FINAL REPORT

The Impact of DNAPL Source-Zone Architecture on Contaminant Mass Flux and Plume Evolution in Heterogeneous Porous Media

SERDP Project ER-1614

August 2013

Mark Brusseau
University of Arizona

SERDP
DOD ▪ EPA ▪ DOE

REPORT DOCUMENTATION PAGE

Form Approved
OMB No. 0704-0188

1. REPORT DATE *(DD-MM-YYYY)*	2. REPORT TYPE	3. DATES COVERED *(From - To)*
30-08-2013	Final	2008-2013

4. TITLE AND SUBTITLE
The Impact of DNAPL Source-Zone Architecture on Contaminant Mass Flux and Plume Evolution in Heterogeneous Porous Media

5a. CONTRACT NUMBER
W912HQ-08-C-0022

5b. GRANT NUMBER

5c. PROGRAM ELEMENT NUMBER

6. AUTHOR(S)
Brusseau, Mark L.

5d. PROJECT NUMBER
ER-1614

5e. TASK NUMBER

5f. WORK UNIT NUMBER

7. PERFORMING ORGANIZATION NAME(S) AND ADDRESS(ES)
University of Arizona
429 Shantz Bldg
Tucson, AZ 85721

8. PERFORMING ORGANIZATION REPORT NUMBER

9. SPONSORING / MONITORING AGENCY NAME(S) AND ADDRESS(ES)
SERDP
4800 Mark Center Drive, Suite 17D08
Alexandria, VA 22305-3605

10. SPONSOR/MONITOR'S ACRONYM(S)
SERDP

11. SPONSOR/MONITOR'S REPORT NUMBER(S)

12. DISTRIBUTION / AVAILABILITY STATEMENT

Approved for public release; distribution is unlimited.

13. SUPPLEMENTARY NOTES

14. ABSTRACT This project was designed to accomplish a systematic study of the mass-transfer behavior of chlorinated-solvent immiscible liquids in heterogeneous porous media at multiple scales, and to investigate the impact of source-zone architecture on mass discharge and plume response. The project involved both bench-scale and field-scale investigations, as well as mathematical modeling analysis. A unique component of the project involved comprehensive long-term studies conducted at a field site (the TIAA site). The analyses employed contaminant mass discharge as an integrative measure of the performance and effectiveness of remediation efforts. The standard approach of characterizing discharge at the source-zone scale was expanded to provide characterization at the plume scale, which was evaluated by examining the change in contaminant mass discharge associated with plume-scale pump-and-treat systems. This approach allows linking the impacts of source-zone remediation to effects on site-wide risk. The studies reported herein investigated the impact of source-zone remediation efforts on contaminant mass discharge and associated plume response at an unprecedented resolution and scale. The results obtained thus provide a significant, unique contribution to our understanding of source-zone dynamics and plume persistence for DNAPL sites. It is anticipated that application of the concepts and tools developed from the project to other DOD sites would provide substantial benefits, including improving the assessment and cost-effective operation of remediation systems for, and enhancing long-term management of, sites contaminated by chlorinated solvents.

15. SUBJECT TERMS
source zone, mass discharge, mass flux, mass removal, back diffusion, mass transfer, contaminant plume, remediation, ISCO, permanganate, persistence, DNAPL

16. SECURITY CLASSIFICATION OF:			17. LIMITATION OF ABSTRACT	18. NUMBER OF PAGES	19a. NAME OF RESPONSIBLE PERSON
U					Mark L. Brusseau
a. REPORT	b. ABSTRACT	c. THIS PAGE	SAR	120	19b. TELEPHONE NUMBER *(include area code)* 520-621-1646

Standard Form 298 (Rev. 8-98)
Prescribed by ANSI Std. Z39.18

Table of Contents

1.0 Abstract……. 1
1.1 Objectives…….…. 1
1.2 Technical Approach……...……. 1
1.3 Results…….. 1
1.4 Benefits……..... 2
2.0 Objective…….. 3
3.0 Background…… 3
3.1 Environmental Issue…….…….. 3
3.2 Summary of Prior Research…… 5
3.2.1 Plume Persistence…….. 5
3.2.2 Characterizing Mass Transfer and Mass Removal…… 7
4.0 Materials and Methods……. 9
4.1 Project Design…… 9
4.2 Bench-scale Experiments…… 9
4.3 Field-scale Experiments……. 11
4.4 Mathematical Modeling……..……... 11
4.5 Analysis of Contaminant Mass Discharge Reduction and Mass Reduction…..…… 13
5.0 Results and Discussion……...……. 15
5.1 Source-zone Dynamics: Mass Removal and Mass Discharge……..…. 15
5.1.1 Impacts of Source-zone Architecture and Age: Bench-scale Results…… 15
5.1.2 Impacts of Source-zone Architecture and Age: Field Results…….…. 27
5.1.3 Impacts of Source-zone Architecture and Age on ISCO: Bench-scale Results. 42
5.2 Field-scale ISCO Application in Heterogeneous Systems…….. 53
5.2.1 ISCO Performance: Mass Removal and Mass Discharge…….. 53
5.2.2 Application of ISCO for Source Containment in a Low-Permeability System. 61
5.3 Plume Response and Persistence…… 63
5.3.1 Impacts of Sorption/Desorption……. 63
5.3.2 Plume Response to Source Remediation…… 72
5.3.3 Plume Response to Source Containment……... 80
5.4 Mathematical Modeling…….. 87
6.0 Conclusions and Implication for Future Research/ Implementation……. 98
6.1 Conclusion and Implications…… 98
6.1.1 Source-Zone Architecture and Age…….. 98
6.1.2 Plume Response and Persistence……..…. 99
6.1.3 Mathematical Modeling……...….. 100
6.1.4 Implications…… 101
6.2 Practical Tools for Site Characterization and Remediation Performance Assessment. 102
6.2.1 Time-Continuous Contaminant Mass Discharge……... 102
6.2.2 The Contaminant Mass Discharge Test……..... 103
6.2.3 Use of Pump-and-Treat Operations Data for Assessing Remediation Efforts... 104
6.2.4 The CMDR-MR Relationship…… 105
6.3 Summary Statement……..... 110
7.0 Literature Cited……..... 110
8.0 Appendices……..... 117
8.1 Supporting Data……..... 117

8.2 List of Scientific/Technical Publications……. 117
8.2.1 Journal Articles……. 117
8.2.2 Presentations……..... 118
8.3 Other Supporting Material…….……...…..... 120

List of Tables

Table 5.1.1-1 Parameters for the initial flow-cell experiment……. 15
Table 5.1.3-1a Summary of experimental conditions……. 42
Tables 5.1.3-1b Summary of experimental conditions…… 43
Tables 5.3.1-1 Summary of miscible-displacement experiments…… 63
Table 5.3.1-2 Parameter values for miscible-displacement experiments…… 64
Table 5.4-1 Summary of methods developed to predict the mass-flux-reduction/mass-removal relationship……. 89
Table 5.4-2 Root-mean-square error (RMSE) values for each method……. 96

List of Figures

Figure 4.3-1 Map of the field site……..... 12
Figure 5.1.1-1 Effluent concentration as a function of the number of pore volumes flushed for the four aqueous flushing experiments……..... 16
Figure 5.1.1-2 Organic –liquid distribution at four different flushing times for the Mixed-Source and Heterogeneous Experiments……...…….. 17
Figure 5.1.1-3 Mass flux reduction versus mass removal behavior for the aqueous flushing and enhanced flushing experiments……. 19
Figure 5.1.1-4 Impact of Source-zone aging on mass flux reduction versus mass removal behavior for the modified Mixed-Source and Heterogeneous experiments (Mixed-Source-2 and Heterogeneous-2, respectively)…… 20
Figure 5.1.1-5 Ganglia-to-pool (GTP) ratio as a function of mass removal for the Mixed-Source and Heterogeneous experiments…….. 22
Figure 5.1.1-6 Mean and variance of organic-liquid saturation distribution for the Mixed-Source and Heterogeneous experiments as a function of mass removal……..…….…… 23
Figure 5.1.1-7 Hydraulic conductivity variance for the Mixed-Source and Heterogeneous experiments as a function of the variance in organic-liquid saturation distribution…… 24
Figure 5.1.1-8 Elution curves for second set of flow-cell experiments…… 25
Figure 5.1.1-9 Relationship between reductions in mass flux and mass for data presented in Figure 5.1.1-8…… 26
Figure 5.1.1-10 Elution curves for flow-cell experiments conducted to investigate the impact of flow rate…… 26
Figure 5.1.1-11 Relationship between reductions in mass flux and mass for data presented in Figure 5.1.1-10……. 27
Figure 5.1.2-1 Maps of the field site…… 29
Figure 5.1.2-2 Schematic of local stratigraphy for the site…….. 29
Figure 3a Sediment-phase trichloroethene (TCE) concentrations for the core samples from the most contaminated cores for each set collected in 2008 (set1 and 2012 (set 2)…… 31
Figure 3b Sediment-phase trichloroethene (TCE) concentrations for core samples from the least contaminated cored for each set collected in 2008 (set 1) and 2012 (set 2)……. 31

Figure 5.1.2-4 Concentrations of trichloroethene (TCE) in groundwater extracted with the two source-area extraction wells and associated flow rates……. 32
Figure 5.1.2-5 Contaminant mass discharge for the source area……... 33
Figure 5.1.2-6 Relationship between the reduction in contaminant mass discharge (CMD) and the reduction in contaminant mass for the source area…… 36
Figure 5.1.2-7 Relationship between the reduction in contaminant mass discharge (CMD) and the reduction in contaminant mass: comparison of measured field data……. 38
Figure 5.1.2-8 Relationship between the reduction in contaminant mass discharge (CMD) and the reduction in contaminant mass: comparison of measured field data from Dover test site 40
Figure 5.1.3-1 Flow-cell schematic for rectangular flow cell with a coarser sand that comprised the matrix and two finer sands were used to create zones 1 and 2…… 44
Figure 5.1.3-2 Photographic images cropped to focus on the lower-K zone 2 and surrounding higher-K matrix sand during the constant permanganate injection…… 45
Figure 5.1.3-3 Photographic image of the lower-K zone 2 and surrounding area after permanganate injection, exhibiting the shadow zone downgradient of the lower-K zone, downgradient manganese oxide tails, and manganese oxide formation around the lower-K zone..... 46
Figure 5.1.3-4a SEM image of sand grain located in the middle of a low-K zone……..… 46
Figure 5.1.3-4b SEM image of sand grain located at the boundary of a low-K zone…..…. 46
Figure 5.1.3-5 Distances in centimeters measured along rectangular flow cell that manganese oxides formed inside and outside of the lower-K zones during flow interruptions of the pulsed permanganate injection experiment…… 47
Figure 5.1.3-6 Effluent TCE concentrations form the rectangular flow-cell experiments with water flooding only (open symbols) and water flooding after pulsed injection of 4.5 pore volumes of 15 mm permanganate (ISCO) (closed symbols)……. 48
Figure 5.1.3-7 Effluent TCE concentrations for the cylindrical flow-cell experiments with water flooding only (open symbols) vs. water flooding after permanganate treatment (ISCO) (closed symbols) for 1 PV injections of the 63.3 mm solution……. 49
Figure 5.1.3-8a Fractional mass-flux reduction as a function of fractional mass removal for the rectangular flow-cell experiments……. 50
Figure 5.1.3-8b Fractional mass-flux reduction as a function of fractional mass removal for the column experiments; (c) cylindrical flow-cell experiments…….. 51
Figure 5.1.3-8c Fractional mass-flux reduction as a function of fractional mass removal for the column experiments…….. 52
Figure 5.2.1-1 Results of contaminant mass discharge tests conducted at the Site 3 source zone before and after ISCO…… 55
Figure 5.2.1-2 Integrated contaminant mass discharge for the entire site, including contributions, from the source zones and the contaminant plume…… 56
Figure 5.2.1-3 Concentrations of the trichloroethene in groundwater collected from monitoring wells located within the Site 3 source zone…… 57
Figure 5.2.1-4 Sediment concentrations of Mn for core samples collected from a single borehole drilled before ISCO and a single borehole drilled after ISCO for Site 3…… 58
Figure 5.2.1-5 Sediment concentrations of trichloroethene for core samples collected from a single borehole drilled before ISCO and a single boreholes drilled after ISCO for Site 3…….. 59
Figure 5.2.2-1 Map of the test site…… 62
Figure 5.3.1-1 Comparison of elution tailing behavior for the long-term, synthetically-aged and freshly-amended aquifer material…… 65

Figure 5.3.1-2 Representative mass removal curves for the long-term aged and freshly-amended aquifer material…… 66
Figure 5.3.1-3 Comparison of long-term, elution tailing behavior for the field-contaminated , synthetically aged, and freshly-amended aquifer material…….. 67
Figure 5.3.1-4 Results of the XRD measurements for the SWy-2 samples…… 68
Figure 5.3.1-5 Results of the XRD measurements for the B-119 samples……. 70
Figure 5.3.1-6 TCE Elution curves for systems flooded with potassium nitrate solution…. 71
Figure 5.3.2-1 Diagram of the study area, compromising the South section of the TIAA site presented in Figure 4.3-1, with locations of extraction wells used for the pump-and-treat system……. 73
Figure 5.3.2-2 Concentration of trichloroethene in groundwater extracted with the pump-and -treat system…… 74
Figure 5.3.2-3 Contaminant mass discharge as a function of time; time zero corresponds to the start of the pump-and-treat operation (April 1987)…….. 75
Figure 5.3.2-4 Contaminant mass discharge for the first 13 years as a function of source; time zero corresponds to the start of the pump-and-treat operation (April 1987)……. 76
Figure 5.3.2-5 Predicted contaminant mass discharge for the cores with and without source-zone remediation; time zero corresponds to the start of the ISCO remediation effort…… 77
Figure 5.3.3-1 Concentrations of trichloroethene (TCE) in groundwater extracted with extraction wells located within the contaminant plume. Zero corresponds to system startup in fall 2007… 81
Figure 5.3.3-2 Change in mean relative TCE concentrations for groundwater sampled from monitoring wells screened separately in the gravel and clay units……... 82
Figure 5.3.3-3 Change in relative areas of the TCE plume for date collected from monitoring wells screened separately in gravel and clay units…… 83
Figure 5.3.3-4 Total contaminant mass discharge for the groundwater contaminant plume extraction-well system…… 84
Figure 5.3.3-5 Relationship between reductions in contaminant mass discharge and reductions in contaminant mass for the plume after source containment……...…. 85
Figure 5.4-1 Relationship between n (parameter from equation 4.1) and ganglia-to-pool (GTP) ration…… 90
Figure 5.4-2 Application of the simple function to measured data…… 90
Figure 5.4-3 Measured and predicted mass-flux reduction versus mass-removal behavior for the Mixed Source and Heterogeneous experiments……. 91
Figure 5.4-4 Mass flux reduction versus mass removal behavior for the Mixed Source and Heterogeneous experiments, and application of the various methods for characterizing mass-flux-reduction/mass-removal behavior……. 93
Figure 5.4-5a Ratio of the source-zone cross-sectional area to the total system cross-sectional area as a function of mass removal for the Mixed Source and Heterogeneous experiments.. 94
Figure 5.4-5b Ratio of the source-zone length to the total system length as a function of mass removal for the Mixed Source and Heterogeneous experiments…… 94
Figure 5.4-6 Measure of the source zone parameters as a function of mass removal for each permeability zone in the Heterogeneous experiment…….. 95
Figure 5.4-7 Measured and simulated elution curves for TCE dissolution……..… 97
Figure 6.2.4-1 Relationships between reduction in contaminant mass discharge and reduction in contaminant mass for three prototypical cases…….. 107

Figure 6.2.4-2 Cumulative mass reduction profiles for three prototypical cases…….. 107
Figure 6.2.4-3 Temporal concentration of CMD profiles for three prototypical cases……. 108
Figure 6.2.4-4 Relationships between reduction in contaminant mass discharge and reduction in contaminant mass for three prototypical cases…….. 109
Figure 6.2.4-5 Relationships between relative contaminant mass discharge and relative contaminant mass for three prototypical cases; log scale…….. 109

List of Acronyms

(D)NAPL = (Dense)Nonaqueous-phase Liquid
CMD = Contaminant Mass Discharge
CMDR = Contaminant Mass Discharge Reduction
DOD = Department of Defense
ISCO = In Situ Chemical Oxidation
ITRC = Interstate Technology and Regulatory Council
MR = Mass Reduction
SERDP = Strategic Environmental Research and Development Program
SVE = Soil Vapor Extraction
TCE = Trichloroethene

Keywords

source zone, mass discharge, mass flux, mass removal, back diffusion, mass transfer, contaminant plume, remediation, ISCO, permanganate, persistence, DNAPL

Acknowledgements

This research was supported by the US Department of Defense Strategic Environmental Research and Development Program (ER-1614), with additional support provided by the National Institute of Environmental Health Sciences Superfund Research Program (P42 ES04940), the US Air Force, and the Tucson Airport Authority. We thank several U of A students and staff that provided field and laboratory assistance, including Dr. Ann Russo, Candice Morrison, and Dr. Jon Mainhagu. We thank Dr. KC Carroll (New Mexico State University) for his collaborative efforts and contributions. We thank George Warner (USAF), Jim Hatton (AECOM), Bill DiGuiseppi (AECOM), Fred Brinker (TAA), and Manfred Plaschke (CRA, Inc) for their support of the field studies. Finally, we thank Andrea Leeson, Hans Stroo, and other members of the SERDP staff for their support.

1.0 Abstract

1.1 Objectives

Chlorinated solvents are the primary contaminants of concern for Department of Defense (DoD) sites. A clear understanding of the mass-transfer and mass-removal behavior of chlorinated solvents in subsurface systems is critical to accurately assess the human-health risks associated with sites contaminated by chlorinated solvents, and to design effective remediation systems for such contamination. The overall goal of the project was to enhance our understanding of the relationships between source-zone architecture, mass-transfer dynamics, and contaminant mass removal for heterogeneous DNAPL source zones, and the associated impacts on plume response. The specific objectives that were addressed in this project are:

1. Investigate the impact of source-zone aging on the relationship between mass removal and mass-flux reduction.
2. Investigate the impact of source-zone architecture and mass-transfer dynamics on contaminant removal, mass flux, and plume response at the field scale.
3. Apply mathematical models to evaluate the impact of porous-medium heterogeneity, nonuniform DNAPL distribution, and mass-transfer processes on mass-flux behavior at multiple scales.
4. Assess the efficacy of methods for estimating mass-flux-reduction/mass-removal behavior.

1.2 Technical Approach

This project was designed to accomplish a systematic study of the mass-transfer behavior of chlorinated-solvent immiscible liquids in heterogeneous porous media at multiple scales, and to investigate the impact of source-zone architecture on mass discharge and plume response. The project involved both bench-scale and field-scale investigations, as well as mathematical modeling analysis. A unique component of the project involved comprehensive long-term studies conducted at a field site (the TIAA site). The analyses employed contaminant mass discharge as an integrative measure of the performance and effectiveness of remediation efforts. The standard approach of characterizing discharge at the source-zone scale was expanded to provide characterization at the plume scale, which was evaluated by examining the change in contaminant mass discharge associated with plume-scale pump-and-treat systems. This approach allows linking the impacts of source-zone remediation to effects on site-wide risk.

1.3 Results

A series of bench-scale and field studies was conducted to investigate the impact of source-zone architecture and flow-field heterogeneity on mass-removal and mass-discharge behavior. In total, the results of the studies demonstrate that the configuration of the source zone with respect to spatial distributions of subsurface properties (porous-media type, permeability, contaminant) exerts a significant control on the magnitudes and rates of mass removal and associated contaminant mass discharge. In particular, it was observed that source-zone age was a critical factor mediating system behavior.

The response of the plume after implementation of source-zone management is a critical issue for chlorinated-solvent sites. This project included two field studies of plume response, one wherein aggressive source remediation efforts were implemented and one for which source control was achieved via hydraulic containment. In total, the results of the project demonstrate that management of source zones can reduce contaminant mass discharge to the groundwater

plume. The analyses indicated that this action can, in turn, reduce the time required to clean up the groundwater plume. However, the results also show that the plumes can be expected to persist for an extended time due to the contributions of back diffusion associated with contaminant mass stored in extensive lower-permeability units within the plume.

The results of this project support the growing consensus that most sites with large groundwater plumes will require many decades before cleanup will be achieved under current methods and standards. The continued use of pump and treat to manage plumes at these sites for the many additional decades anticipated will result in an enormous aggregate operations and maintenance cost. Hence, there is a critical need to evaluate alternative methods, such as monitored natural attenuation, permeable reactive barriers, and deep reactive treatment zones that can be used to cost-effectively manage these plumes while continuing to meet all remedial objectives. More effective methods for treating poorly accessible contaminant are also needed. In addition, there is a critical need to develop methods that can provide higher-resolution site characterization that: (a) are cost effective, (b) are specifically designed to minimize disruption of operating remedial systems, and (c) can readily provide temporal updates of site conditions, thus supporting adaptive responses of the remedial systems to changing site conditions.

1.4 Benefits

This project demonstrated that time-continuous measurements of contaminant mass discharge can provide useful information to characterize mass-transfer processes, assess mass-removal magnitudes and conditions, and estimate contaminant distributions and quantities, as well as quantify mass discharge. Time-continuous profiles of contaminant mass discharge can be obtained by conducting extended contaminant mass discharge tests or by capturing operational fluid-extraction data. This project demonstrated the utility of both methods, and presented methods of data analysis and interpretation. Specifically, the project showed that our approach for comprehensive analysis of operational pump-and-treat data is a powerful, cost-effective method for providing higher-resolution, value-added characterization of contaminated sites. Advantages of the method include: (a) use of data that typically exists for operating sites, thus minimizing data-collection costs, (b) no disruption of the operating remediation system, (c) ability to update the analysis at any time, providing a means to periodically revise the site conceptual model, and the operation of the remediation system.

Temporal profiles of contaminant mass discharge, combined with knowledge of initial contaminant mass, can be used to evaluate the relationship between reductions in contaminant mass discharge (CMDR) and reductions in contaminant mass (MR). In this project, we developed CMDR-MR relationships for a well-detailed field site, and also for several other prior field projects. These data represent the first comprehensive field-based analysis of this entity. The results indicate that the CMDR-MR relationship is a defining characteristic of system behavior, and is mediated by system properties and conditions such as permeability distribution, contaminant distribution, and mass-transfer processes.

The studies reported herein investigated the impact of source-zone remediation efforts on contaminant mass discharge and associated plume response at an unprecedented resolution and scale. The results thus provide a significant, unique contribution to our understanding of source-zone dynamics and plume persistence for DNAPL sites. It is anticipated that application of the concepts and tools developed from the project to other DOD sites would provide substantial benefits, including improving the assessment and cost-effective operation of remediation systems for, and enhancing long-term management of, sites contaminated by chlorinated solvents.

2.0 Objective

Chlorinated solvents are the primary contaminants of concern for Department of Defense (DoD) sites (SERDP, 2006). They are also among the most common groundwater contaminants in the USA due to their prior widespread use for numerous military, industrial, and commercial applications. These compounds occur in the form of nonaqueous-phase (immiscible) organic liquids (DNAPLs) and are long-term sources of vadose zone and groundwater contamination. Given their toxicity, widespread occurrence, persistence, and complex behavior, chlorinated solvents continue to pose a significant risk to human health and the environment.

A clear understanding of the mass-transfer and mass-removal behavior of chlorinated solvents in subsurface systems is critical to accurately assess the human-health risks associated with sites contaminated by chlorinated solvents, and to design effective remediation systems for such contamination. The Strategic Environmental Research and Development Program of DoD released a Statement of Need (SON) in 2007 titled "Improved Understanding and Prediction of Plume Response to DNAPL Source Zone Architecture and Depletion". The stated objective of this SON was to improve the understanding and ability to predict the response of the chlorinated solvent dissolved phase plume to the architecture and possible depletion of the DNAPL source zone.

The overall goal of the project was to enhance our understanding of the relationships between source-zone architecture, mass-transfer dynamics, and contaminant mass removal for heterogeneous DNAPL source zones, and the associated impacts on plume response. The specific objectives that were addressed in this project are:

1. Investigate the impact of source-zone aging on the relationship between mass removal and mass-flux reduction.
2. Investigate the impact of source-zone architecture and mass-transfer dynamics on contaminant removal, mass flux, and plume response at the field scale.
3. Apply mathematical models to evaluate the impact of porous-medium heterogeneity, nonuniform DNAPL distribution, and mass-transfer processes on mass-flux behavior at multiple scales.
4. Assess the efficacy of methods for estimating mass-flux-reduction/mass-removal behavior.

3.0 Background

3.1 Environmental Issue

As noted above, chlorinated solvents are the primary contaminants of concern for DoD sites. Extensive dissolved-phase groundwater contaminant plumes typically form at sites contaminated by these compounds because of their relatively high aqueous solubilities (in comparison to regulatory standards), limited retardation, and generally low (or very site dependent) transformation potential. In many cases, the plumes are hundreds of meters to several kilometers long. These large plumes are very expensive to contain and remediate, and present difficult challenges to the long-term management and closure of the sites.

Pump and treat has been the primary method used to contain and treat groundwater contaminant plumes at chlorinated-solvent sites. After approximately 30 years of experience gained, it is now clear that most sites with large groundwater plumes comprising these contaminants will require many more decades before cleanup will be achieved under current methods and standards (e.g,, DOD, 2011; NRC, 2013). The continued use of pump and treat to manage plumes at these sites for the many additional decades anticipated will result in an

enormous aggregate operations and maintenance cost. For example, it is estimated that DoD may spend more than $100 million annually for hydraulic containment at chlorinated-solvent sites using pump-and-treat technologies, with total lifetime aggregate costs exceeding $2 billion (SERDP, 2006). Furthermore, it has been estimated that aggregate annual pump-and-treat costs for the estimated 15,000 to 25,000 sites in the U.S. with DNAPL contamination could range from $2.7 to $4.5 billion dollars, with lifetime aggregate costs exceeding $100 billion (EPA, 2003).

The results of prior investigations have clearly indicated that the presence of organic-liquid contamination in the subsurface, i.e., the existence of DNAPL source zones, is typically a primary factor limiting the cleanup of chlorinated-solvent sites. DNAPLS serve as long-term sources of subsurface contamination, and their presence contributes greatly to the significant costs and time required for site remediation discussed above. Recognition of the importance of source zones to overall site cleanup led to major investments and research into source-zone remediation over the past two decades.

The obvious goal for source-zone remediation is complete removal of all DNAPL mass from the subsurface. Unfortunately, because of the complexities associated with the transport, retention, distribution, and mass transfer of DNAPLs, as well as the heterogeneity of subsurface environments, it is generally not possible to remove all DNAPL mass from the source zone (e.g., SERDP, 2001; ITRC, 2002; EPA, 2003; NRC, 2004). A recent publication based on prior SERDP-supported research highlights these issues (8). Thus, in most situations, application of a source-zone remediation technology will result in only partial reduction of DNAPL mass. A critical question then is what benefit does partial source reduction have for overall site cleanup, and particularly, what impact would partial source remediation have on the groundwater contaminant plume? One ramification of this issue is illustrated by the conclusion reported in an expert panel review (NRC, 2004) “The technical difficulties involved in characterizing and remediating source zones and the (associated) potential costs are so significant that there have been no reported cases of large chlorinated solvent sites where remediation has restored the site to drinking water standards.”

An argument for source-zone remediation, even when only partial source reduction is expected, is that the reduction in source-zone mass will result in reduced mass discharge to the plume over the long term, thus reducing the time-scale required for pump and treat. Another argument for implementing source-zone remediation involves the concept of integrated remedial strategies wherein aggressive source-zone remediation is combined with low-cost methods for managing the contaminant plume. A prime example of this approach is combining source-zone treatment with monitored natural attenuation. If the mass discharge of contaminant from the source zone is too large, the attenuation capacity of the system will be exceeded and the contaminant plume will not be contained. However, implementing source reduction may reduce the mass discharge such that the attenuation processes can effect plume containment. In either case, it is hypothesized that implementing source-zone remediation will ultimately result in accelerated site closure and reduced long-term site management costs.

Resolving whether source remediation would be effective for a given site requires a determination of its relative costs and benefits. The key set of questions to address in determining cost-benefit are: (1) what degree of source reduction is expected to be accomplished with the selected remedial technology for the given site conditions (i.e., mass removal), (2) what impact would this level of mass reduction have on the amount of contaminant emanating from the source zone (i.e., contaminant mass discharge), and (3) would this reduction in mass

discharge result in a significant reduction in risk and/or remedial costs (i.e., plume response). Clearly, these questions can be accurately answered only if we fully understand the impact of the remedial action on DNAPL mass reduction and resultant mass-discharge reduction across the spectrum of conditions and scales inherent to subsurface environments.

3.2 Summary of Prior Research

The distribution, mass-transfer dynamics, and mass removal of chlorinated solvents and other organic liquids in the subsurface have been examined in numerous studies conducted over the past few decades. Thus, there exists a significant level of information and understanding about the behavior of organic-liquid contaminants in the subsurface. However, the current understanding of mass-transfer and mass-removal processes is far from complete, and many challenges remain. These challenges were documented in a Workshop report that examined the critical issues and research needs for remediation of chlorinated-solvent contaminated sites (SERDP, 2006). Among the priority research needs identified were:

- improved understanding of the relationship between mass removal and mass flux
- improved understanding of plume response to source-zone remediation
- improved understanding of mass transfer and mass removal for source zones that have poorly accessible ("flow-limited") NAPL

The project whose results are presented in this report was designed to address these and related issues.

3.2.1 Plume Persistence

The migration, removal, and persistence of groundwater contaminant plumes have been a focus of research and field investigations for several decades. This is discussed in more detail in a manuscript in preparation (18). Conceptually, the factors contributing to plume persistence have long been established, including uncontrolled source zones, dispersed reservoirs of dissolved and sorbed contaminant, and non-optimal well-field performance (e.g., Keely, 1989; Mackay and Cherry, 1989). Recently, the persistence of plumes after source remediation has re-emerged as a focus of concern. This has led to a "rediscovery" of the role of dispersed sources of mass and the transfer of such mass to advective domains on plume persistence. Aqueous-phase contaminant stored in lower-permeability zones within and/or adjacent to large plumes is one reservoir of mass. Another is contaminant sorbed to sediment within the plume. As noted, the potential impact of such mass on plume removal was conceptualized long ago (e.g., Keely, 1989; Mackay and Cherry, 1989).

The specific impact of dispersed mass storage on plume migration and removal has been investigated in a number of mathematical-modeling studies. For example, Johnson and Pankow (1992) reported the results of numerical simulations that illustrated that contaminant mass residing within a lower-permeability unit could serve as a long-term source of contamination to a groundwater plume. Several investigators have used numerical simulations to illustrate the impact of spatial variability of hydraulic conductivity and of sorption, and associated mass transfer, on rates of contaminant removal.

The impact of dispersed mass storage on plume migration and removal has been investigated in a few field studies. Bahr (1989) reported the results of a small-scale contaminant elution test conducted in a groundwater plume in Ottawa, Canada. A mathematical model was applied to the measured data, and it was concluded that mass removal was affected by rate-

limited desorption. Brusseau (1993) analyzed the field data reported by Bahr (1989) using a multi-factor nonideal transport model, and delineated the relative contributions of back diffusion and rate-limited desorption on contaminant removal. A field study was conducted by Ball and colleagues (c.f. Liu and Ball, 2002) at Dover AFB, DE to evaluate the impact of mass transfer (desorption; diffusion between lower and higher permeability units) on migration and removal of a chlorinated-solvent groundwater contaminant plume. The studies, involving coring, contaminant elution tests, and mathematical modeling, were conducted using two 10 by 3.7 meter sheet-pile cells isolated from the surrounding contaminant plume. The results of the study indicated that a lower-permeability unit downgradient of the source zone became contaminated via diffusive mass transfer from the plume as it migrated in the aquifer, and that water flushing via pump and treat removed a minimal fraction of the contaminant mass residing in the lower-permeability unit.

Rivett et al. (2006) examined the behavior of a small, three-component (trichloromethane, trichloroethene, tetrachloroethene) groundwater contaminant plume after hydraulic isolation of the source. They observed delayed contaminant removal, which was attributed primarily to the impact of inter-well stagnation zones. They concluded that back diffusion and nonideal desorption processes had minimal measurable impact on plume behavior, which is likely due to a combination of a mildly heterogeneous field site (no major silt/clay zones) and the fact that the plume was freshly created for the study (resident for ~1 year). Chapman and Parker (2005) conducted a study at a chlorinated-solvent contaminated site in CT to investigate plume behavior after isolation of the source zone. Initial concentrations of trichloroethene, which ranged between 5000 and 30,000 ug/L, declined to between 200 and 3000 ug/L within approximately three years after isolation of the source zone. However, the plume was observed to persist for several years beyond the time estimated for removal via hydraulic flushing. The results of sediment coring and mathematical modeling indicated that diffusive mass transfer of contaminant (back diffusion) from a laterally extensive lower-permeability unit into the aquifer mediated long-term plume response. Parker et al (2008) investigated the impact of hydraulic source isolation on plume persistence for a trichloroethene -contaminated site in FL. The results of mathematical modeling suggested that back diffusion from laterally extensive lower-permeability units into the aquifer caused the observed persistence of the plume. Rasa et al. (2011) concluded, based on mathematical modeling and analysis of field data, that back diffusion was the cause of a plume of tert-butyl alcohol persisting for several years after source removal at a site in CA.

Brusseau and colleagues conducted an extensive study of source-zone remediation efforts and associated plume behavior for a chlorinated-solvent contaminated site in AZ undergoing pump-and-treat remediation (Nelson and Brusseau, 1996; Blue et al., 1998; Brusseau et al., 1999; Zhang and Brusseau, 1999; Nelson and Brusseau, 2003; Brusseau et al., 2007). Multiple methods, including contaminant elution tests, multiple-solute tracer tests, coring, analysis of historic pump-and-treat operations data, laboratory experiments, and mathematical modeling, were used to characterize the relative impacts of plume-scale back diffusion, plume-scale sorption/desorption, and dissolution of organic liquid trapped in the source zones on contaminant transport. The results indicated that all three mass-transfer processes were influencing plume removal and persistence, with organic-liquid dissolution the primary factor (Zhang and Brusseau, 1999; Brusseau et al., 2007). In addition, the results showed that contaminant concentrations were generally higher within the laterally extensive lower-permeability units compared to the more permeable units, suggesting that pump and treat was ineffective at flushing the lower-

permeability units. Assessment of the historic integrated plume-scale contaminant mass discharge, along with the results of mathematical modeling, indicated that the plume would persist for many decades even with the isolation or removal of the source zones, primarily due to back diffusion of contaminant associated with the lower-permeability units (Brusseau et al., 2007, 2011b).

3.2.2 Characterizing Mass Transfer and Mass Removal

High-resolution sampling of groundwater and sediment is the standard method used to characterize contaminant distributions. Such data are sometimes used to evaluate potential processes influencing mass transfer and mass removal. For example, such analyses provide direct evidence of the presence of contamination within a lower-permeability unit. Multiple samples can be collected from within the same area as a function of time to characterize temporal changes in concentration distributions, and thereby assess the dynamics of diffusive mass transfer. Studies conducted in this manner may require relatively long times (years) to resolve mass-transfer dynamics. Other methods for characterizing the occurrence and contributions of mass transfer include the multiple-solute tracer test and the induced-gradient contaminant elution test.

Multiple-solute Tracer Tests

The multiple-solute tracer test was developed to characterize the occurrence of diffusive mass transfer and its impact on contaminant transport (Brusseau, 1993; Maloszewski and Zuber, 1993). This method is based on the use of multiple non-reactive tracers with different aqueous diffusivities. For a system influenced by a diffusive mass-transfer process, the rate of mass transfer will be greater for solutes with larger diffusion coefficients. Thus, tracers with different diffusion coefficients should exhibit non-identical breakthrough curves (e.g., different amounts of spreading, different extents of tailing) for a given set of conditions. For example, a tracer test employing two non-reactive tracers with different diffusion coefficients was conducted in the field to characterize the contribution of diffusive mass transfer to contaminant transport in a sedimentary aquifer (Nelson et al., 2003). Greater spreading was observed for the tracer with the smaller diffusion coefficient, indicating an impact of rate-limited diffusive mass transfer between zones of lower and higher permeability on transport. Because the larger tracer has a smaller diffusion coefficient, more time was required for it to diffuse in and out of the lower-permeability units, thus resulting in greater spreading.

The multiple-solute tracer test method has been used successfully in both laboratory and field studies. In some situations, however, the resolution of the tracer test may not be sufficient to fully assess the contribution of diffusive mass transfer to plume behavior. For example, the relatively short residence times associated with induced-gradient tracer tests may not be sufficient to fully capture diffusive mass-transfer behavior, particularly for systems containing thick, laterally extensive lower-permeability layers. In addition, difficulties are often encountered in obtaining accurate analyses of tracers at lower concentrations, further limiting resolution of the test.

Induced-Gradient Contaminant Elution Tests

Induced-gradient contaminant elution tests have been used to characterize and evaluate the impact of mass-transfer processes on contaminant transport and mass removal for a variety of field sites. Bahr (1989) first presented the method, which was conducted in the plume region of the site. Most applications since have also been implemented within the plume. Brusseau and

colleagues (Nelson and Brusseau, 1997; Blue et al., 1998; Brusseau et al., 1999; 2007) extended the test to source zones and demonstrated its utility for characterizing contaminant mass discharge.

The induced-gradient contaminant elution test is conducted within an existing zone of groundwater contamination, wherein an extraction well is pumped for an extended period and contaminant concentrations in the effluent are monitored. An injection well is sometimes used in conjunction with the extraction well (a well couplet) to inject clean water and thereby help isolate and flush the target zone. A nonreactive tracer solution is sometimes injected to support data analysis and interpretation. The effluent concentration data are used to produce a contaminant elution curve. The nature of the contaminant elution curve obtained from the test is examined to evaluate the potential impact of rate-limited mass-transfer processes on contaminant transport. Specifically, the presence and extent of "tailing" (asymptotic approach to low concentrations) is used as an indicator of potential rate-limited mass transfer constraints. In addition, flow-interruption or rebound tests are often conducted in conjunction with the induced-gradient contaminant elution test. This is accomplished by continued monitoring of contaminant concentrations after cessation of pumping. Observation of increased contaminant concentrations (rebounding) is another indicator of potential mass-transfer constraints. Mathematical modeling is often used to assist in analysis and interpretation of the test results.

Interpretation of the results of an induced-gradient contaminant elution test is relatively straightforward for a system in which a single mass-transfer process is operative. However, for many systems, contaminant transport is influenced by multiple mass-transfer processes (desorption from the solid phase, diffusive mass-transfer from low-permeability zones, dissolution from an immiscible-liquid phase). For such systems, it may in some cases be difficult to separate the effects of diffusive mass transfer from those of the other mass-transfer processes. Another issue with interpretation of test results is the potential contributions of hydraulic phenomena to the observed tailing and rebound, particularly for situations wherein the test site is located within a large contaminant plume. Such phenomena include the influx of contaminated water from outside the swept zone, and its potential impact on tailing and rebound, and the impact of desaturation and resaturation of contaminated zones on rebound for unconfined aquifer systems.

4.0 Materials and Methods

4.1 Project Design

The impact of porous-medium heterogeneity and non-uniform DNAPL distributions (i.e., source-zone architecture) on DNAPL mass-transfer dynamics (and associated mass removal behavior) at larger (field) scales is not fully understood. Concomitantly, the relationship between source-zone architecture and the "source function" (i.e., contaminant mass discharge), and how reductions in source-zone mass impact mass discharge, remains ill-defined. Furthermore, the influence of coupled processes such as DNAPL mass transfer, sorption/desorption, and matrix-associated diffusive mass transfer on long-term contaminant mass discharge is unclear. This project was designed to accomplish a systematic study of the mass-transfer behavior of chlorinated-solvent immiscible liquids in heterogeneous porous media at multiple scales, and to investigate the impact of source-zone architecture on mass discharge and plume response.

The project involved both bench-scale and field-scale investigations, as well as mathematical modeling analysis. The bench-scale experiments were designed to investigate the impact of porous-medium heterogeneity and non-uniform NAPL distribution on mass-removal and mass-discharge behavior under well-defined and controlled conditions. The impact of different types of source-zone architectures was investigated. A major aspect of this component involved the use of imaging methods. These methods were used to obtain direct, in-situ, quantitative measurements of DNAPL configuration and dissolution dynamics. Another major component of the project was the collaborative field study conducted at a federal Superfund site in Tucson. This study provided a unique opportunity to directly examine the impact of DNAPL source-zone mass removal on mass discharge reduction and plume response for an actual field site. Another component of the project involved the application of mathematical modeling at multiple scales to assist in data analysis and interpretation.

Note that in the following sections, references to specific publications produced from the project are cited where relevant. The citations are keyed to the numbered publications listed under the "Journal Articles subsection (8.2.1) of the "Publications" section.

4.2 Bench-scale Experiments

A series of column experiments was conducted to investigate the impact of sorption/desorption interactions on contaminant transport (1,9,13). Aquifer sediment collected from the project field site was used for these experiments. Trichloroethene, the primary contaminant of concern at the field site, was used as the model contaminant. Methods we have developed and used successfully in prior research were employed (e.g., 1).

A set of experiments was conducted to examine the potential for intercalation of TCE by clay minerals associated with aquifer sediments. The sediment samples collected from the field site were used, along with two Montmorillonite specimen clays that were used as controls. X-ray diffraction (XRD), conducted with a controlled-environment chamber, was used to characterize smectite interlayer d-spacing for three treatments (bulk air-dry sample, sample mixed with synthetic groundwater, sample mixed with TCE-saturated synthetic groundwater). The methods used are presented in (9).

Several sets of experiments were conducted using flow cells to investigate the impact of source-zone architecture on DNAPL dissolution and the impact of remediation efforts (2,3,12). The design, preparation, and implementation of the flow-cell experiments followed methods we have used in prior experiments (Brusseau et al., 2000; 2002). A specially designed light

reflection visualization (LRV) imaging system was used for some of these experiments to characterize the in-situ DNAPL distribution (7).

Light transmission and reflection theory has been described in detail by other researchers. Therefore, only a description of the imaging method is provided herein. A high resolution digital camera (Nikon D70 with an AF-S Nikkor 18-70 mm lens) was used for raw data collection. All images included an optical density photographic card (Kodak) to correct for lighting differences and to convert pixel intensity to optical density. Images were imported into MATLAB as 3-D matrices, with the dimensions representing the red (R), green (G) and blue (B) color values, respectively. Next, the images were converted into a 1-D matrix of intensity (I) values:

$$I = \frac{(R+G+B)}{(3\cdot 255)} \qquad I \in [0,1]$$

The optical density of each pixel was calculated using the average intensity of the white step of the optical density card:

$$OD = -\log_{10}\left(\frac{I_i}{I_0}\right)$$

where OD is the pixel optical density, I_i is the intensity of the pixel, and I_0 is the average intensity of the white step of the optical density card.

An optical density and organic-liquid saturation calibration curve was obtained for the two sands that contained TCE liquid in the flow cell experiments. A series of 40-ml glass vials were prepared by mixing known volumes of deionized water, organic liquid and sand in a beaker. Then, a quarter of the sand mixture at a time was transferred into the vials and compacted using a glass bar. When the vial was filled, the cap was placed onto the vial and sealed using parafilm. Vials were prepared to represent approximately 50%, 30%, 20% and 10% organic liquid saturation. A vial representing 100% organic liquid saturation was prepared by filling the vial with a known volume of organic liquid. Next, sand was added to the vial and compacted using a glass bar. A 0% organic liquid saturation vial was prepared in a similar fashion, using deionized water instead of organic liquid. Once prepared, the vials were photographed next to an optical density photographic card. The actual organic-liquid saturation for each vial was then determined by solvent extraction using methanol. The extraction efficiency for these relatively ideal media was greater than approximately 95%.

For the flow cell experiments, a series of three high-resolution (pixel size of ~175 um) photographs was taken of the front face of the flow cell at each time of interest. Image sets were collected at several times throughout organic-liquid injection and dissolution. As noted above, each photograph contained the optical density photographic card to convert pixel intensity to optical density. The images were imported into MATLAB and the OD value of each pixel was determined, as described above. An average pixel-by-pixel optical density value for a given time was determined by averaging the optical density of the three images of a given image-time set. The impact of slight variations in lighting across the front of the flow cell was accounted for by normalizing the OD values to a background set of OD values collected prior to TCE injection. High OD values registered near the edge of the image where no organic liquid existed due to reflection of the flow cell frame. These anomalous values were removed from the image.

Variations in the light source among image sets (i.e., from one collection time to another) were corrected by selecting an observation window within the flow cell that was organic-liquid free throughout the course of the experiment. The average OD within this window was monitored over time. To correct the image data, OD values were multiplied by the ratio of the

average OD of the calibration standard with no organic liquid (the reference standard) and the average OD of the observation window for the specific collection time.

The entire image was smoothed by averaging OD over a 5 x 5 pixel area. A threshold value was selected to remove noise due to changes in the lighting or the camera. Organic-liquid saturation was calculated based on the aforementioned organic-liquid saturation versus optical density calibration curve. The volume of organic liquid was calculated by multiplying the organic-liquid saturation by the pixel volume (~7.2 x 10^{-4} cm^3).

4.3 Field-scale Experiments

Field studies were conducted at sites located within the Tucson International Airport Area (TIAA) federal Superfund site (Figure 4.3-1). The TIAA site was placed on the National Priorities List in 1983. Trichloroethene and dichloroethene are the primary groundwater contaminants of concern. The site comprises multiple sources of contamination, three primary groundwater contaminant plumes (southern, central, northern), and several responsible parties are involved in remediation activities. The subsurface is very heterogeneous at the site, with hydraulic conductivities spanning many orders of magnitude. Low-permeability units reside both below and above the regional and surficial aquifers, and data indicate high levels of contamination associated with these units. Large-scale pump-and-treat systems have been in operation for many years for the southern and northern plumes. A pump-and-treat system was started in 2007 for the central plume.

Studies were conducted at the southern and central sites as part of this project. For the southern site, historic operations data for the pump-and-treat system were used to evaluate mass removal and mass discharge behavior (6). In addition the impact of using in-situ chemical oxidation (ISCO) to treat the DNAPL source zones was assessed (5). Contaminant mass discharge tests were conducted before and after ISCO implementation. In addition, monitoring wells were sampled and sediment cores were collected before and after implementation. Details of the methods used for these studies are presented in (5,6).

For the central site, the study involved investigating the impact of source containment on mass removal and mass discharge for the source zone (10), and the response of the contaminant plume (11). The study included high-resolution sampling of sediment cores, periodic sampling of monitoring wells, and monitoring of contaminant mass discharge. Details of the methods used for these studies are presented in (10).

4.4 Mathematical Modeling

Mathematical models and associated relationships based on the use of up-scaled rate coefficients were developed and used in the project to simulate aqueous concentrations as a function of DNAPL dissolution (14). One approach was based on the use of a continuous-distribution representation. Another was based on the use of the multiple-domain representation. Models based on these two approaches were applied to data obtained from the flow-cell experiments, as presented in the “Results” section.

In another study, the efficacy of a simple mass-removal function for characterizing mass-discharge-reduction/mass-removal behavior for organic-liquid contaminated source zones was evaluated using data obtained from the flow-cell experiments (4). A widely used function was employed,

$$1-\frac{CMD_f}{CMD_i}=\left(1-\frac{M_f}{M_i}\right)^n \qquad (4.1)$$

where CMD is contaminant mass discharge [M/T], M is source zone mass [M], n is a fitting parameter, and the subscripts i and f represent initial and final, respectively. Methods to improve the performance of this function, based on the use of system-indicator parameters were investigated, as detailed in the "Results" section.

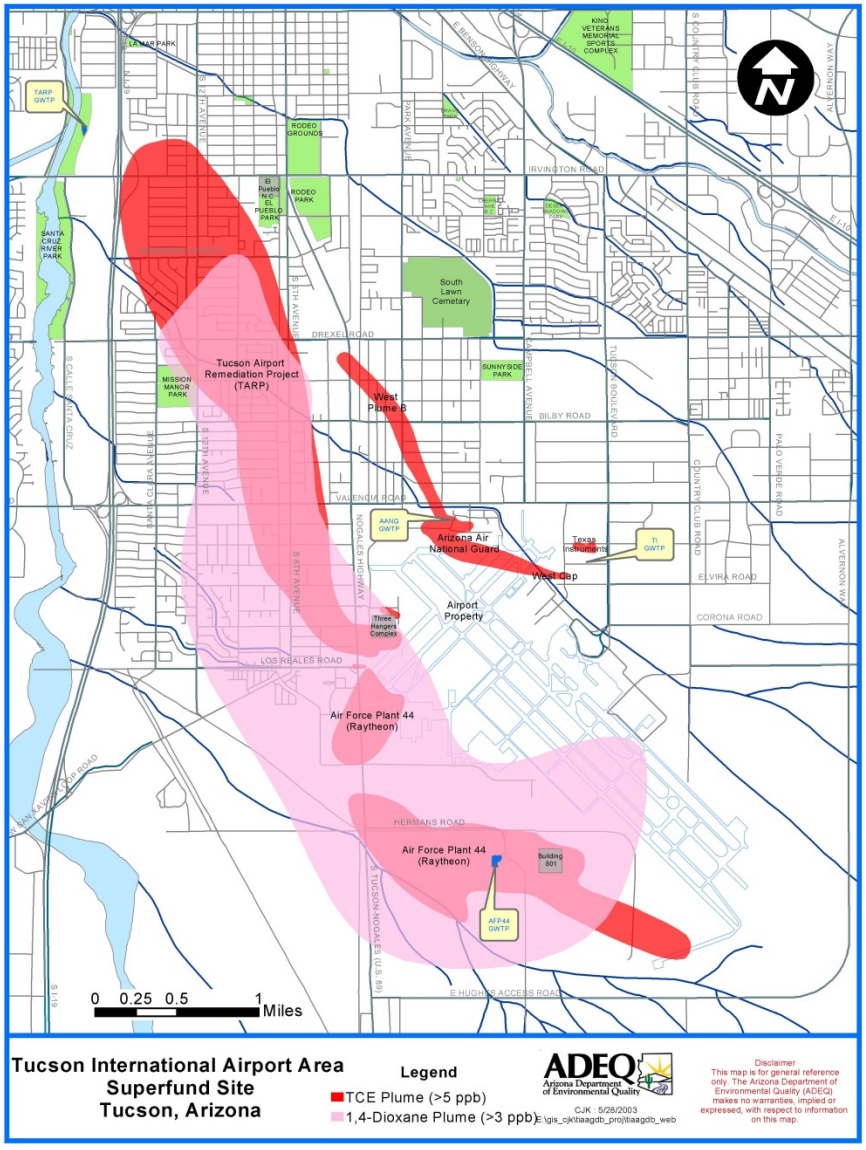

Figure 4.3-1. Map of the field site.

4.5 Analysis of Contaminant Mass Discharge Reduction and Mass Reduction

The relationship between reductions in contaminant mass discharge and reductions in contaminant mass is a key index to system behavior. This index was used to evaluate the data collected for the bench-scale and field-scale studies. The data needed to develop this relationship are temporal measures of contaminant mass discharge and mass reduction, as well as determination of the initial contaminant mass present in the system. The first two are readily obtained by collecting continuous measures of groundwater discharge and associated contaminant concentrations for the system. For the bench-scale systems, initial mass is known. However, it is not known for the field sites. Two methods were used to estimate this quantity for the study conducted at the central plume site (10), as detailed below.

The first method is a slight variation of the standard approach employing sediment-core data. With the standard approach, sediment-phase concentrations of the contaminant obtained for example by solvent extraction of core data are used in conjunction with values for the bulk density and volume of contaminated media to calculate absolute values of contaminant mass. However, uncertainty in bulk densities and especially domain volumes can add to overall method uncertainty. This source of uncertainty can be minimized by using core data collected at two times to determine the relative change in concentrations and mass. This information, combined with the mass-removed quantity determined from integration of the extraction-well CMD data, can be used to estimate an initial mass (M_0) using the relation:

$$M_0 = M_{\Delta t}/\Delta M_f + M_{t-1} \qquad (4.2)$$

where $M_{\Delta t}$ is the quantity of contaminant mass removed in the period between collection of the two sets of cores determined from integration of the CMD data (442 kg), ΔM_f is the fractional mass reduction for the period between collection of the two sets of cores, which was obtained from the core data (0.82), and M_{t-1} is the mass removed prior to collection of the first core set (245 kg), also determined from integration of the CMD data. This latter term accounts for the fact that the first set of cores was obtained a year after the start of the source-control operation. The ΔM_f term was calculated as $1 - \bar{C}_2/\bar{C}_1$, where $\bar{C}_1$ and $\bar{C}_2$ are the mean, aggregate sediment-phase contaminant concentrations obtained from the core data for sets 1 and 2, respectively.

The second method used to estimate the initial contaminant mass present in the saturated zone of the source area is based on fitting a mass-depletion function to the temporal CMD data. In general, a mechanistic-based reactive transport model can be calibrated to historical concentration data to solve the inverse problem for M_0. However, the use of advanced transport models for field sites is typically constrained by a lack of information needed to parameterize the model. In lieu of this approach, simplified mass-depletion functions can be fit to measured data to estimate M_0. For example, simplified functions have been fit to temporal concentration data collected from monitoring wells located within contaminant plumes to provide estimates of source mass (Butcher and Gauthier, 1994; Basu et al., 2009). It is anticipated that CMD data measured directly for the source area via a contaminant mass discharge test will provide a more robust data set for estimation of source mass.

The method is based on a conservation of mass argument for a system undergoing fluid extraction:

$$dM/dt = -Q_t C_t \qquad (4.3)$$

where M is contaminant mass (M), Q is fluid discharge (L^3/T), C (M/L^3) is the concentration of the contaminant in the extracted fluid, and it is assumed that there are no other sources of mass reduction, and that mass discharge into the system is 0. A selected source-depletion function can now be specified to relate changes in concentrations and mass discharge to changes in mass. The power function is one such, widely used, function (e.g., Zhu and Sykes, 2004; Falta et al., 2005):

$$C_t/C_0 = (M_t/M_0)^{\Gamma} \qquad (4.4)$$

where C_0 is initial contaminant concentration and Γ is the power index term, representing the impact of a host of conditions and processes on mass-removal behavior. Substituting equation 4 into 3 yields:

$$dM/dt = -(Q_0C_0/M_0^{\Gamma})M^{\Gamma} \qquad (4.5)$$

Given that the terms in parentheses are constants, one can define $k = Q_0C_0/M_0^{\Gamma}$ as a source depletion rate coefficient, as noted in prior applications (e.g., Zhu and Sykes, 2004; Falta et al., 2005). For the special case wherein $\Gamma = 1$, the equation reduces to a first-order, exponential function, with a solution for CMD given as $QC_t = QC_0\exp(-kt)$. The function was fit to the measured CMD data, optimizing for k. M_o was then calculated with the optimized k and the known value for initial CMD (Q_0C_0).

5.0 Results and Discussion

5.1 Source-zone Dynamics: Mass Removal and Mass Discharge

5.1.1 Impacts of Source-zone Architecture and Age: Bench-scale Results

A total of four experiments were conducted for the first part of the study (Table 5.1.1-1). The Control and Homogeneous experiments both consisted of a homogeneous pack of 40/50 sand. A residual saturation of TCE was emplaced within these two flow cells, the only difference being that TCE was uniformly distributed within the entire system for the former experiment whereas it resided in a subsection of the system for the latter. The Homogeneous-EF experiment was identical in setup to the Homogeneous experiment. The Mixed-Source experiment consisted of a homogeneous pack of 40/50 mesh sand with a 2-cm thick capillary barrier of 70/100 mesh sand along the bottom boundary. This distribution promoted the formation of a zone of higher organic-liquid saturation (e.g., pool) at the material boundary. The Heterogeneous and Heterogeneous-EF experiments consisted of a matrix of 40/50 mesh sand with lenticular lenses of 20/30 mesh and 70/100 mesh sands. Details of the methods and systems are presented in the published paper (3).

The efficacy of the light reflection visualization (LRV) imaging method was tested through comparison of measured and known volumes of organic liquid for experiments conducted with a two-dimensional flow cell. Two sets of experiments were conducted, with source-zone configurations representing two archetypical residual-and-pool architectures. LRV measurements were collected during the injection of organic liquid and during a dissolution phase induced by water flushing. There was a strong correlation between measured and known organic-liquid volumes, with the LRV-measured values generally somewhat lower than the known volumes. Errors were greater for the system wherein organic liquid was present in multiple zones comprised of porous media of different permeabilities, and for conditions of multiphase flow. This method proved effective at determining organic-liquid distribution in a two-phase system using minimal specialized equipment. Details of the results are presented in the published paper (7).

Table 5.1.1-1. Parameters for the initial flow-cell experiments.

Experiment	Q (ml/min)	v (cm/hr)	L (cm)	A (cm^2)	$S_{n,global}$ [a]	$GTP_{initial}$ [b]	$\mu_{Sn,\ initial}$ [c]	$\sigma^2_{Sn,\ initial}$ [c]
Control	0.6	30.1	7	3.5	0.18	Inf	0.18	0
Homogeneous	2.7	9.4	10	48.5	0.01	Inf	6.7×10^{-3}	1.9×10^{-4}
Mixed-Source	3.3	9.1	40	61.8	0.01	1.7	6.6×10^{-3}	1.1×10^{-3}
Heterogeneous	3.3	9.7	40	59.5	0.02	1.2	5.3×10^{-3}	9.3×10^{-4}

[a] $S_{n,\ global}$ is defined as the volume of organic liquid divided by the pore volume of the entire system (source zones plus matrix).

[b] Ganglia-to-pool ratio, defined as the volume of organic liquid occurring as "ganglia" ($S_n \leq$ residual saturation) divided by the volume of organic liquid residing in pools ($S_n >$ residual saturation). Residual saturation thresholds for the 40/50 and 20/30 sand were 0.2 and 0.16, respectively (Dobson et al. 2006).

[c] The mean and variance in organic-liquid distribution was calculated for the entire system.

Contaminant Elution Behavior

The contaminant elution curves obtained from the flow-cell and control experiments are presented in Figure 5.1.1-1. As expected, the initial effluent concentration for the control experiment was equal to the aqueous solubility of TCE and the concentration remained high until almost all of the organic-liquid mass was removed. The effluent concentrations for the other flow-cell experiments were less than aqueous solubility values, as expected, due to dilution effects associated with the system configuration. The effluent concentrations for the Homogeneous experiment initially remained steady and gradually decreased after 14 pore volumes of water flushing. The elution curves for the Mixed-Source and Heterogeneous experiments exhibited relatively extensive periods wherein the concentrations decreased gradually (the first 25 pore volumes for the Mixed-Source experiment and 70 pore volumes for the Heterogeneous experiment), reflecting the impacts of mass-removal constraints associated with system configuration.

For the Mixed-Source experiment, organic-liquid mass associated with the hydraulically-accessible region (i.e., the residual zone within the matrix) was completely removed after approximately 25 pore volumes of water flushing (Figure 5.1.1-2). The mass associated with the less hydraulically-accessible, higher-saturation region above the capillary barrier was the last to be removed. Removal of mass from this region occurred along a dissolution front moving progressively down gradient, similar to results reported in previous studies (e.g. Brusseau et al., 2000; Brusseau et al., 2002; Imhoff et al., 1994). This resulted in steady effluent concentrations for an extended period of flushing from approximately 30 to 100 pore volumes (Figure 5.1.1-1). Additional images of organic-liquid distribution during the experiment are presented in the published paper (3).

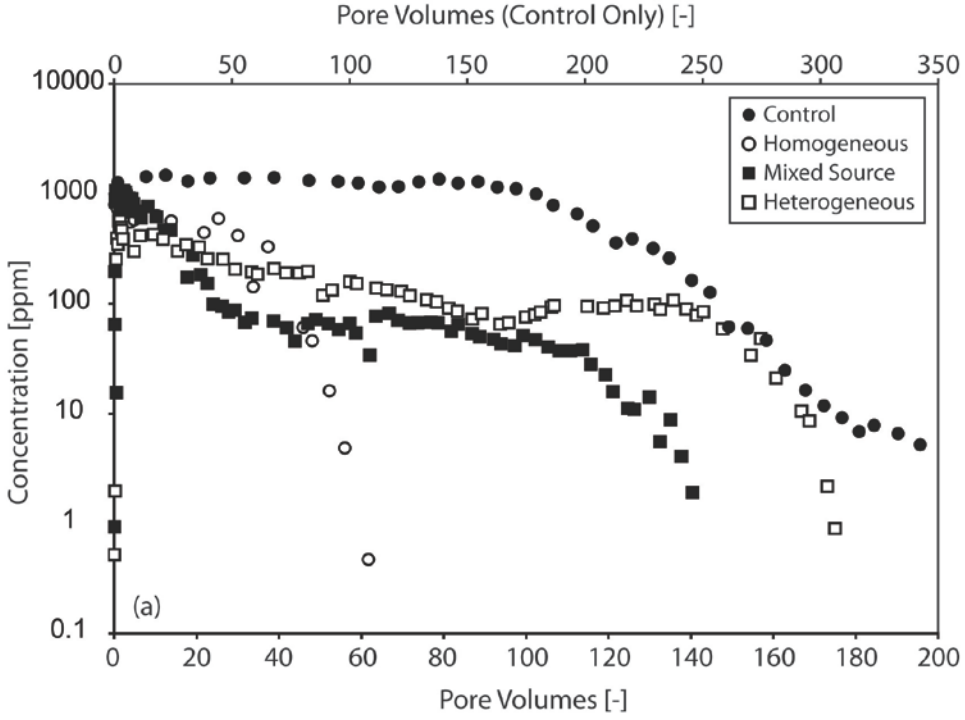

Figure 5.1.1-1. Effluent concentration as a function of the number of pore volumes flushed for the four aqueous flushing experiments.

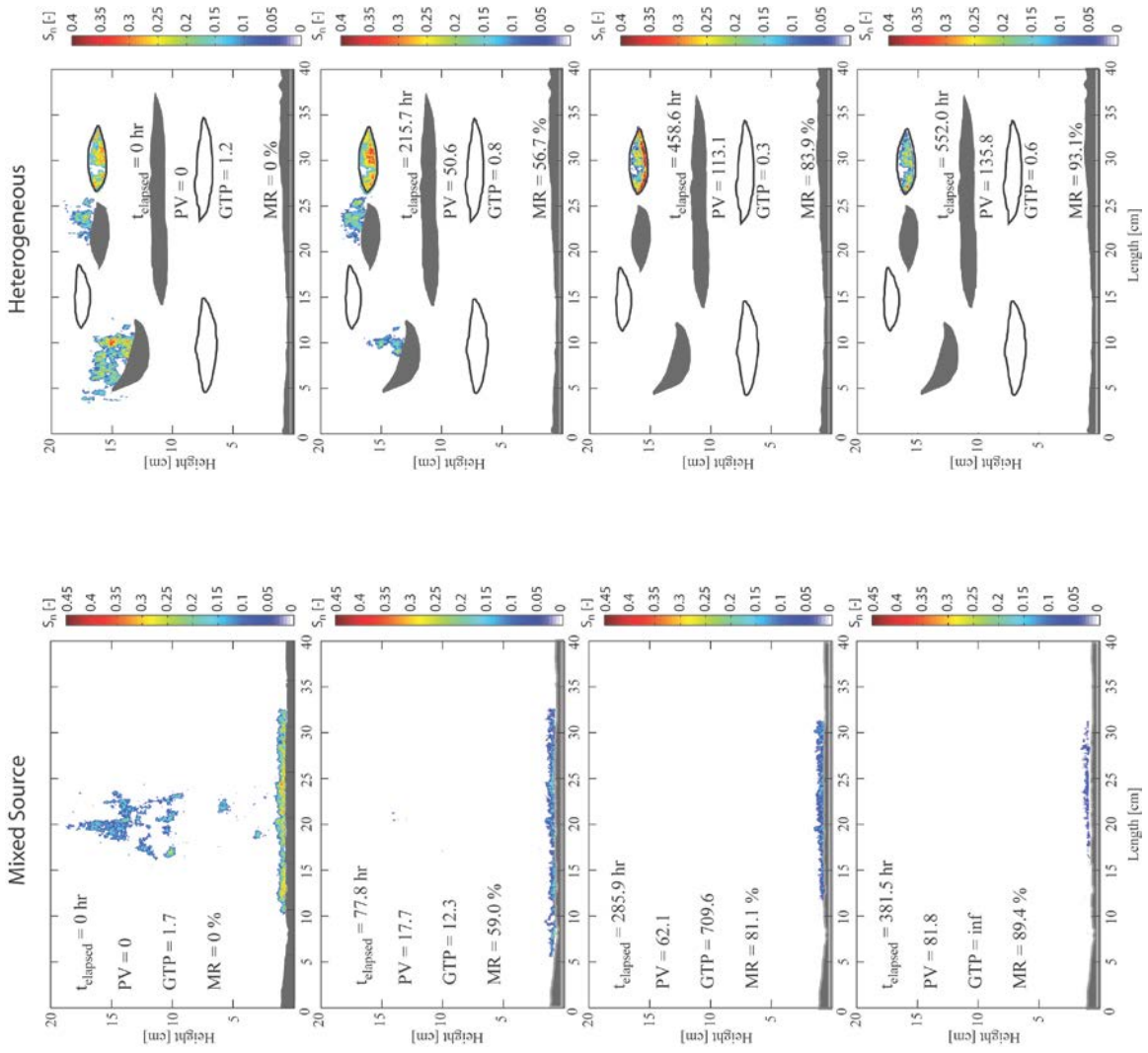

Figure 5.1.1-2. Organic-liquid distribution at four different flushing times for the Mixed-Source and Heterogeneous experiments. Organic-liquid saturation was determined using imaging as described in the text. The matrix of the Mixed-Source experiment was composed of 40/50 sand and the gray zone was composed of 70/100 sand. The matrix of the Heterogeneous experiment was composed of 40/50 sand. The black-outlined zones were composed of 20/30 sand and gray zones were composed of 70/100 sand. The organic-liquid saturation is defined using the color scale, where warm colors indicate high organic-liquid saturation and cool colors represent low saturation. The ganglia-to-pool (GTP) ratio was calculated using the image data with a residual-saturation threshold of 0.20 for the 40/50 sand and 0.16 for the 20/30 sand. The percent mass removed (MR) was calculated based on moment analysis of the elution data. PV is pore volumes of water flushed. The spatial resolution for each image was 0.02 mm^2.

The elution curve for the Heterogeneous experiment also displayed an initial period wherein effluent concentration gradually decreased with flushing (Figure 5.1.1-1). The initial decrease in concentration reflects the preferential removal of organic-liquid mass from the 40/50 matrix (Figure 5.1.1-2). During flushing, the organic-liquid mass in the 20/30 zone remained relatively constant with time until all of the organic-liquid mass was removed from the matrix. The delay in removal of organic liquid from the 20/30 zone was primarily due to the presence of organic-liquid sources located directly upgradient. This behavior is similar to that observed in prior modeling studies (Sale and McWhorter, 2001). After approximately 60 pore volumes of flushing, the organic liquid associated with the 20/30 zone mobilized within this zone. After approximately 94 pore volumes, the concentration eluting from the flow cell increased from 66 mg/L to 95 mg/L and remained constant until only a small portion of the pool remained. This increase resulted from changes in the relative permeability (k_r) associated with flushing of the 20/30 pool zone, and is similar to behavior observed in prior work (Powers et al., 1998; Nambi and Powers, 2000). Additional images of organic-liquid distribution during the experiment are presented in the published paper (3).

Mass-Flux-Reduction/Mass-Removal Behavior

For both the Control and Homogeneous experiments, significant reductions in mass flux did not occur until relatively large fractions of mass (>50%) were removed (Figure 5.1.1-3). Such mass-removal behavior is evident from the contaminant elution curves obtained for the two experiments (Figure 5.1.1-1), wherein concentrations are maintained at or near maximal levels for the majority of flushing. The mass-flux-reduction/mass-removal behavior observed for the Homogeneous experiment was generally similar to that of the Control experiment even though the organic liquid was not uniformly distributed throughout the flow field as it was for the Control. For the control experiment, minimal mass flux reduction occurred until approximately 75% of the mass was removed. For the Homogeneous experiment, reduction in mass flux occurred after removing approximately 50% of the mass, with the earlier reduction due to the shorter length of the source zone in the direction of flow and associated mass-transfer constraints. The general behavior observed for both experiments is expected for systems wherein organic liquid is distributed relatively homogeneously (e.g., occurs only as residual) and is accessible to water flow, illustrating the impact of relatively ideal mass-transfer and displacement on mass flux and mass removal, as observed in prior studies (Fure et al., 2006; Brusseau et al., 2008).

The mass-flux-reduction/mass-removal relationships for both the Mixed-Source and Heterogeneous experiments exhibited nonsingular or multi-step behavior (Figure 5.1.1-3). Such multi-step mass-flux-reduction/mass-removal behavior has been observed in prior flow-cell experiments (Brusseau et al., 2008), selected individual realizations in recent mathematical-modeling studies (Lemke et al., 2004; Phelan et al., 2004; Soga et al., 2004; Lemke and Abriola, 2006), and in measured field data (Brusseau et al., 2007; DiFilippo and Brusseau, 2008). Measurement of the temporal evolution of organic-liquid saturation distribution for the present study allows an analysis of this behavior, which has not been characterized or discussed to a significant extent in prior work. The multi-step behavior comprised two distinct stages. In the first stage, reductions in mass flux were observed after removing less than 2% of the total mass in the flow cell. These early reductions in mass flux reflect the preferential removal of organic liquid residing at lower saturations in hydraulically-accessible regions of the flow cell (Figure 5.1.1-2). The mass flux from the flow cell continued to decrease until all of the highly-accessible

organic liquid mass was removed. The final stage of the mass-flux-reduction/mass-removal relationship reflects the removal of the higher saturation, more poorly-accessible organic-liquid mass.

For the Mixed Source experiment, the removal of organic-liquid mass from the region of high saturation resulted in steady effluent concentrations for many pore volumes of flushing. The steady effluent concentrations resulted in minimal reductions in mass flux until almost all of the organic-liquid mass was removed from the system, which produced the change in slope in the mass-flux-reduction/mass-removal relationship observed after greater than 60^{+}% mass removal. For the Heterogeneous experiment, changes in the relative permeability of the 20/30 zone during dissolution resulted in an increase in effluent concentrations and, consequently, an increase in the mass flux from the flow cell. This increase produced the change in slope observed in the mass-flux-reduction/mass-removal relationship. Following this, there was an extended period during which mass flux remained constant due to steady state effluent concentrations associated with the dissolution of mass within the region of high saturation.

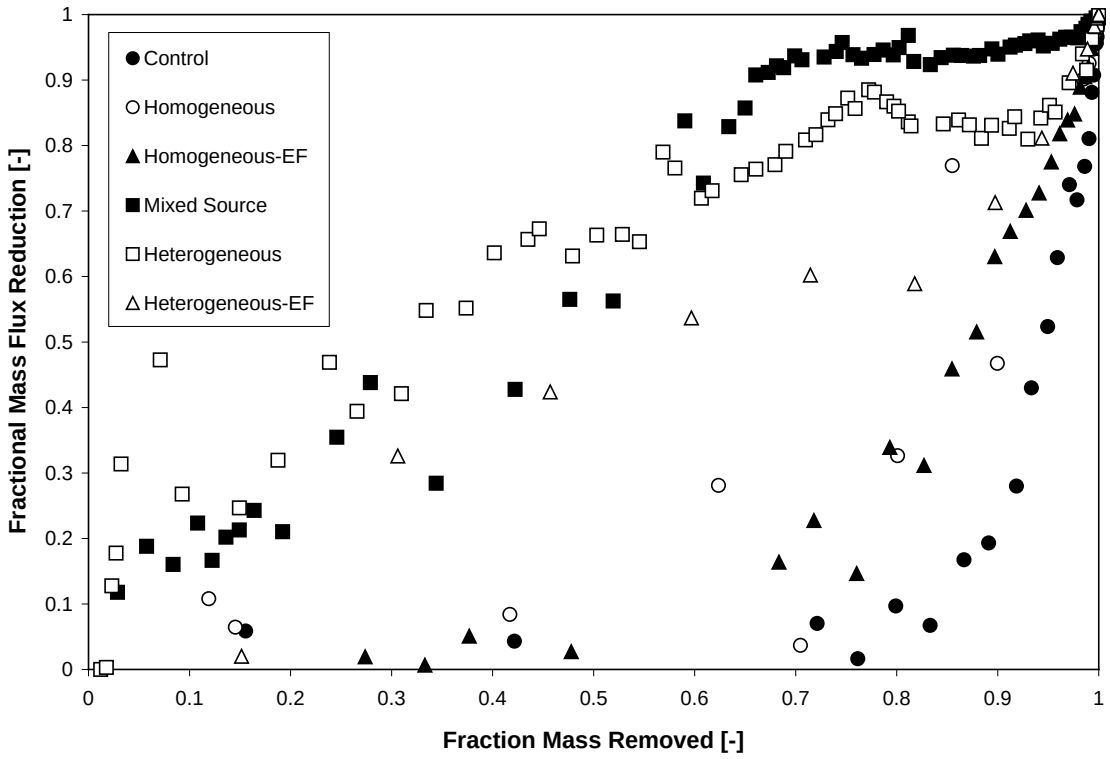

Figure 5.1.1-3. Mass flux reduction versus mass removal behavior for the aqueous flushing and enhanced flushing experiments.

Impact of Source-Zone Age

Sites where organic-liquid contamination has existed for many years will likely have had a portion of the highly accessible source-zone mass removed prior to the initiation of source-zone characterization and remediation. Behavior observed for such systems may differ from that observed for newly contaminated systems such as represented by the flow-cell experiments discussed above. The impact of source-zone age was investigated for the Mixed-Source and Heterogeneous experiments by re-assessing the mass-flux-reduction/mass-removal behavior after the most highly accessible mass was removed. For the Mixed-Source experiment, a new initial condition was established after 29 pore volumes of flushing. This coincides with the complete removal of the highly accessible organic liquid within the center of the flow cell, leaving only the more poorly accessible higher-saturation organic liquid located along the top of the capillary barrier. The new initial condition for the Heterogeneous experiment was established after 106 pore volumes of flushing, corresponding to the complete removal of organic liquid from the 40/50 matrix. The mass-flux-reduction/mass-removal relationships were then recalculated based on these new initial conditions (Figure 5.1.1-4).

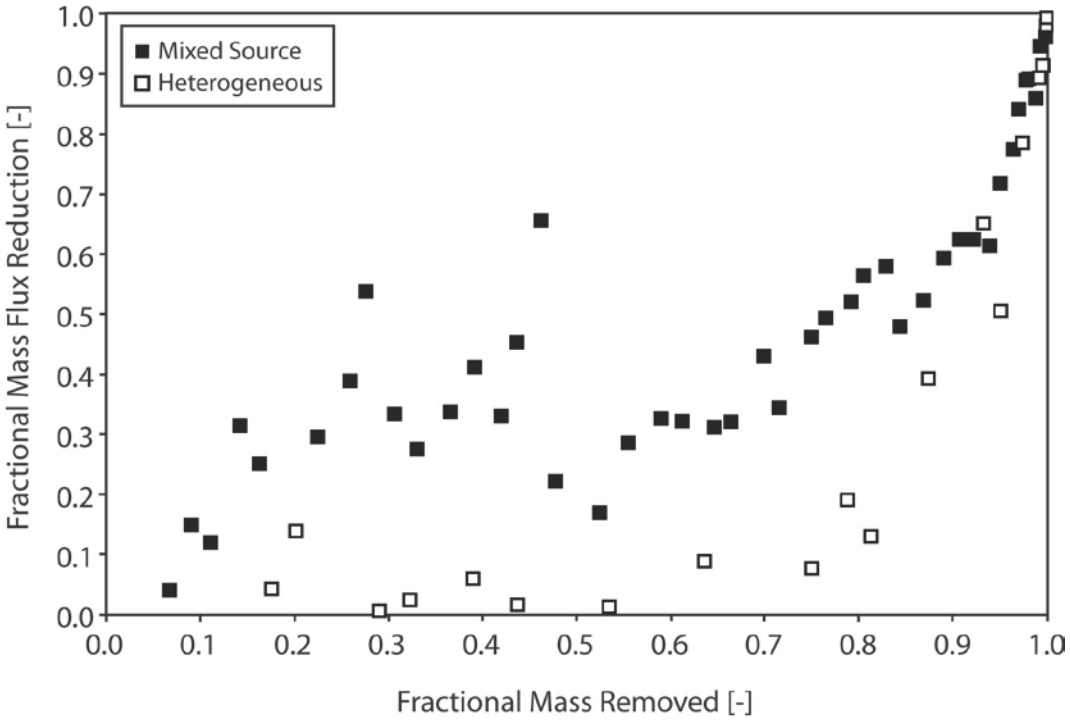

Figure 5.1.1-4. Impact of Source-zone aging on mass flux reduction versus mass removal behavior for the modified Mixed-Source and Heterogeneous experiments (Mixed-Source-2 and Heterogeneous-2, respectively). For the Mixed-Source experiment, a new initial condition was established after 29 pore volumes of flushing. This coincides with the complete removal of the highly accessible residual organic liquid, leaving only the more poorly accessible organic liquid pool located along the top of the capillary barrier. The new initial condition for the Heterogeneous experiment was established after 106 pore volumes of flushing, corresponding to the complete removal of organic liquid mass from the 40/50 matrix.

The mass-flux-reduction/mass-removal behavior for these high-saturation-dominated systems is significantly different from the initial relationships derived for these experiments. The modified Mixed-Source data set (hereafter referred to as Mixed-Source-2) exhibited multi-step behavior, marked by three distinct stages. Although the original Mixed-Source data set also displayed multi-step behavior, the three stages for the Mixed-Source-2 data set occurred significantly earlier in relation to relative mass removal. In the initial stage, reductions in mass flux were observed after removing less than 10% of the mass. This initial reduction in mass flux reflects the preferential removal of the accessible mass along the top boundary of the source zone. Next, there was a period of minimal reduction in mass flux associated with the downgradient progression of the dissolution front through the source zone. In the final stage, there were again large reductions in mass flux associated with the complete removal of the remaining organic-liquid mass from the source zone.

The modified Heterogeneous data set (hereafter referred to as Heterogeneous-2) exhibited minimal reductions in mass flux until nearly all of the source-zone mass was removed. This behavior is in great contrast to that observed for the original data set, and is similar to that observed in a modeling-based study for source zones consisting of only pooled organic liquid (Sale and McWhorter, 2001). Although the mass flux emanating from the systems are significantly different, the mass-flux-reduction/mass-removal behavior exhibited by the Heterogeneous-2 data set is similar to that of the Control experiment (Figure 5.1.1-3). This is related to the fact that both systems have relatively unimodal distributions of organic liquid.

Impact of Organic-Liquid Distribution

Changes in organic-liquid distribution and their impact on observed mass-flux-reduction/mass-removal behavior can be examined by evaluating the ganglia-to-pool (GTP) ratio, which is the ratio of the volume of residual to pooled organic liquid (e.g., Lemke et al., 2004; Parker and Park, 2004; Lemke et al., 2006). This ratio was calculated at various flushing times for the experiments (Figure 5.1.1-5). The Mixed-Source experiment had an initial GTP of 1.7. During flushing, the GTP ratio increased until all of the organic-liquid mass was present at or below residual saturation (GTP = ∞). Therefore, the system became more residual dominated with time as would be expected. The initial GTP ratio for the Heterogeneous experiment was 1.2 and the GTP ratio remained relatively constant until approximately 30% of the total mass was removed from the system. After this, the GTP ratio decreased at a gradually increasing rate until 85% mass removal, indicating that the system became more pool dominated as the hydraulically-accessible organic liquid present at lower saturations was removed. The final portion of the decrease in the GTP ratio corresponded to the late-stage increase in effluent concentration observed in Figure 5.1.1-1, indicating that organic liquid present at lower (residual) saturations in the 20/30 higher-saturation zone was preferentially removed during this time. Eventually, the GTP ratio for this zone increased, indicating a more residual dominated system, as mass removal proceeded to completion.

In prior studies, larger fractions of mass removal were required to induce mass flux reductions for systems with higher GTP ratios, whereas smaller fractions of mass removal were required for systems with moderate to low ratios (Lemke et al., 2004; Phelan et al. 2004; Lemke and Abriola, 2006; Suchomel and Pennell, 2007; Brusseau et al., 2008). The initial GTP ratios for all four experiments are presented in Table 5.1.1-1. In general, our results agree with the prior studies, in that larger fractions of mass removal were required to induce mass flux reductions for experiments with higher initial GTP ratios (Control and Homogeneous) and smaller fractions of

mass removal were required for experiments with lower initial GTP ratios (Mixed-Source and Heterogeneous). In contrast, the Heterogeneous-2 data set had a low initial GTP ratio (0.3) but displayed minimal reduction in mass flux until nearly all of the source-zone mass was removed. This disparity illustrates a limitation associated with use of the GTP ratio for source zones comprising a single-source type in physically heterogeneous systems. The present case of organic liquid occurring at only high saturation (pool dominated system) is one such example. Another case for which use of the GTP ratio is limited is that wherein organic liquid at low saturation resides within lower-permeability zones (residual dominated system), as discussed by Brusseau et al. (2008).

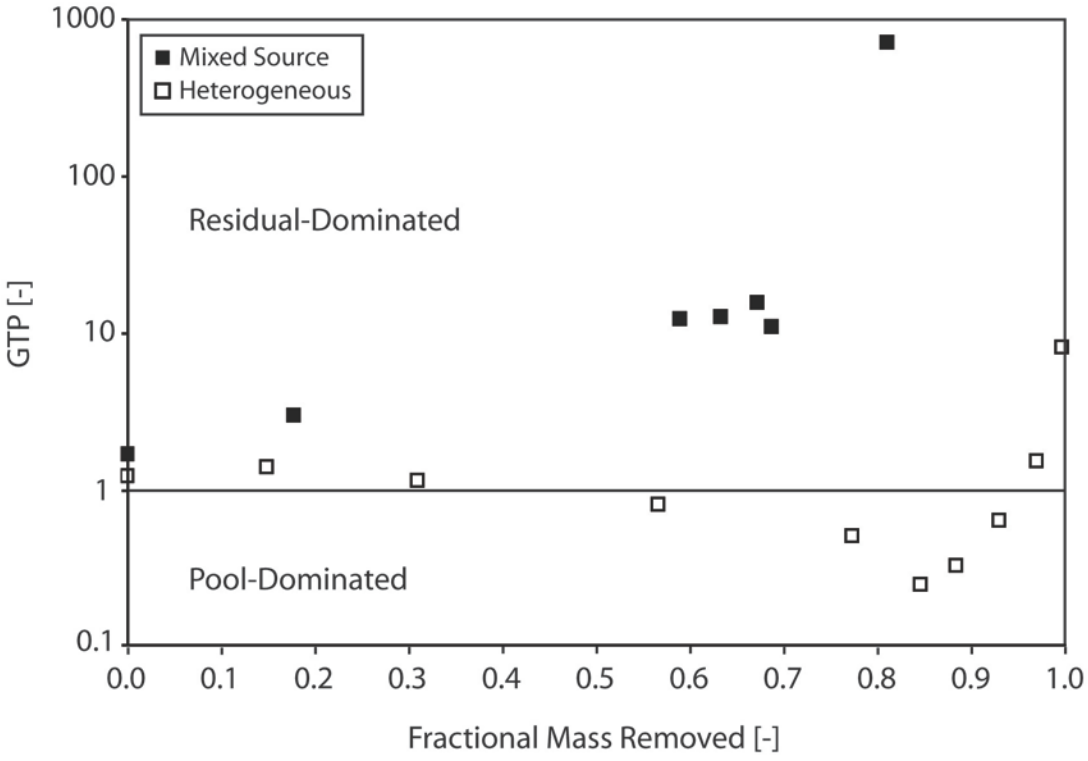

Figure 5.1.1-5. Ganglia-to-pool (GTP) ratio as a function of mass removal for the Mixed-Source and Heterogeneous experiments. The GTP ratio is the ratio of the volume of organic liquid ≤ residual (ganglia) to volume > residual (pool).

Source-zone architecture can also be described using statistical measures of saturation distribution (e.g., Mayer and Miller, 1996; Saenton and Illangsasekare, 2007; Basu et al., 2008). The initial mean (μ) and variance (σ^2) for the spatial distribution of organic-liquid saturation for the entire flow field is presented in Table 5.1.1-1 for each experiment. Reductions in mass flux were observed at earlier stages of mass removal for the systems with larger saturation variance.

Changes in organic-liquid distribution through time were characterized by determining the mean and variance for only the regions with organic-liquid present (i.e., organic-liquid free regions of the flow field were not included) (Figure 5.1.1-6). For the Mixed-Source experiment, the mean organic-liquid saturation decreased once the mass associated with the residual-dominated matrix was removed and remained constant until almost all of the remaining mass was removed from the system. This further illustrates the sequential down-gradient progression of the dissolution front in the region just above the capillary barrier. The variance in saturation remained relatively constant until the majority of mass was removed. For the Heterogeneous experiment, the mean remained relatively constant until only the mass associated with the pool remained, at which time there was a sharp increase in the mean saturation. The variance in saturation distribution displayed similar behavior, indicating that organic-liquid distribution was more uniform in the 40/50 matrix than in the 20/30 zone. The observed results with respect to saturation variance are similar to those obtained from model simulations reported by Basu et al. (2008).

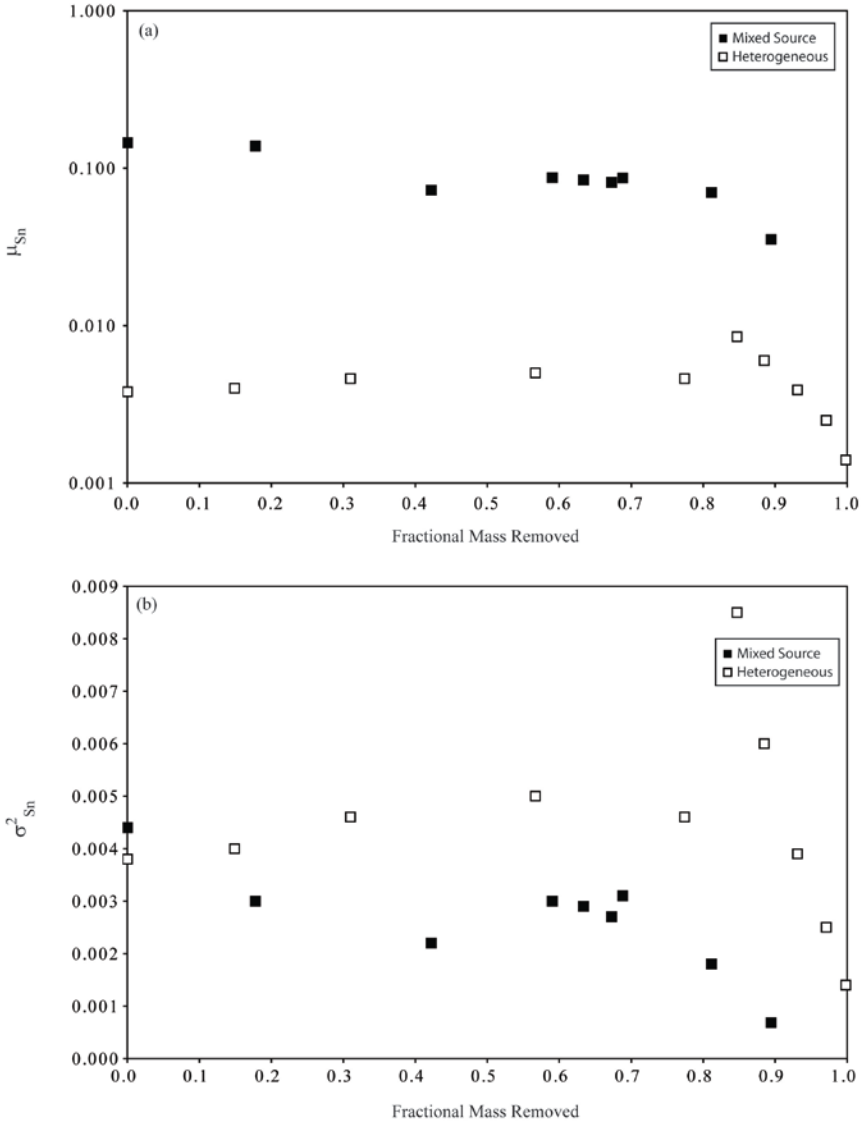

Figure 5.1.1-6. Mean (μ_{Sn}) and variance (σ^2_{Sn}) of organic-liquid saturation distribution for the Mixed-Source and Heterogeneous experiments as a function of mass removal. The mean and variance were calculated for only the regions of the flow cell where organic-liquid was present. (a) Mean, (b) Variance

Impact of Flow-Field Heterogeneity

Changes in flow-field heterogeneity and its associated impact on mass-flux-reduction/mass-removal behavior were examined by evaluating the spatial variance in organic-liquid distribution and hydraulic conductivity at various times during flushing (Figure 5.1.1-7). The variances presented in this figure were calculated for the entire system in order to evaluate the impact of the entire flow field on reductions in mass flux. The calculated hydraulic conductivity for each image set incorporates the impact of organic liquid on relative permeability.

For the Mixed-Source experiment, the variance in hydraulic conductivity decreased linearly as organic liquid was removed from the system (i.e., decrease in the variance in Sn). This is consistent with flow occurring in a physically homogeneous domain and continued removal of the organic liquid resulting in a lessening impact of relative-permeability effects. For the Heterogeneous experiment, the variance in hydraulic conductivity increased non-linearly as mass was removed from the system. This is due to the fact that the presence of regions of high organic-liquid saturation in the 20/30 zone reduced the relative permeability of this zone, and therefore reduced the initial hydraulic-conductivity disparity of the system. However, removal of organic liquid from the 20/30 zone reduced the relative-permeability effect, resulting in an increase in the hydraulic-conductivity disparity (towards the maximum value associated with the intrinsic-permeability differences).

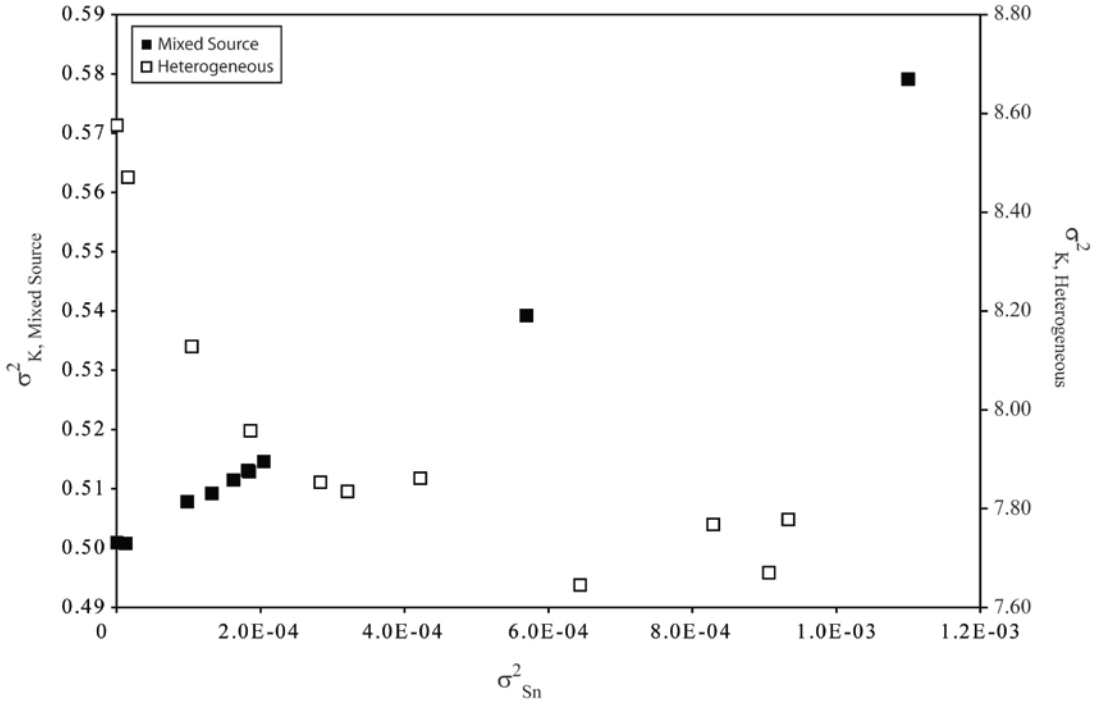

Figure 5.1.1-7. Hydraulic conductivity variance (σ^2_K) for the Mixed-Source and Heterogeneous experiments as a function of the variance in organic-liquid saturation distribution (σ^2_{Sn}). The variance in hydraulic conductivity and organic-liquid saturation were calculated for the entire flow cell, including organic-liquid free regions.

Impact of Flushing Agent

Two experiments were conducted to determine if the multi-step mass-removal/mass-flux-reduction behavior observed under water-flooding conditions may also be observed for enhanced-solubilization conditions. A solution of 2% (wt.) Tween-80 was chosen because it has been shown to significantly enhance TCE dissolution without mobilization (e.g., Suchomel and Pennell, 2006). The mass-removal/mass-flux-reduction behavior for the two enhanced flushing experiments is presented in Figure 5.1.1-3. The observed behavior for the Homogeneous-EF experiment is similar to that observed for the Homogeneous experiment, indicating that mobilization did not occur during the surfactant flushing. The mass-removal/mass-flux-reduction behavior for the Heterogeneous-EF experiment displays similar nonsingular behavior compared to the Heterogeneous experiment, indicating that increased rates of mass removal may not be sufficient to overcome the hydraulic accessibility constraints of the source zone.

Additional experiments were conducted to further examine organic-liquid dissolution, mass removal, and contaminant mass flux reduction under the influence of enhanced flushing solutions (12). Details of the methods and systems are presented in the manuscript (12). The results were similar to those discussed above, in that multi-step behavior was observed (Figure 5.1.1-8). Inspection of Figure 5.1.1-9 shows that the relationship between reductions in mass flux and reductions in mass are similar for the enhanced-solubilization solutions (SDS) and water. This indicates that while the presence of an enhanced-solubility reagent may impact the magnitude and rate of mass removal, it does not appear to significantly alter the inherent mass-removal process.

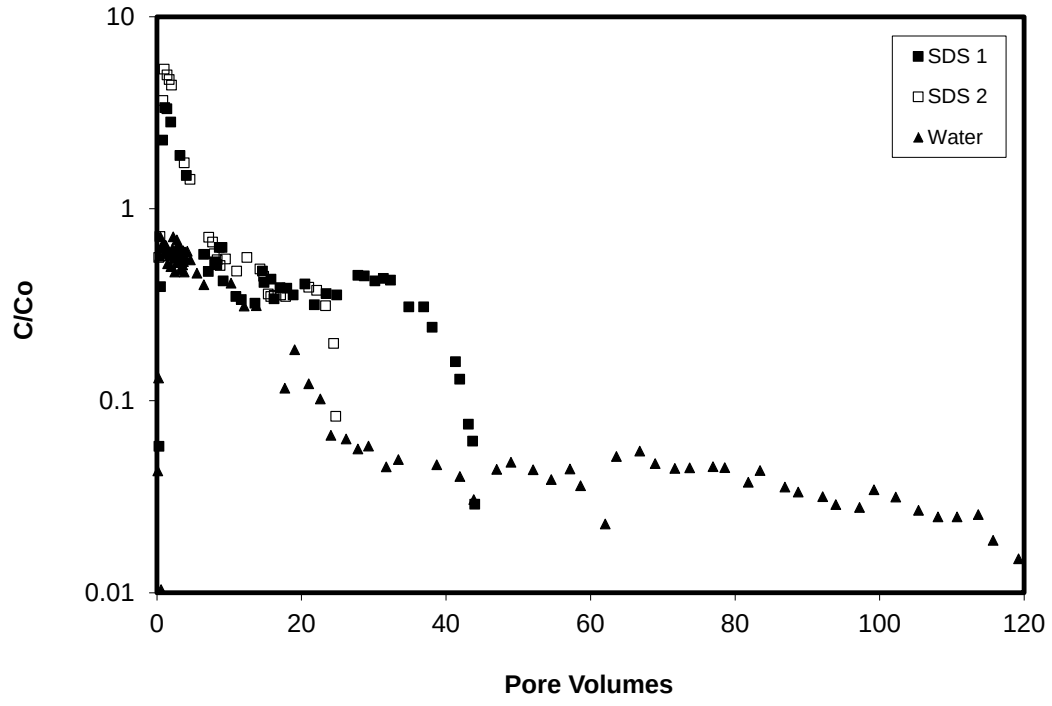

Figure 5.1.1-8. Elution curves for second set of flow-cell experiments; SDS = sodium dodecylsulfate.

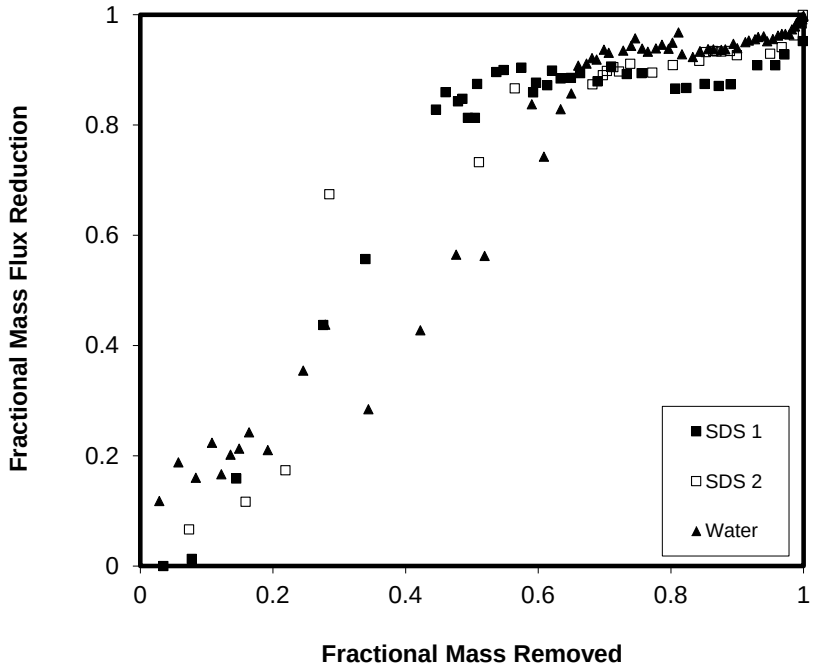

Figure 5.1.1-9. Relationship between reductions in mass flux and mass for data presented in Figure 5.1.1-8.

Measuring contaminant mass discharge at field sites can be done using downgradient "fences" of multilevel sampling devices arrayed in a line normal to groundwater flow, or by conducting induced-gradient contaminant mass discharge tests. The former method is typically employed under natural-gradient conditions, while the latter is under induced-gradient conditions. There has been some question as to the comparability of results obtained with the two methods. This was investigated by conducting two experiments (see publication 12), one with a faster flow rate (equivalent to a pore-water velocity of 3 m/d) and one with a slower flow rate (equivalent to a pore-water velocity of 0.2 m/d). The lower velocity is representative of those observed for natural-gradient flow at field sites.

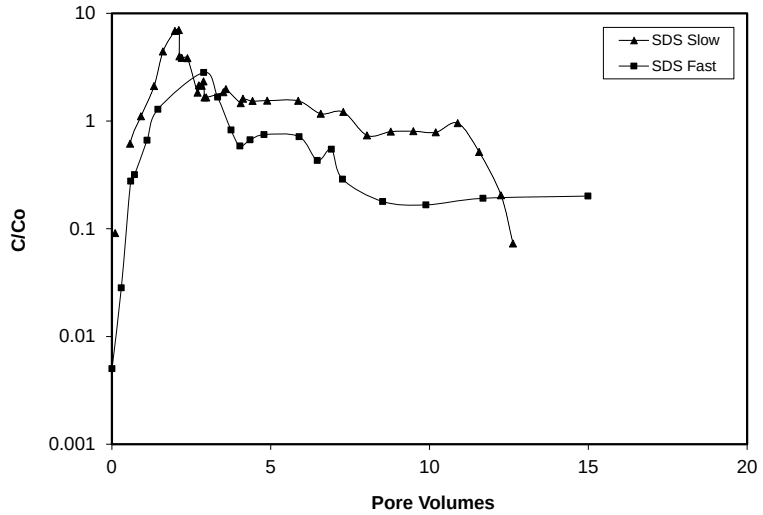

Figure 5.1.1-10. Elution curves for flow-cell experiments conducted to investigate the impact of flow rate; SDS = sodium dodecylsulfate.

The elution curves obtained for the two experiments are similar in shape (see Figure 5.1.1-10). Inspection of Figure 5.1.1-11 shows that the relationship between reductions in mass flux and reductions in mass are also similar for the two experiments. This indicates that while the magnitude and rate of mass removal may be influenced by flow rate, it does not appear to significantly alter the inherent mass-removal process.

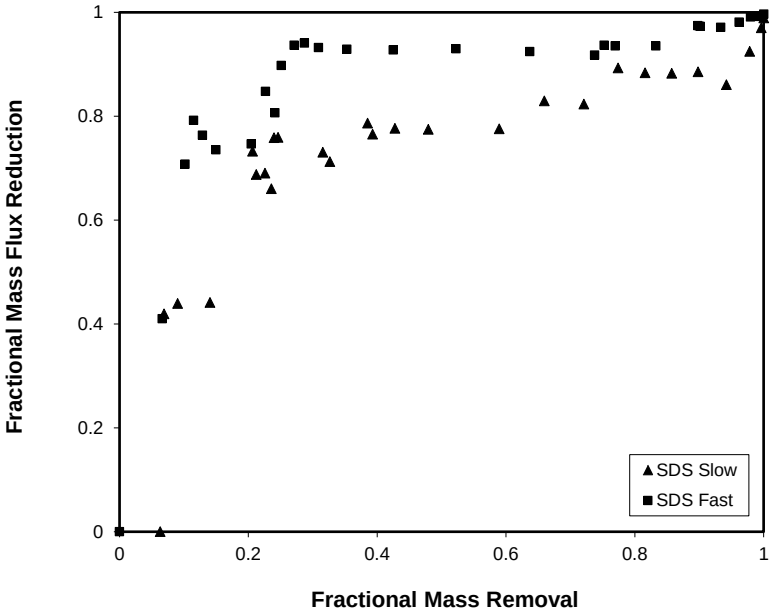

Figure 5.1.1-11. Relationship between reductions in mass flux and mass for data presented in Figure 5.1.1-10.

Summary

A series of flow-cell experiments was conducted to investigate the impact of source-zone architecture and flow-field heterogeneity on the mass-removal/mass-flux-reduction relationship. Our results illustrate the impact of organic-liquid distribution and hydraulic accessibility on mass-flux-reduction/mass-removal behavior. Large fractions of mass removal may be required to induce significant reductions in mass flux for systems with uniform distributions of organic liquid (i.e., all residual or all pool) residing in hydraulically-accessible flow domains. Conversely, significant reductions in mass flux may be induced with relatively minimal mass removal for systems wherein organic liquid is present at both residual and higher saturations. Multi-step behavior was observed for the heterogeneous source-zone systems, and characterization of the organic-liquid saturation distribution throughout flushing allowed identification of the cause of the nonideal behavior. Such behavior will complicate estimation and prediction efforts based on simplified approaches.

5.1.2 Impacts of Source-zone Architecture and Age: Field Results

The site that was the focus of the study is part of the Tucson International Airport Area (TIAA) federal Superfund site in southern Arizona. The study site comprises a local saturated zone, referred to as the shallow groundwater zone, which exists as a persistent feature above the regional aquifer. The site consists of a small source area (approximately 8400 m^2) and a groundwater contaminant plume extending approximately 600 m to the west (Figure 5.1.2-1). Trichloroethene is the primary groundwater contaminant, and aqueous concentrations upwards of

100 mg/L (~10% of solubility) and greater have been reported for samples collected from groundwater monitoring wells within the source area. The source area corresponds to a facility that was used in the past to clean aircraft parts and the external surfaces of military aircraft. TCE vapor degreasers, decarbonizers, and parts-cleaning tanks were located in several small buildings at the site. The activities at the site in conjunction with the high observed aqueous concentrations suggest that liquid TCE is likely present in the subsurface. A technical impracticability waiver was granted by the U.S. EPA for the source area based on the degree of contamination and extensive lower-permeability materials present.

Site Conditions

A simplified schematic of the stratigraphy for the shallow groundwater zone is presented in Figure 5.1.2-2. The subsurface consists of clay and silty clay units with localized and discontinuous intervals/lenses of silt, sand, and gravel. The clay is typically highly plastic, and is comprised primarily of muscovite, illite, and montmorillonite (Matthieu et al., 2012). A prominent feature is a sand and/or gravel unit, termed the gravel sub-unit, of significant areal extent present between approximately 34 and 38 m below land surface (bls). The clay layer below the gravel sub-unit separates the shallow groundwater zone from the regional aquifer. The potentiometric surface for the shallow groundwater zone is approximately 28-29 m bls in the vicinity of the source area, resulting in a saturated zone spanning the interval between approximately 29-37 m bls. The shallow groundwater zone merges with the regional aquifer at the western edge of the site, and thus the leading edge of the shallow-groundwater-zone contaminant plume is indeterminate as it merges into the regional aquifer at this transition zone (CRA, 2010).

A multi-element remediation project was initiated at the shallow groundwater zone site in the fall of 2007. The effort consists of three components: soil vapor extraction for the vadose-zone section of the source area, hydraulic containment for the saturated-zone section of the source area, and pump and treat for the groundwater-contaminant plume. Two extraction wells are used for source control (Figure 5.1.2-1), and currently four extraction wells are operated within the plume. The extraction wells are screened at depth intervals of 35 – 38 m bls, corresponding to the gravel sub-unit. The total extraction rate for the two source-control wells (CRA-5 and DP-1) is currently approximately 75 m^3/d, while the total for the plume wells is approximately 300 m^3/d. Four extraction wells are used for the soil vapor extraction system, which has a total discharge of approximately 20,000 m^3/d. The vapor extraction wells are screened at two depth intervals, approximately 9 - 15 and 18 - 23 m bls. The source-zone groundwater extraction and soil vapor extraction systems have to date removed approximately 690 and >3000 kg of TCE, respectively. The contaminant mass discharge (CMD) associated with operation of the source-control wells has been monitored since system startup. Details of the methods and systems are presented in the published paper (10).

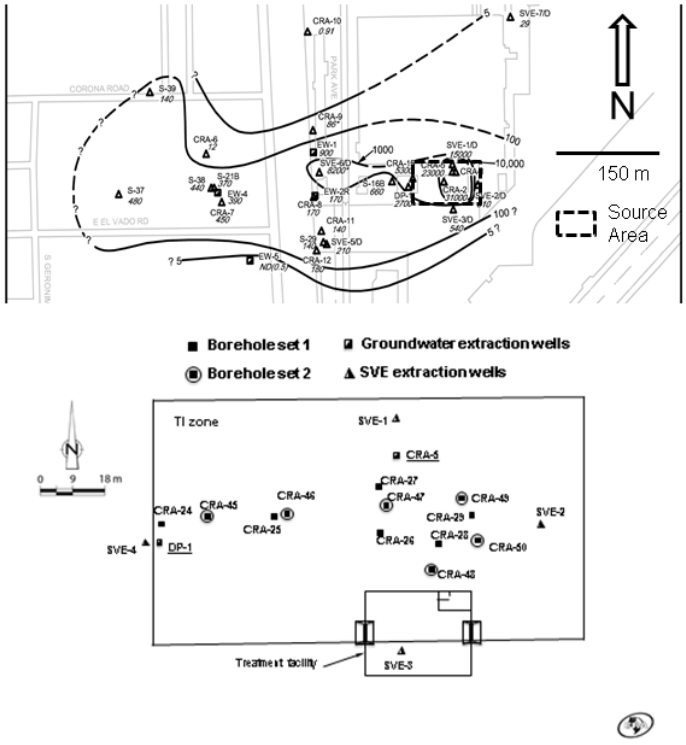

Figure 5.1.2-1. Maps of the field site. The upper figure presents contours of TCE concentrations (µg/L) in the gravel sub-unit for 2007 prior to the start of groundwater extraction; the lower figure is a schematic of well and borehole locations in the source area.

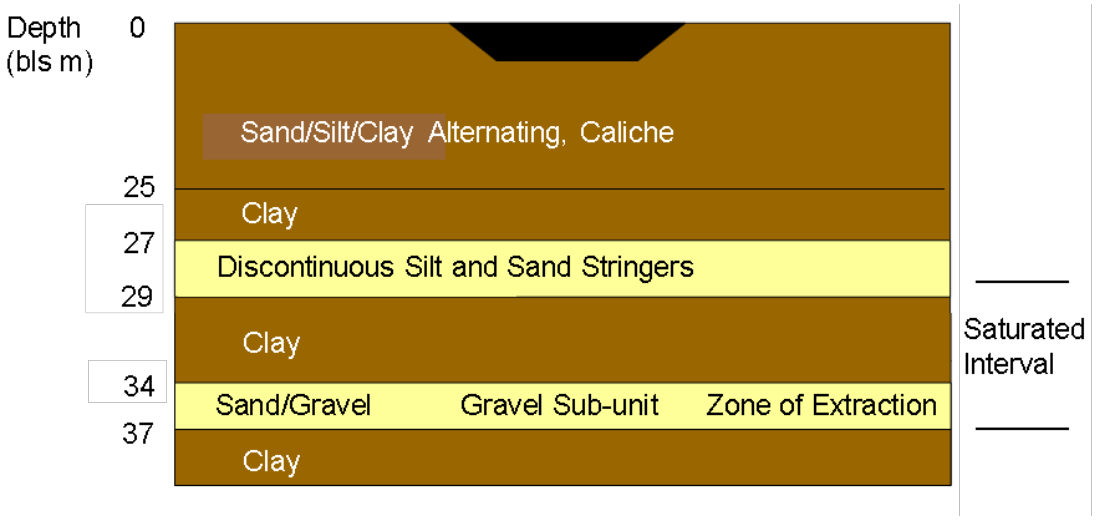

Figure 5.1.2-2. Schematic of local stratigraphy for the site.

Sediment Coring

Two sets of six boreholes were drilled within the source area to collect complete sets of sediment cores from each borehole (see Figure 5.1.2-1). One set of cores (set-1) was collected in the fall of 2008, approximately one year after the start of the remediation effort. The second set of cores (set-2) was collected in the spring of 2012. The cores were obtained using roto-sonic drilling, which is a useful method for collecting continuous cores. The drilling was terminated in each borehole at the base of the gravel sub-unit (37-38 m bls) to avoid penetrating the clay aquitard that overlies the regional aquifer. The cores were analyzed with high spatial resolution (~6-cm intervals in saturated and confining units; lesser resolution for the vadose zone) wherein 10-mL subsamples were collected from the internal central axis of the core with disposable open-tip plastic syringes. The samples were analyzed by GC/MS/MS (gas chromatography tandem mass spectrometry). The detection limit for sediment-phase concentrations of TCE was approximately 0.03 mg/kg-dry sediment.

Textural evaluation of the core material collected from the source area confirmed the stratigraphic model presented in Figure 5.1.2-2. The results of the laboratory hydraulic-conductivity measurements were consistent with the results of the field tests, wherein values for subsamples of the gravel-sub-unit were 2-3 orders-of-magnitude greater than those measured for the clay subsamples. The organic-carbon contents for the subsamples ranged from 0.02 to 0.08%.

The concentrations of TCE were measured for sediment samples collected from the boreholes drilled in 2008 (set 1) and 2012 (set 2). Approximately 1400 total samples were collected for each set. Illustrative results are presented in Figure 5.1.2-3 for the two most contaminated and two least contaminated cores for each set.

The highest concentrations for the set-1 cores were obtained for core CRA-26 (Figure 5.1.2-3a), ranging up to almost 20 mg/kg and with a mean of 2 mg/kg for the interval 28-38 m bls. These concentrations may be somewhat low for samples associated with suspected DNAPL presence (e.g., Feenstra et al., 1991). However, it must be noted that this first set of samples was collected more than a year after startup of groundwater extraction, and that 245 kg of TCE was extracted from the source area prior to core collection. For all 6 set-1 cores, the highest concentrations were associated with the interval between 25 to 30 m bls. This interval corresponds to the lower-permeability silty clay layer in which the interface between the vadose zone and saturated zone resides (Figure 5.1.2-2). Some of the cores had another smaller peak at the interval 33-35 bls, which corresponds to the bottom of the clay layer above the gravel sub-unit. The lowest concentrations for the two sets are presented in Figure 5.1.2-3b.

The mean concentration for all 6 set-1 cores was approximately 0.9 mg/kg for the interval 28-38 m bls. The TCE concentrations for the set-2 cores were significantly lower, with a mean of 0.14 mg/kg for the interval 28-38 m bls. The set-2 cores had approximately 4 times as many non-detects as did set 1 (45% vs. 12%). Comparison of the two sets of data suggests that a significant, ~80%, reduction in aggregate TCE concentrations occurred between sediment-sampling events for the 28-38 m interval. This value was calculated using the 0.03 mg/kg detection limit as a conservative estimate to quantify values for samples for which non-detects were reported. This apparent reduction would be the result of mass removal via water flushing, with a possible contribution from soil vapor extraction for the uppermost section of the interval.

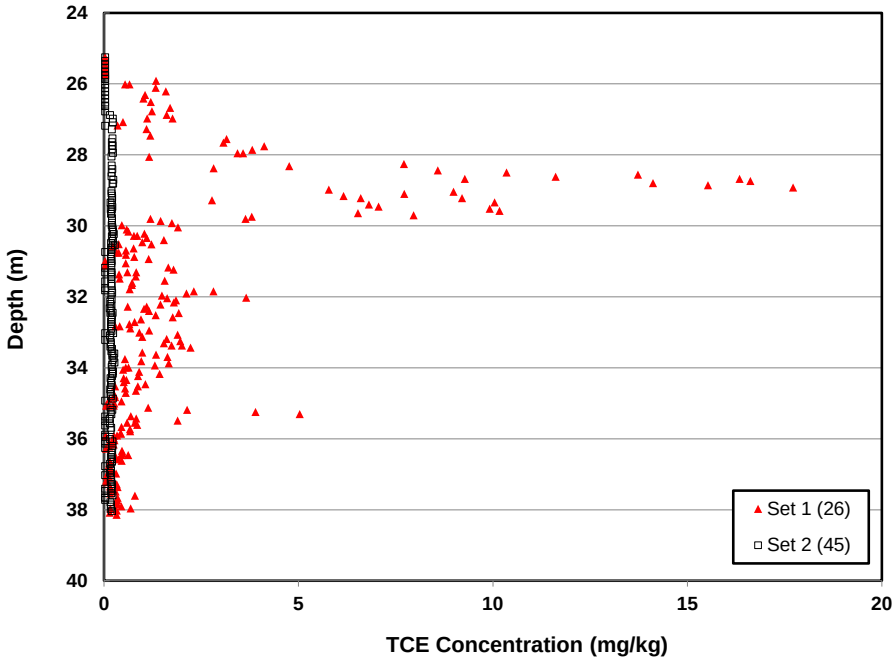

Figure 5.1.2-3a. Sediment-phase trichloroethene (TCE) concentrations for core samples from the most contaminated cores for each set collected in 2008 (set 1) and 2012 (set 2); see Figure 5.1.2-1 for key to locations. Specific borehole numbers (minus CRA prefix) are noted in parentheses. Note that the paired cores are not co-located.

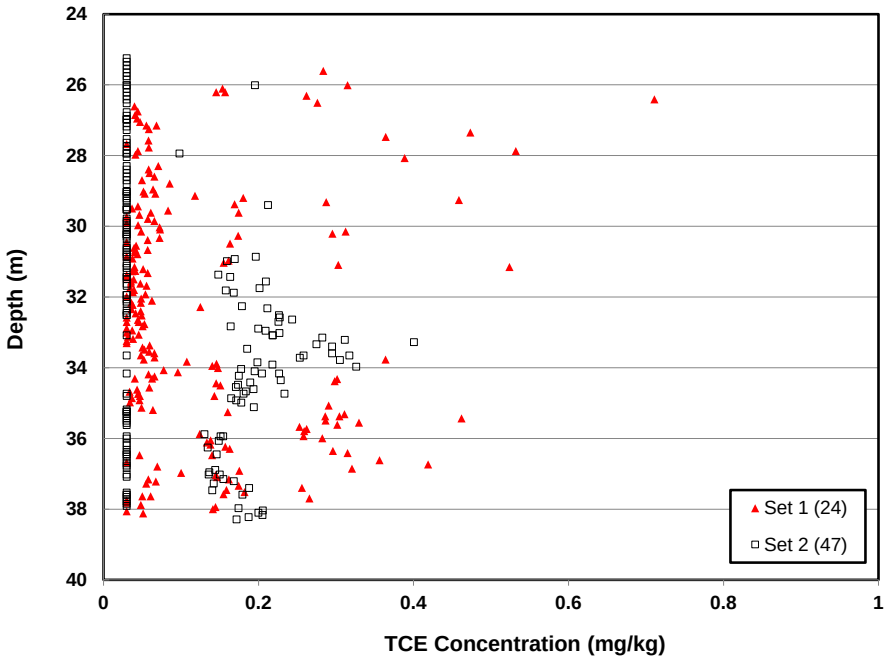

Figure 5.1.2-3b. Sediment-phase trichloroethene (TCE) concentrations for core samples from the least contaminated cores for each set collected in 2008 (set 1) and 2012 (set 2).

Contaminant Concentrations and Mass Discharge

The concentrations of TCE in the groundwater pumped from the two source-area extraction wells are presented in Figure 5.1.2-4. After an initial peak, the concentrations declined relatively rapidly for some time, and currently exhibit asymptotic tailing. The peak and asymptotic concentrations are 30 and 2 mg/L, respectively, for well CRA-5 and 8 and 1 mg/L, respectively, for well DP-1. These concentrations are quite high considering that they are associated with extraction wells as opposed to monitoring wells. As noted above, concentrations of 100 mg/L and higher have been observed for samples collected from monitoring wells in the source area. These high concentrations, and the quantity of TCE removed with soil vapor extraction, are consistent with the presence of liquid TCE (DNAPL) in the subsurface.

The flow rates for the source extraction wells are also presented in Figure 5.1.2-4. The extraction rate has remained relatively constant for DP-1, with a factor-of-two decrease in later years, and has increased over time for CRA-5. Operation of the source-control wells has established containment of the source area, which has resulted in its isolation from the contaminant plume. This, in combination with the operation of the plume extraction wells, is expected to minimize the impact of the plume on mass discharge measured with the source-control wells. A hydraulic residence time of ~1 year is estimated for the source area based on the extraction rates and the estimated domain volume and porosity. Thus, it is estimated that the total groundwater extraction to date equates to approximately 4 pore volumes of flushing.

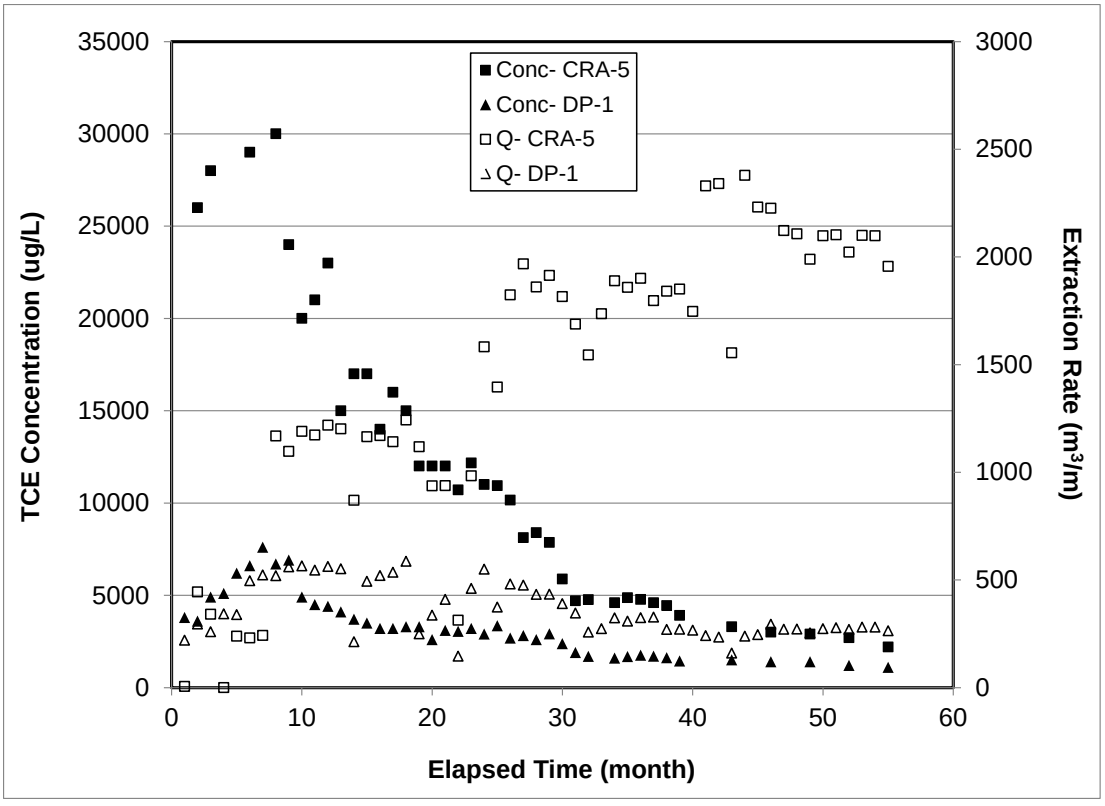

Figure 5.1.2-4. Concentrations of trichloroethene (TCE) in groundwater extracted with the two source-area extraction wells and associated flow rates. Zero time corresponds to system startup in fall 2007.

The contaminant mass discharge associated with operation of the source-control wells is presented in Figure 5.1.2-5. The initial peak values averaged approximately 1 kg/d. These are at the very high end of the range of values reported in a recent survey of mass-discharge field data (ITRC, 2010). More than 90% of the total mass discharge is associated with well CRA-5, which is expected given that it is located near the center of the source, whereas well DP-1 is located near the downgradient edge. The total contaminant mass discharge has declined asymptotically to a current value of approximately 0.15 kg/d. The total mass of TCE removed from the source area via groundwater extraction as of spring 2012 is 687 kg based on integration of the data presented in Figure 5.1.2-4.

The total contaminant mass discharge has decreased significantly, approximately 85%, since the initiation of groundwater extraction. This decrease is a direct function of the reduction in TCE concentrations observed for the extraction wells, given that the total extraction flow rate has actually increased over the course of operations. The decrease in TCE concentrations may be a result of reductions in contaminant mass, changes in hydraulic conditions, or some combination thereof. As noted above, a significant reduction in aggregate sediment-phase concentration of TCE was observed for the core data. This observation, in conjunction with the large quantity of TCE removed via groundwater extraction indicates that there was a significant reduction in contaminant mass for the system. Regarding potential hydraulic effects, the extraction wells have been operated consistently since startup, with no individual well cycling, etc. However, the extraction rate for CRA-5 has increased with time, and it is possible that effects associated with the increased flow rate (dilution due to expanded zone of influence, increased mass-transfer constraints) may have contributed to the decrease in TCE concentration.

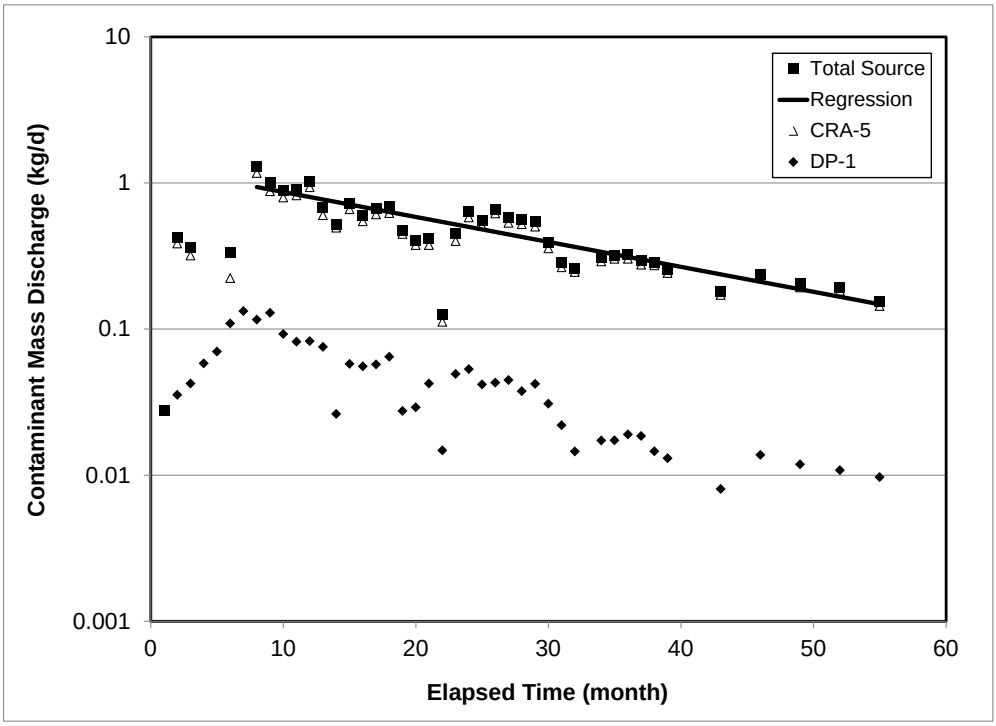

Figure 5.1.2-5. Contaminant mass discharge for the source area. Zero time corresponds to system startup in fall 2007. The regression represents a fit of the exponential-depletion function to total CMD ($r^2 = 0.86$).

Inspection of Figure 5.1.2-4 shows that after initial startup there were three periods wherein extraction rates for CRA-5 were essentially uniform, the first from months 8-23, the second from months 24-40, and the third from month 40 to current. Inspection of Figures 5.1.2-4 and 5.1.2-5 shows that TCE concentration and contaminant mass discharge decreased during each of these many-month-long periods of steady state extraction. The decreases in TCE concentrations observed during these periods would be primarily induced by reductions in contaminant mass. In addition, the contaminant mass discharge has decreased by approximately 90% for DP-1, whereas the extraction rate for DP-1 has decreased by a factor of two (as opposed to the increase registered for CRA-5). In summary, the results indicate that the observed reduction in contaminant mass discharge is associated primarily with a reduction in contaminant mass.

Estimation of Initial Contaminant Mass

The contaminant mass discharge for the source-area hydraulic-control system is known with a relatively high degree of certainty, based on the resolution of data collection. The total quantity of contaminant mass removed via groundwater extraction for the two source-area control wells is also known with relatively high certainty as it reflects the same data set. What is not known is the mass of contaminant present in the saturated zone of the source area at the start of remediation operations, which is typical for most sites. Two methods were used to estimate this initial source mass.

Based on the core data and the mass-removed quantity determined from the extraction-well CMD data, the initial TCE mass was estimated to be 784 kg using method 1. The total fraction of mass reduction to date based on this estimated initial mass is ~86%. The estimated initial mass is recognized to have potential significant uncertainty, the degree of which depends on the representativeness of the core data for the entire source area. For example, it is possible that the coring missed zones of higher contaminant concentrations; the impact of this is likely to be more significant for the initial coring given the higher aggregate concentrations present. Another potential source of uncertainty is the possibility that the soil vapor extraction system may have contributed to removal of mass for the interval of interest. Thus, it is anticipated that the estimation method is more likely to produce an under-estimate rather than over-estimate of initial mass. Assuming an arbitrary 25% error for illustrative purposes produces an estimate of approximately 1000 kg for the initial mass, which translates to a total to-date fractional mass reduction of ~70%.

Inspection of Figure 5.1.2-5 shows that the exponential depletion function provides a good fit to the CMD data. An optimized value of 0.47 yr^{-1} was obtained for k. Using this value, and an initial CMD of 1.28 kg/d, produces an estimate of 993 kg for M_0. The total fraction of mass reduction to date based on this estimated initial mass is 69%. Uncertainty in the estimated value would depend upon the representativeness of the CMD data for the entire target zone, and the robustness with which the fitted function describes the measured data throughout the mass-depletion history. The zones of influence of the extraction wells span the entire source area, and thus the measured CMD data is considered to be representative. Considering this and the fact that the function provides a good fit to approximately 4 years of CMD data, it is likely that the estimated M_0 is relatively robust. Interestingly, the value obtained based upon the core data is approximately 20% lower than the value obtained by fitting the CMD data. This is consistent with the discussion above regarding potential underestimation using the core data.

The methods discussed above were used to estimate the mass of TCE present in the saturated zone of the source area at the start of remediation. Also of interest is the mass of TCE initially present in the saturated zone of the source prior to development of the groundwater contaminant plume, i.e., the mass of TCE that initially entered the saturated zone. Determining this quantity requires estimates of the mass associated with the plume in addition to the source. The plume-associated mass was estimated in part as the sum of the mass of TCE present in the plume at the end of the project and the mass of TCE that has been removed from the plume via groundwater extraction during the project, which totals approximately 170 kg. In addition, the mass of TCE lost to the regional aquifer at the western, leading edge of the plume was estimated using an average hydraulic gradient of 0.0075, a mean hydraulic conductivity (K) of ~8.6 m/d, a mean C of 0.1 mg/L, and the estimated cross-sectional area, producing a CMD of ~0.02 kg/d. Applying this natural-gradient CMD for an elapsed time of 60 years results in a mass of ~390 kg.

Adding the two plume-associated masses to the initial source mass (M_0) estimated above produces 1342 and 1539 kg for methods 1 and 2, respectively. Based on these values, it is estimated that approximately one-third of the TCE mass that initially entered the saturated zone of the source area had been removed (generating the observed contaminant plume) prior to the start of the source-control effort. Using the K and gradient values noted above, and the dimensions of the source area, it is estimated that the equivalent of approximately 40 pore volumes of water had been flushed through the source area prior to the start of remediation. A removal of one-third of the initial mass is reasonable given this estimated magnitude of flushing. The total initial spill masses estimated for the saturated-zone source area are less than one-half of the contaminant mass (>3000 kg) that has been removed to date from the vadose zone via soil vapor extraction. This is reasonable given the surface-application mode of disposal of the waste materials.

Relationship Between Reductions in Contaminant Mass Discharge and Contaminant Mass

The relationship between the measured reduction in contaminant mass discharge and the estimated reduction in contaminant mass for the source area was determined using the CMD data and M_0 values discussed above, where $CMDR = 1\text{-}CMD_t/CMD_0$ and $MR = 1\text{-}M_t/M_0$. The data associated with the initial few months of operation were not used in the calculations given that the system had not attained quasi-steady-state, as reflected in the initial rise in CMD (Figure 5.1.2-5). The contaminant mass removed during this initial stage (~95 kg) was subtracted from the tabulation of initial mass and mass reduction. Two curves are presented in Figure 5.1.2-6, one for each of the two M_0 estimates reported above. A line representing one-to-one correspondence is included for reference.

The mass discharge is observed to decrease essentially immediately upon initiation of mass reduction. The data exhibit a curvilinear convex-upward profile that resides above the one-to-one reference line. A few prior CMDR-MR profiles have been reported based on laboratory experiments and mathematical modeling (e.g., Rao et al., 2002; Jayanti and Pope, 2004; Phelan et al., 2004; Jawitz et al., 2005; Fure et al., 2006; Brusseau et al., 2008; Kaye et al., 2008; Maji and Sudicky, 2008; Carroll and Brusseau, 2009; Christ et al., 2009, 2010; Tick and Rincon, 2009; DiFilippo et al., 2010; Marble et al., 2010). The results span a wide range of behavior, from convex-downward curves residing below the reference line (for which there is relatively small reduction in CMD during the early stages of mass reduction), to approximately one-to-one profiles, to convex-upward profiles similar to those observed herein.

The convex-upward profile is generally associated with systems wherein significant quantities of mass are present in hydraulically poorly accessible domains, for which mass removal is influenced by mass-transfer constraints. It is reasonable to expect that a large fraction of the contaminant mass present at the study site at the start of the project would be poorly accessible, given the presence of extensive silt and clay layers and the fact that ~60 years of natural-gradient groundwater flushing most likely removed a major portion of the more accessible mass. The data obtained from the sediment cores, which showed that the highest TCE concentrations were associated with lower-permeability units, supports this contention.

The CMDR-MR relationship is often simulated using a simple power function, wherein $CMDR = MR^n$ (e.g., Rao et al., 2002). The parameter *n* defines the specific CMDR-MR relationship, and is a lumped-process term that incorporates the impact of contaminant distribution, flow-field dynamics, and mass-transfer processes. The curves obtained with this function, with n = 0.55 and 0.4, match the measured data relatively well (Figure 5.1.2-6).

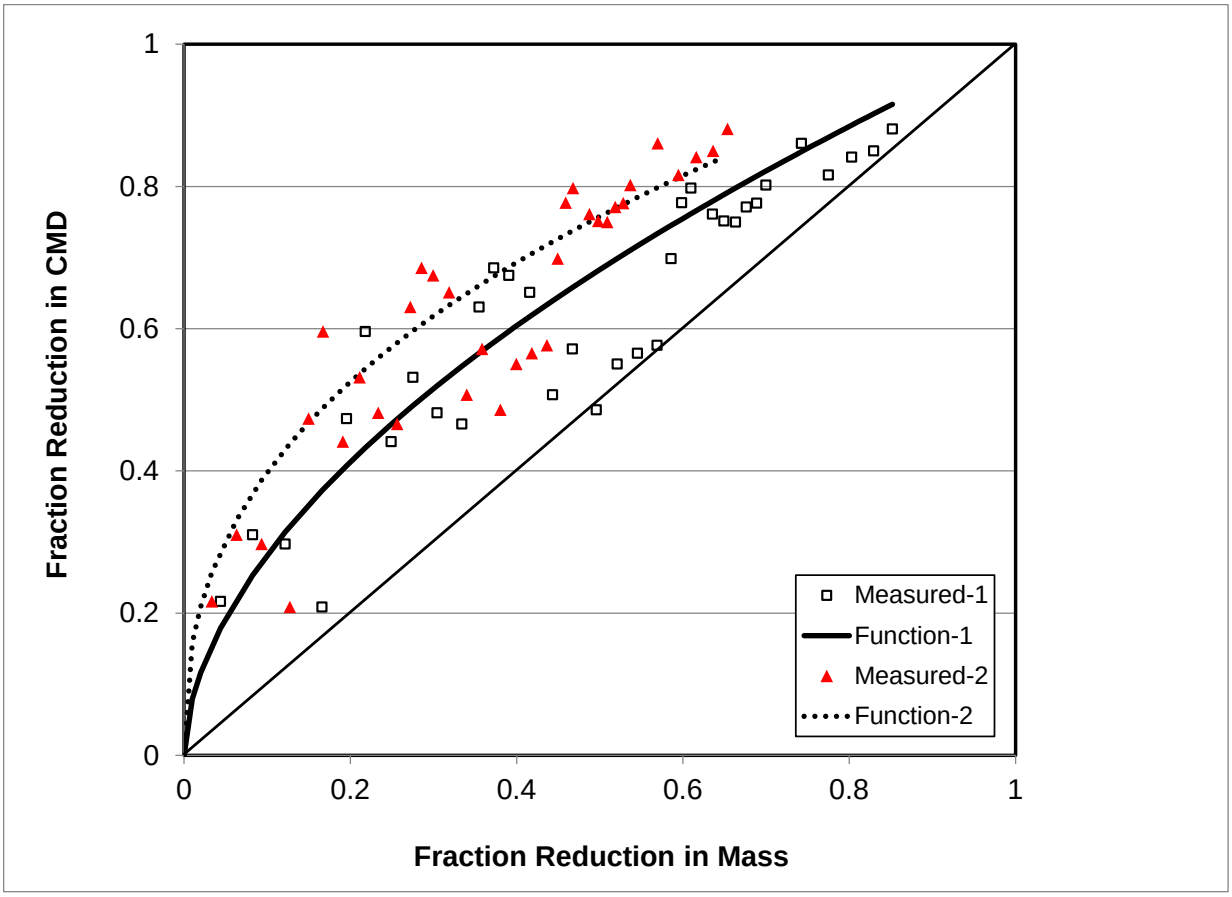

Figure 5.1.2-6. Relationship between the reduction in contaminant mass discharge (CMD) and the reduction in contaminant mass for the source area. Methods 1 and 2 refer to the two methods used to estimate initial contaminant mass (see text). Also shown are fitted simulations produced with a simple function $CMDR = MR^n$.

Comparison to Other Field Data

Very few measurements of time-continuous profiles of contaminant mass discharge have been reported to date for field systems. The lack of such measurements, in combination with the typical uncertainty regarding initial contaminant mass for most sites, limits the opportunities for time-continuous-based characterization of the CMDR-MR relationship for field systems. Initial time-continuous-based characterizations of CMDR-MR relationships for field sites were reported by Brusseau et al. (2007) and DiFilippo and Brusseau (2008). Brusseau et al. (2007) determined the integrated CMDR-MR relationship associated with combined pump and treat of the sources and groundwater contaminant plume for the south section of the TIAA complex. DiFilippo and Brusseau (2008) determined the CMDR-MR relationships for emplaced-source experiments conducted at the Borden site in Canada, using raw concentration and flow-rate data reported by Broholm et al. (1999) and Rivett and Feenstra (2005). For these experiments, known quantities of three-component chlorinated-solvent liquids were introduced into the subsurface, after which mass removal under natural-gradient groundwater (Rivett and Feenstra (2005) or sequential groundwater and cosolvent (Broholm et al., 1999) floods was monitored in detail. In addition, DiFilippo and Brusseau (2008) compared the behavior observed for the Borden data to that of the south-TIAA site, including the integrated source and plume data as well as data for a single source area.

The data obtained for the current study are compared to the data reported for the single source area of the south-TIAA site (Site 3) and the Borden experiments in Figure 5.1.2-7. Distinctly different CMDR-MR relationships are observed for the various sites. For example, relatively small reductions in contaminant mass discharge are observed up to approximately 40% mass reduction for the Borden data, in contrast to the essentially immediate reduction observed for the present study. The profile for the south-TIAA site is intermediate to the other two. Differences in the nature of the MDR-MR relationships observed for the different sites are most likely manifestations of differences in system properties and conditions, such as permeability distribution, contaminant distribution, and mass-transfer processes. It is possible that differences in experiment conditions, such as spatial scale, hydraulic gradient, and the use of three-component DNAPL for the Borden experiments, may also have had some influence. The issue of the three-component DNAPL was addressed in part by determining the aggregate CMD and mass removal based on mole fractions (DiFilippo and Brusseau, 2008). The issues of scale and hydraulic-gradient conditions are addressed in a following paragraph.

Regarding differences in system properties and conditions, the Borden site has a comparatively small degree of permeability variability, with the target subsurface zone comprised of medium- to fine-grained lacustrine sand with occasional beds of coarse sand/gravel and silt (Broholm et al., 1999). Conversely, the TIAA sites are very heterogeneous, with extensive sequences of clay alternating with laterally discontinuous lenses of silts, sands, and gravels. Furthermore, the Borden sites were freshly-contaminated systems, with monitoring of mass discharge commencing soon after emplacement of the contamination. In contrast, the TIAA sites are mature sites, with characterization commencing many years after contamination emplacement (approximately 60 and 35 years for the central-TIAA and south-TIAA sites, respectively). Mass transfer and mass removal processes occurring during the intervening decades, as documented by the extensive groundwater contaminant plumes present at the TIAA sites, would be expected to have significantly altered the contaminant distribution within the source areas, with much of the mass preferentially removed from the more accessible domains. For example, for the current study site, it was estimated above that approximately one-third of

the initial contaminant mass in the saturated-zone source area was removed via natural-gradient flushing prior to the start of characterization and remediation activities. In total, it is likely that a larger fraction of contaminant mass was accessible for mass removal via advective and diffusive transport for the Borden experiments compared to the TIAA sites. The CMDR-MR relationships observed for the Borden versus the TIAA sites are consistent with this supposition that site age through its impact on contaminant distribution and accessibility is a significant discriminatory factor. In addition, it is possible that the difference observed between the two TIAA sites may be related in part to the significant difference in source-zone age associated with the two sites.

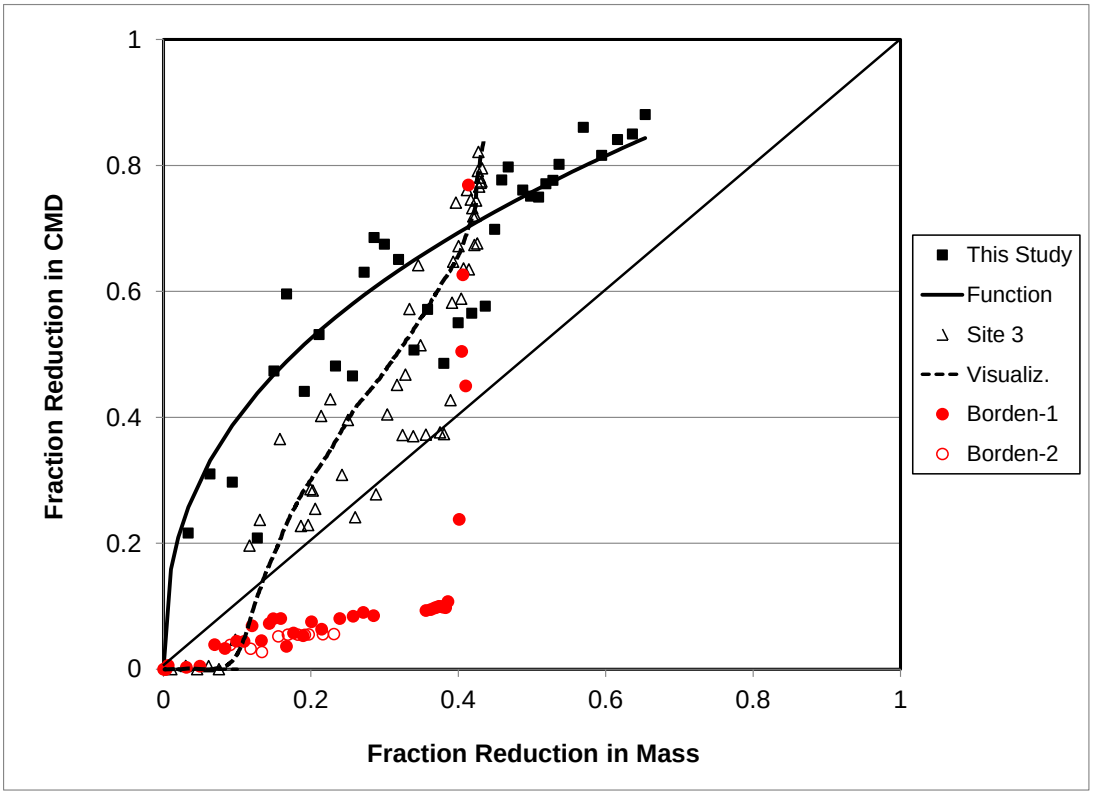

Figure 5.1.2-7. Relationship between the reduction in contaminant mass discharge (CMD) and the reduction in contaminant mass: comparison of measured field data. The relationships for Site 3 and Borden were calculated and reported originally by DiFilippo and Brusseau (2008), using raw concentration and flowrate data reported by Brusseau et al. (2007) for Site 3, Broholm et al. (1999) for Borden-1, and Rivett and Feenstra (2005) for Borden-2. The line for the Site 3 data is for visualization purposes and is not produced with a mathematical function. The data for this study are based on the M_0 obtained with method 2.

Additional illustration of the impact of contaminant accessibility is presented by the Borden-1 data. Interestingly, a significant reduction in CMD is observed to begin at ~40% mass reduction for this data set. The marked change in the profile indicates a significant change in mass-removal conditions, transitioning from a system controlled by more-accessible mass to one controlled by less-accessible mass (Brusseau et al., 2008; DiFilippo et al., 2010; Christ et al., 2010). Excavation and characterization of the source after experiment completion indicated that

the majority (~85%) of the remaining contaminant mass was associated with a single 0.5-cm thick, areally extensive pool of DNAPL (Broholm et al., 1999). This mass would be expected to be poorly accessible to water flushing. These results support the conclusion that mass removal at the latter stage of the experiment was controlled by poorly accessible mass. Furthermore, based on the characterization results, 50% or more of the initial contaminant mass was present as pools (i.e., was relatively poorly accessible). This is consistent with the observed CMDR transition point, which occurred at approximately 40% mass reduction (with that fraction likely representing the more accessible mass). Characterization of CMD and mass removal for the Borden-1 source area after the more accessible mass has been removed (i.e., an aged source) produces a CMDR-MR profile that is shifted leftward and is more similar to that observed for the TIAA-site 3 site (data not shown).

As noted, another major difference between the Borden and TIAA sites is spatial scale, wherein the Borden experiment systems are small (~4 x 5 m) and the TIAA source areas are much larger (~100 x 100 m). The potential impact of scale was investigated by examining two additional characterizations of field-scale CMDR-MR relationships that were determined herein using raw concentration and flow-rate data reported in the literature. These experiments were conducted at the Dover AFB test site, using a sheet-pile enclosed cell (3 x 4.6 m) emplaced in the subsurface, into which tetrachloroethene was injected under controlled conditions. The experiment zone is a shallow, unconfined aquifer that consists of medium to fine sands with interbedded gravels, silts, and clay lenses (Tick et al., 2003). After initial contamination, an alcohol flood was conducted (Brooks et al., 2004), followed by a surfactant flood (Childs et al., 2006) and a complexing-sugar flush (Tick et al., 2003). The three experiments were conducted sequentially in the same cell, with the primary difference being that the surfactant flood employed vertical-circulation extraction wells for a majority of the flood whereas the complexing-sugar flush (CSF) employed a standard horizontal line-drive system. Additional tetrachloroethene was injected into the cell prior to both the surfactant and CSF experiments.

The CMDR-MR relationships determined for the surfactant and CSF experiments are presented in Figure 5.1.2-8. The curves are similar wherein there is minimal reduction in CMD for the initial stage of mass reduction, followed by a sharp, significant reduction in CMD that starts at approximately 15-25% mass reduction. The similarity of the two profiles suggests that the fluid-control configuration (vertical versus horizontal floods) did not have a significant impact on observed behavior. Each of the three treatments removed only a portion of the total tetrachloroethene mass present, and this mass was therefore present for the subsequent experiments. Thus, the system can be considered to have been under partially aged conditions for the surfactant and CSF experiments, with a combination of more-accessible mass (a portion of the newly added mass) and poorly accessible mass (a portion of the newly added mass and the mass remaining from the prior test). The observed CMDR-MR profiles are consistent with these conditions.

The CMDR-MR profiles observed for the two Dover experiments are generally similar to those observed for the TIAA-Site 3 and Borden-1 data sets (Figure 5.1.2-7). The scale of the Dover experiment site is very similar to that of the Borden experiment sites, and much smaller than that of the TIAA sites. Given this, it appears that the difference in scale did not contribute significantly to the differences in behavior observed between the Borden and TIAA sites. In addition, the Dover experiments, as well as the TIAA studies, were conducted under induced-gradient conditions. Conversely, the Borden experiments were conducted under natural-gradient conditions. For example, the mean pore-water velocity for the Dover CSF experiment was 1 m/d

(Tick et al., 2003) compared to 0.1 m/d for the Borden-1 experiment (Broholm et al., 1999). The fact that similar CMDR-MR profiles were obtained for the Borden-1, Dover, and TIAA-site 3 systems indicates that hydraulic-gradient status did not have a significant impact on the underlying mass-removal behavior. It should be noted that the two Dover experiments involved enhanced-solubility floods, while the Borden-1 experiment comprised a sequential water and cosolvent flood and the TIAA studies involved strictly water flushing. The similarity of the CMDR-MR profiles among the different systems indicates that the composition of the flooding solution also did not have a significant impact on the underlying mass-removal behavior. This is consistent with results obtained from laboratory experiments (Carroll and Brusseau, 2009; Tick and Rincon, 2009; DiFilippo et al., 2010). It should also be noted that the Dover data sets as well as the Site 3 and Borden-1 data exhibit non-singular ("S-shaped") profiles that cannot be simulated with the simple CMDR-MR function, which has also been observed in prior studies (Brusseau et al., 2008; DiFilippo and Brusseau, 2008; Christ et al., 2010; DiFilippo et al., 2010).

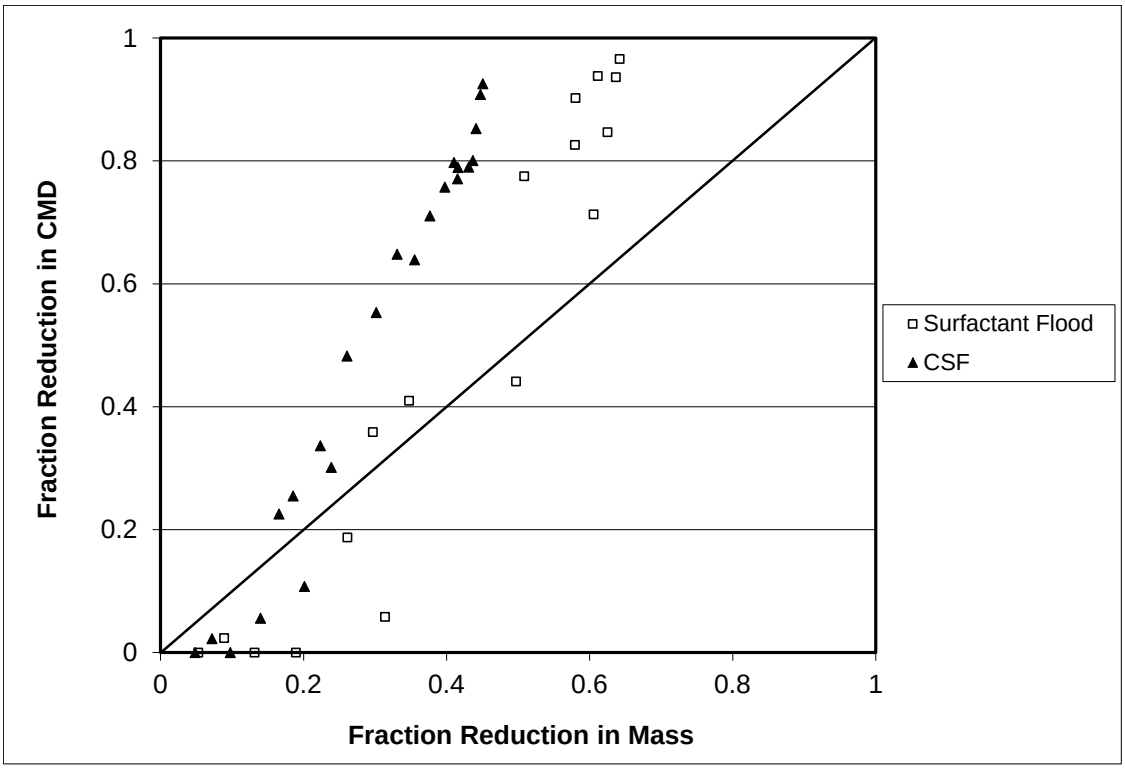

Figure 5.1.2-8. Relationship between the reduction in contaminant mass discharge (CMD) and the reduction in contaminant mass: comparison of measured field data from Dover test site. Relationships calculated using raw concentration and flowrate data reported by Childs et al. (2006) for the surfactant flood and Tick et al. (2003) for the CSF (complexing sugar flush).

Summary

The use of contaminant-mass-discharge measurements to characterize site conditions and evaluate remediation performance is becoming a critical component of site assessment. Time-

continuous measurements of contaminant mass discharge, obtained by conducting extended contaminant mass discharge tests or by capturing operational fluid-extraction data, can provide useful information to characterize mass-transfer processes, assess mass-removal magnitudes and conditions, and estimate contaminant distributions and quantities. In the present study, the temporal behavior of contaminant mass discharge was characterized for a very heterogeneous source-zone field site contaminated by TCE DNAPL. The results showed that contaminant mass discharge decreased asymptotically with time, from approximately 1 to 0.15 kg/d. Comparison of two sets of core data, collected 3.5 years apart, suggests that aggregate sediment-phase TCE concentrations decreased by ~80% between sampling events. The results reported herein provide insight to the impact of hydraulic-based remedial efforts on contaminant mass discharge for heterogeneous, DNAPL-contaminated source zones.

Two methods were used to estimate the mass of contaminant initially present in the source area, and they produced reasonably similar results. Each method has associated sources of uncertainty, as well as requirements that can limit their use. Limitations associated with method 1, sediment coring, are well known. Regarding the second method, it is based on fitting a mass-depletion function to temporal CMD data, and obviously requires availability of such data. Prior similar efforts of estimating source mass have been implemented by fitting simplified functions to temporal concentration data collected from monitoring wells located within contaminant plumes (Butcher and Gauthier, 1994; Basu et al., 2009). This approach has broad potential applicability given the general widespread availability of monitoring-well data for many sites. However, it is anticipated that CMD data (rather than solely concentration data) measured directly for the source area via an extended contaminant mass discharge test as done herein will provide a more robust data set for estimation of source mass. The second method is a useful alternative to standard coring, particularly for cases wherein coring is technically or economically impractical. The method is also useful for cases wherein temporal CMD data can be captured from analysis of operational data for fluid-extraction systems such as pump and treat or soil vapor extraction. Such analysis of historic-operations data provides a simple means by which to estimate initial contaminant mass for the treatment domain.

Contaminant mass discharge data can be integrated with measurements of initial mass to characterize the relationship between reductions in contaminant mass discharge and reductions in contaminant mass. The CMDR-MR relationship is a defining characteristic of system behavior, reflecting system properties and conditions. These relationships are typically characterized using time-continuous CMD data, which provides the means to assess the temporal dynamics of mass removal as influenced by changes in contaminant distribution and configuration, and resultant impacts on flow and mass-transfer processes. However, CMDR-MR relationships can also be obtained for specific snapshots of time by collecting spatially discrete data. For example, Brooks et al. (2004) reported CMDR-MR data obtained from two sets of measurements (before and after a remedial action) collected at six monitoring locations, and used these spatial data to represent a CMDR-MR profile for the alcohol-flood pilot test conducted at Dover AFB that was discussed above.

As noted, very few time-continuous measurements of CMDR-MR relationships have been reported to date for field systems (Brusseau et al., 2007; DiFilippo and Brusseau, 2008). The data collected during the study were used develop such a relationship for the source area of the site. The profile exhibited by the data is consistent with a system wherein significant quantities of mass were present in hydraulically poorly accessible domains, for which mass removal is influenced by mass-transfer constraints. This contention is supported by the sediment-

core data, which showed that the highest concentrations of TCE are associated with lower-permeability units, and by the estimates of the amount of groundwater flushing and associated contaminant mass removal experienced by the source area in the ~60 years prior to project startup. The results obtained from the present study were compared to those obtained from other field studies to evaluate the impact of system properties and conditions on behavior. The results indicated that factors such as domain scale, hydraulic-gradient status (induced or natural), and flushing-solution composition had insignificant impact on the CMDR-MR profiles and thus on underlying mass-removal behavior. Conversely, source-zone age, through its impact on contaminant distribution and accessibility, was implicated as a critical factor influencing the nature of the CMDR-MR relationship. This is consistent with the results of mathematical modeling studies and laboratory experiments (Jawitz et al., 2005; Brusseau et al., 2008; DiFilippo et al., 2010).

5.1.3 Impacts of Source-zone Architecture and Age on ISCO: Bench-scale Results

The effectiveness of permanganate for in situ chemical oxidation of organic liquid (trichloroethene) trapped in lower-permeability (K) zones located within a higher-permeability matrix was examined in a series of flow-cell experiments (Table 5.1.3-1).

Table 5.1.3-1a. Summary of experimental conditions

Flow Cell	System Description	Matrix Mesh	Zone 1 Mesh (upper)	Zone 2 Mesh (lower)	System Length (cm)	Organic-Liquid Source Length (cm)	Average Pore Velocity (cm/hr)	Initial S_n
Rectangular	2 lower K zones with organic liquid	20/30	70/100	40/50	40	16	3.5	0.15
Rectangular	2 lower K zones with organic liquid	20/30	70/100	40/50	40	16	4.5	0.19
Rectangular	2 lower K zones with organic liquid	20/30	70/100	40/50	40	16	4.0	0.18
Cylindrical	1 lower K zone with organic liquid	20/30	40/50	-	10	2.5	20	0.11
Cylindrical	1 lower K zone with organic liquid	20/30	40/50	-	10	2.5	21	0.17
Cylindrical	1 lower K zone with organic liquid	20/30	40/50	-	10	2.5	20	0.12
Cylindrical	Uniform organic liquid distribution	20/30	-	-	7	7	21	0.12
Cylindrical	Uniform organic liquid distribution	20/30	-	-	7	7	21	0.03

Table 5.1.3-1b. Summary of experimental conditions

Flow Cell	Initial Experiment Mass (g)	Initial Water Flood Mass (g)	Fraction Oxidized by $KMnO_4$	Source Zone Treatment
Rectangular	32.2	-	0.20	Constant injection of 15mM $KMnO_4$ to 4.9 PV
Rectangular	41.8	33.0	0.14	Pulsed injections of 15mM $KMnO_4$ to 4.5 PV followed by water flood
Rectangular	38.8	38.8	-	Water flood control experiment
Cylindrical	1.1	0.4	0.65	Constant injection of 63.3 mM $KMnO_4$ to 1 PV followed by water flood
Cylindrical	1.1	0.1	0.92	Pulsed injection of 63.3 mM $KMnO_4$ to 4.2 PV followed by water flood
Cylindrical	1.1	1.1	-	Water flood control experiment
Cylindrical	1.5	1.5	-	Homogeneous medium/source water flood
Cylindrical	0.4	0.4	-	Homogeneous medium/source water flood

Details of the methods and systems are presented in the published paper (2).

Permanganate Transport and Oxidation-Reaction Product Formation

The first experiment conducted with the rectangular flow cell (Figure 5.1.3-1) comprised continuous injection of 4.5 pore volumes of a 15 mM permanganate solution. The permanganate solution exhibited plug flow until reaching the lower-K zones, at which point the solution bypassed the lower-K zones and continued to move downgradient toward the outlet of the flow cell. A time series of photographic images of one of the lower-K zones and surrounding higher-K matrix during permanganate solution injection is presented in Figure 5.1.3-2. Brown manganese oxide precipitates initially formed at the interface between the surrounding media and the lower-K zones, except at the downgradient end. Conrad et al. (2002) also observed the formation of manganese oxide precipitate adjacent to zones of high saturation of organic liquid. In addition, gas bubbles, presumed to be carbon dioxide, formed at the interfaces. “Shadow” zones within the higher-K matrix into which the permanganate solution did not enter were observed downgradient of both lower-K zones (Figure 5.1.3-3), and were attributed to by-pass flow effects. Precipitates formed at the top and bottom edges of the shadow zones, forming tails. The precipitate-affected zones increased in thickness during the experiment, indicating continued flux of aqueous TCE from the lower-K zones into the higher-K matrix. Similar behavior was also observed in experiments conducted by Reitsma and Marshall (2000).

Following completion of the permanganate treatment, subsamples were collected to determine remaining TCE mass and for SEM analysis. SEM photomicrographs of samples collected from the matrix and from the center of the lower-K zones indicate precipitates did not

form at those locations during the treatment (Figure 5.1.3-4a). In addition, solid-phase manganese was not detected with the EDS analysis. Conversely, the samples collected from the interface between the matrix and lower-K zones had noticeable precipitates, which were observed to have a fibrous and semi-amorphous crystalline structure that formed as a coating on the surface of the sand grains (Figure 5.1.3-4b). Previous researchers have used X-Ray diffraction to determine that the precipitate typically formed is potassium-rich birnessite (Li and Schwartz, 2004b). The EDS analysis of the precipitates described herein revealed the presence of manganese, chlorine, and potassium in addition to the quartz sand components (silica and oxygen), indicating that chlorine and potassium by-products of TCE oxidation were being incorporated (e.g., coprecipitation) into the manganese oxide crystal structure.

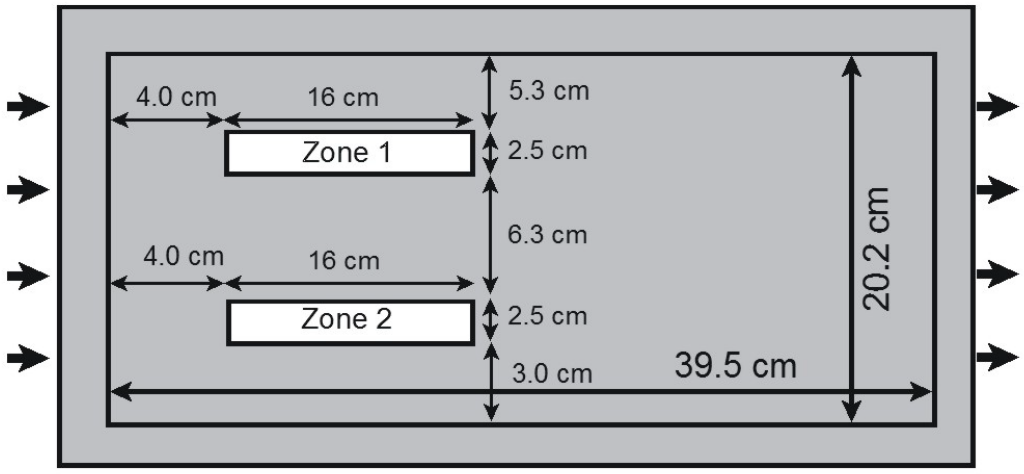

Figure 5.1.3-1. Flow-cell schematic for rectangular flow cell with a coarser sand (20/30 mesh; 724 um) that comprised the matrix and two finer sands were used to create zones 1 (70/100 mesh; 172 um) and 2 (40/50 mesh; 360 um);

The second experiment conducted with the rectangular flow cell consisted of a series of three pulses totaling ~4.5 pore volumes, with periods of no flow between the pulses. The transport behavior observed during the first pulse was similar to that of the constant-injection experiment wherein the permanganate solution exhibited plug flow until coming into contact with the lower-K zones, which were bypassed, causing shadow zones to form downgradient of both lower-K zones. During the no-flow periods, permanganate solution diffused into the shadow zones. In addition, pore water in the matrix changed from purple to clear, and precipitation occurred in the matrix surrounding both lower-K zones. This indicates that TCE was diffusing from the lower-K zones and reacting with permanganate during the flow interrupts. At the completion of the permanganate treatment, 54% of the area comprising lower-K zone 2 contained noticeable precipitates compared to 21% for lower-K zone 1. Differences in the extent of precipitate formation likely reflect the differences in advective penetration of the zones by the permanganate solution (Figure 5.1.3-5), consistent with the permeability differences between the two media comprising the zones.

The formation of brown manganese-oxide precipitates and gas bubbles was also observed during the cylindrical flow cell experiments. Two permanganate-injection experiments were conducted with the cylindrical system, both employing a 63.3 mM permanganate solution. One experiment comprised a continuous injection of 1 pore volume of permanganate solution, and the other comprised four equal-volume injections (total of 4.2 pore volumes of solution) alternated with flow interruptions. For the continuous-injection experiment, manganese-oxide precipitate was observed in the matrix but not in the lower-K zone. Precipitate formation was more extensive for the pulsed-injection experiment compared to the continuous-injection experiment, consistent with the greater volume of permanganate solution injected. In addition, a significant amount of precipitate was observed within the lower-K zone. This indicates that permanganate diffused into the lower-K zone during the flow-interruption periods. Diffusive mass transfer of permanganate into lower-K zones has been observed in a prior study (Struse et al., 2002).

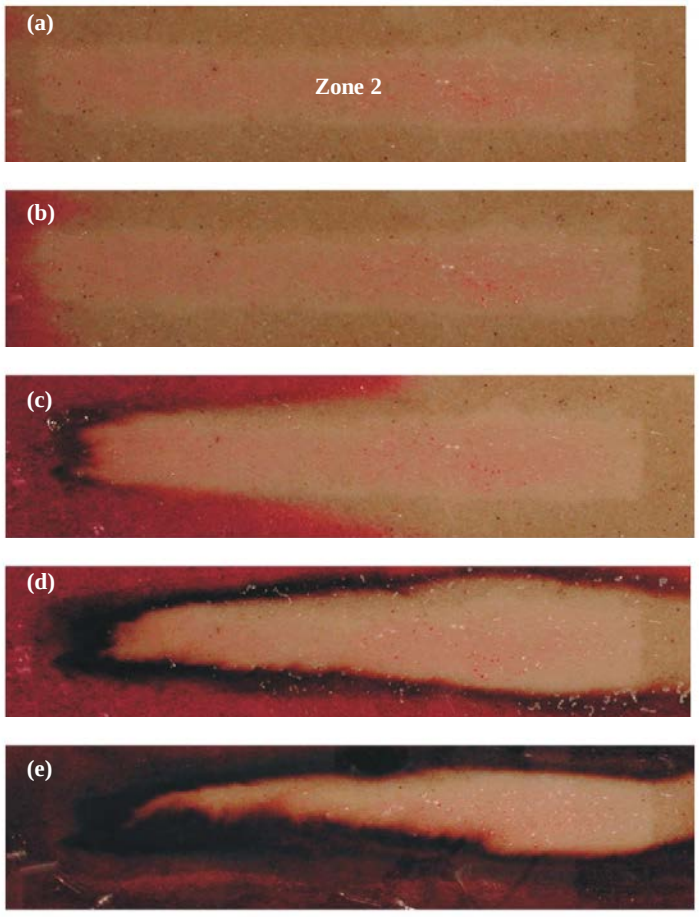

Figure 5.1.3-2. Photographic images cropped to focus on the lower-K zone 2 (40/50 mesh; 360 um) and surrounding higher-K matrix sand during the constant permanganate injection: (a) 0.01 pore volume, (b) 0.03 pore volume, (c) 0.14 pore volume (d) 1.0 pore volume, and (e) 4.0 pore volumes.

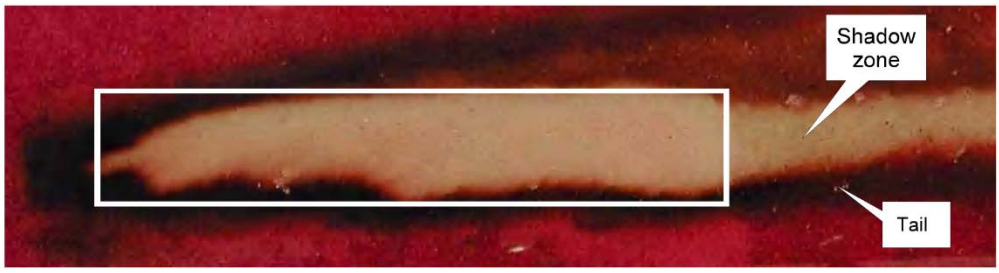

Figure 5.1.3-3. Photographic image of the lower-K zone 2 and surrounding area after permanganate injection, exhibiting the shadow zone downgradient of the lower-K zone, downgradient manganese oxide tails, and manganese oxide formation around the lower-K zone. The white box represents the outline of the source zone.

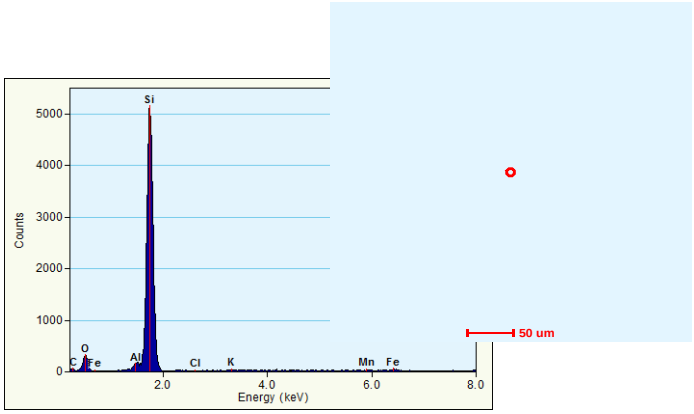

Figure 5.1.3-4a. SEM image of sand grain located in the middle of a low-K zone. Qualitative elemental analyse of the mineral-surface chemistry collected at locations indicated (red circle) on the SEM photomicrograph was obtained using an energy dispersive x-ray spectroscopy detector.

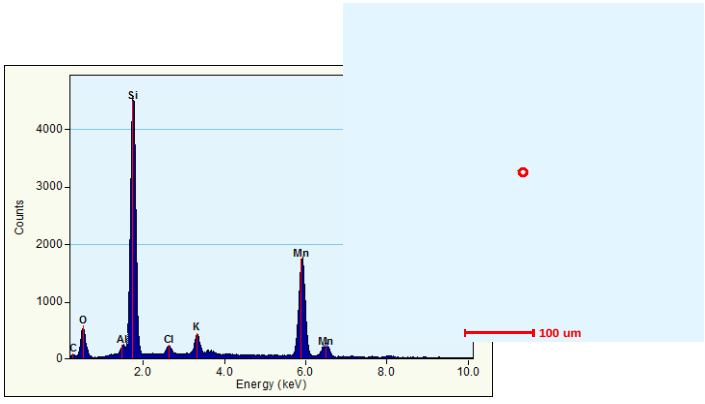

Figure 5.1.3-4b. SEM image of sand grain located at the boundary of a low-K zone. Qualitative elemental analyses of the mineral-surface chemistry collected at location indicated (red circle) on the SEM photomicrograph was obtained using an energy dispersive x-ray spectroscopy detector.

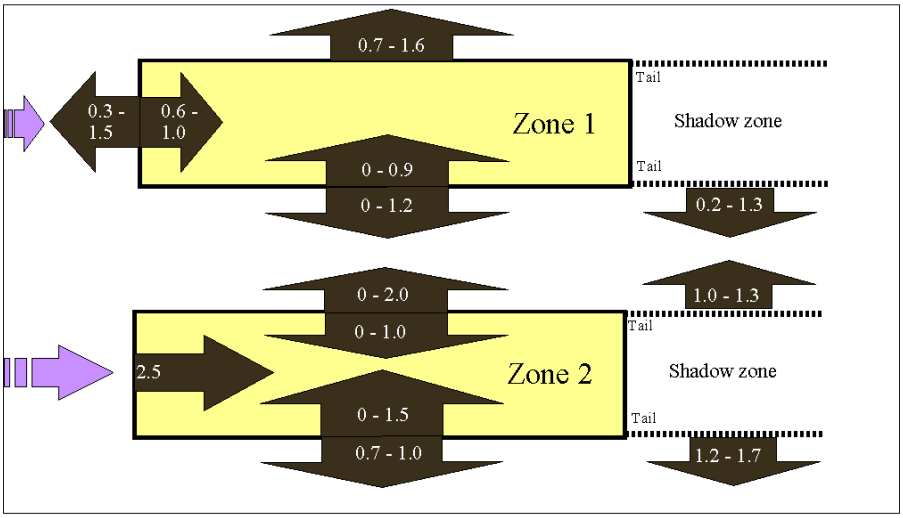

Figure 5.1.3-5. Distances in centimeters measured along rectangular flow cell that manganese oxides formed inside and outside of the lower-K zones during flow interruptions of the pulsed permanganate injection experiment.

Mass Removal and Mass Flux

Loss of TCE mass from the lower-K source zones during the experiments occurred first by permanganate-induced oxidation and then by dissolution and associated mass flux during the subsequent water flood. Concentration data from solvent extraction and effluent samples were used to determine mass removed due to dissolution and subsequent transport and elution. Mass loss due to transformation was calculated by mass balance (Table 5.1.3-1). For the pulsed permanganate-injection experiment conducted with the rectangular flow cell, 3.1(±0.4) grams of TCE were eluted during the permanganate injection and 26.3(±2.6) grams were eluted during the subsequent water flood, for a total of 29.4(±3) grams. The mass of TCE remaining at experiment completion was determined to be 6.7(±0.9) grams. A total of 5.7(±0.7) grams of TCE was calculated to have been oxidized by permanganate, which is approximately 14% of the initial TCE mass. Approximately 13.7(±1.8) grams of permanganate would be required for oxidation of this quantity of TCE, which is approximately 80% of the total amount injected. This value is somewhat uncertain given the uncertainties in determining mass remaining.

As noted above, the permanganate injection caused a reduction in TCE mass. A question of interest is what impact, if any, did this mass reduction have on post-treatment effluent concentrations and associated mass flux. After the multiple permanganate pulses, water was flushed through the flow cell for an additional 37 pore volumes to characterize mass flux following the permanganate treatment. TCE effluent concentration data exhibit an initial increase to 750 mg/L (Figure 5.1.3-6), which was attributed to the concentration rebound during the flow interruption period. The concentration gradually decreased to 290 mg/L by the end of the water flood. TCE effluent concentrations were 230 mg/L after 40 pore volumes for the water-flood (aqueous dissolution) control experiment. The relatively small observed difference in concentrations for the two experiments may reflect experiment variability, or may be associated with the impact of permanganate treatment on subsequent water flow and organic-liquid dissolution, as observed by Heiderscheidt et al. (2008). The similarity of effluent TCE

concentrations observed during the control and permanganate experiments suggests that manganese oxide precipitates did not significantly inhibit mass transfer from the lower-K zones.

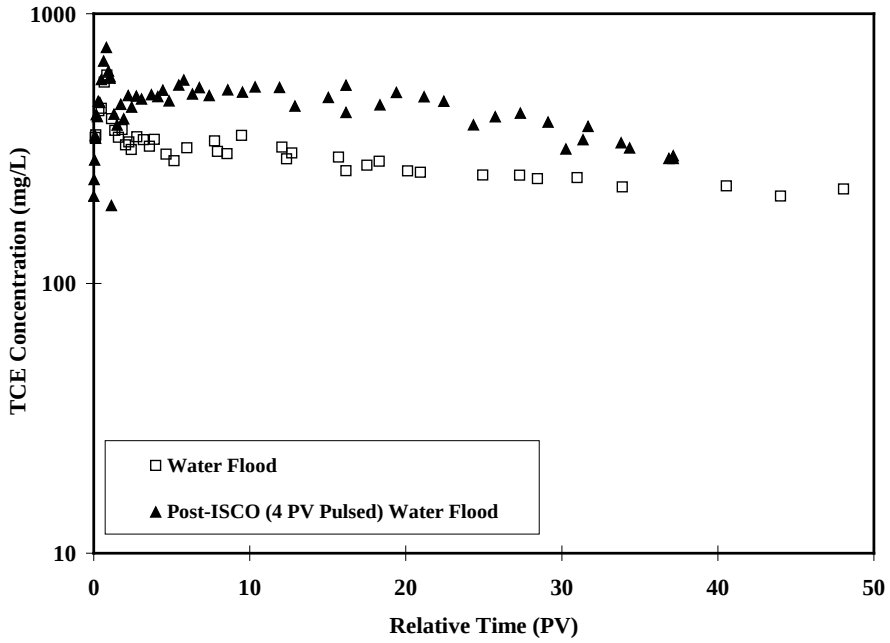

Figure 5.1.3-6. Effluent TCE concentrations from rectangular flow-cell experiments with water flooding only (open symbols) and water flooding after pulsed injection of 4.5 pore volumes (PV) of 15 mM permanganate (ISCO) (closed symbols).

The similarity in mass fluxes observed for the experiments discussed above indicates that the permanganate treatment did not significantly impact post-treatment mass flux. However, the fraction of mass reduction associated with permanganate treatment was relatively small. As noted above, the cylindrical flow cell experiments were conducted to examine mass-removal and mass-flux-reduction behavior for conditions of complete mass removal. The results are presented in Figure 5.1.3-7.

For the water-flood experiment, the effluent concentration dropped quickly and then remained steady for an extended period. A steady-state phase was also observed for the continuous permanganate-injection experiment. The steady-state concentration of approximately 90 mg/L observed for the experiments is much lower than aqueous solubility, and reflects the impact of dilution given that the TCE-contaminated zone encompassed only a portion of the flow-cell cross section. The steady-state period was shorter for the continuous permanganate-injection experiment as compared to the water-flood control experiment despite nearly identical initial saturations (Table 5.1.3-1), which reflects the impact of mass removal by *in situ* oxidation. In contrast to the prior two experiments, there was no extended period of relatively constant effluent concentrations for the pulsed permanganate-injection experiment, due presumably to permanganate oxidation of the majority of the organic liquid prior to water flooding.

Approximately 140 pore volumes of water flushing were required to decrease effluent concentrations to approximately 0.1 mg/L for the water-flood control experiment. Conversely, 60 pore volumes were required for the continuous permanganate-injection experiment and less than 50 pore volumes for the pulsed permanganate-injection experiment. These results indicate that the permanganate treatment had a significant impact on long-term mass flux, and concomitantly the amount of water flushing required to reach a relatively low aqueous concentration.

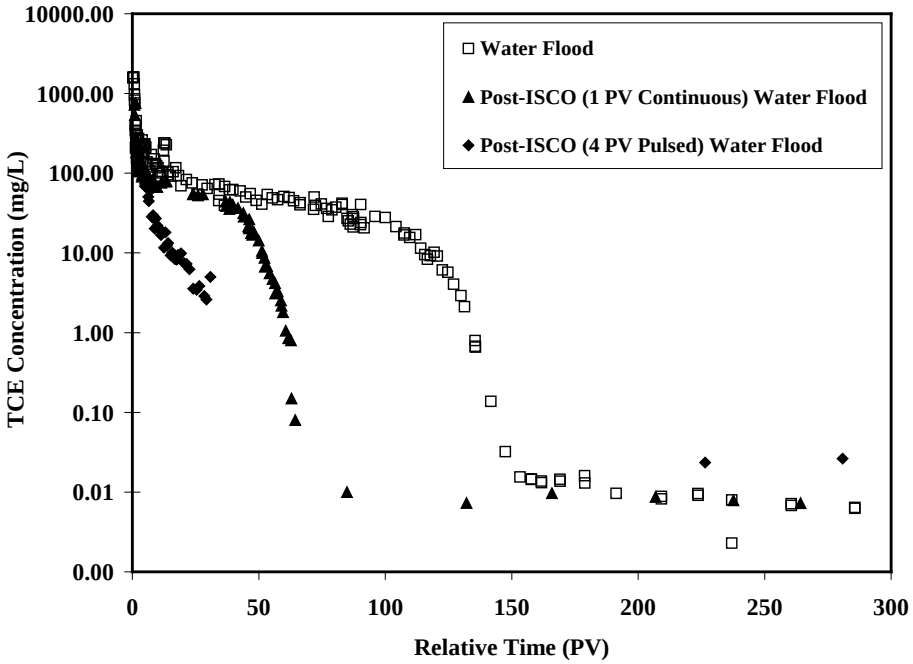

Figure 5.1.3-7. Effluent TCE concentrations for the cylindrical flow-cell experiments with water flooding only (open symbols) vs. water flooding after permanganate treatment (ISCO) (closed symbols) for 1 PV and 4 PV injections of the 63.3 mM solution.

Relationship between Mass Flux Reduction and Mass Removal

Several factors influence the nature of the mass-flux-reduction/mass-removal relationship for a given system. These include the amount of contaminant and its distribution, mass-transfer processes, and flow-field dynamics. Implementation of a source-zone remediation effort may alter mass-flux-reduction/mass-removal behavior. For example, preferential removal of contamination from particular locations or the formation of oxidation reaction products may alter the flow field and modify contaminant accessibility. This was evaluated by conducting water floods after completion of the permanganate injections.

The mass-flux-reduction/mass-removal data for the rectangular flow-cell experiments conducted with and without permanganate treatment are compared in Figure 5.1.3-8a. The TCE saturation was approximately 15% at the start of the water flood conducted for the permanganate experiment, which is similar to the initial saturation of 18% for the water-flood control experiment. An approximately one-to-one relationship between mass flux reduction and mass

removal was observed for the water-flood control experiment. This behavior is expected for a system in which a portion of the contamination is poorly accessible (e.g., Fure et al., 2006; Brusseau et al., 2008). In contrast, a minimal reduction in mass flux was observed until approximately 30% mass removal for the water flood conducted after the permanganate injection. After this point, mass flux decreased at an increasing rate through the end of the experiment. These results suggest that mass-transfer and mass-removal efficiency were greater for the post-permanganate water flood compared to the water-flood control. As noted above, a significant degree of manganese-oxide precipitation occurred in the matrix surrounding the lower-K zones. This precipitate formation may have decreased the effective permeability of the matrix adjacent to the lower-K zones, thus reducing the permeability contrast and concomitantly by-pass flow, thereby leading to a greater degree of flushing (greater hydraulic accessibility) for the source zone.

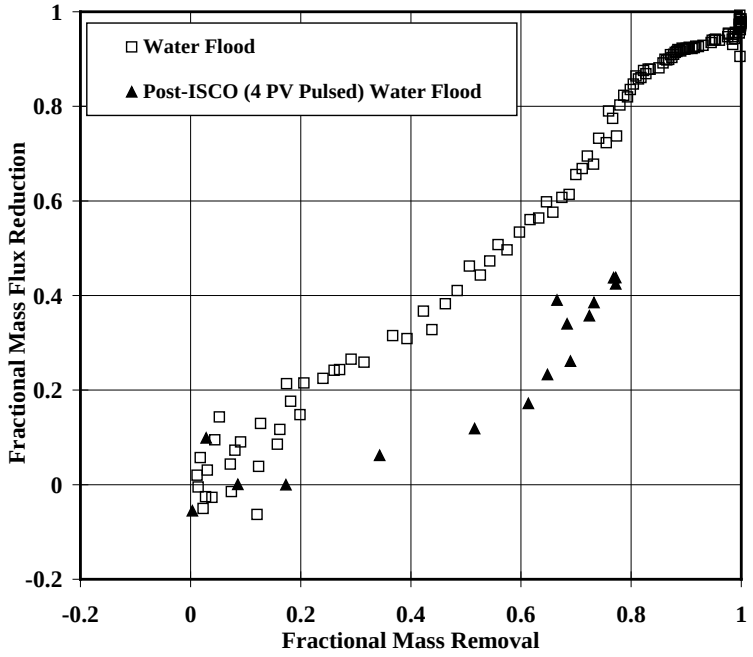

Figure 5.1.3-8a. Fractional mass-flux reduction as a function of fractional mass removal for the rectangular flow-cell experiments.

The mass-flux-reduction/mass-removal data for the experiments conducted with the cylindrical flow cell are presented in Figure 5.1.3-8b. The fraction of mass removed during the permanganate treatments was significantly greater for the two cylindrical flow-cell experiments (65% and 92% for the continuous and pulsed experiments, respectively) compared to that of the rectangular flow-cell experiments. These mass reductions resulted in initial TCE saturations of approximately 3-4% for the post-permanganate water floods, which are significantly smaller than the initial saturation of 12% for the water-flood control experiment. The impact of initial organic-liquid saturation on mass-flux reduction/mass-removal behavior was evaluated with control experiments wherein TCE was uniformly distributed in homogeneously packed columns at initial saturations of 3% and 12%. The data exhibit relatively efficient mass-removal behavior as expected, with significant mass-flux reductions occurring only after the majority of mass has

been removed (Figure 5.1.3-8c). Mass flux begins to decrease at a smaller mass-removal fraction for the lower-saturation experiment (~0.5 vs ~0.7), reflecting the impact of reduced initial contaminant mass.

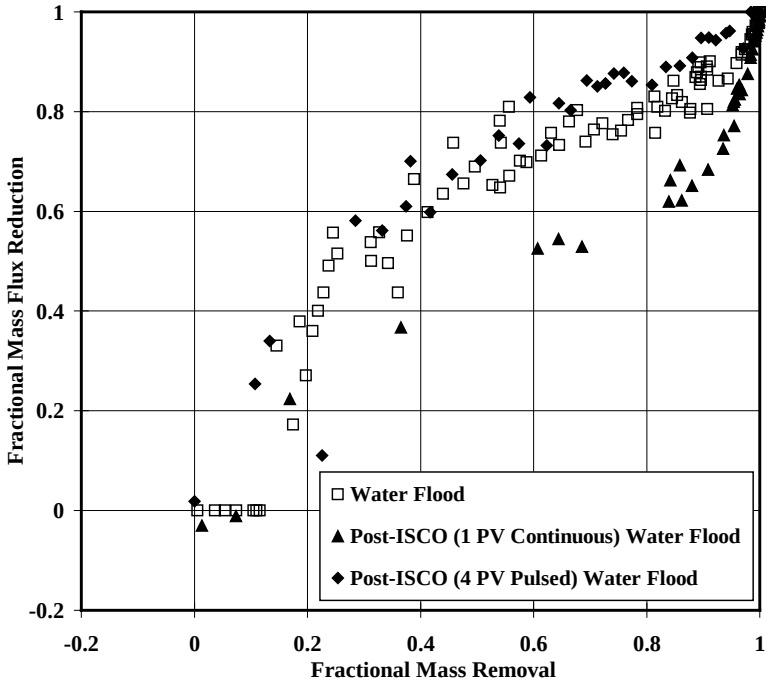

Figure 5.1.3-8b. Fractional mass-flux reduction as a function of fractional mass removal for the column experiments; (c) cylindrical flow-cell experiments.

Inspection of Figure 5.1.3-8b shows that the initial mass-flux reduction behavior was relatively similar for the water flood conducted after the continuous permanganate-injection and for the water-flood control experiment, whereas it differed for the water flood conducted after the pulsed-permanganate experiment (the latter experiment will be discussed in a following section). However, a smaller reduction in mass flux was observed for the post-permanganate water flood at larger mass-removal fractions. This latter result suggests that mass-transfer and mass-removal efficiency were greater for the post-permanganate water flood compared to the water-flood control. For the continuous- injection permanganate experiment, manganese-oxide precipitate was observed within the matrix but not within the lower-K zone. Similarly to the results of the rectangular flow-cell experiments discussed above, it is possible that the precipitate reduced the permeability contrast between the matrix and the lower-K source zone, thereby increasing the hydraulic accessibility of the source zone. As noted above, the initial TCE saturation at the start of the water flood was significantly smaller for the permanganate-injection experiment. Thus, the potential impact of lower initial mass on mass-flux-reduction/mass-removal behavior (as illustrated in Figure 5.1.3-8c) appears to have been offset by the greater mass-removal efficiency.

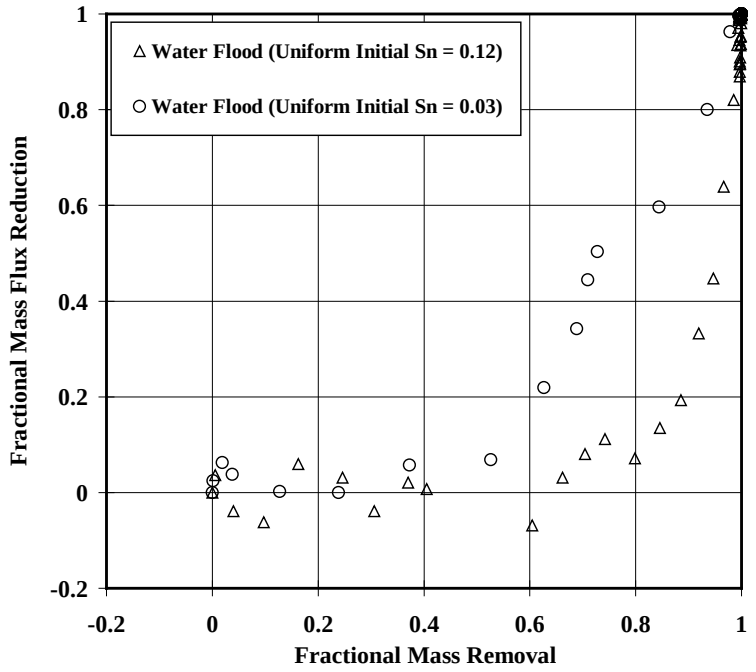

Figure 5.1.3-8c. Fractional mass-flux reduction as a function of fractional mass removal for the column experiments.

An apparent increase in mass-transfer and mass-removal efficiency has been observed for the post-permanganate water floods compared to the water-flood controls for both the cylindrical and rectangular flow-cell experiments. For both cases, manganese-oxide precipitate formed in the matrix surrounding the lower-K source zones, which is suspected to have influenced the flow field and thus hydraulic accessibility of the contaminant. For the continuous-injection cylindrical flow-cell experiment, one pore volume of permanganate solution was injected in continuous mode, and the concentration of permanganate was four times higher than that used for the rectangular flow-cell experiment. Conversely, 4.5 pore volumes of lower-concentration solution were injected in successive pulses for the rectangular flow-cell experiment. Thus, similar relative amounts of permanganate were introduced for the two experiments. The similarity of overall results suggests that the injection mode did not have a significant impact on behavior for the conditions and configurations employed.

For the water flood conducted after the pulsed permanganate injection (cylindrical flow-cell experiment), mass flux decreased essentially immediately, in contrast to the water flood conducted after the continuous permanganate injection (Figure 5.1.3-8b). In addition, the reduction in mass flux was significantly greater for essentially the entire water flood. Thus, the mass-flux-reduction/mass-removal behaviors are significantly different for the two permanganate experiments, despite the fact that both experiments had similar initial TCE saturations at the start of their respective water floods. These results indicate that mass transfer and mass removal was more constrained for the water flood conducted after the pulsed-injection experiment compared to the single-injection experiment. The amount of permanganate injected was 4 times greater for the pulsed-injection experiment, and manganese-oxide precipitation was significantly greater (as noted above). In addition, precipitate was observed to have formed inside the lower-K source

zone for the pulsed experiment (and not for the continuous experiment), which is hypothesized to have resulted in decreased permeability and hence reduced hydraulic accessibility, thereby constraining mass transfer and mass removal. This is consistent with the observation that the reduction in mass flux for the water flood conducted after the pulsed permanganate injection was greater than that observed for the water-flood control experiment for mass-removal fractions greater than approximately 0.7 (Figure 5.1.3-8b).

Summary

A series of flow-cell experiments was conducted to determine the effectiveness of ISCO using permanganate, and the associated impacts on contaminant mass flux, for systems wherein organic-liquid contaminant was located in hydraulically poorly-accessible lower-K zones. Permanganate was able to degrade TCE in the lower-K zones as confirmed by the formation of dissolved gas and manganese-oxide precipitates. The impact of permanganate treatment on long-term mass flux behavior was examined by conducting water floods after permanganate injection. The results were compared to those of water-flood control experiments. The amount of water flushing required for complete contaminant mass removal was reduced for all permanganate treatments for which complete mass removal was evaluated. However, the nature of the mass-flux-reduction/mass-removal relationship observed during water flooding varied as a function of the specific permanganate treatment. The disparity in behavior was attributed to the varied impact of precipitate formation on the flow field and contaminant accessibility. The results presented herein illustrate the impact of ISCO on mass-flux reduction/mass-removal behavior.

5.2 Field-scale ISCO Application in Heterogeneous Systems

5.2.1 ISCO Performance: Mass Removal and Mass Discharge

A key issue for implementing in-situ chemical oxidation (ISCO) and other source-zone remediation methods at a given site is their relative costs and benefits in comparison with existing (typically pump and treat) and other potential remediation efforts. Assessing the quantitative performance of a source-zone remediation effort is central to evaluating associated costs and benefits. In their extensive review of 242 ISCO projects conducted over the past decade, Krembs et al. (2010) found that only four of the projects were assessed using estimates or measurements of contaminant mass discharge. Discounting the two that used estimates rather than actual measurements, and including an additional non-tabulated project, results in a total of three ISCO projects for which performance has been assessed based on measurements of contaminant mass discharge. Furthermore, these very few comprise relatively small-scale pilot tests, with two of them having been conducted at the Borden test site. As noted by the authors of these latter studies, relatively ideal subsurface conditions at the Borden site produced optimal performance results for ISCO that are unlikely to be representative for many sites. Thus, there is great interest in assessing the performance of a large-scale ISCO project based on contaminant mass discharge measurements for a site with highly heterogeneous subsurface conditions.

A large-scale permanganate-based ISCO effort has been conducted over the past ten years at a federal Superfund site in Tucson, AZ, for which trichloroethene (TCE) is the primary contaminant of concern. There are two objectives for this study. The first is to assess the performance of a full-scale remediation effort employing ISCO for a site that is representative of the many large, complex chlorinated-solvent contaminated sites present in the USA and elsewhere wherein multiple source zones have contributed to the creation of a large (~10's km^2) contaminant plume. The second is to illustrate an enhanced approach for performance

assessment of source-zone remediation efforts. The performance of the ISCO project is assessed through analysis of changes in contaminant mass discharge. We first employ the standard approach, which involves measuring source-zone discharge once before and once after ISCO implementation. We then employ an additional approach based on a high-resolution, real-time characterization of contaminant mass discharge at the plume scale. This latter approach provides a more robust analysis of discharge perturbations, including potential rebound effects, and provides a means by which to link source-zone remediation to impacts on site-wide risk. The performance assessment covers a period of approximately 10 years, including several years of pre and post monitoring. The site that was the focus of the study is part (Southern section) of the Tucson International Airport Area (TIAA) federal Superfund site in southern Arizona that is discussed above. Details of the site and ISCO project are presented in the published paper (5).

Contaminant Mass Discharge

The results of the contaminant mass discharge tests conducted at the Site 3 source zone before and after permanganate injection are presented in Figure 5.2.1-1. The initial contaminant mass discharge for the short-term test conducted prior to ISCO was approximately 0.6 kg/d. The values decreased over the course of the test to an asymptotic value of 0.1 kg/d. The results obtained for the longer-term test, which was 21 months in duration, are similar to those for the one-month test. These results suggest that the short-term test provided a representative characterization of contaminant mass discharge for the source zone.

The initial contaminant mass discharge for the test conducted after ISCO was approximately 0.04 kg/d (Figure 5.2.1-1). The values decreased over the course of the test to an asymptotic value of approximately 0.025 kg/d. Thus, both the peak and asymptotic contaminant mass discharge values were lower after permanganate injection, by factors of 15 and 4, respectively. The reduction in contaminant mass discharge is approximately 75% based on comparison of the respective asymptotic values. The magnitude of observed reduction is consistent with reductions reported for several pilot-scale source-zone remediation efforts employing a variety of methods.

The impact of ISCO at the plume scale was evaluated by examining the change in contaminant mass discharge associated with the pump-and-treat system. The integrated contaminant mass discharge for the entire pump-and-treat system as a function of time is shown in Figure 5.2.1-2. The composite contaminant mass discharge was relatively constant for several years prior to implementation of ISCO, with a value of approximately 0.7 kg/d. This behavior indicates that mass removal via pump and treat had stabilized to a quasi steady-state under the extant conditions. Contaminant mass discharge began to decrease almost immediately upon ISCO startup due to a combination of source-zone concentration reduction and flow reduction, and declined to a final value of 0.1 kg/d at the completion of injections. After year 4, the contaminant mass discharge began to increase, before stabilizing at the current value of approximately 0.2 kg/d. Based on these data, implementation of in-situ chemical oxidation resulted in a reduction in plume-scale contaminant mass discharge of approximately 70%.

As noted above, the contaminant mass discharge exhibited a rebound after the completion of permanganate injections. The rebound period lasted for approximately one year before the discharge stabilized. The observation of rebound effects is consistent with results observed for prior ISCO applications wherein rebound is often observed in monitoring-well concentrations. The collection of the high-resolution integrated discharge data provided a means to monitor for rebound to ensure that the source-zone tests were conducted after the rebound period. According

to the review of Krembs et al. (2010), there have been no prior studies evaluating post-ISCO rebound based on continuous measurements of contaminant mass discharge.

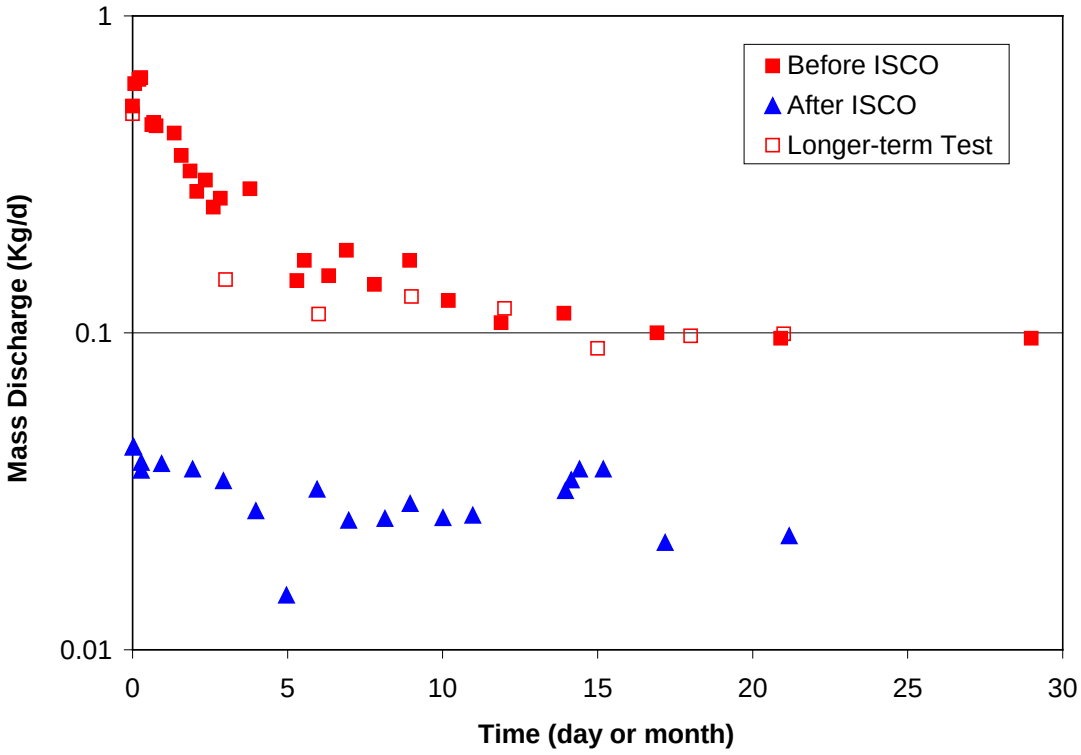

Figure 5.2.1-1. Results of contaminant mass discharge tests conducted at the Site 3 source zone before and after ISCO. Tests labeled "Before ISCO" and "After ISCO" have a time scale of days; the longer-term test (conducted before ISCO) has a time scale of months.

In the prior discussions, the reductions in contaminant mass discharge were attributed solely to ISCO. However, the potential impact of other activities and conditions at the site should be evaluated. There is no evidence of natural attenuation of TCE via biotic or abiotic transformation reactions at this site. Hence, aside from the oxidation associated with the ISCO applications, there are no other transformation processes present to contribute to TCE concentration reductions. Full-scale soil vapor extraction operations were implemented at the source zones starting in mid-1996, and were completed in July 2004. Hence, the ISCO implementation at Site 3 occurred after completion of SVE operations. These conditions, in conjunction with the steady-state behavior observed for the integrated (plume-scale) contaminant mass discharge before and after ISCO, indicate that the observed changes in contaminant mass discharge can be attributed to the impact of the ISCO project.

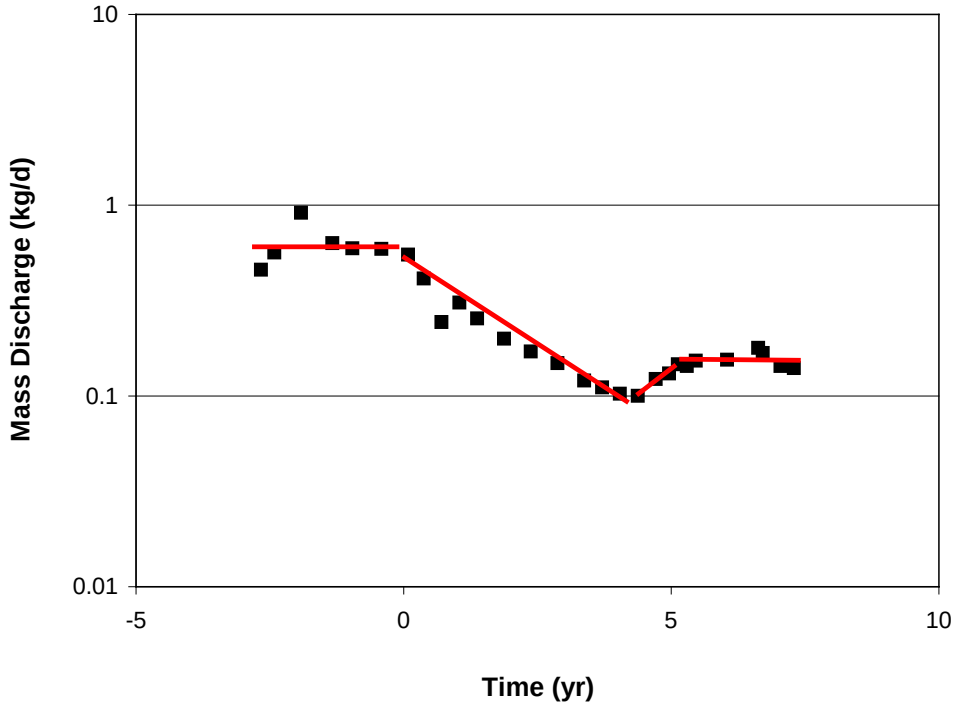

Figure 5.2.1-2. Integrated contaminant mass discharge for the entire site, including contributions from the source zones and the contaminant plume. Time 0 denotes the start of ISCO. The lines are included for visualization purposes and do not represent any type of quantitative analysis.

Groundwater and Sediment Concentrations

The concentration of Mn in groundwater samples collected from the extraction well used for the contaminant mass discharge tests ranged from approximately 2-10 ug/L throughout the post-injection test. These values are consistent with background Mn concentrations measured for multiple wells located in the injection zone, which ranged from approximately 1 to 20 ug/L. The results obtained for dissolved oxygen, oxidation-reduction potential, dissolved solids, and color were also all consistent with background values measured prior to permanganate injection. These results indicate that the injected permanganate had dissipated significantly prior to the post-ISCO characterization efforts. Concentrations of Mn in the influent to the treatment plant have remained below the detection limit throughout operation of the pump-and-treat system, including during and after the permanganate injections.

The concentrations of TCE in groundwater samples collected before and after ISCO from a number of monitoring wells within Site 3 are presented in Figure 5.2.1-3. The TCE concentrations prior to ISCO ranged from 33 to 1000 ug/L. A wide range in concentration reductions was observed, with a mean reduction of 68%. The mean concentration reduction is similar to the reductions in contaminant mass discharge determined from both the source-zone and plume-scale analyses. A mean reduction in TCE concentrations of 87% was observed for Site 2. The greater reduction observed for Site 2 may be related in part to the greater amount of permanganate used at that site.

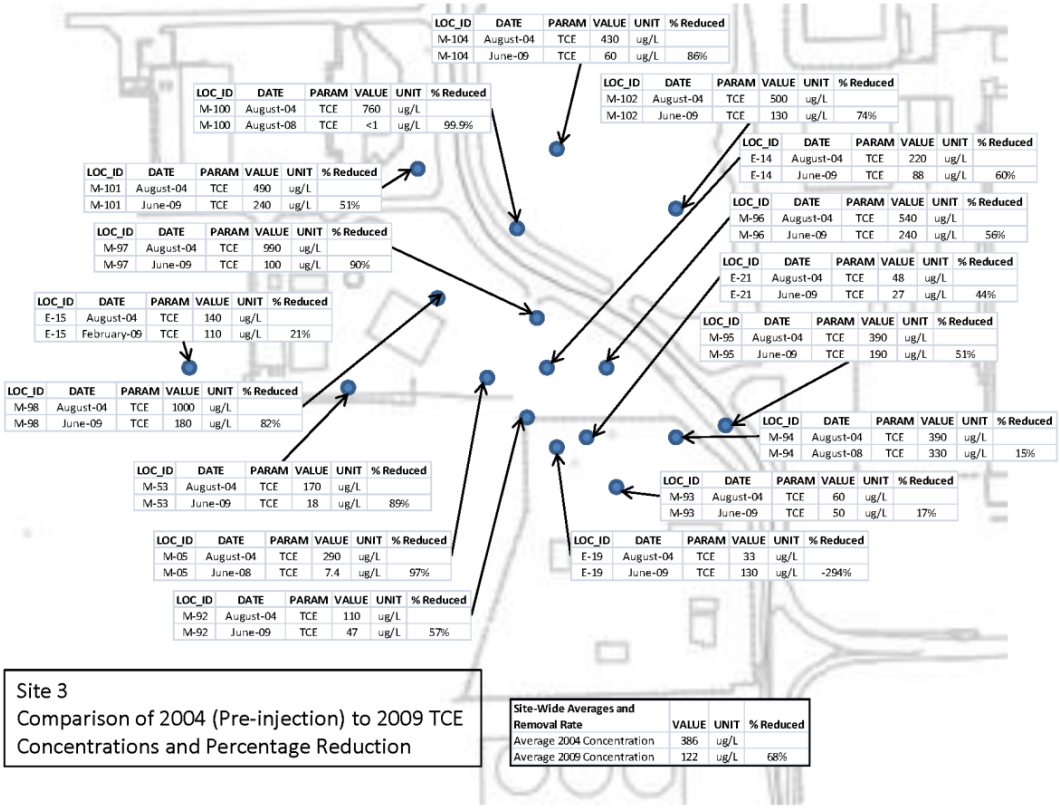

Figure 5.2.1-3. Concentrations of trichloroethene in groundwater collected from monitoring wells located within the Site 3 source zone. These monitoring wells were used for permanganate injection. Well E-14, used for the source-zone contaminant mass discharge tests, is located in the center of the plot.

Concentrations of Mn determined for the sediment samples are presented in Figure 5.2.1-4. The results show that the sediments contain high and somewhat spatially variable background levels of Mn. In addition, while the natural oxidant demand associated with the sediment is low, there could be some impact of permanganate reaction with sediment organic matter. These conditions limit the use of manganese-oxide presence as an indicator of TCE oxidation. However, as noted above, the borehole used to collect the sediment was located approximately 5 m from a well used for permanganate injections. Given such close proximity, it is likely that permanganate solution contacted the sediment. In addition, the significant reductions in sediment-phase TCE concentrations discussed below serve as an indirect indictor of permanganate contact. The similar range of Mn concentrations for before and after ISCO suggests that the use of permanganate and the associated formation of oxides would have minimal impact on hydraulic conductivity. The potential for much higher concentrations of oxide (e.g., rinds) to form in localized association with pockets of organic liquid can not be discounted. Such formation could potentially impact local-scale mass transfer and mass flux, as observed in prior laboratory experiments (e.g., 24-26).

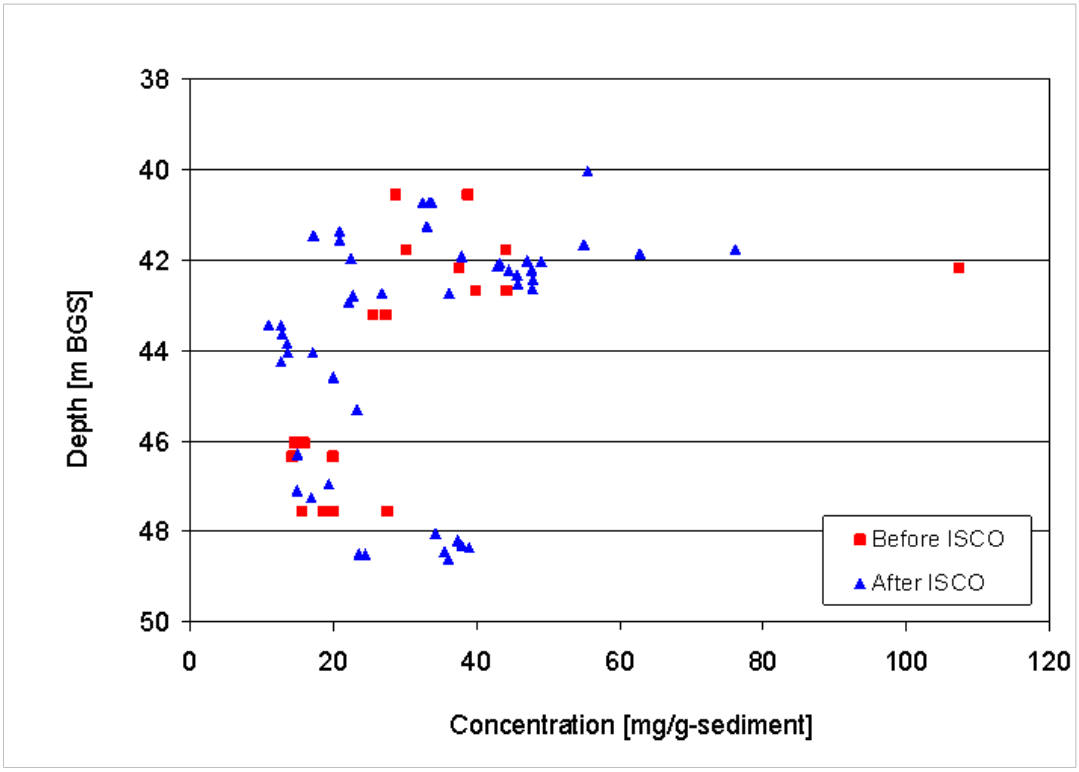

Figure 5.2.1-4. Sediment concentrations of Mn for core samples collected from a single borehole drilled before ISCO and a single borehole drilled after ISCO for Site 3.

The concentrations of TCE for sediment samples collected from boreholes drilled before and after ISCO are presented in Figure 5.2.1-5. The highest concentrations prior to ISCO are associated with the lower-permeability layer that adjoins the top of the Upper Aquifer. The measurable TCE concentrations remaining after ISCO are associated with the bottom portion of that lower-permeability layer. Remediation of this unit via a hydraulic-based method such as ISCO is expected to be less effective than for the adjacent higher-permeability units. Comparison of the two sets of data indicates that a significant reduction (aggregate ~90%) in TCE concentrations occurred between sampling events. This reduction is the combined result of mass reduction via ISCO and mass removal via water flushing (pump and treat). The impact of pump and treat on mass removal was examined in prior simulations of contaminant transport for the site, which produced an estimated reduction in total source-zone mass of ~15% over an 11-year period of pump and treat (21). While local mass-reduction rates are expected to exhibit significant spatial variability, the modeling results provide an indication that mass reduction via water flushing would in general be expected to be relatively low for the 10-year ISCO project. This suggests that the significant reduction observed for the sediment data was caused primarily by ISCO.

Figure 5.2.1-5. Sediment concentrations of trichloroethene for core samples collected from a single borehole drilled before ISCO and a single borehole drilled after ISCO for Site 3. For the post-ISCO core, approximately 100 samples were analyzed; only 25% of that total is presented in the figure (concentrations for all samples except the two shown in the figure were below the detection limit).

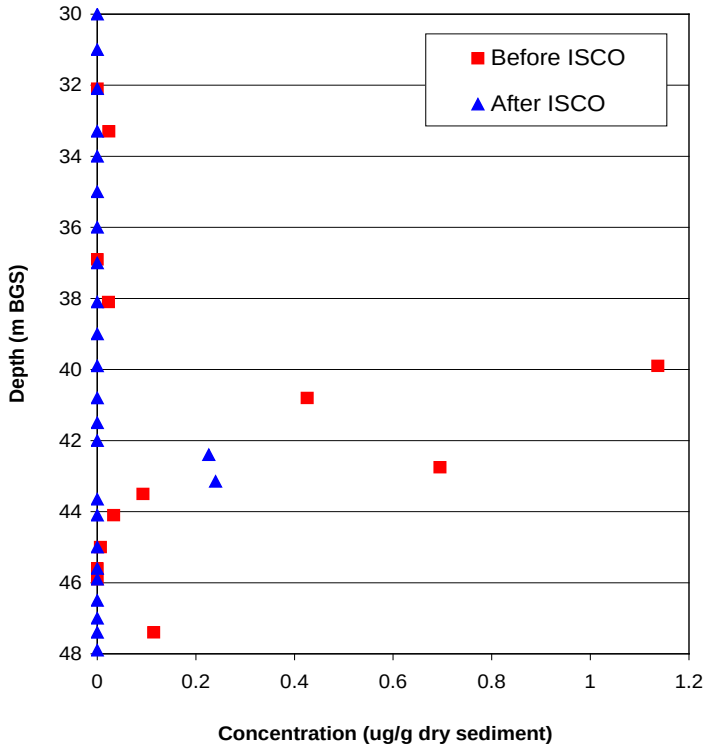

Impact of Source-zone Architecture and Mass-transfer Phenomena on Reductions in Contaminant Mass and Mass Discharge

Maximum discharge rates were observed at the beginning of each contaminant mass discharge test, followed by asymptotic conditions (Figure 5.1.4-1), as noted above. The extraction well was not pumped for at least several months prior to the start of each test, which allowed quasi-equilibrium conditions to form with respect to contaminant distribution between the advective and poorly-accessible domains. The peak discharge at the beginning of the test thus represents removal of a "maximum" loading of mass from the advective domain that was generated during the preceding non-pumping period. Conversely, the asymptotic discharge represents primarily mass removal associated with transfer from the poorly-accessible domains. The rebound of integrated contaminant mass discharge observed after completion of ISCO (Figure 5.1.4-2) is attributed to mass transfer of TCE from the poorly-accessible domains, with additional contribution from displacement by upgradient groundwater. The approximate one year of rebound incorporates the time for permanganate to dissipate once injections ceased, in addition to the inherent characteristic times of contaminant mass transfer and transport.

Measurements of flow and contaminant concentration for each extraction well of the pump-and-treat system allow calculation of the relative contributions of each source zone and the plume to the total integrated contaminant mass discharge. For the three years prior to the start of ISCO, Sites 2 and 3 contributed approximately 47% to total contaminant mass discharge. This was reduced significantly after ISCO. Interestingly, the aggregate mass discharge associated with the plume also decreased after ISCO. This decrease is due partly to reductions observed for four extraction wells that are all located downgradient of the Site 3 source zone, with distances ranging from approximately 200 to 1100 meters. Significant decreases in TCE concentrations occurred for these wells at varying times after the start of ISCO. For example, distinct decreases in TCE concentrations are observed approximately seven months and three years after the start of ISCO for wells EL02 and E23, respectively, which are located approximately 180 and 675 meters from the perimeter of Site 3. A mean pore-water velocity of approximately 0.7 m/d is estimated based on the elapsed times and distances; this value is similar to the estimated upper range of mean pore-water velocities (~1 m/d) in that area based on measured hydraulic gradients and conductivities. Given this, it is possible that the concentration reductions observed for these plume extraction wells reflect the impact of ISCO implementation at the Site 3 source zone.

The significant reduction in contaminant mass discharge observed for the ISCO project suggests that the permanganate injections produced an appreciable reduction in contaminant mass. Direct analysis of mass reductions was not feasible for the project, which is typically the case. Permanganate consumption associated with aqueous-phase TCE and natural sediment demand is estimated to have comprised roughly 10% of the total injected. Hence, given the estimated contaminant mass present and the amount of permanganate injected, it is projected that there was sufficient permanganate to cause a significant reduction in contaminant mass.

While the reduction in mass discharge obtained for this study was significant, it is lower than the weighted-average reduction of approximately 92% observed for a small-scale permanganate-ISCO test conducted at the Borden research site in Canada (Thomson et al., 2007). The reduction in contaminant mass discharge produced by a reagent-injection-based method such as ISCO will be controlled by reagent-contaminant contact, which in turn is a function of several factors including reagent-injection conditions, mass-transfer processes, and source-zone architecture. Thus, contaminant mass discharge results should be interpreted in light of site-specific conditions. One factor likely contributing to the disparity in observed reductions is the degree of heterogeneity associated with the two sites, and the resultant expected differences in mass-removal behavior. The test domain at the Borden site is comprised primarily of a sand unit with a relatively small degree of heterogeneity. Given this and the method by which organic liquid was introduced to the test domain, it would be anticipated that the organic liquid would be relatively accessible to flowing groundwater (and permanganate solution) and thus that mass removal would be minimally influenced by mass-transfer limitations. That such is the case is supported by the results of prior research. In contrast, a large fraction of the contaminant mass at the TIAA site appears to be poorly accessible to flowing groundwater, which significantly constrains mass removal and associated mass discharge.

Different reagent-injection approaches were used for the two sites. The permanganate was introduced via an induced-gradient recirculation approach for the Borden project, which would be anticipated to maximize reagent-contaminant contact for the Borden site conditions. Conversely, the use of such an induced-gradient approach for the source-zone architecture present at the TIAA site would be anticipated to exacerbate mass-transfer constraints and thus

further limit reagent-contaminant contact. Hence, permanganate was introduced via an injection/natural-dissipation mode for the TIAA site.

Summary

The performance of a large-scale permanganate-based ISCO project was assessed by examining the impact of treatment on contaminant mass discharge. While the effectiveness of ISCO may have been influenced by the high degree of heterogeneity present at the site, a significant reduction in contaminant mass discharge was achieved. One anticipated benefit of this reduction is a decrease in the length of time required to operate the pump-and-treat system. The implementation of ISCO reduced, but did not eliminate, contaminant mass discharge from the source zones. Based on these results, continued management of contaminant mass discharge from the source zones will need to be considered as part of the long-term management of the site. This scenario is likely to be manifest at many of the large chlorinated-solvent contaminated sites in the USA.

The use of contaminant mass discharge, rather than contaminant mass, as a performance metric has several advantages, including greater accessibility, less uncertainty, and greater relevance for risk-based assessment. An enhanced approach for characterizing contaminant mass discharge was illustrated that extends the standard source-zone scale measurements to incorporate additional characterization at the plume scale. Collection of integrated plume-scale contaminant mass discharge data before, during, and after the ISCO treatment period provided a high-resolution, real-time analysis of discharge perturbations, including rebound effects. This approach provides a robust means by which to link source-zone remediation to impacts on site-wide risk, and is anticipated to have broad utility for assessing remediation effectiveness.

5.2.2 Application of ISCO for Source Containment in a Low-Permeability System

Source zones located in relatively deep, low-permeability formations provide special challenges for remediation. Such a source zone is located in an isolated section of the TIAA site. 1,1-Dichloroethene (DCE) contamination is present at the Samsonite Building Area (SBA), with aqueous concentrations averaging 30 µg/L for the local shallow groundwater system. A significant fraction of DCE is thought to be located in lower permeability strata adjacent to the water table. Information collected by site consultants indicate contamination occurs as dissolved and sorbed phases, with no evidence of organic liquid being present. A small groundwater contaminant plume has formed downgradient of the source zone.

Given the site conditions, source containment using hydraulic-based methods or permeable reactive barriers is impractical, and aggressive mass-removal approaches based on reagent injection (e.g., ISCO, enhanced-solubility reagents) are likely to be ineffective. In-situ thermal or electrokinetic methods may be feasible, but are relatively expensive. Considering the hypothesized contaminant distribution, and the low contaminant mass discharge, these latter two methods are likely to be cost-ineffective. One possible approach for such conditions is to create a persistent treatment zone for purposes of containment.

The objective of this approach is to reduce the contaminant mass discharge from the source zone via source containment. In this case, containment is effected by creation of a persistent treatment zone through injection of permanganate solution. Given the site conditions (low permeability, low hydraulic gradient), it was hypothesized that the reagent solution would remain primarily within the source area for several years. Thus, a single round of injection was designed, minimizing costs. Details of methods are presented in the manuscript (16).

Multiple injection wells were emplaced in the source zone area (Figure 5.1.5-1), with well screens spanning both the vadose and saturated zones (23 to 28 meters below ground surface). Core subsamples collected during borehole drilling were analyzed for organic matter and extracted for DCE. Bench-scale studies using core material determined that DCE was readily degraded by $KMnO_4$, even at lower reagent concentrations (< 1 mM). The natural oxidant demand was determined to be 1.0×10^{-5} grams of $KMnO_4$ per gram of sediment.

The reagent injections commenced in 2005. The injection wells (IW) were each injected with approximately 250 kilograms of ~1.7% $KMnO_4$ solution. Several groundwater parameters were measured pre- and post-injection within the treatment zone. Groundwater collected from two downgradient monitoring wells was also monitored.

The programs MODFLOW-2000 and MT3D3 were employed, using hydraulic conductivity values and additional physical parameters from the site, to simulate the $KMnO_4$ injection. The results of the simulations indicated that the injected reagent solution would persist within the source zone for several years.

As of February 2012, $KMnO_4$ is still present in the source zone (Figure 5.2.2-1). This result substantiates the persistence of the treatment zone per the initial hypothesis. Site monitoring continues in an effort to determine the long-term effectiveness of $KMnO_4$ injection on DCE concentrations. DCE concentrations in groundwater collected from two downgradient monitoring wells (CRA-13, S-42) have been monitored periodically. The concentrations for samples collected from S-42 during a seven-year period prior to ISCO averaged approximately 6.5 ug/L. Concentrations for the past two years have averaged approximately 2.8 ug/L. Concentrations for samples collected from CRA-13 have decreased from approximately 1 to 0.6 ug/L. These results indicate that the treatment zone is causing a reduction in contaminant concentrations of groundwater discharging from the source zone. In summary, the results support the effectiveness of the method for containing a source zone in a deep, low-permeability system.

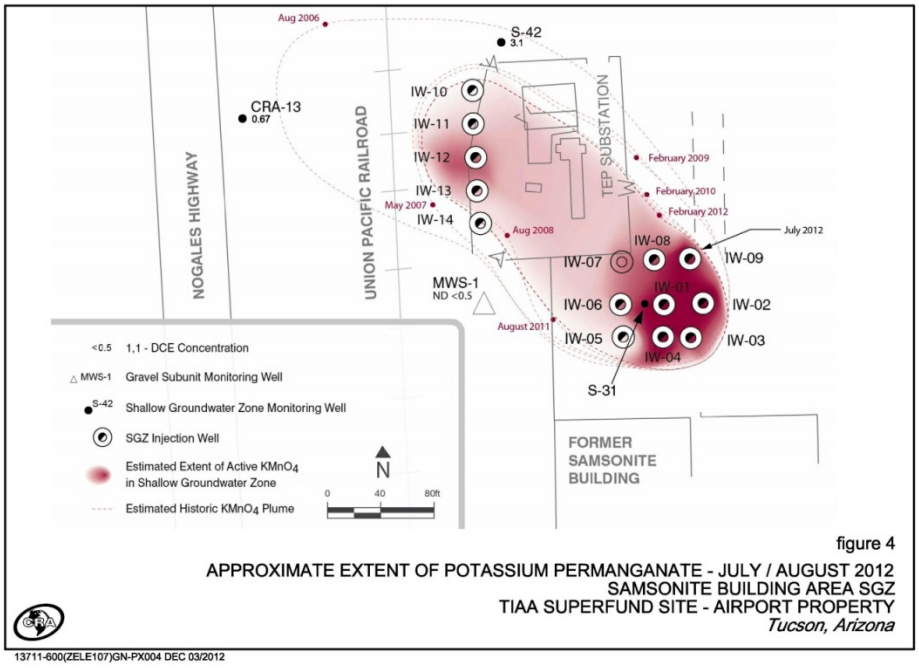

Figure 5.2.2-1. Map of test site. Injection and monitoring wells are marked. The region influenced by the permanganate solution is noted annually.

5.3 Plume Response and Persistence

5.3.1 Impacts of Sorption/Desorption

This study investigated the effect of contaminant aging on the sorption/desorption and transport of trichloroethene in a low organic-carbon content aquifer material, comparing mass removal and long-term, low-concentration elution tailing for field-contaminated, synthetically-aged (contact times of approximately four years), and freshly-amended aquifer material. The experiments conducted for the initial set of experiments are enumerated in Table 5.3.1-1. Additional experimetns, as noted below, were conducted to examine the impact of clay minerals on sorption and transport. Details of the methods and materials used are presented in the published papers and manuscript in preparation (1,9,13).

Table 5.3.1-1. Summary of miscible-displacement experiments.

Column	Experiment	Sand %	Silt %	Clay %	ρ_b[a] g cm^{-3}	n[b]	V[c] cm h^{-1}	Slope of Low-Concentration Elution Tail[d]
A	Aged	95.7	1.8	2.5	1.72	0.34	22.4	-0.008
	Fresh						22.2	-0.008
B	Aged	99.0	0.0	1.1	1.56	0.37	23.3	-0.003
	Fresh						20.4	-0.003
C	Aged	97.5	1.3	1.3	1.81	0.32	24.2	-0.008
D	Fresh	96.3	1.8	2.0	1.80	0.33	23.4	-0.02
E	Field-Contaminated	NM[f]	NM	NM	~1.73	~0.37	~25.0	-0.007

[a]Bulk density (ρ_b).
[b]Porosity.
[c]Pore-water velocity
[d]Calculated for the low-concentration elution tail.

Impact of Aging

The observed retardation factors and apparent distribution coefficients (K_d) obtained for trichloroethene from the miscible-displacement experiments (i.e., as a function of the initial trichloroethene aqueous-phase concentration) are presented in Table 5.3.1-2. These values are similar to values reported in the literature for trichloroethene (ranging from 0.01 to 0.24 mL g^{-1}) for aquifer materials with similarly low organic-carbon contents. Previous experimental results have shown that sorption of trichloroethene by the aquifer material is nonlinear. Specifically, the magnitude of the sorption coefficient is smaller for the experiments conducted with the higher trichloroethene input concentration. This nonlinearity was described using a Freundlich isotherm (r^2 = 0.93), with a Freundlich-sorption coefficient (K_f) equal to 0.05 mg$^{(0.17)}$ L$^{0.83}$ kg^{-1} and Freundlich exponent equal to 0.83. Nonlinear sorption is often hypothesized to result from interactions of sorbate with so-called hard carbon, a condensed, amorphous organic matter matrix, which would be consistent with the organic-carbon properties of the aquifer material (composed of approximately 61% hard carbon, e.g., kerogen and black carbon).

Table 5.3.1-2. Parameter values for miscible-displacement experiments.

Column	Experiment	R_{TCE}[a]	K_d[b] mL g^{-1}	Fraction TCE Sorbed Mass[c], %	Percent recovery
A	Aged	1.003	0.001	0.3	99.3
	Fresh	1.09	0.017	8.5	99.1
B	Aged	1.1	0.026	11	98.8
	Fresh	1.2	0.038	14	100.7
C	Aged	1.07	0.012	6.6	99.8
D	Fresh	1.08	0.015	8.1	99.9

[a]Retardation factor obtained through moment analysis of trichloroethene's elution tail.
[b]Apparent distribution coefficient as a function of the initial trichloroethene aqueous-phase concentration.
[c]For initial condition such that total mass includes trichloroethene present in the aqueous phase.

The results of experiments designed to determine the potential effects of the experimental apparatus on the transport behavior of trichloroethene are shown in Figure 5.3.1-1. Comparison of these elution curves indicates that there is minimal retention and elution tailing of trichloroethene associated with the experimental apparatus. These results are supported by a comparison of the nonreactive tracer results obtained for the experimental apparatus (i.e., a column containing no aquifer material) compared to those obtained for trichloroethene in the same system (results not shown).

The elution behavior of trichloroethene observed for the long-term, synthetically-aged treatments is compared to that observed for the fresh treatments in Figure 5.3.1-1. The overall elution behavior of trichloroethene, specifically the rapid concentration decrease and the long tail, is essentially identical for the two treatments. The elution of trichloroethene to the detection limit required greater than 200 pore volumes of flushing for the low-C_o experiments and greater than 150 pore volumes of flushing for the high-C_o experiments, despite the minimal retention of trichloroethene by the aquifer material. This nonideal behavior indicates that significant mass-transfer constraints are influencing transport of trichloroethene in the system. For example, approximately 98% of the total trichloroethene mass (including resident aqueous-phase mass) was removed in the first four pore volumes for Column C, whereas the remaining trichloroethene mass removal required greater than 150 pore volumes of additional flushing (see Figure 5.3.1-2). This 2% of total mass represents approximately 29% of the initial sorbed mass prior to elution. The similarity in elution behavior observed for the two treatments suggests minimal impact of aging.

The data obtained from the miscible-displacement experiments were analyzed by moment analysis to determine mass recoveries, which ranged from 98.8% to 100.7% (Table 5.3.1-2). No effect of contaminant aging on removal efficiencies was observed. Following the complete elution of trichloroethene (i.e., effluent concentrations below the detection limit), solvent extractions of the aquifer material were performed for Columns C and D. The concentration of trichloroethene was below detectable levels (corresponding to <0.1% of the initial TCE mass) for

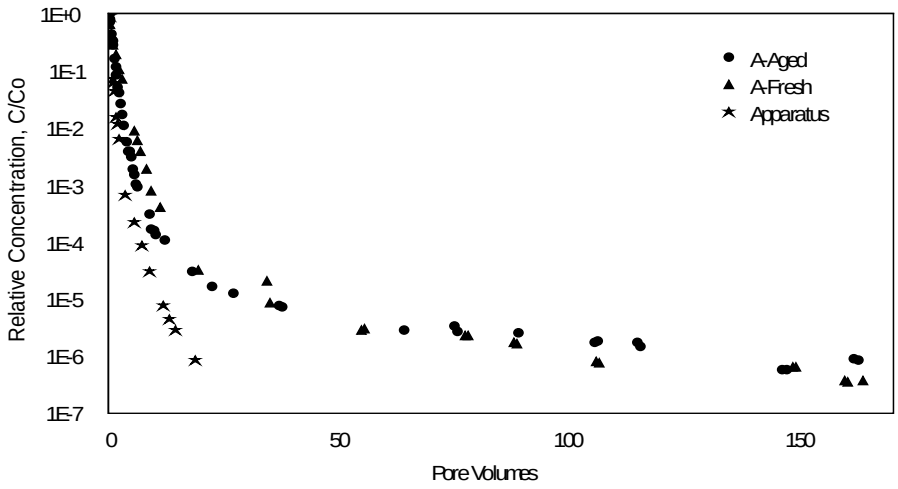
1E+0
1E-1
1E-2
1E-3
1E-4
1E-5
1E-6
1E-7
Relative Concentration, C/Co
0
50
100
150
Pore Volumes
A-Aged
A-Fresh
Apparatus

A

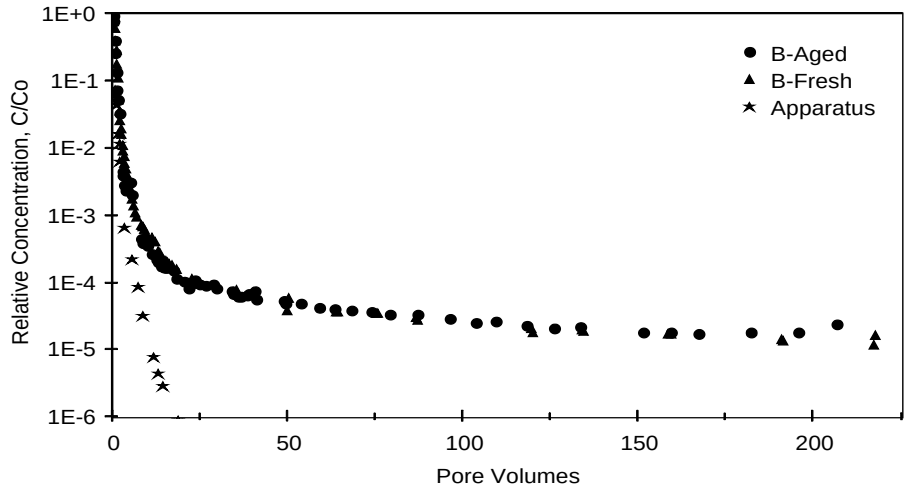
1E+0
1E-1
1E-2
1E-3
1E-4
1E-5
1E-6
Relative Concentration, C/Co
0
50
100
150
200
Pore Volumes
B-Aged
B-Fresh
Apparatus

B

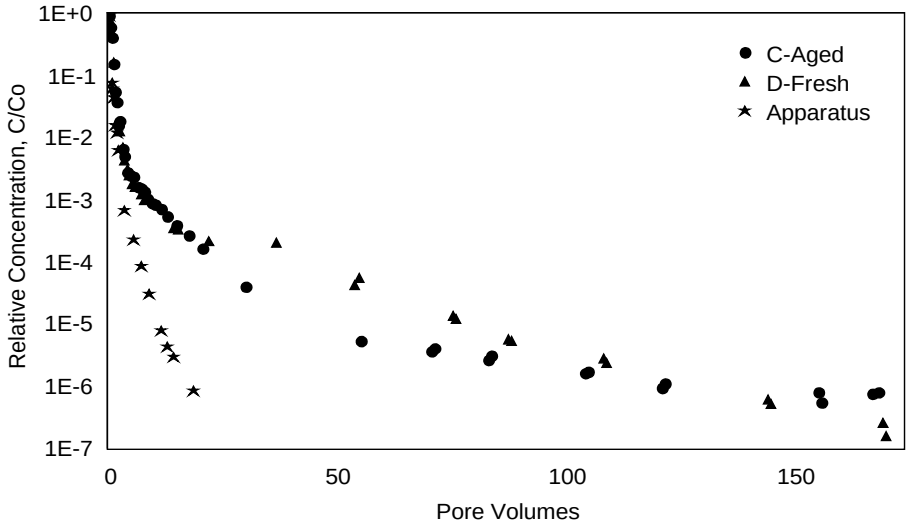
1E+0
1E-1
1E-2
1E-3
1E-4
1E-5
1E-6
1E-7
Relative Concentration, C/Co
0
50
100
150
Pore Volumes
C-Aged
D-Fresh
Apparatus

C

Figure 5.3.1-1. Comparison of elution tailing behavior for the long-term, synthetically-aged and freshly-amended aquifer material. Also included are results obtained for an experiment conducted using a column containing no aquifer material (Apparatus). (A) Column A: High-concentration trichloroethene (~900 mg L^{-1}) sequential miscible-displacement experiments. (B) Column B: Low-concentration trichloroethene (~10 mg L^{-1}) sequential miscible-displacement experiments. (C) Column C and Column D: Independent, high-concentration trichloroethene (~900 mg L^{-1}) miscible-displacement experiments.

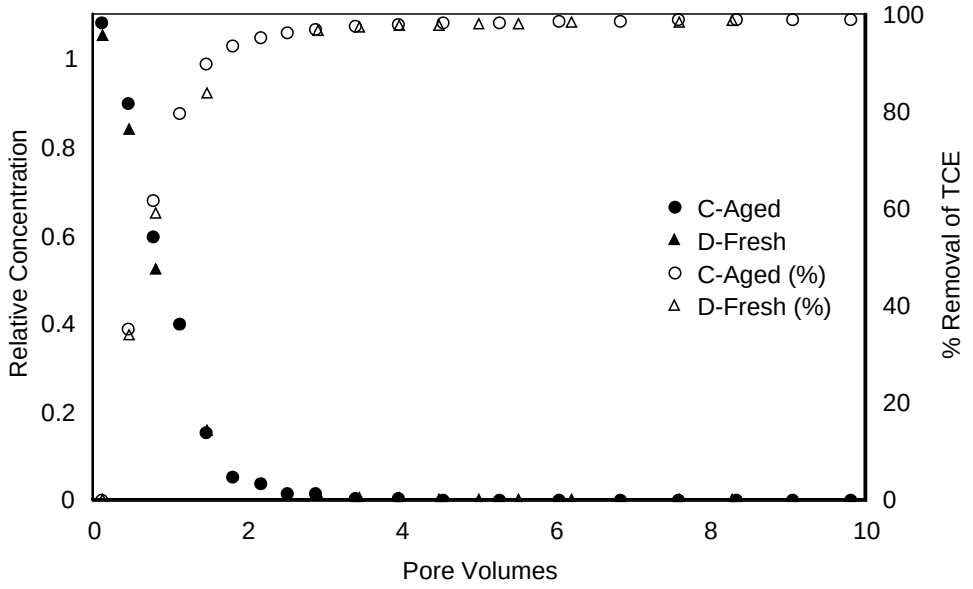

Figure 5.3.1-2. Representative mass removal curves for the long-term aged and freshly-amended aquifer material.

both cases, independent of contaminant aging, which is in agreement with the elution mass recovery values reported in Table 5.3.1-2. The efficiency of the solvent extraction using dichloromethane may be somewhat constrained for systems comprising condensed, carbonaceous organic material. However, as noted previously, the mass balance is consistent between the solvent-extraction and elution-recovery analyses. In addition, the results are consistent with those of the flow-interruption experiments described below.

Flow-interruption experiments were performed at the end of selected trichloroethene elution experiments wherein flow was interrupted for 13 days. The aqueous-phase concentrations increased after flow was resumed, indicating the existence of nonuniform concentration distributions and associated rate-limited mass transfer (i.e., nonequilibrium conditions) in the system. Additionally, moment analysis of these flow-interruption experiments yielded nearly identical mass recoveries (1.0 μg and 0.93 μg, for Aged-A and Fresh-A, respectively) for the two treatments, i.e., independent of trichloroethene=s contact time with the aquifer material. This is consistent with the observations reported above.

A comparison of the elution tailing behavior of the field-contaminated, synthetically-aged, and freshly-amended aquifer material is shown in Figure 5.3.1-3. While some uncertainty is associated with the elution curve for the field-contaminated aquifer material due to the flow-interruptions, very similar low-concentration elution tailing is observed for all cases, independent of contaminant aging. Furthermore, the slopes of the elution tails (log-concentration versus pore volumes) for the field-contaminated (-0.007), Aged-A (-0.008), and Fresh-A (-0.008), for example, are very similar (see Table 5.3.1-1). This analysis indicates similar low-concentration elution behavior for the field-contaminated, synthetically-aged, and freshly-amended aquifer material (representing contact times of >40 years, ~4 years, and <8 hours, respectively), supporting the finding mentioned previously that the general nonideal behavior of trichloroethene is independent of contaminant aging.

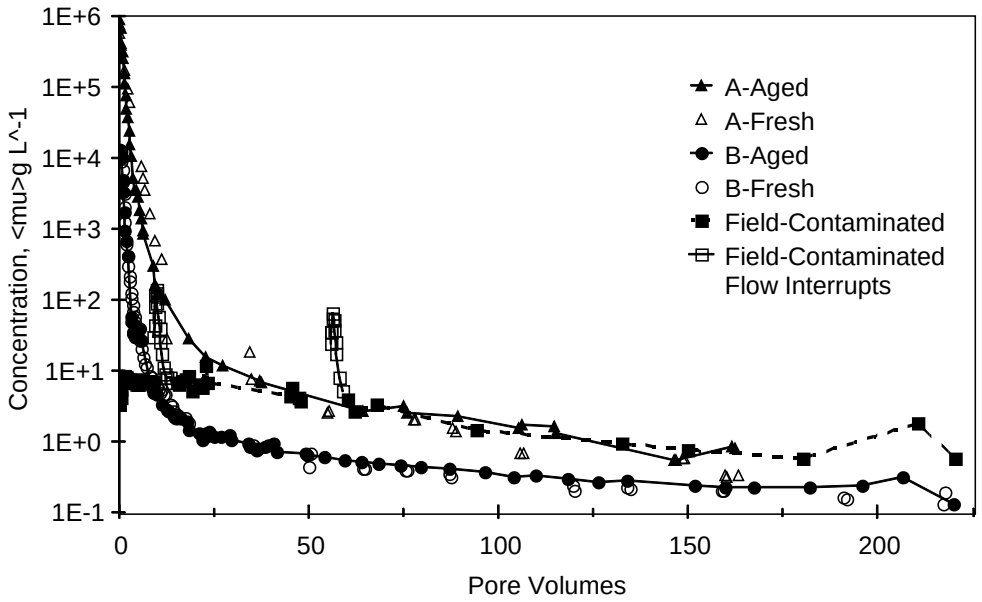

Figure 5.3.1-3. Comparison of long-term, elution tailing behavior for the field-contaminated, synthetically-aged, and freshly-amended aquifer material. Column A: High-concentration trichloroethene (~900 mg L^{-1}) sequential miscible-displacement experiments. Column B: Low-concentration trichloroethene (~10 mg L^{-1}) sequential miscible-displacement experiments.

Intercalation of TCE by Clays

The objective of this research was to examine the potential for intercalation of trichloroethene (TCE) by clay minerals associated with aquifer sediments. Sediment samples were collected from the TIAA field site in Tucson, AZ. Two widely used Montmorillonite specimen clays were employed as controls. X-ray diffraction, conducted with a controlled-environment chamber, was used to characterize smectite interlayer d-spacing for three treatments (bulk air-dry sample, sample mixed with synthetic groundwater, sample mixed with TCE-saturated synthetic groundwater). Details of the materials and methods used are presented in the published paper (9).

The results of the XRD measurements for Na-Montmorillonite (SWy-2) are presented in Figure 5.3.1-4. The baseline scan for untreated Na-Montmorillonite, shown as the solid line in Figure 1, shows a smectite peak at 8.35 º2θ. This measurement was used to calculate a d-spacing of 10.6 Å. Chipera et al (2001) measured a d-spacing of 11.2 Å for SWy-2. Diffractograms of smectite clays exhibit variability due to relative humidity and other factors. Considering this variability, the d-spacing of the smectite clay measured in the current experiment is within the range of literature values. The XRD measurements for the treated SWy-2 samples are compared to this baseline scan to determine if a change in the d-spacing occurred as a result of treatment.

One of the TCE-saturated synthetic groundwater treatments shows a well-defined smectite peak at 4.85 º2θ with a d-spacing of 18.2 Å. There is no significant smectite peak present at or near the 8.35 º2θ position, which was the peak location observed for the baseline untreated scan. The difference between the d-spacing values for the baseline untreated sample and the sample treated with TCE-saturated synthetic groundwater is 7.6 Å. Figure 5.3.1-4 shows the results of a second sample that was treated with TCE-saturated synthetic groundwater. A smectite peak with a d-spacing of 15.2 Å is present at 5.83 º2θ. Similar to the prior scan, there was no smectite peak present at 8.35 º2θ. The difference in d-spacing of this sample treated with TCE-saturated synthetic groundwater and the untreated sample is 4.6 Å. The observed increases in the d-spacing indicate that the SWy-2 expanded when it was treated with TCE-saturated synthetic groundwater.

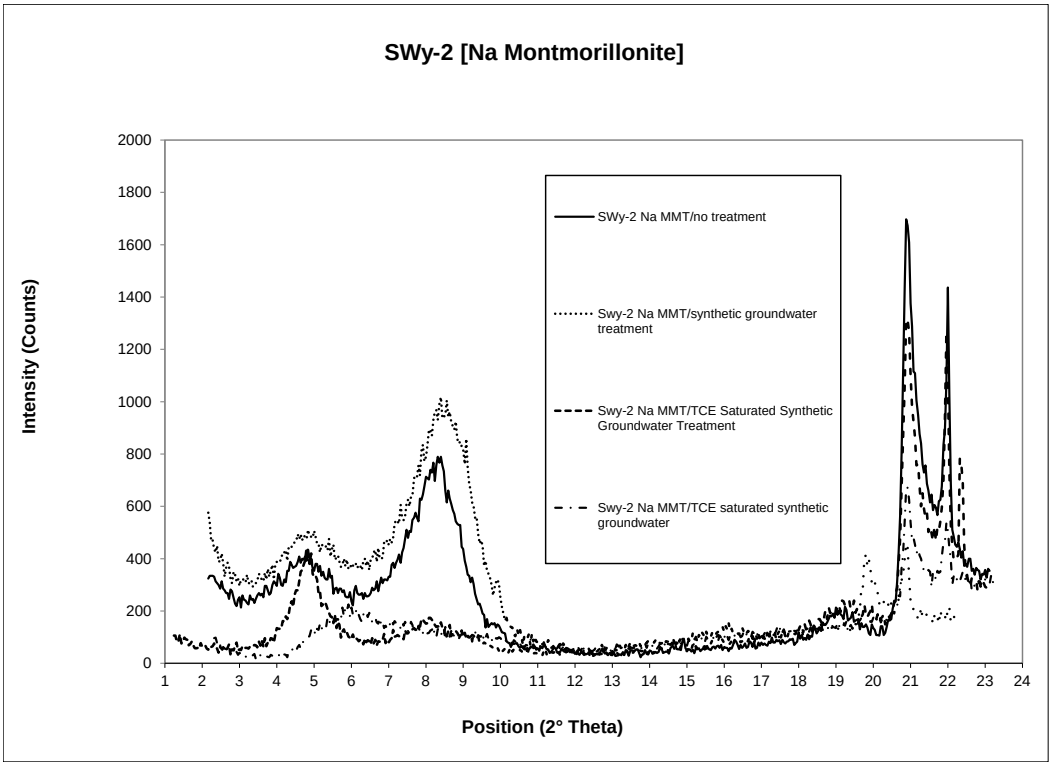

Figure 5.3.1-4. Results of the XRD measurements for the SWy-2 (Na montmorillonite) samples.

The diffractogram for the treatment where the SWy-2 was exposed to synthetic groundwater with no TCE (Figure 5.3.1-4) is similar to that of the untreated sample (the baseline scan). This indicates that the presence of the synthetic groundwater solution alone caused no measurable expansion for the SWy-2. The similarity of d-spacings for the untreated baseline sample and the sample treated with synthetic groundwater is expected given that both samples have a common origin and therefore are likely to have identical interlayer ion compositions, and that the baseline sample was air-dried rather than oven-dried. These results in conjunction with the increase in d-spacing observed for the samples treated with TCE-saturated groundwater indicate that TCE was intercalated within the interlayer space of the clay mineral.

Similar results were obtained for the Ca-montmorillonite (STx-1b) sample. The STx-1b base scan with no treatment shows a smectite peak at 6.90 º2θ with a d-spacing of 12.8 Å. There was no significant change for the sample treated with synthetic groundwater, which had a d-spacing of 12.3 Å. In contrast, when the STx-1b was treated with TCE-saturated synthetic groundwater, the smectite peak appeared at 5.72 º2θ, and the d-spacing was 15.4 Å.

For the B-119 sediment, the smectite peak was at 5.83 º2θ, with a d-spacing of 15.2 Å for the untreated sample (Figure 5.3.1-5). For the TCE-saturated synthetic groundwater treatment, the smectite peak occurred at 4.76 º2θ, and the d-spacing was 18.6 Å. Conversely, there was no change observed for the synthetic groundwater treatment in comparison to the untreated sample.

For the CRA-26 sediment, the smectite peak was present at 5.97 º2θ, and the d-spacing was 14.8 Å for the untreated sample. For the TCE-saturated synthetic groundwater treatment, the smectite peak occurred at 4.41 º2θ, and the d spacing was 20.0 Å. Again, there was no change observed for the synthetic groundwater treatment in comparison to the untreated sample.

For the M-72 44 to 46 m BGS sediment, the smectite peak was present at 5.85 º2θ, and the d-spacing was 15.1 Å for the untreated sample. For the TCE-saturated synthetic groundwater treatment, the smectite peak occurred at 4.70 º2θ, and the d-spacing was 18.8 Å. For the synthetic groundwater treatment, the smectite peak occurred at 6.22 º2θ and had a d-spacing of 14.2 Å, which is a slight decrease compared to the control.

For the M-72 46 to 48 m BGS sediment, the smectite peak was present at 5.88 º2θ, and the d-spacing was 15.0 Å for the untreated sample. For the TCE-saturated synthetic groundwater treatment, the smectite peak occurred at 4.62 º2θ, and the d-spacing was 19.1 Å. Conversely, there was no significant change observed for the synthetic groundwater treatment in comparison to the untreated sample.

The results obtained for the four sets of sediments are consistent with those obtained for the two specimen clays. For all cases, the d-spacing was observed to increase for the treatment with TCE-saturated synthetic groundwater, whereas no significant change was observed for the treatment with synthetic groundwater alone. The increase in the d-spacing ranged from approximately 3 to 5 Å for the sediments, similar to that observed for the specimen clays. This is consistent with the thickness of the TCE molecule. These results indicate that TCE was intercalated by the clay minerals. The kinetics of the TCE-clay interaction was not investigated in our study. However, the apparent observed intercalation obviously occurred within the treatment period (24 hours), which provides an outer-bound for the reaction time scale.

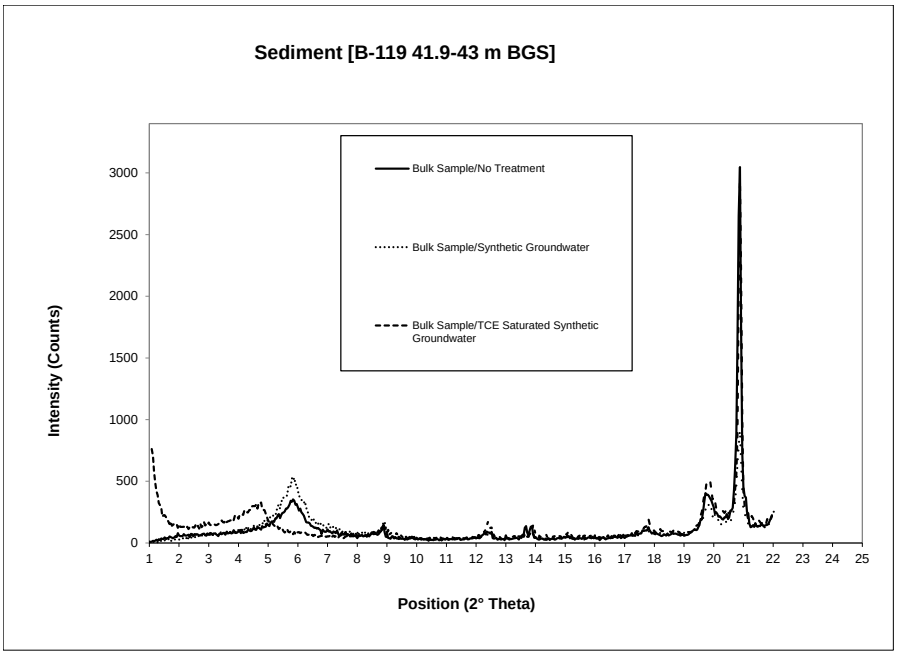

Figure 5.3.1-5. Results of the XRD measurements for the B-119 (41.91 to 43 m BGS) samples.

The results of prior miscible-displacement experiments conducted with these sediments show that TCE elution exhibits extensive tailing (discussed in prior subsection), wherein more than 100 pore volumes of water flushing were required to reduce TCE concentrations to the 1 ug/L range. This is despite the fact that sorption of TCE by these sediments is quite low, with retardation factors less than 1.2. This behavior indicates that some type of recalcitrant interaction is influencing TCE desorption and transport. The results of the present study suggest that the observed behavior may in part be influenced by intercalation of TCE by clay minerals present in the sediment. Such interactions could potentially exacerbate diffusive mass-transfer limitations at the field scale and, for example, impact plume removal via pump and treat.

The Impact of Changes in the Ionic Composition of Groundwater

Silt/clay units are common in sedimentary subsurface environments, and it is well recognized that these units can store significant quantities of contaminant mass. Many remediation approaches are based on injection of an aqueous solution comprising one or more reagents. It is well known that the physical and geochemical properties of clay minerals in particular are sensitive to aqueous geochemical conditions. Hence, it is possible that injecting a reagent solution may in some cases impact the properties of clays associated with lower-permeability units in the treatment zone. This issue was investigated using ISCO with potassium permanganate as the test system.

The impact of a change in ionic composition of groundwater was investigated by conducting a series of column experiments involving elution of sorbed TCE from aquifer sediment. Two sets of experiments were conducted, one with groundwater composition (synthetic groundwater) matched to the site groundwater (suite of salts) and one with potassium nitrate solution. The latter electrolyte was selected to represent for example the introduction of potassium via use of potassium permanganate. The experiments were conducted in pairs, with an

initial TCE elution test conducted prior to flooding, and a second TCE elution test conducted after the column was flooded with either solution for many pore volumes. Aquifer sediment collected from the TIAA site was used. Details of the materials and methods used are presented in the manuscript in preparation (13).

The results of the experiments showed that the extent of elution tailing increased for the systems flooded with the potassium nitrate solution (Figure 5.3.1-6). In addition, this behavior was also observed for tests conducted with non-reactive tracers. Conversely, no change was observed for the systems flooded with synthetic groundwater. Also no change was observed for sediment samples that had minimal clay minerals present (data not shown). These results suggest that the change in ionic composition of the water altered solute transport behavior. It is hypothesized that this effect is caused by a change in clay mineral properties induced by the change in ionic composition.

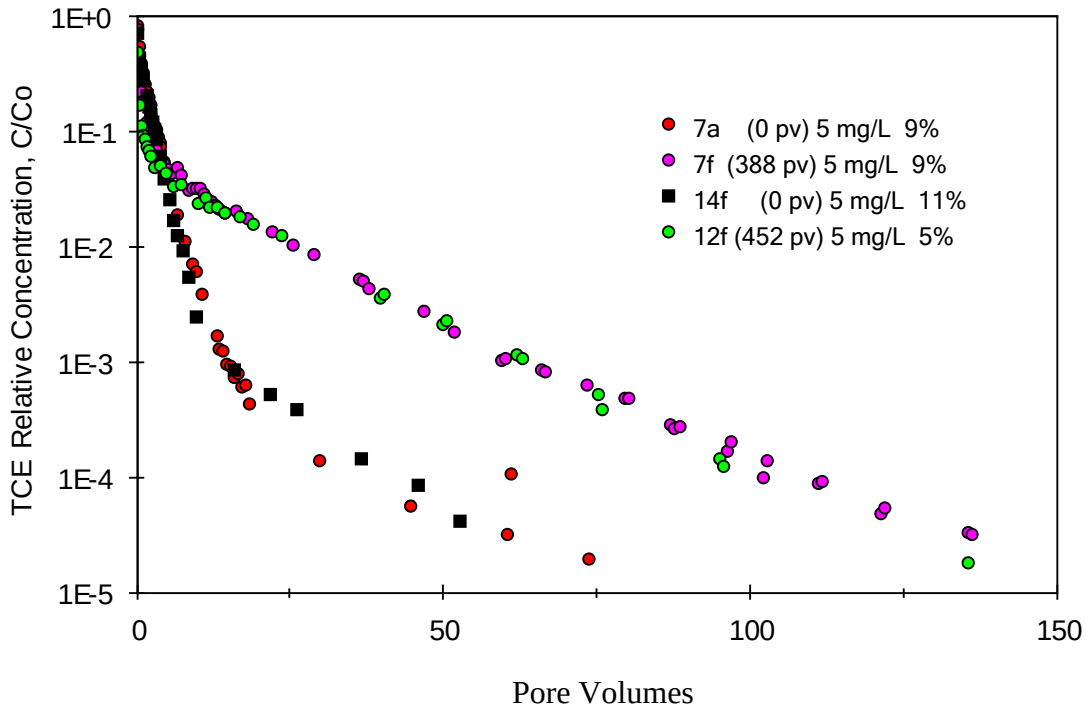

Figure 5.3.1-6. TCE Elution curves for systems flooded with potassium nitrate solution. There are two pairs of data. One set represent controls with no flooding prior to the experiments; these are denoted with (0) in the legend. The other set were flooded with ~400 pore volumes of potassium nitrate solution.

Summary

Elution of trichloroethene from a low organic-carbon-content aquifer material exhibited extensive low-concentration tailing, despite minimal retention of trichloroethene by the aquifer material. The observed nonideal behavior clearly indicates that significant mass-transfer constraints influence trichloroethene transport in this aquifer material. The elution behavior of trichloroethene from field-contaminated aquifer material was essentially identical to that for the

synthetically-aged treatment (approximately four years) and for the freshly-amended treatment (contact time <8 hours). In addition, the results of three independent mass-balance analyses, total mass eluted, solvent-extraction analysis of residual sorbed mass, and flow-interruption rebound showed equivalent recoveries for the aged and fresh treatments. These results indicate that long-term contaminant aging did not influence sorption/desorption and transport of trichloroethene in this low organic-carbon aquifer material.

Several researchers have reported significant effects of aging on the sorption/desorption behavior of hydrophobic organic contaminants in natural porous media. However, most of these studies have involved soils or sediments with moderate or greater organic-carbon contents (greater than approximately 0.1%), and few have been conducted using media with low organic-carbon contents. In the present study, organic-carbon content of the aquifer material was 0.03% (∀ 0.009%). While the objectives of this study did not include a detailed analysis of mechanisms responsible for the sorption/desorption of trichloroethene, a few preliminary conclusions can be drawn from the results. First, the fact that the elution behavior of trichloroethene was essentially identical between the three treatments, irrespective of the contact time, indicates that the attainment of sorption equilibrium was relatively rapid. Second, trichloroethene=s nonlinear sorption suggests the presence of variable and heterogeneous sorption energies, the existence of which is often associated with condensed, carbonaceous material, consistent with the organic-carbon properties of the aquifer material (found to be composed of approximately 61% hard carbon, e.g., kerogen and black carbon). Previous research has shown that that sorption of organic compounds by condensed, carbonaceous materials is often nonlinear and can be relatively rapid. For example, rapid equilibration times for the sorption of polyaromatic hydrocarbons to small particles of soot have been reported by several researchers. These observations suggest that the interaction of trichloroethene with hard-carbon components of the aquifer material mediates the transport and fate behavior of trichloroethene for this system. The observed minimal impact of aging may be related at least in part to the weathered state of this geologically older aquifer material.

The potential intercalation of solutes into interlayers of clay minerals is a question of interest regarding contaminant transport, fate, and remediation. Prior studies have focused primarily on use of specimen clays. In this study, the potential for TCE intercalation by clay mineral components of aquifer sediments was examined. Four sets of sediment samples were collected from the TIAA field site in Tucson, AZ. Two widely used Montmorillonite specimen clays were used as controls. X-ray diffraction, conducted with a controlled-environment chamber, was used to characterize smectite interlayer d-spacing for three treatments (bulk air-dry sample, sample mixed with synthetic groundwater, sample mixed with TCE-saturated synthetic groundwater). The results of the XRD analysis show a greater d-spacing for the samples treated with TCE-saturated synthetic groundwater for all field samples as well as the specimen clays. These results indicate that TCE was intercalated by the clay minerals, which may have contributed to the extensive elution tailing observed in prior miscible-displacement experiments conducted with this sediment. A change in ionic composition of groundwater was shown to affect solute transport behavior.

5.3.2 Plume Response to Source Remediation

The long-term impact of source-zone remediation efforts was assessed for the Southern section of the TIAA site, at which groundwater is contaminated by a very large trichloroethene plume (Figure 4.3-1). The impact of the remediation efforts (soil vapor extraction and in-situ

chemical oxidation) was assessed through analysis of plume-scale contaminant mass discharge, which was measured using a high-resolution data set obtained from 23 years of operation of a large pump-and-treat system. The well field configuration is shown in Figure 5.3.2-1. The methods and details of the study are presented in the published paper (6).

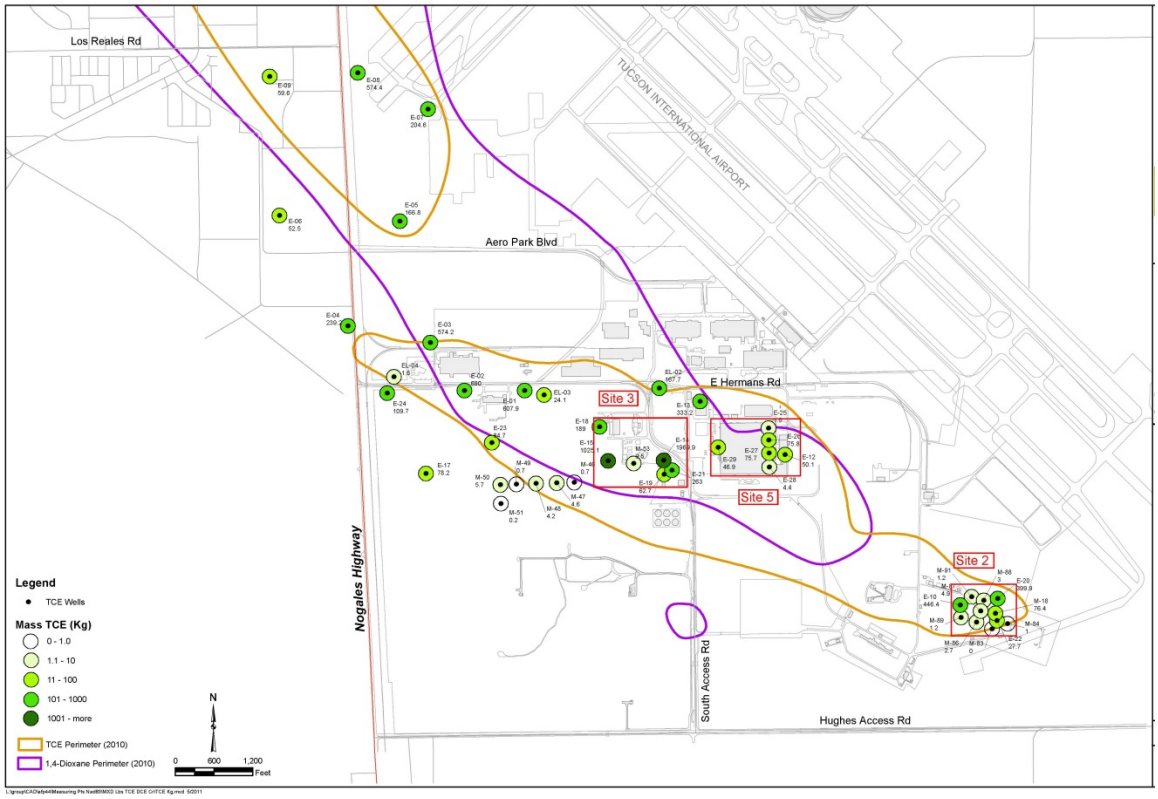

Figure 5.3.2-1. Diagram of the study area, comprising the South section of the TIAA site presented in Figure 4.3-1, with locations of extraction wells used for the pump-and-treat system.

Contaminant Mass Removal

The pump-and-treat system has been in operation for approximately 23 years. Approximately 12,000 kg of solvent mass have been removed with the system to date. This quantity is approximately twice the amount of mass that was estimated to be initially present in the dissolved and sorbed phases prior to startup of pump and treat. In addition, it is approximately half of the total mass, including organic liquid, estimated to have been initially present in the water-saturated portion of the subsurface (i.e., excluding vadose-zone mass) based on the results of partitioning tracer tests and mathematical modeling (Nelson and Brusseau, 1996; Zhang and Brusseau, 1999; Brusseau et al., 2007).

The concentration of trichloroethene in the extracted groundwater is shown as a function of time in Figure 5.3.2-2. After an initial increase with system startup, the concentrations declined rapidly for the first three years of operation. At that point, asymptotic behavior began, with concomitant reductions in the rate of mass removal. Concentrations have declined from approximately 100 µg/L at the start of the asymptotic stage to 15 µg/L at present. The results of prior characterization efforts conducted at the site, using several methods of analysis, provided

strong evidence that organic liquid was present in both the unsaturated and saturated portions of the primary source zones (Nelson and Brusseau, 1996; Brusseau et al., 1999, 2007; Zhang and Brusseau, 1999; Simon and Brusseau, 2007). The results of field tests, laboratory experiments, and mathematical modeling indicated that the asymptotic behavior observed in Figure 5.3.2-2 was caused primarily by constrained mass removal of poorly-accessible organic liquid present in the source zones, with additional contributions from diffusive mass transfer of aqueous mass between zones of lower and higher permeability within and adjacent to the contaminant plume (i.e., "back diffusion") and nonideal (nonlinear, rate-limited) sorption/desorption (Nelson and Brusseau, 1997; Blue et al., 1998; Brusseau et al., 1999, 2007; Zhang and Brusseau, 1999; Johnson et al., 2003a,b,2009; Nelson et al., 2003).

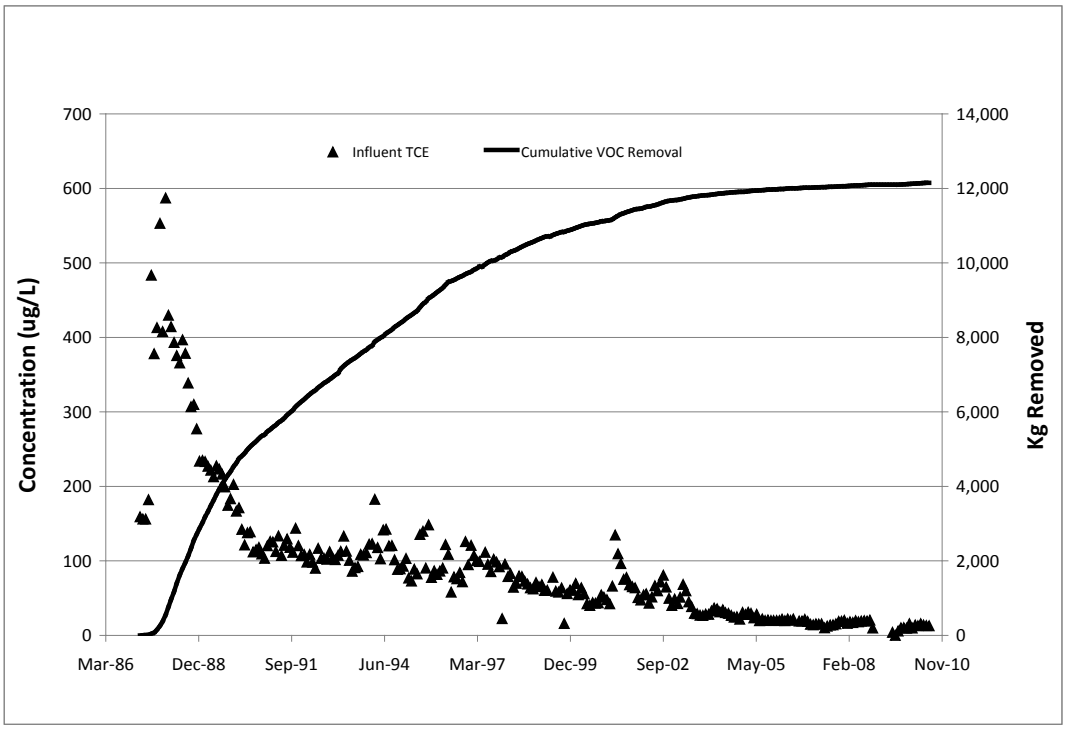

Figure 5.3.2-2. Concentration of trichloroethene in groundwater extracted with the pump-and-treat system. Also shown is cumulative solvent mass removed.

Contaminant Mass Discharge Prior to Source-zone Remediation

The contaminant mass discharge as a function of time is presented in Figure 5.3.2-3. Inspection of the data reveals several stages of distinct behavior. After an initial increase, the mass discharge attained a peak value of approximately 7 kg/d. The mass discharge then decreased relatively rapidly over the next three years to a value of approximately 2 kg/d. This reduction reflects the removal of high-concentration aqueous-phase contamination during initial operation of the pump-and-treat system. After year 3, the contaminant mass discharge began to exhibit quasi steady-state behavior wherein the values decreased relatively minimally over the next approximately six years. As noted above, this behavior reflects the impact of mass-removal constraints.

Contaminant concentration and groundwater extraction data are collected for each extraction well, which allows an assessment of the relative contributions of the source zones and

of the plume to total contaminant mass discharge (see Figure 5.3.2-4). Inspection of Figure 5.3.2-4 reveals significantly different behavior for the plume and source zones, wherein the discharge for the plume decreases relatively steadily through year 10 while that for the source zones remains essentially constant. Thus, the gradual net decrease in total contaminant mass discharge observed during this period is due primarily to reductions associated with the plume contribution. It is estimated that the three source zones contributed approximately two thirds of the total discharge during this period, with Site 3 contributing approximately half (contaminant mass discharge of ~1 kg/d).

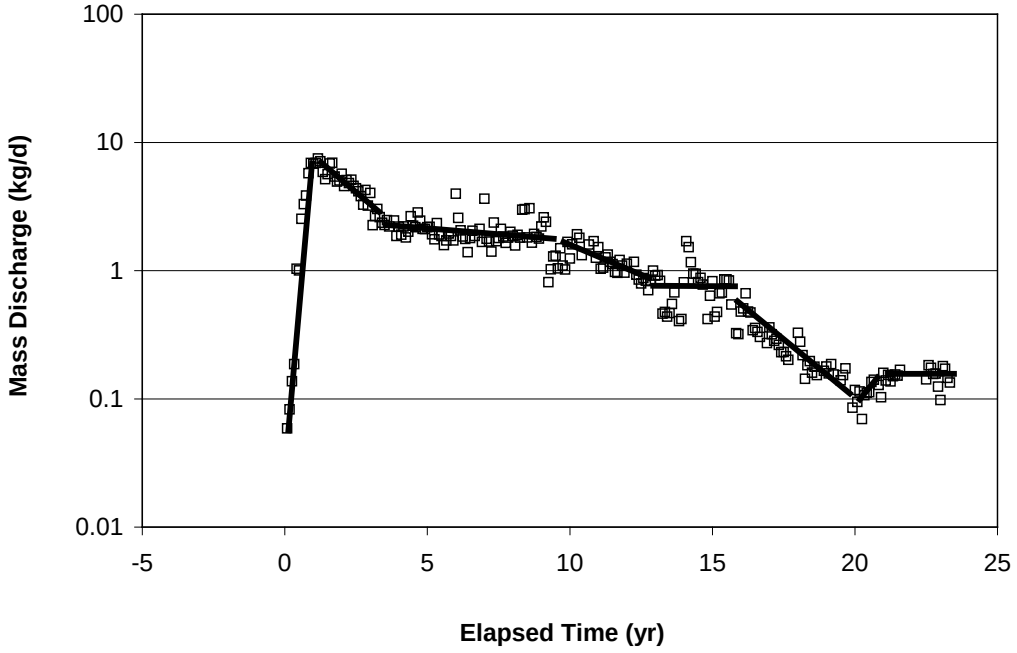

Figure 5.3.2-3. Contaminant mass discharge as a function of time; time zero corresponds to the start of the pump-and-treat operation (April 1987).

A compilation of contaminant mass discharge measurements was reported recently by the ITRC (2010). Data were collected for approximately 40 sites, which comprised a variety of contaminants and site types. The reported values for conditions prior to source-zone remediation efforts, and excluding natural-attenuation effects if applicable, ranged primarily from 0.001 to 1 kg/d. The quasi steady-state contaminant mass discharge measured for the site reported herein, prior to source-zone remediation, is larger than all of the values obtained from the survey, and one or more orders-of-magnitude larger than the vast majority of the values. In addition, the value measured for the Site 3 source zone is similar to the largest values reported in the survey.

The contaminant mass discharge of approximately 2 kg/d observed during the quasi steady-state period represents the inherent long-term rate for the pump-and-treat system under the extant mass-transfer limited conditions. It is likely that this behavior would have persisted for a significant time without the advent of the source-zone remediation efforts. This potential was examined by Brusseau et al. (2007), who conducted predictive simulations to evaluate the impact of source-zone management on plume-scale remediation. The predictions were obtained using

the model presented by Zhang and Brusseau (1999), employing the same conditions and parameters that they used to successfully simulate the observed plume-scale contaminant transport behavior over the course of the first 10-plus years of the pump-and-treat operation. For the modeling conducted by Zhang and Brusseau (1999), a three-dimensional heterogeneous hydraulic-conductivity field was generated using information obtained from borehole logs and pumping tests. Sorption and local-scale mass transfer parameters were obtained from laboratory experiments conducted with aquifer material collected from the site. Initial organic-liquid saturations were based on the results of partitioning tracer tests conducted at the site. For the predictive simulations presented in Brusseau et al. (2007), it was assumed for the case of source-zone remediation that all organic-liquid mass in the saturated portion of the source zones was removed prior to the start of the simulation period (the impact of vadose-zone mass was not evaluated). This assumption represents a limiting case to the actual conditions expected for partial mass removal. A single, constant set of flow rates was used for the injection and extraction wells. Thus, the influence of flow-rate variations associated with changes in the pump-and-treat operation was not reflected in the predictions.

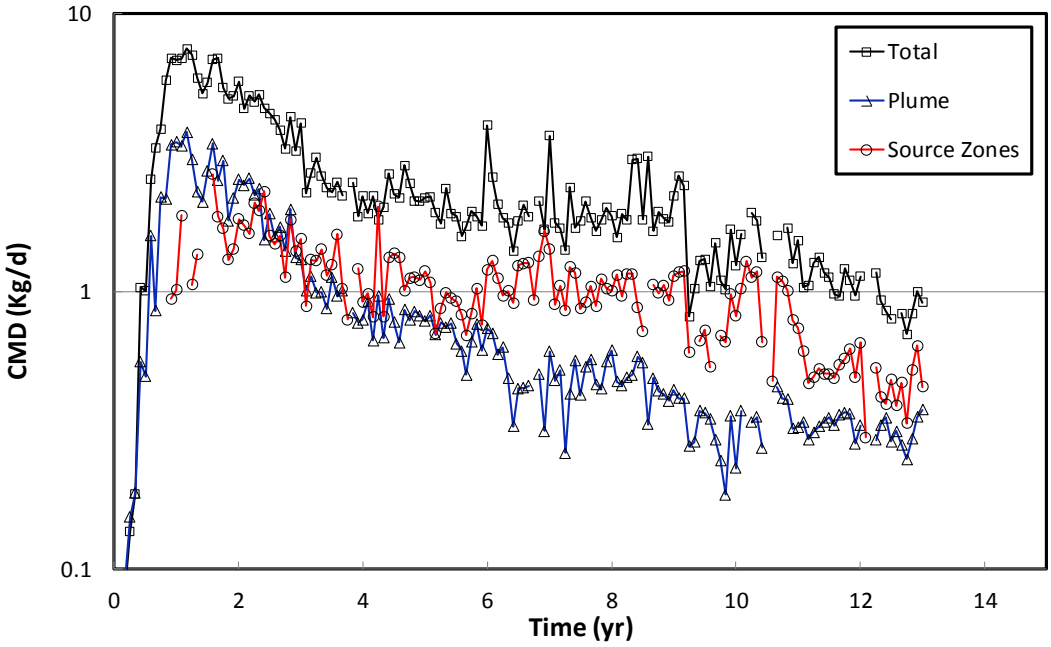

Figure 5.3.2-4. Contaminant mass discharge for the first 13 years as a function of source; time zero corresponds to the start of the pump-and-treat operation (April 1987).

The predicted composite trichloroethene concentrations reported by Brusseau et al. (2007) were combined herein with the average measured extraction rate for the pump-and-treat system to calculate predicted values for contaminant mass discharge. The predicted values for the cases with and without source-zone remediation are presented with the measured values for the period after the start of ISCO in Figure 5.3.2-5. The results for the simulation without source-zone remediation illustrate that contaminant mass discharge is predicted to decrease at a small

rate in the absence of source-zone remediation (i.e., under the influence of only pump and treat). For example, it is estimated that it would take approximately 75 years from the start of the simulation period for the pump-and-treat system to attain the current mass discharge (~0.2 kg/d).

The prediction obtained for the case with source-zone remediation provides a reasonably good representation of the measured data, considering the assumptions employed. No organic-liquid contaminant mass was present in the system for this simulation. Hence, the simulation represents the condition wherein the mass removed is that associated solely with the aqueous and sorbed phases. Inspection of the contaminant elution curve (see Brusseau et al., 2007) and of Figure 5.3.2-5 reveals asymptotic behavior, which indicates that mass removal is constrained. For example, under the simulation conditions, it is estimated that it would require approximately 63 years of pump and treat to reach an influent concentration of 5 ug/L (equivalent to a reduction in contaminant mass discharge of roughly 99%) after source-zone remediation. This is approximately 7-times longer than would be expected under ideal mass-removal conditions, given an approximate hydraulic residence time of six years (Brusseau et al., 2007) and assuming essentially complete removal within 1.5 pore volumes for ideal conditions. The extended time required for removal of the aqueous and sorbed mass (i.e., plume-associated mass) illustrates the impact of back diffusion and nonideal sorption/desorption on plume persistence.

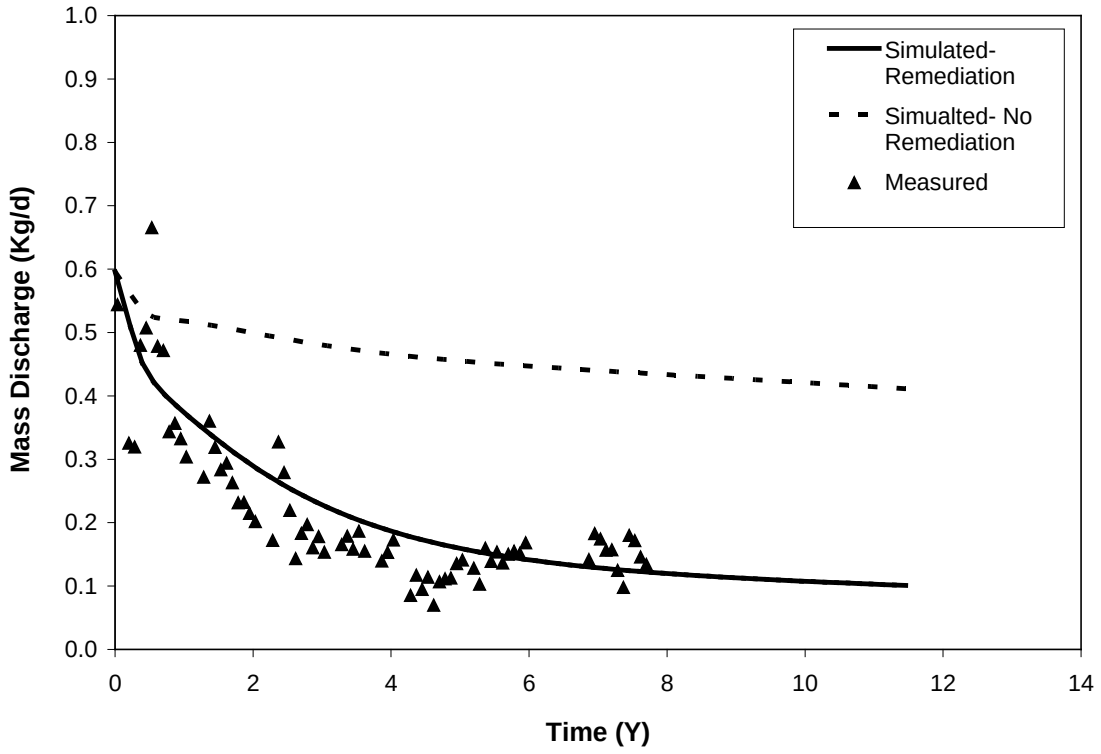

Figure 5.3.2-5. Predicted contaminant mass discharge for cases with and without source-zone remediation; time zero corresponds to the start of the ISCO remediation effort.

Contaminant Mass Discharge After Source-zone Remediation

Full-scale soil vapor extraction was initiated at the source zones in years 8 to 9. The SVE operations removed approximately 49,000 kg of solvent mass, which is more than four times the

amount removed via pump and treat to date. The mass-removal rates for the SVE systems were relatively constant for the first few years of operation, averaging approximately 38, 3, and 2 kg/d for Sites 2, 3, and 5, respectively. Interestingly, these values are significantly larger than the respective source-zone aqueous-phase mass discharges associated with pump and treat.

The vapor-phase contaminant mass discharges began to decline relatively rapidly after the first few years of operation for all three sites. The discharges decreased to values approximately 100-times smaller than the initial values (~99% reduction) within three years after the start of the decline, at which point the SVE systems were shut down. The extracted vapor concentrations at this point were very low (~3 µg/L). Sampling of vapor monitoring wells a year after SVE closure showed minimal rebound of contaminant concentrations. In addition, contaminant concentrations for almost all of the sediment samples collected from several boreholes drilled within the source zones after SVE completion were below regulatory screening levels. These results suggest that most of the contaminant mass initially present in the vadose zone portion of the source zones was removed by the SVE operations.

After startup of the SVE operations, the site-wide aqueous-phase contaminant mass discharge began to decrease at a significantly greater rate (Figure 5.3.2-3), declining from approximately 1.8 to approximately 0.7 kg/d over the first four years after startup. Inspection of Figure 5.3.2-4 shows that the plume-associated mass discharge remained relatively constant for this period, whereas the discharge for the source zones decreased. The decrease in source-zone discharge corresponds to significant (factor of ~4) decreases in trichloroethene concentrations for groundwater pumped from the primary source-zone extraction wells. As noted above, a low-permeability layer exists above the saturated zone. However, the integrity and areal extent of this layer is uncertain, and windows wherein the layer is not present appear to exist (Zhang and Brusseau, 1998). In addition, measurements from pressure transducers and of water levels indicate the likely existence of a hydraulic connection between the vadose zone and the saturated zone. While these results suggest that SVE implementation may have contributed to the observed reduction in discharge, it is difficult to definitively and quantitatively address this issue given the uncertainties associated with the site regarding the impact of vadose-zone contaminant mass on groundwater. However, removal of the very large quantity of solvent from the vadose zone is likely to have ameliorated a long-term source of contamination to groundwater.

In-situ chemical oxidation was initiated at two of the two primary source zones (Sites 2 and 3) in year 16. Almost immediately, the aqueous-phase contaminant mass discharge began to decrease at a significantly greater rate (Figure 5.3.2-3). The mass discharge decreased from approximately 0.7 to 0.1 kg/d after implementation of in-situ chemical oxidation. This reduction was due to a combination of reductions in trichloroethene concentrations and reductions in flow rates for source-zone extraction wells (Brusseau et al., 2011). More than 37,000 kg of permanganate was injected into the two primary source zones over a three and a half year period. While it is not possible to quantify the mass depletion associated with this effort, evaluation of system conditions, including the mass of contaminant present and natural oxidant demand, indicated that the amount of permanganate injected was sufficient to cause a significant depletion in contaminant mass (5). This is consistent with the significant reduction in contaminant mass discharge observed after the implementation of in-situ chemical oxidation. The contaminant mass discharge rebounds to a value of approximately 0.2 after year 20, which corresponds to completion of the in-situ chemical oxidation effort. The increase in mass discharge was due primarily to an increase in trichloroethene concentrations (5). The ISCO project and its impact on contaminant mass discharge are discussed in detail by Brusseau et al. (5).

Contaminant mass discharge has stabilized once again (Figure 5.3.2-3), with minimal change observed for the past three years (2008-2010). The current quasi steady-state mass discharge reflects mass-removal behavior associated with the remaining contamination. This remaining contaminant mass is hypothesized to comprise poorly-accessible mass in the source zones, as well as aqueous (and sorbed) mass present in the extensive lower-permeability units located within and adjacent to the contaminant plume.

Assessing the Benefits of Remediation

The initial quasi steady-state period observed during years 4 to 9 in Figure 5.3.2-3 represents the inherent long-term mass-removal behavior for the pump-and-treat system under the extant mass-transfer limited conditions, as discussed above. As noted, it is likely that this behavior would have persisted for a significant time without the advent of the source-zone remediation efforts. The rate of decline in mass discharge over this period can be used to estimate mass discharge values for future times under conditions wherein pump and treat was the sole remediation action. This allows an assessment of the benefit of employing the source-zone remediation efforts in terms of the additional reduction in mass discharge attained compared to the projected decrease that would have occurred solely from pump and treat. Treating the decrease in mass discharge as a first-order function, the estimated mass discharge with no source-zone remediation is projected to be approximately 1.1 kg/d for the current year. This corresponds to a projected reduction in contaminant mass discharge of approximately 40% achieved from the pump-and-treat operation alone. The measured contaminant mass discharge was reduced from approximately 1.85 kg/d at the end of the initial quasi steady-state period to approximately 0.2 kg/d currently, a total reduction of approximately 89%. These results suggest that the source-zone remediation efforts significantly enhanced the reduction in mass discharge beyond the projected reduction that would have been achieved solely with the pump-and-treat operation.

The rate of decline in mass discharge for the initial quasi steady-state period can also be used to estimate the time required for mass-discharge values to reach a specified target via only the pump-and-treat operation (no source zone remediation). For example, it is estimated that it would take approximately 65 years from year 9 for the pump-and-treat system to attain the current mass discharge (~0.2 kg/d). This estimated value is within the range of the estimated time of approximately 75 years obtained from the predictive modeling noted above. The implementation of the source-zone remediation efforts is thus projected to have in effect eliminated approximately 50 years of pump-and-treat operations (accounting for the time elapsed during source-zone remediation). The operations and maintenance costs for pump-and-treat (roughly $1 million per year) associated with this reduction can be compared to the costs associated with implementation of the source-zone remediation efforts (roughly $15 M and $1 M for SVE and ISCO, respectively) to evaluate relative cost effectiveness. A complete cost assessment would require an accounting of several factors and is beyond the scope of this research.

Summary

The data collected during 23 years of remediation operations at the TIAA site represent a valuable data set that can be used to assess the impact of remediation efforts on plume-scale contaminant mass discharge and associated risk at an unprecedented resolution and scale. The results indicate that these efforts resulted in significant reductions in mass discharge. Use of the

data to evaluate the reduced length of pump and treat operations afforded by the source-zone remediation efforts, which can be used to estimate the cost savings associated with the decreased operational period, was illustrated. While it is recognized that such extrapolation-based analyses are fraught with uncertainty, they can provide useful information for purposes of site assessment and remediation-performance evaluation.

The analysis presented herein was based on employing contaminant mass discharge as an integrative measure of the performance and effectiveness of remediation efforts. The standard approach of characterizing discharge at the source-zone scale was expanded to provide characterization at the plume scale, which was evaluated by examining the change in contaminant mass discharge associated with the site-wide pump-and-treat system. This approach allows linking the impacts of source-zone remediation to effects on site-wide risk. There are several potential sources of uncertainty associated with this analysis, including the impact of natural-attenuation processes, the influence of temporal variability of the pump-and-treat operations, and uncertainty regarding the impact of vadose-zone sources on groundwater quality (this latter factor was discussed above). As discussed by Brusseau et al. (6), there appears to be minimal impact from natural-attenuation processes at the site. Regarding the second factor, overall extraction and injection flow rates for the pump-and-treat system have varied temporally, as have the specific sets of wells employed at a given time. Quantifying the impact of this flow-field variability on contaminant mass discharge would be a complex endeavor for a site such as this, with multiple source zones and multiple extraction wells, and wherein mass-transfer constraints are operative. For example, the impact of changes in flow rate is not straightforward (e.g., a reduction in flow will not necessarily result in a lower mass discharge), as the change in flow rate may impact contaminant concentrations due to factors such as mass-transfer constraints and spatially variable contaminant distributions. Similarly, turning off a given extraction well does not necessarily eliminate the associated mass discharge, as it may be captured by another extraction well.

While significant reductions were attained, it is evident that implementation of the source-zone remediation efforts has not completely eliminated contaminant mass discharge. Remaining contaminant mass contributing to the current mass discharge is hypothesized to comprise poorly-accessible mass in the source zones, as well as aqueous (and sorbed) mass present in the extensive lower-permeability units located within and adjacent to the contaminant plume. The results of mathematical modeling illustrated the impact of back diffusion and nonideal sorption/desorption on the time required for removal of the plume-associated mass, and the implications for plume persistence. The fate of these sources is an issue that is likely to be of critical import for many chlorinated-solvent contaminated sites. Development of methods to address these sources will be required to achieve successful long-term management of such sites and to ultimately transition them to closure.

5.3.3 Plume Response to Source Containment

Hydraulic containment is one approach available for management of source zones contaminated by chlorinated solvents and other organic liquids. The objective of this study was to characterize the behavior of a groundwater contaminant plume after implementation of a source-containment operation at the Central section of the TIAA site. The system was monitored since start-up to measure the change in contaminant concentrations within the plume, the change in plume area, the mass of contaminant removed, and the integrated contaminant mass discharge. Methods used and details of the study are presented in the manuscript in review (11).

Concentration Data

Operation of the two source-control wells appears to have established hydraulic containment of the source area, based on measurement of hydraulic gradients (see Figure 3). This has resulted in isolation of the source from the contaminant plume. The operation of the source control wells, in combination with the operation of the plume extraction wells, is expected to minimize the impact of the source on mass discharge measured for the plume.

The composite concentrations of TCE in groundwater extracted with the contaminant-plume extraction wells are presented in Figure 5.3.3-1. The concentrations are observed to increase during the first six months of operation, after which they peak at approximately 950 ug/L. The delay in attaining the peak reflects stabilization of the flow and concentration fields. The concentrations decrease relatively rapidly over the following year, and begin to exhibit asymptotic behavior approximately 20 months after system startup.

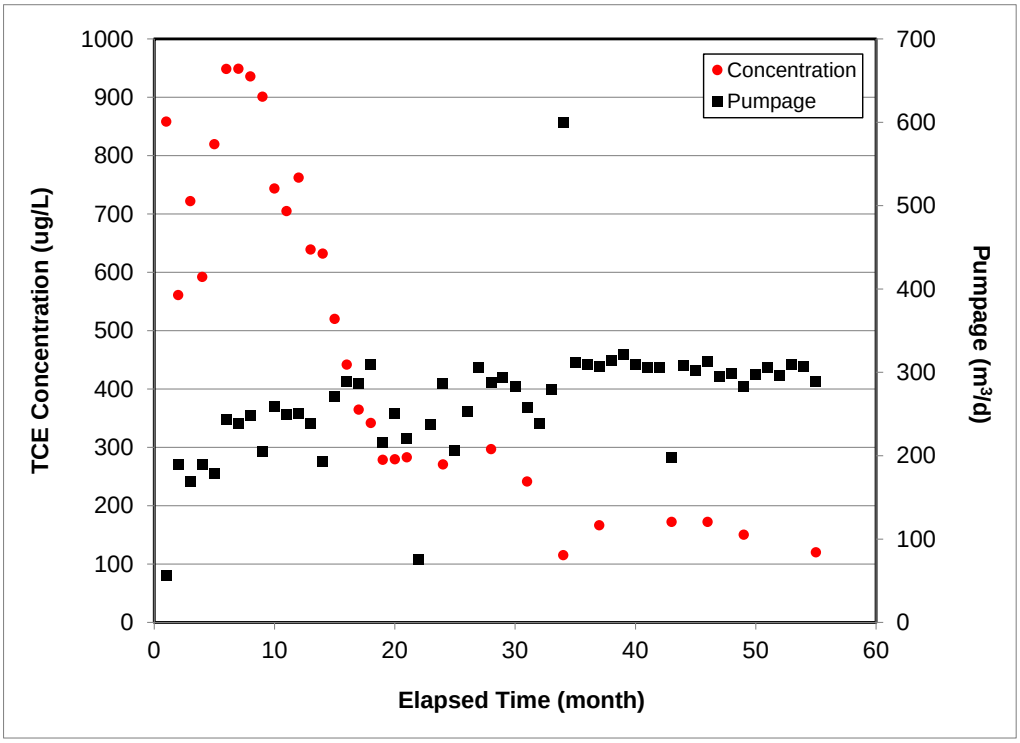

Figure 5.3.3-1. Concentrations of trichloroethene (TCE) in groundwater extracted with extraction wells located within the contaminant plume. Also shown is aggregate pumpage. Zero time corresponds to system startup in fall 2007.

The volume of groundwater pumped for the plume extraction wells is presented in Figure 5.3.3-1. Rates of extraction increased gradually for the first 30 months of operation, and have been relatively constant thereafter. The gradual increase is related to optimization efforts implemented by the operator. A total of approximately 430,000 m^3 of groundwater had been removed with the plume extraction wells at the time of data analysis. This corresponds to the equivalent of more than three pore volumes of flushing, or 0.06 pore volumes per month, based on the estimated pore volume of the gravel unit.

Forty groundwater monitoring wells located within the plume area were sampled periodically. Data were collected separately for wells screened in the gravel unit and those screened in the clay unit above. The mean baseline concentrations of TCE prior to system start-up were 794 and 62 ug/L for groundwater sampled from the gravel and clay units, respectively. The mean concentrations for the August 2012 sampling event were 56 and 34 ug/L, respectively. These data reflect concentration reductions of 93 and 46% for the gravel unit and clay unit, respectively, after 60 months of system operation. The temporal changes in mean relative concentrations are presented in Figure 5.3.3-2. The relative concentration is observed to decrease more rapidly for the wells screened in the gravel unit. It is important to note that these data represent mean concentrations for all wells sampled, and that the two sets of wells screened in the gravel and clay units are not co-located. Thus, the mean values cannot be used to assess the direction of the concentration gradient between the two layers.

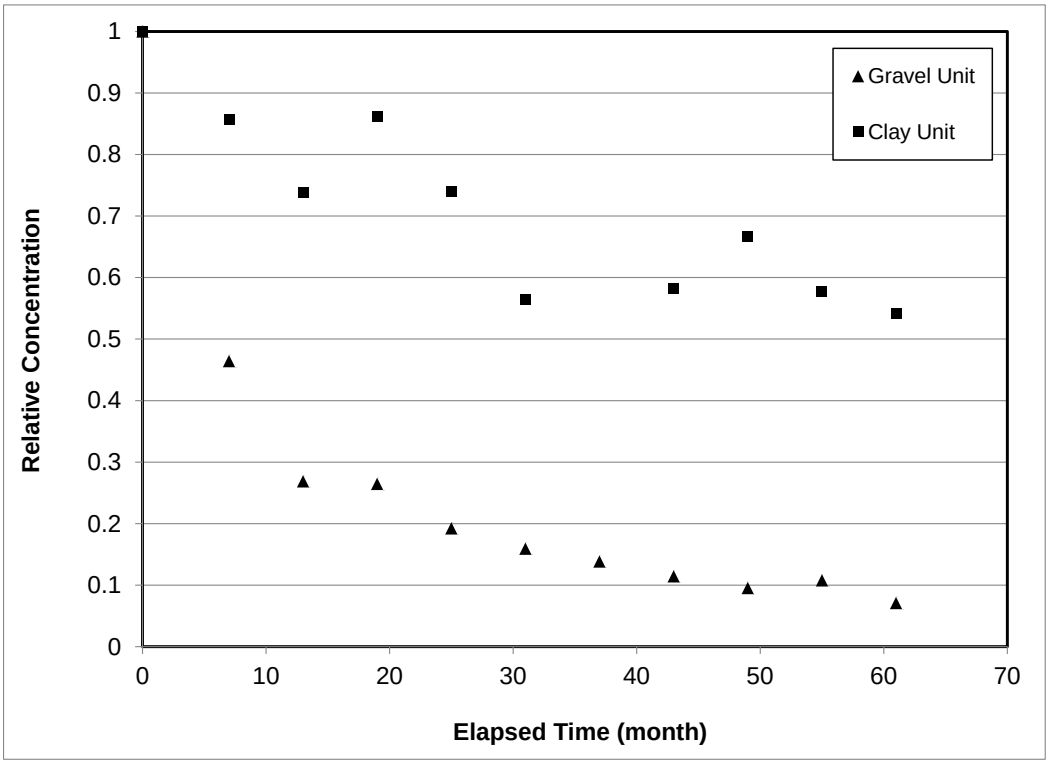

Figure 5.3.3-2. Change in mean relative TCE concentrations for groundwater sampled from monitoring wells screened separately in the gravel and clay units. The concentrations are the mean for data collected for 20 and 25 wells, respectively. Zero time corresponds to system startup in fall 2007.

The spatial areas encompassed by the contaminant plumes for the gravel and clay units were approximately 200,000 m^2 and 245,000 m^2, respectively, in 2007 (prior to system startup). It is assumed that quasi steady state conditions had developed with respect to plume size by this point, given that the plume has existed at the site for several decades, the presence of the flow-control boundary on the western (downgradient) edge of the plume, and the presence of the uncontrolled source on the eastern edge. Evidence of steady state conditions is presented by examination of TCE concentration data collected from 1997 to 2007 for a well located at the

downgradient edge of the plume. The coefficient of variation for this data set is ~13%, indicating small temporal variability. Under such conditions, the sizes of the plumes in the adjacent units would be expected to be similar. The plumes for the two units differ by approximately 20%, which is considered reasonable similarity given the uncertainty associated with the estimation method.

The plume areas in August 2012 were approximately 87,000 m^2 and 130,000 m^2, for the gravel and clay units, respectively. The relative decrease in plume areas was 53% for the gravel unit and 43% for the clay unit. A significant decrease in area associated with TCE concentrations greater than 100 ug/L was observed for both units. The temporal changes in relative plume area are presented in Figure 5.3.3-3. The maximum reduction in area observed for the plume in the gravel unit occurred essentially within the first year, whereas the reduction in area occurred more gradually for the clay-unit plume. This is consistent with the data presented in Figure 5.3.3-2.

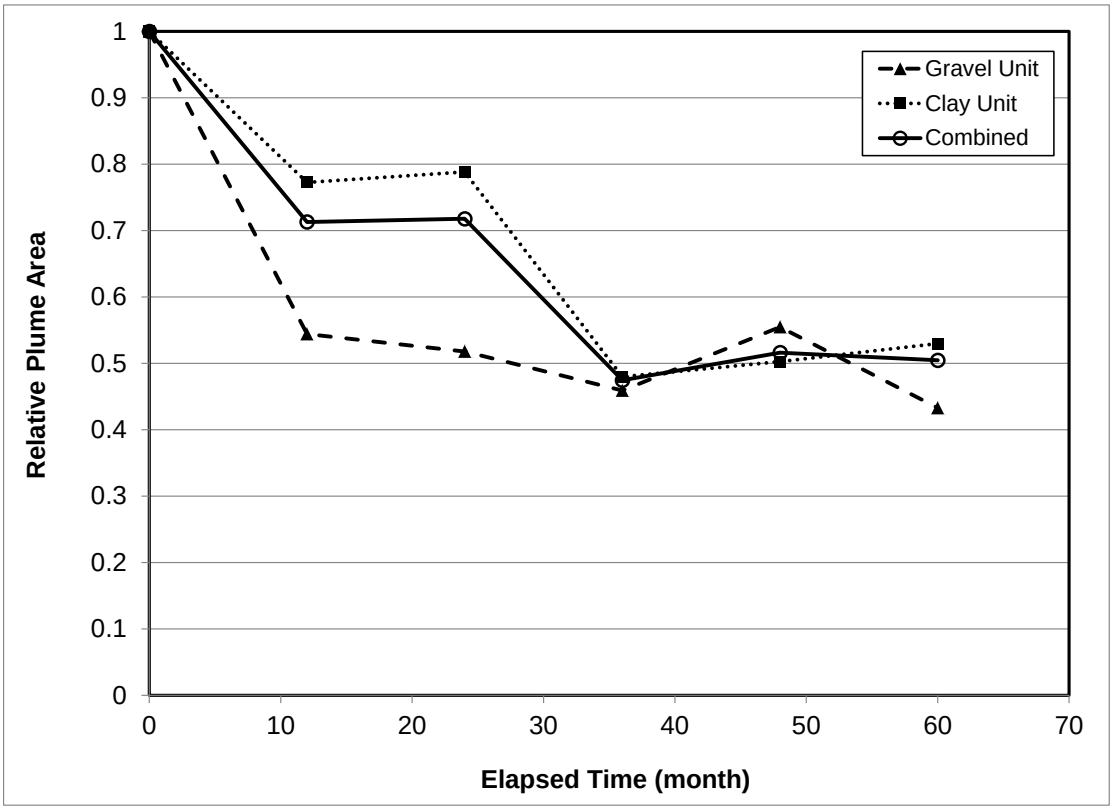

Figure 5.3.3-3. Change in relative areas of the TCE plume (defined by the 5 ug/L contour) for data collected from monitoring wells screened separately in the gravel and clay units. Zero time corresponds to system startup in fall 2007.

Contaminant Mass Removal and Mass Discharge

A total of approximately 140 kg of TCE has been removed with the plume extraction wells as of mid-2012, based on integration of the concentration and pumpage data. The rate of mass removal began to decrease greatly after approximately 10 months, and attained asymptotic conditions after approximately 20 months (data not shown). An estimate of the mass of TCE currently present within the plume can be obtained using the estimated pore volume, the mean

concentration for the plume, and an assumption that sorption contributes an additional approximately 15% to the total mass (Zhang and Brusseau, 1999; Brusseau et al., 2007). This produces an estimated mass of approximately 20 kg, which translates to an initial mass of 160 kg and an associated mass reduction of approximately 87%.

The distribution of TCE mass between the gravel and clay units can be estimated using the TCE concentrations measured for groundwater sampled from the monitoring wells located within the plume. It is estimated that 83% of the mass resided within the gravel unit and 17% within the clay prior to remediation startup. The relative fraction associated with the gravel unit declined after startup, while that associated with the clay increased. As of the August 2012 sampling round, it is estimated that 46% of the remaining mass resided within the gravel unit and 54% within the clay.

The total contaminant mass discharge (CMD) associated with operation of the plume extraction wells is presented in Figure 5.3.3-4. The discharge peaked at 0.23 kg/d approximately 6 months after system start up. The delay in attaining the peak reflects the behavior observed for the concentration data. The peak value is at the higher end of the range of values reported in a recent survey of mass-discharge field data (ITRC, 2010). The mass discharge decreased significantly during the next year of operation, and thereafter began an asymptotic decline to a current value of approximately 0.03 kg/d. This represents an approximate 87% reduction in mass discharge since the initiation of the plume pump-and-treat system. This reduction is a function of the reduction in TCE concentrations observed for the extraction wells, given that the system flow rate increased over the first half of the operations period and thereafter has remained relatively constant. This then suggests that the reduction in mass discharge is associated with contaminant mass removal as opposed to other factors, such as changes in hydraulic conditions.

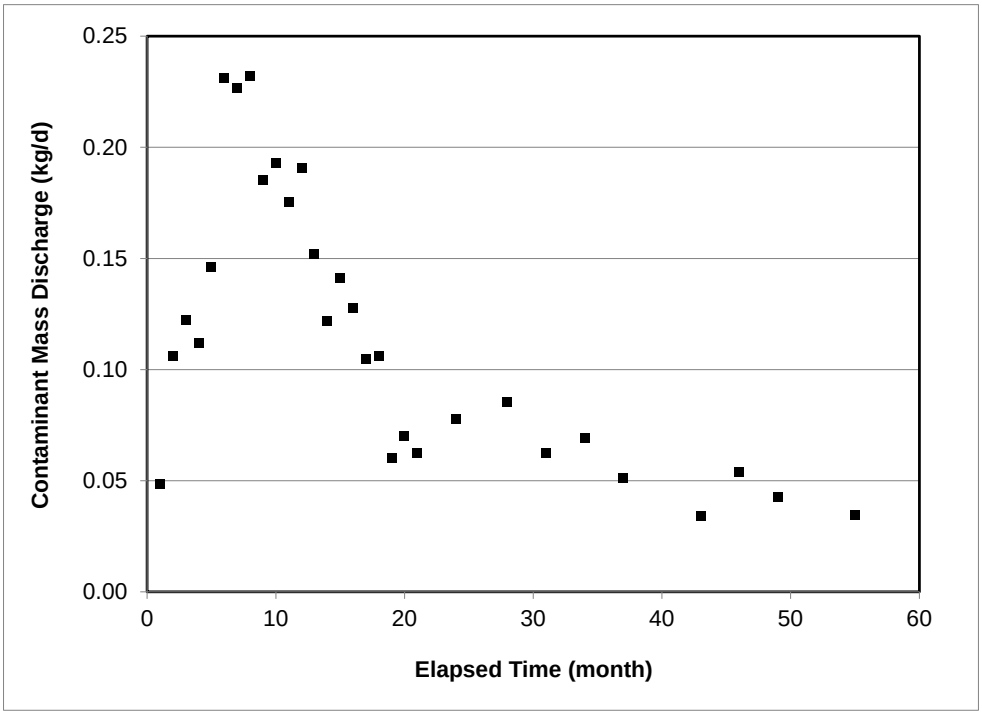

Figure 5.3.3-4. Total contaminant mass discharge for the groundwater contaminant plume extraction-well system. Zero time corresponds to system startup in fall 2007.

Evaluating the response of contaminant mass discharge to mass removal or reduction efforts is facilitated by determining the relationship between reductions in contaminant mass discharge and reductions in contaminant mass (e.g., Rao et al., 2002; Brusseau et al., 2007; DiFilippo and Brusseau, 2008). The relationship was determined using the data collected for the plume, and is presented in Figure 8. It is observed that the data exhibit an approximate one-to-one relationship between reductions in contaminant mass discharge associated with pump-and-treat remediation of the plume and reductions in contaminant mass within the plume. Such behavior is often considered to reflect the existence of poorly accessible mass that constrains the overall mass-removal rate (e.g., Jawitz et al., 2005; Brusseau et al., 2008; DiFilippo and Brusseau, 2008; Christ et al., 2010; DiFilippo et al., 2010; Brusseau et al., 2013).

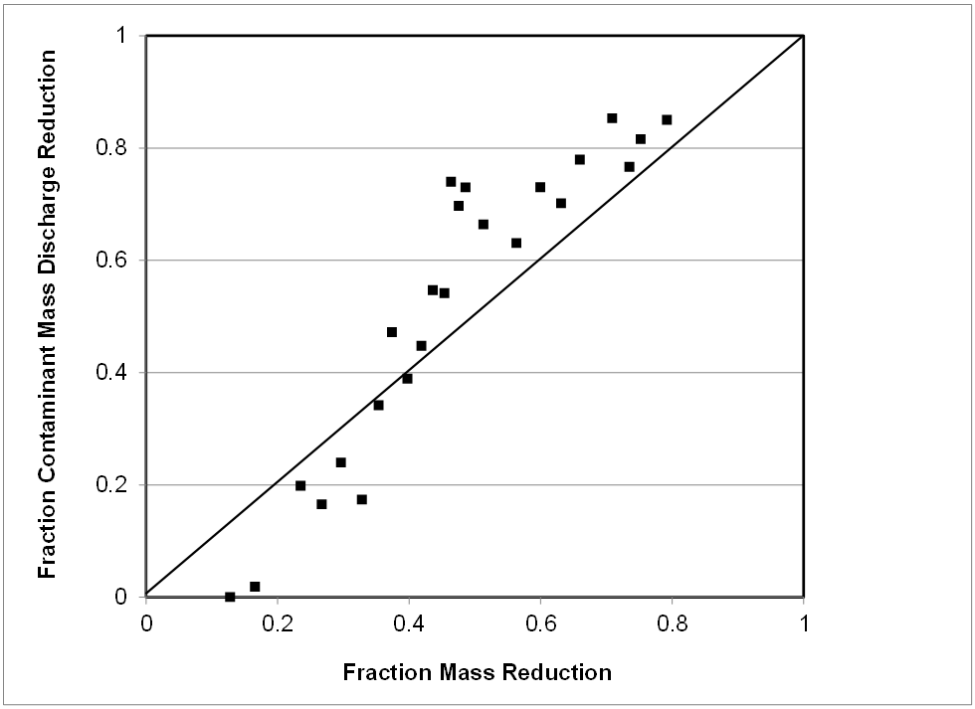

Figure 5.3.3-5. Relationship between reductions in contaminant mass discharge and reductions in contaminant mass for the plume after source containment.

Plume Persistence

Plume migration at the site is considered to be driven by longitudinal advective transport in the gravel unit, with such transport in the clay units adjacent to the gravel considered to be insignificant. This hypothesis is supported by the TCE-concentration data collected for the groundwater monitoring wells. As reported above, the mean concentration of TCE within the plume was more than ten-times higher in the gravel compared to the clay prior to system startup. Conversely, the mean concentrations of TCE in the source zone prior to system start-up were 12,320 and 16,300 ug/L for monitoring wells screened in the gravel and clay, respectively. The concentrations are comparable for the two units in the source area as would be expected for the extant contamination scenario, which involved surface disposal of waste. In contrast, the order-

of-magnitude disparity observed for the plume data is consistent with advective transport in the gravel unit serving as the primary control on plume migration, with diffusive mass transfer serving as the transport vector for contaminant delivery to the clay units adjacent to the gravel.

Inspection of Figure 5.3.3-1 shows that the integrated TCE concentrations (and the associated CMD, Figure 5.3.3-4) decreased rapidly from the peak, attaining asymptotic conditions within 20 months of operation. This time period corresponds to the equivalent of roughly one pore volume of groundwater removal (with pore volume based on the gravel unit). This observation is consistent with the behavior expected for ideal hydraulic flushing. These observations suggest that the mass removed prior to the start of asymptotic conditions represents primarily contaminant present in the advective (e.g., higher-permeability) domain, namely the gravel unit, which is consistent with the observed changes in TCE concentration and mass distributions reported above for the gravel versus clay units. This supports the contention that the gravel unit is the primary domain for plume migration and removal.

The equivalent of an additional approximately 2.5 pore volumes of groundwater have been flushed through the contaminated zone since the start of asymptotic conditions. However, the spatial area encompassed by the plume has decreased by only approximately 50% since containment of the source. In addition, the rate of decrease in contaminant mass discharge is significantly lower after asymptotic conditions were attained (Figure 5.3.3-4). These observations indicate a significant decrease in mass-removal effectiveness. The potential causes of this behavior are of interest in assessing and predicting long-term response of the plume.

The clay units adjacent to the gravel unit have low permeabilities and thus experience minimal direct water flushing. Data for groundwater collected from wells screened in the clay shows that TCE is present at substantial concentrations, as noted above. Hence, the clay units are likely to serve as an extensive, distributed source of TCE via diffusive mass transfer (back diffusion) to the gravel unit. As presented above, aggregate reductions of 93 and 46% were observed for TCE concentrations in groundwater sampled from monitoring wells screened in the gravel and clay units, respectively, with implementation of site remediation. The significantly lower reduction observed for the wells screened in the clay is likely associated with the impact of diffusive mass-transfer constraints on mass removal. Concomitantly, the relative distribution of TCE mass has shifted from being predominantly associated with the gravel unit, to an approximate 50:50 distribution between the gravel and clay units. Furthermore, the relative decrease in plume size observed for TCE in the gravel was slightly larger than, but relatively similar to, the decrease observed for TCE in the clay unit (Figure 5.3.3-3). This is despite the fact that the rapid decreases in resident TCE concentrations and plume area observed for the gravel unit, as well as the rapid initial decrease observed for integrated CMD, indicate that flushing of the gravel unit due to the pump-and-treat operation should have already eliminated the plume if mass-removal conditions were ideal.

All of these observations suggest that contaminant transport and removal within the gravel unit is hindered by mass transfer of TCE from the clay to the gravel. This supports the contention that the clay units are serving as an extensive, distributed source of TCE. However, other factors such as sorption-related processes and hydraulic phenomena (e.g., well-field hydrodynamics) may also be important. The low–permeability sediments comprise a high percentage of clay minerals, including smectitic clays (Matthieu et al., 2013). The results of studies conducted with sediments from the site indicate that TCE can be intercalated within the interlayer spaces of clay minerals associated with the site sediments (Matthieu et al, 2013). This intercalation may contribute to recalcitrance and plume persistence by constraining desorption.

The results of prior experiments conducted using sediment collected from the TIAA site indicate that sorption/desorption of TCE is rate limited (Johnson et al., 2003, 2009). In addition, the results of prior experiments show that sorption of TCE by the site sediments in nonlinear, which can also influence rates of mass removal. However, given that sorption of TCE by the site sediments is quite low, with retardation factors of approximately <1.2, it is anticipated that the impact of sorption/desorption associated factors may be relatively minor compared to that of diffusive mass transfer associated with the extensive clayey units.

Summary

Hydraulic containment is being used to manage the source area at the study site. Operation of two source-control wells appears to have established containment of the source area, which has resulted in isolation of the source from the contaminant plume and elimination of source mass discharge to the plume. A critical issue associated with hydraulic source-containment systems is the response of the contaminant plume, which is mediated by properties of the site and processes occurring therein. The results of this study indicate that operation of the plume-scale pump-and-treat system has resulted in a significant reduction in contaminant mass, mass discharge, and areal extent for the plume. For example, concentrations of TCE within the gravel unit decreased by 90% after implementation of source containment. In addition, the mass of TCE and the contaminant mass discharge associated with the plume have both decreased by approximately 87%.

However, TCE concentrations and associated mass discharge began to exhibit an asymptotic decline after the equivalent of approximately one pore volume of groundwater removal. In addition, the areal extent of the plume has decreased by only 50% despite the flushing of the equivalent of more than three pore volumes of groundwater. The results of groundwater sampling show that a significant reservoir of contaminant mass resides in the clay units adjacent to the sand/gravel unit. Diffusion of TCE from the clay units into the sand/gravel unit (back diffusion) is concluded to be a primary constraint to rapid removal of the plume, and is likely to cause the plume to persist for many decades. This result is consistent with those obtained in prior field studies. The potential impact of hydraulic factors is currently being assessed.

The use of pump-and-treat operations data to supplement characterization based on monitoring-well information was illustrated to enhance the analysis. The operations data provide an integrated measure of plume behavior that can support a more comprehensive assessment of the system. For example, the data were used herein to determine the relationship between reductions in contaminant mass discharge and reductions in contaminant mass for the plume. To our knowledge, this represents the first such measurement for an isolated contaminant plume.

5.4 Mathematical Modeling

Two primary uses for mathematical models in Hydrology are the investigation of fundamental processes and site-specific management applications. Regarding the former, mathematical models are a powerful means by which to integrate process-based information for complex systems, and thus are a key method for investigating phenomena over a wide range of conditions that are problematic to investigate by other means. Regarding the second use, mathematical modeling has become a critical component of risk assessment, characterization, and remediation-system development efforts for hazardous-waste sites. Unfortunately the use of advanced, multi-process mathematical models for such applications is often greatly constrained

by insufficient knowledge of subsurface properties and contaminant distributions. This is particularly the case for immiscible-liquid contaminated sites, for which the location and architecture of the sources zones is rarely known in detail. Thus, it is often necessary to use simpler models (referred to as lumped-process models) for simulating mass removal and mass flux at larger scales, particularly the field scale.

A critical issue associated with the use of simpler models is how to translate mechanistic information (e.g., pore-scale processes) into the simplified models. This is often referred to as the "upscaling" issue. This issue is critical for accurate and effective modeling of field-scale systems. A primary focus of interest regarding upscaling issues has been the scalability of the first-order mass transfer approach typically used to represent immiscible-liquid dissolution (e.g., Zhang and Brusseau, 1999; Saba and Illangasekare, 2000; Brusseau et al., 2002; Park and Parker, 2005; Christ et al., 2006; Marble et al., 2008). When applied to a column system for example, the mass-transfer coefficient clearly represents the pore-scale mechanisms mediating dissolution at the local scale. However, when this approach is applied to larger-scale systems, the mass-transfer coefficient represents all factors influencing dissolution that are not otherwise explicitly represented in the model. In such cases, the mass-transfer rate coefficient becomes in essence a macro-scale model-calibration parameter. Current research is focused on how to use mechanistic-based information to upscale this macro-scale mass-transfer parameter (or macrodissolution coefficient).

The use of simple lumped-process models to predict transport requires determination of the macro-scale mass-transfer coefficient. This is often done via model calibration. However, this approach is limited by several constraints, one of them being that calibration cannot be done for situations wherein historical data are not available for such calibration. An alternative approach is to use some method to produce estimates of the macro-scale mass-transfer coefficient. One potential approach is to use system-indicator functions, such as the ratio of NAPL occurring as residual-phase (ganglia) to that as pools, source-length:system-length ratio, and source-area:system-area ratio (cross-sectional area). It is hypothesized that the macro-scale mass-transfer coefficient (which is a function of source-zone architecture) will correlate in some manner with these system-indicator parameters, which are simple measures of source-zone architecture.

The efficacy of a simple mass-removal function for characterizing mass-flux-reduction/mass-removal behavior for organic-liquid contaminated source zones was evaluated in this study (4). The investigation made use of data obtained from the series of flow-cell experiments discussed above, and presented in the relevant published paper (3). The flow-cell systems were designed to reflect a variety of organic-liquid distributions and flow-field heterogeneities. The methods employed for the modeling study are presented in detail in the published paper (4).

Simple Mass-Removal Function

The performance of the simple mass-removal function (equation 4.1) was evaluated using two approaches. In the first set of analyses, the efficacy of the function for characterizing mass-flux-reduction/mass-removal behavior was evaluated by examining its ability to match the data obtained from the flow-cell experiments (i.e., curve-fitting). In the second set of analyses, the ability of the function to independently simulate observed behavior was investigated. Using the function in the latter mode requires a means by which to determine a priori values for the n parameter.

The Initial GTP (IGTP) method (Table 5.4-1) was developed to provide estimates of *n* based on a parameter used to account for source accessibility, the measured initial GTP. The IGTP method is based on establishing a relationship between *n* and GTP, similar to the approach used by Christ et al., 2006, who presented a relationship between the exponent of the first-order concentration/mass-depletion function and GTP. In the current study, data reported by Lemke and Abriola (2006), who used a numerical model to simulate organic-liquid distribution and dissolution in heterogeneous porous media, were used as the source data to characterize a relationship between *n* (exponent for the mass-flux-reduction/mass-removal function) and GTP. Specifically, the concentration/mass-removal data reported by Lemke and Abriola (2006) were first converted to mass-flux-reduction/mass-removal curves, after which the simple mass-removal function was fit to each curve using a least-squares-regression routine to determine a value for the *n* parameter. The *n* values were then regressed against the GTP values reported for each simulation. A positive correlation was obtained between *n* and GTP, which was best expressed by a power-law model (Figure 5.4-1). This regression, which is in terms of the mass-flux-reduction function, spans a reasonably large range of GTP ratios ($0.17 < GTP < 65.6$, $R^2 = 0.93$), and provides an alternative to the regression presented by Christ et al. (2006), which is in terms of the concentration/mass-depletion function. As will be discussed below, additional functions were developed and evaluated to characterize *n* as a function of changing system conditions.

Table 5.4-1. Summary of methods developed to predict the mass-flux-reduction/mass-removal relationship.

Method	Equation*	Figure
Initial GTP (IGTP)	$n = 0.65\left(GTP_i\right)^{0.52}$	5.4-3
Variable GTP (VGTP)	$n = f\left(GTP_t\right)$	5.4-4a
Variable Source Size (VS)	$n = n_0\left(\frac{A_{sz,t}}{A_{tot}}\right)\left(\frac{L_{sz,t}}{L_{tot}}\right)$ where $n_0 = 0.65\left(GTP_i\right)^{0.52}$	5.4-4b
Multi-Domain (MD)	$n = n_0\left(\sum_{i=1}^{k} A_{norm,i} L_{norm,i} f_i\right)$	5.4-4c
Multi-Domain Relative Permeability (MDRP)	$n = n_0\left(\sum_{i=1}^{k} A_{norm,i} L_{norm,i} K_{norm,i} f_i\right)$	5.4-4d

* $A_{norm} = \frac{A_{sz,t}}{A_{sz,0}}$, $L_{norm} = \frac{L_{sz,t}}{L_{sz,0}}$, $K_{norm} = \left(\frac{K_t}{K_0}\right)^3$, $K = k_r K_{sat}$

GTP_i is the initial GTP ratio for the experiment [-], A_{sz} is the source zone area [L^2], L_{sz} is the source-zone length [L], A_{tot} is the total cross-sectional area of the flow cell [L^2], L_{tot} is the total length of the flow cell [L], K is hydraulic conductivity [L/t], k_r is the relative permeability [-], K_{sat} is the water saturated hydraulic conductivity [L/t], f is the fraction of organic-liquid mass in each zone, k is the total number of zones, and the subscripts *0* and *t* represent initial time and later time *t*, respectively. The threshold values for residual saturation for each sand mesh sizes

used in our experiments are provided by Dobson et al., (2006). The relative permeability for each system was obtained from image analysis.

Application of the Simple Mass-Removal Function

The simple mass-removal function was applied to the data sets reported herein (Figure 5.4-2). The best-fit values for *n* were determined using a least-squares-regression routine. For the Control and Homogeneous experiments, the measured data were well simulated by the simple mass-removal function. The initial behavior for the Mixed Source and Heterogeneous experiments was also well simulated by the function. However, the non-singular behavior observed at larger mass removals was poorly simulated.

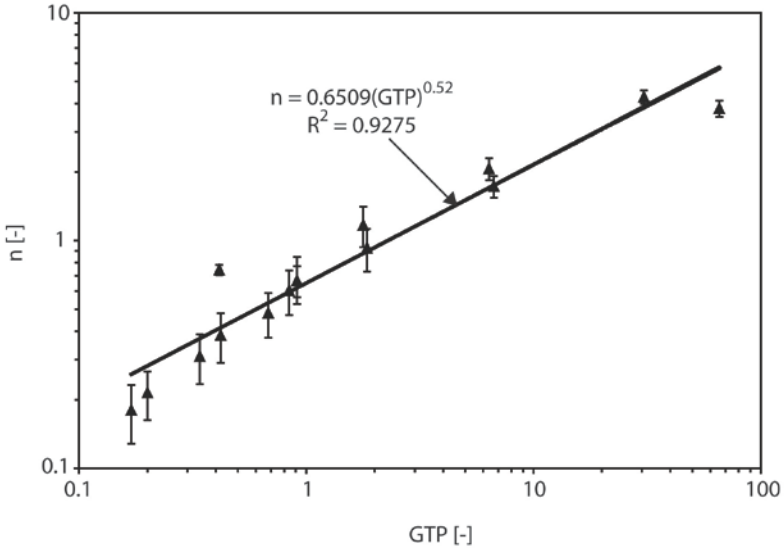

Figure 5.4-1. Relationship between *n* (parameter from equation 4.1) and ganglia-to-pool (GTP) ratio. See text for description of data source and analysis methods.

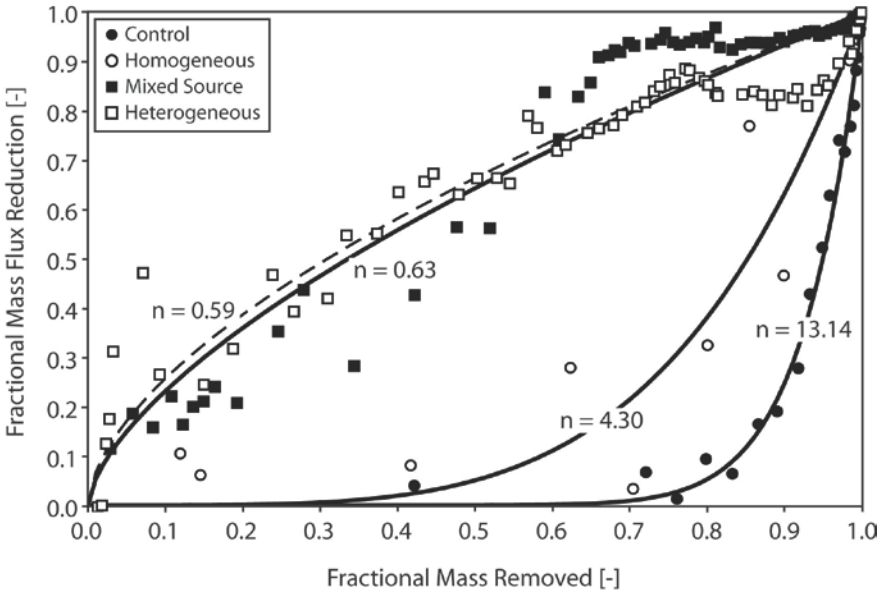

Figure 5.4-2. Application of the simple function to measured data.

The relationship between *n* and GTP reported in Figure 5.4-1 was used to determine an initial value for the *n* parameter used in the simple mass-removal function. Using the initial GTP ratio from the image analysis, *n* values of 0.86 and 0.72 were calculated for the Mixed Source and Heterogeneous experiments, respectively. These values are similar in magnitude to the best fit *n* values determined using least squares regression (shown in Figure 5.4-2). The predicted curves reasonably match the measured data for approximately the first 40% of the total mass removed (Figure 5.4-3). These results support the robustness of the *n*-GTP correlation, and suggest that the IGTP method may be useful for providing first-order characterization of initial mass-flux-reduction/mass-removal behavior.

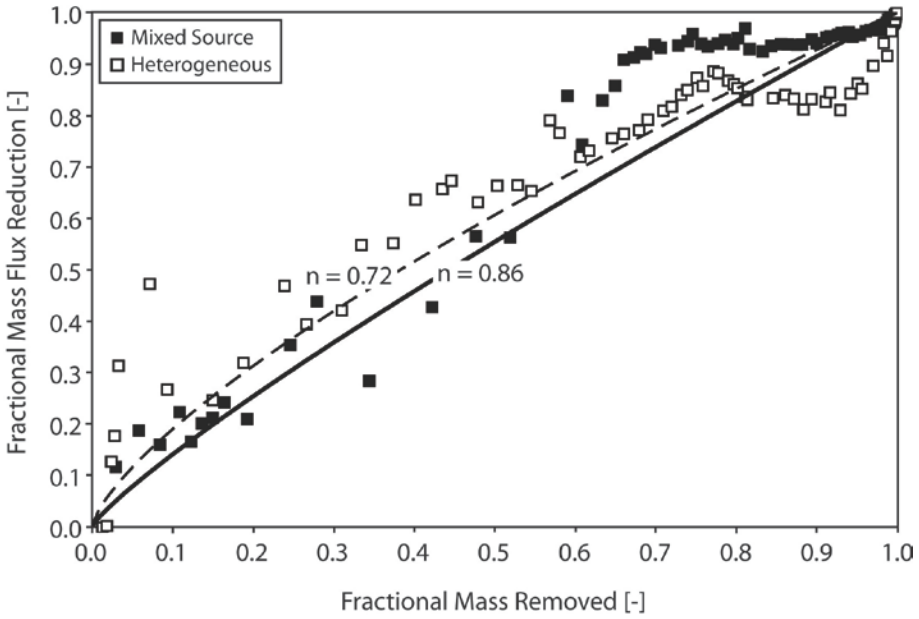

Figure 5.4-3. Measured and predicted mass-flux-reduction versus mass-removal behavior for the Mixed Source and Heterogeneous experiments. The solid (Mixed-source) and dashed (Heterogeneous) lines were obtained with the simple mass-flux-reduction/mass-removal function wherein the values for the n parameter were obtained independently using the initial GTP ratio (IGTP method).

While the IGTP method provided reasonable predictions for initial mass removal, the predicted curves were unable to capture the later, nonsingular mass-flux-reduction/mass-removal behavior. In addition, whereas the initial GTP ratios for the Control and Homogeneous experiments were the same, the mass-flux-reduction/mass-removal behavior for these two experiments was different due to different source zone areas and lengths. These results illustrate that the initial GTP ratio alone is not sufficient for characterizing the complete mass-flux-reduction/mass-removal relationship. This conclusion is consistent with results presented in previous studies (Christ et al., 2006; Basu et al., 2008; Brusseau et al., 2008; DiFilippo and Brusseau, 2008).

Organic-liquid distribution and flow-field conditions change as organic liquid is depleted from the source zone. Therefore, it can be anticipated that describing mass-flux-reduction/mass-removal behavior with a simple function parameterized solely on initial source-zone characteristics would be limited. For the specific case of the simple function used herein

(equation 4.1), singular mass-flux-reduction/mass-removal curves are produced when *n* is a constant (a function only of initial conditions). However, non-singular or multi-step mass-flux-reduction/mass-removal behavior has been observed in prior flow-cell experiments (e.g., Brusseau et al., 2008; Kaye et al., 2008; DiFilippo et al., 2010; Marble et al., 2010), mathematical-modeling studies (e.g., Lemke et al., 2004; Phelan et al., 2004; Soga et al., 2004; Lemke and Abriola, 2006; Basu et al., 2008b; Maji and Sudicky, 2008; Christ et al., 2009), and for measured field data (Brusseau et al., 2007; DiFilippo and Brusseau, 2008). This non-singular behavior is a result of changes in organic-liquid distribution and relative permeability during the course of mass removal. For the simple mass-removal function to adequately simulate the non-singular behavior, the parameter *n* would need to change as a function of mass removal to reflect changes in organic-liquid distribution and flow-field conditions. For example, by changing *n* from 0.63 to 0.25 once 66% of the total mass has been removed, the mass-removal function provides a better representation of the measured data for the Mixed Source experiment. Similarly, the mass-removal function is able to capture the behavior observed for the Heterogeneous experiment if *n* is allowed to gradually increase from 0.56 to 2.5 once 80% of the total mass is removed from the system. These results show that, as would be expected, the performance of the simple mass-removal function can be improved significantly by allowing *n* to vary with mass removal.

System-Indicator Parameters and Mass-Removal Dependent Functions

The simple mass-removal function can simulate the non-singular behavior observed for the measured data by allowing *n* to change as a function of mass removal. However, to use the mass-removal function in a predictive manner, the mass-removal dependency of *n* needs to be characterized. One possible approach is to relate *n* to system-indicator parameters that change during the course of mass removal. The following analysis evaluates system parameters that may be considered as surrogates representing major factors that influence organic-liquid dissolution and associated mass flux (Table 5.4-1). Specifically, the nature of contact (dilution effects, contact time) will be represented though use of source zone cross-sectional area and length. Organic-liquid accessibility is represented through the GTP ratio and relative permeability.

Changes in organic-liquid distribution can be characterized by determining the GTP ratio at multiple times throughout mass removal. The GTP ratio for both the Mixed Source and Heterogeneous experiments varied significantly as organic-liquid mass was removed through dissolution. The Variable GTP (VGTP) method attempts to account for changes in organic-liquid distribution by allowing *n* to change as a function of the changing GTP ratio (Table 5.4-1). For this method, *n* was updated at each imaging timestep by use of the measured GTP ratio and the regression equation presented in Figure 5.4-1. The simulated mass-flux-reduction/mass-removal relationships obtained using the VGTP method are presented in Figure 5.4-4a. This method was able to capture the initial behavior observed for the Heterogeneous experiment; however, it was unable to capture the increase in mass flux associated with mass removal from the pool zone. It was also unable to simulate the observed behavior for the Mixed Source experiment. These results are consistent with those above regarding the limitation of the GTP ratio.

The Variable Source Size (VS) method accounts for changes in mass flux by allowing *n* to change as a function of changes in dilution and residence time (cross-sectional area and length of the source zone) (Table 5.4-1). Changes in the organic-liquid distribution were defined by the ratios of the source-zone cross-sectional area and length to the total cross-sectional area and

length of the system. The method uses the initial GTP ratio to calculate an initial value for *n*, providing a measure of the initial organic-liquid distribution and relative accessibility.

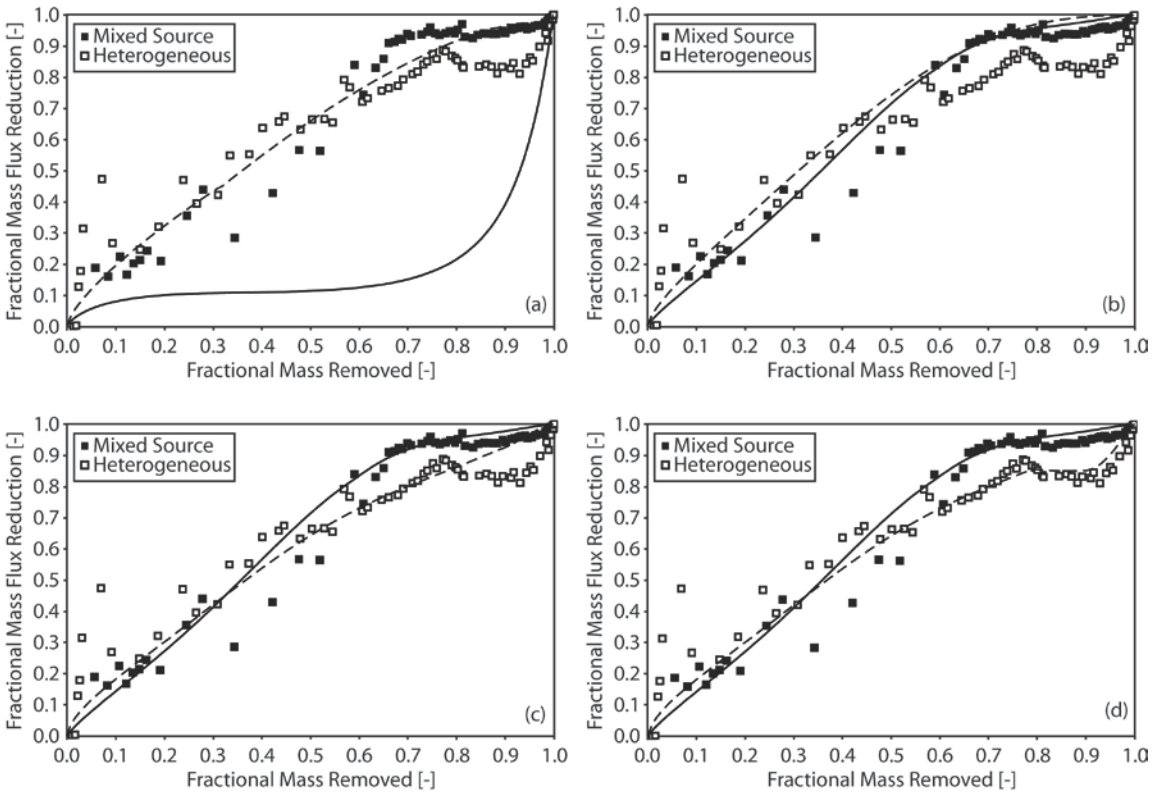

Figure 5.4-4. Mass flux reduction versus mass removal behavior for the Mixed Source and Heterogeneous experiments, and application of the various methods for characterizing mass-flux-reduction/mass-removal behavior. (a) Variable GTP method (VGTP), (b) Variable Size method (VS), (c) Multi-Domain method (MD), and (d) Multi-Domain Relative Permeability method (MDRP). The model simulations for the Mixed Source and Heterogeneous experiments are represented by the solid and dashed lines, respectively.

The mass-flux-reduction/mass-removal relationships simulated using the VS method are presented in Figure 5.4-4b. Changes in source-zone cross-sectional area and length are presented in Figure 5.4-5. This method provided a reasonable simulation of the multi-step behavior exhibited for the Mixed Source experiment. However, the VS method over-calculated the amount of mass flux reduction observed for the Heterogeneous experiment at high mass removals and was unable to simulate the increased mass flux observed when only the pool source remained.

The Multi-Domain (MD) method is a modification of the VS method, wherein the source-zone is sub-divided into regions based on intrinsic permeability (Table 5.4-1). This method accounts for the presence of multiple sub-regions of differing properties within the source zone, and is similar in concept to the two-region/multi-region models widely used in contaminant hydrology. The relative importance of each region to the overall mass flux behavior is a function of the relative fractions of organic liquid present in each region. Only one region was required for the Mixed Source experiment since all of the organic liquid was present in a

single porous medium. The source zone for the Heterogeneous experiment was divided into two regions, the matrix and the higher intrinsic-permeability zone located in the upper right-hand corner of the flow cell. The dimensions employed for the two regions were based on the physical dimensions of the permeability units. Additional simulations produced for the Heterogeneous experiment employing more than two regions did not improve the performance of this method. As for the prior method, the initial GTP ratio is used to calculate an initial value for *n*.

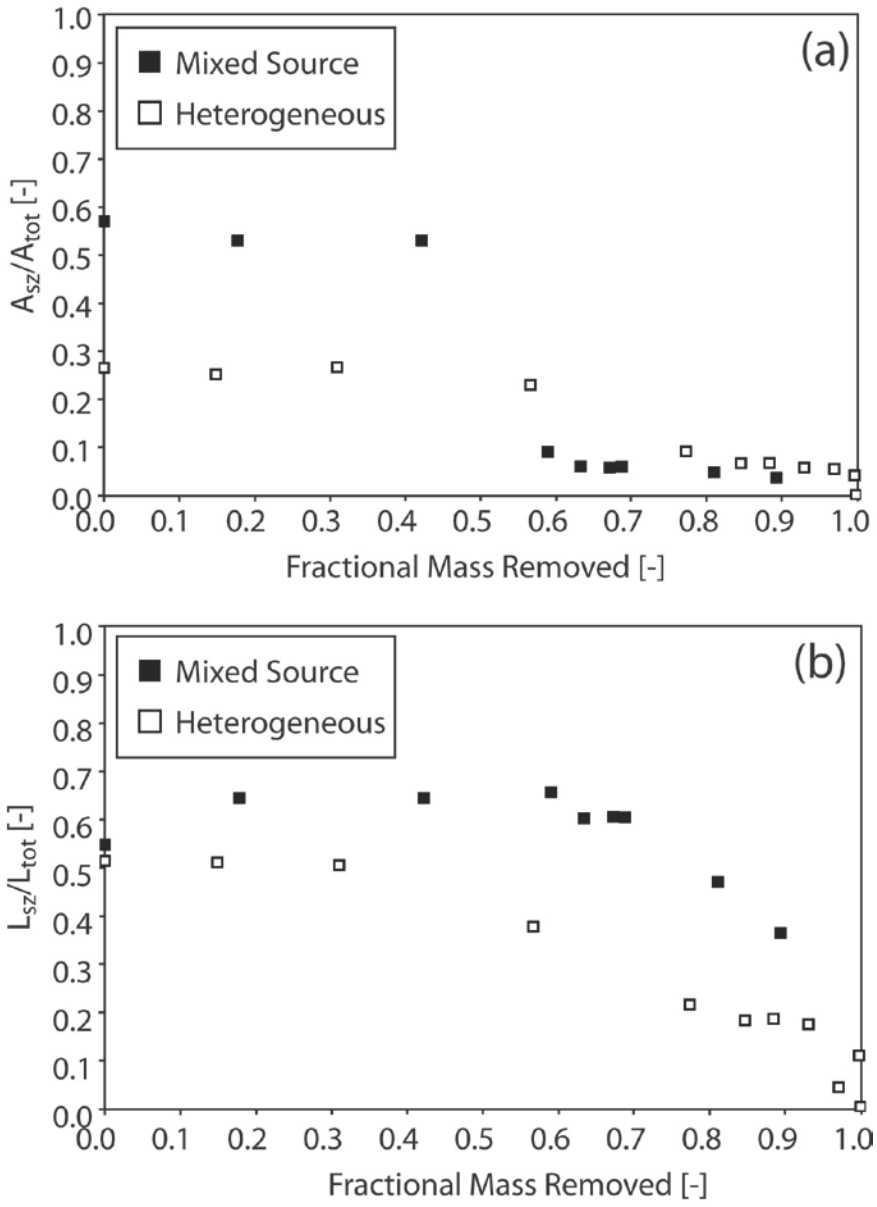

Figure 5.4-5. (a) Ratio of the source-zone cross-sectional area to the total system cross-sectional area as a function of mass removal for the Mixed Source and Heterogeneous experiments. (b) Ratio of the source-zone length to the total system length as a function of mass removal for the Mixed Source and Heterogeneous experiments.

The mass-flux-reduction/mass-removal relationships simulated using the MD method are presented in Figure 5.4-4c. Changes in source-zone cross-sectional area and length (in the flow direction) for each permeability zone in the Heterogeneous experiment are presented in Figure 5.4-6. This method captured the early behavior exhibited by the Heterogeneous experiment; however, it was unable to simulate the multi-step behavior observed at later stages of mass removal. In addition, the MD method over-calculated the amount of mass flux reduction observed at early stages of mass removal for the Mixed Source experiment. Evaluation of both the VS and MD methods shows that accounting for the initial organic-liquid distribution and dilution effects was not sufficient to fully simulate the measured mass-flux-reduction/mass-removal behavior.

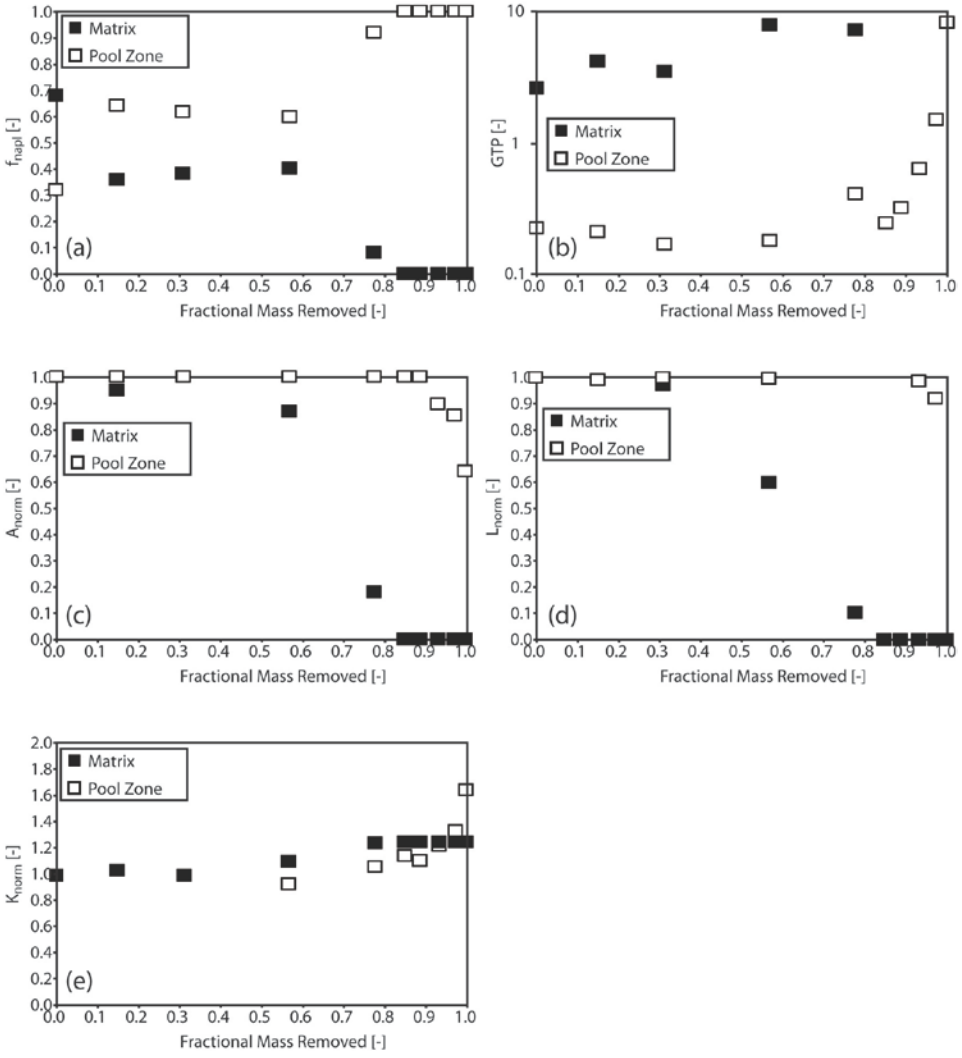

Figure 5.4-6. Measure of the source zone parameters as a function of mass removal for each permeability zone in the Heterogeneous experiment. The matrix refers to portion of the organic liquid present in the 40/50 matrix and the pool refers to the portion of the organic liquid that is present initially at high saturation in the 20/30 zone. (a) Fraction of organic liquid, (b) GTP ratio, (c) normalized source-zone cross-sectional area, (d) normalized source zone length, (e) normalized hydraulic conductivity.

The Multi-Domain Relative Permeability (MDRP) method accounts for changes in source-zone accessibility through changes in relative permeability, in addition to accounting for initial organic-liquid distribution and dilution effects (Table 5.4-1). With this method, the source zone was sub-divided into regions based on the intrinsic permeability of the porous medium, and the impact of changes in dilution and residence time (cross-sectional area and length of the source zone) was accounted for (as done for the MD method). In addition, the impact of relative permeability on organic-liquid accessibility was accounted for using a simple relative permeability function. Changes in permeability were defined by the ratio of the hydraulic conductivity at a given time to the initial hydraulic conductivity of the region. The zones were weighted based on the fraction of organic liquid present in each zone. For the Mixed Source experiment, the MDRP method reduced to the VS method (assuming negligible reductions in relative permeability), given all of the organic liquid was present in one permeability zone.

The mass-flux-reduction/mass-removal relationships simulated using the MDRP method are presented in Figure 5.4-4d. Changes in the hydraulic conductivity for each permeability zone in the Heterogeneous experiment are presented in Figure 5.4-6. This method provided the most representative simulations of the behavior exhibited by both the Mixed Source and Heterogeneous experiments. Of particular note, this method was able to simulate the increase in mass flux (decrease in mass flux reduction) observed for the Heterogeneous experiment at approximately 75% mass removal.

The relative differences between the model simulations and the measured data were quantified using the root-mean-square error (RMSE):

$$RMSE = \sqrt{\frac{1}{k}\sum_{i=1}^{n}\left(S_i - O_i\right)^2}$$

where k is the total number of samples [-], S is the method simulated reduction in mass flux [-], and O is the observed reduction in mass flux [-]. The computed RMSE value for each method is presented in Table 5.4-2. The MDRP method best represented the observed behavior for both the Mixed Source and Heterogeneous experiments. This was expected since this method is the most inclusive in accounting for changes in both organic-liquid distribution and the flow field.

Table 5.4-2. Root-mean-square error (RMSE) values for each method*

	IGTP	VGTP	VS	MD	MDRP
Mixed Source	0.10	0.52	0.05	0.08	0.05
Heterogeneous	0.08	0.08	0.11	0.08	0.07

*High values represent poorer predictions and vice versa.

Additional Modeling

Additional modeling efforts were conducted using data sets obtained from the column and flow-cell data reported herein to test other approaches for upscaled simulation of organic-liquid dissolution. One approach was based on the use of a continuous-distribution representation wherein the dissolution rate coefficient is represented by a log-normal distribution function defined by a mean and variance. Another was based on the use of the multiple-domain representation wherein the source is discretized into multiple domains, and for which dissolution

for each domain is governed by a different set of coefficient values. The results clearly show that the continuous-distribution based model cannot adequately simulate the multi-step elution curves typically obtained from the experiments. Such behavior was adequately simulated with the multi-region model. An example is presented in Figure 5.4-7. Full details are presented in the manuscript in preparation (14).

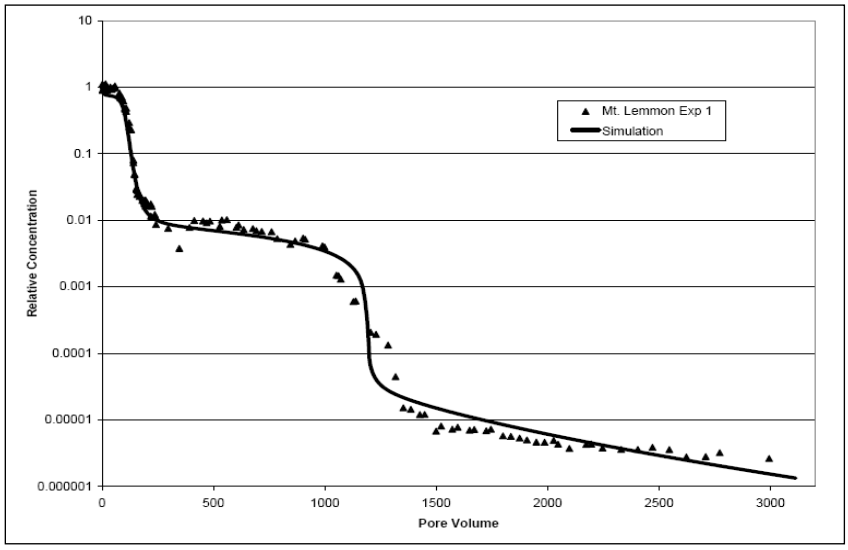

Figure 5.4-7. Example measured and simulated elution curves for column experiment. TCE liquid was present at residual saturation; the column was flushed with water. The model domain comprised three regions for TCE dissolution.

Summary

Several methods were developed herein to describe the mass-flux-reduction/mass-removal relationship using a dynamic mass-removal function and measurable system indicator parameters. The methods incorporated measures of source zone architecture (GTP ratio, source zone cross-sectional area and length) and flow field dynamics (changes in relative permeability). Methods that incorporated only the GTP ratio were adequate for obtaining a first-order approximation of initial mass-flux-reduction/mass-removal behavior. However, these methods were unable to describe the later-stage, non-singular behavior observed in the data sets. A method that incorporated parameters accounting for the source zone cross-sectional area and length as well as changes in relative permeability provided the most representative simulations of the observed data. This is consistent with the results of prior work wherein inclusion of relative-permeability dynamics has been shown to improve model performance (e.g., Powers et al., 1998; Brusseau et al., 2002; Zhang et al., 2008).

As has been discussed, approaches based solely on an initial characterization of the system often have difficulty in providing adequate simulations of observed mass-flux-reduction/mass-removal behavior for complex systems (e.g., Christ et al., 2006; Brusseau et al., 2008; DiFilippo and Brusseau, 2008; Zhang et al., 2008). The approach presented herein represents an attempt to mediate this constraint, and based on the results presented herein, has the potential to improve characterization of mass-flux-reduction/mass-removal behavior. However, this approach requires determination of system indicator parameters multiple times during the course of a mass-removal event. As is widely acknowledged, such measurements may be difficult to obtain for many field applications, and multiple measurements will increase costs. More work is needed to investigate readily measurable system parameters useful as indicators of mass-removal and mass-flux behavior.

6.0 Conclusions and Implications for Future Research/Implementation

6.1 Conclusion and Implications

6.1.1 Source-Zone Architecture and Age

A series of flow-cell experiments was conducted to investigate the impact of source-zone architecture and flow-field heterogeneity on mass-removal and mass-flux behavior. Our results illustrate the impact of organic-liquid distribution and hydraulic accessibility on mass-flux-reduction/mass-removal behavior. Large fractions of mass removal may be required to induce significant reductions in mass flux for systems with uniform distributions of organic liquid (i.e., all residual or all pool) residing in hydraulically-accessible flow domains. Conversely, significant reductions in mass flux may be induced with relatively minimal mass removal for systems wherein organic liquid is present at both residual and higher saturations. These results are consistent with the few prior published laboratory and modeling studies.

A unique component of the project involved comprehensive long-term studies conducted at a field site (the TIAA site). In one study, the temporal behavior of contaminant mass discharge for a DNAPL source zone was characterized. The results showed that contaminant mass discharge decreased asymptotically with time, from approximately 1 to 0.15 kg/d. Comparison of two sets of core data, collected 3.5 years apart, suggests that aggregate sediment-phase TCE concentrations decreased by ~80% between sampling events. The results indicate that contaminant mass discharge decreased significantly during five years of system operation.

Contaminant mass discharge data can be integrated with measurements of initial mass to characterize the relationship between reductions in contaminant mass discharge and reductions in contaminant mass. The data collected during the study were used develop such a relationship for the source area of the site. The profile exhibited by the data is consistent with a system wherein significant quantities of mass were present in hydraulically poorly accessible domains, for which mass removal is influenced by mass-transfer constraints. This contention is supported by the sediment-core data, which showed that the highest concentrations of TCE are associated with lower-permeability units, and by the estimates of the amount of groundwater flushing and associated contaminant mass removal experienced by the source area in the ~60 years prior to project startup.

The results obtained from the present study were compared to those obtained from other field studies to evaluate the impact of system properties and conditions on behavior. The results indicated that factors such as domain scale, hydraulic-gradient status (induced or natural), and flushing-solution composition had insignificant impact on the CMDR-MR profiles and thus on underlying mass-removal behavior. Conversely, source-zone age, through its impact on contaminant distribution and accessibility, was implicated as a critical factor influencing the nature of the CMDR-MR relationship. This is consistent with the results of mathematical modeling studies and laboratory experiments (Jawitz et al., 2005; Brusseau et al., 2008; DiFilippo et al., 2010).

In total, the results of the bench-scale and field studies demonstrate that the configuration of the source zone with respect to spatial distributions of subsurface properties (porous-media type, permeability, contaminant) exerts a significant control on the magnitudes and rates of mass removal and associated contaminant mass discharge. In particular, it was observed that source-zone age was a critical factor mediating system behavior. The results meet Objective 1 of the project: “Investigate the impact of source-zone aging on the relationship between mass removal and mass-flux reduction”.

6.1.2 Plume Response and Persistence

It is well established that remediation of large groundwater contaminant plumes requires cleanup or control of the source zones. The response of the plume after implementation of source-zone management is a critical issue for chlorinated-solvent sites. This project included two field studies of plume response, one wherein aggressive source remediation efforts were implemented (SVE and ISCO) and one for which source control was achieved via hydraulic containment. The analysis presented herein was based on employing contaminant mass discharge as an integrative measure of the performance and effectiveness of remediation efforts. The standard approach of characterizing discharge at the source-zone scale was expanded to provide characterization at the plume scale, which was evaluated by examining the change in contaminant mass discharge associated with the plume-scale pump-and-treat system. This approach allows linking the impacts of source-zone remediation to effects on site-wide risk.

The results for the Southern section of the TIAA site indicated that aggressive source-zone remediation resulted in significant reductions of contaminant mass discharge to the plume. However, while significant reductions were attained, it is evident that implementation of the source-zone remediation efforts has not completely eliminated contaminant mass discharge. Remaining contaminant mass contributing to the current mass discharge is hypothesized to comprise poorly-accessible mass in the source zones, as well as aqueous (and sorbed) mass present in the extensive lower-permeability units located within and adjacent to the contaminant plume. The results of mathematical modeling illustrated the impact of back diffusion and nonideal sorption/desorption on the time required for removal of the plume-associated mass, and indicated the plume would persist for many decades.

The results for the Central section of the TIAA site demonstrate that hydraulic containment of the source zone has resulted in isolation of the source from the contaminant plume and elimination of mass discharge to the plume. The results of this study indicate that operation of the plume-scale pump-and-treat system after source containment has resulted in a significant reduction in contaminant mass, mass discharge, and areal extent for the plume. For example, concentrations of TCE within the gravel unit decreased by 90% after implementation of source containment. In addition, the mass of TCE and the contaminant mass discharge associated with the plume have both decreased by approximately 87%. However, TCE concentrations and associated mass discharge began to exhibit an asymptotic decline after the equivalent of approximately one pore volume of groundwater removal. In addition, the areal extent of the plume has decreased by only 50% despite the flushing of the equivalent of more than three pore volumes of groundwater. The results of sediment-core and groundwater sampling show that a significant reservoir of contaminant mass resides in the clay units adjacent to the sand/gravel unit. This latter unit is considered to be the primary avenue for longitudinal plume migration. Diffusion of TCE from the clay units into the sand/gravel unit (back diffusion) is concluded to be the primary constraint to rapid removal of the plume, and is likely to cause the plume to persist for many decades.

In total, the results of the project demonstrate that management of source zones can reduce contaminant mass discharge to the groundwater plume. The analyses indicated that this action can, in turn, reduce the time required to clean up the groundwater plume. However, the results also show that the plumes can be expected to persist for an extended time due to the contributions of back diffusion associated with contaminant mass stored in lower-permeability units located within or adjacent to the plume. The studies reported herein assessed the impact of source-zone remediation efforts on plume-scale contaminant mass discharge and plume response

at an unprecedented resolution and scale, thus providing a significant, unique contribution to our understanding of plume behavior. Hence, the results met Objective 2 of the project: "Investigate the impact of source-zone architecture and mass-transfer dynamics on contaminant removal, mass flux, and plume response at the field scale".

6.1.3 Mathematical Modeling

Significant effort has been directed at developing models for simulating dissolution of organic liquids and associated source-zone mass-removal and mass-flux behavior. It has been clearly demonstrated through comparison of simulations to measured data that complex dissolution models can be used successfully to simulate organic-liquid dissolution in heterogeneous systems when sufficient information is available regarding the spatial distribution of permeability and organic-liquid mass (e.g., Powers et al., 1998; Frind et al., 1999; Zhang and Brusseau, 1999; Detwiler et al., 2001; Brusseau et al., 2002; Brusseau et al., 2007; Marble et al., 2008). However, the application of complex mathematical models requires detailed characterization of the system, which is often not possible for field sites. This leads to the alternative of employing simplified models, and the host of issues associated with such an approach.

One major issue associated with the simplified approaches such as the function presented in equation 4.1, as well as streamtube-based source-depletion models (e.g., Soerens et al., 1998; Jawitz et al., 2005) and deterministic dissolution models employing continuous-distribution dissolution functions (e.g., Garg and Rixey, 1999; Zhang and Brusseau, 2004) is that they typically produce singular mass-flux-reduction/mass-removal curves. Conversely, as noted above, non-singular (multi-step) behavior is often observed for complex systems. While simulations produced by the simplified models may be deemed to adequately represent measured non-singular behavior in some cases, the error associated with the simulated curves may be quite significant, particularly at the field scale where deviations may translate to many years of system operation and attendant costs. Modifying these approaches to represent the existence of distinct regions of differing conditions within the system (e.g, through the use of multi-region approaches) may in some cases improve performance. However, their effectiveness remains constrained by the use of only initial-condition information. One potential approach to improving the performance of simplified models for simulating mass-flux-reduction/mass-removal behavior, and in particular non-singular behavior, is to dynamically inform (update) the model via system indicator parameters throughout the course of mass removal.

Several methods were developed herein to describe the mass-flux-reduction/mass-removal relationship using a dynamic mass-removal function and measurable system indicator parameters. The methods incorporated measures of source zone architecture (GTP ratio, source zone cross-sectional area and length) and flow field dynamics (changes in relative permeability). Methods that incorporated only the GTP ratio were adequate for obtaining a first-order approximation of initial mass-flux-reduction/mass-removal behavior. However, these methods were unable to describe the later-stage, non-singular behavior observed in the data sets. A method that incorporated parameters accounting for the source zone cross-sectional area and length as well as changes in relative permeability provided the most representative simulations of the observed data. This is consistent with the results of prior work wherein inclusion of relative-permeability dynamics has been shown to improve model performance (e.g., Powers et al., 1998; Brusseau et al., 2002; Zhang et al., 2008).

As has been discussed, approaches based solely on an initial characterization of the system often have difficulty in providing adequate simulations of observed mass-flux-reduction/mass-removal behavior for complex systems (e.g., Christ et al., 2006; Brusseau et al., 2008; DiFilippo and Brusseau, 2008; Zhang et al., 2008). The approach presented herein represents an attempt to mediate this constraint, and based on the results presented herein, has the potential to improve characterization of mass-flux-reduction/mass-removal behavior. These results met Objective 3: "Apply mathematical models to evaluate the impact of porous-medium heterogeneity, nonuniform DNAPL distribution, and mass-transfer processes on mass-flux behavior at multiple scales".

6.1.4 Implications

Plume Persistence and Long-term Management

In addition to chlorinated solvents, several other types of contaminants of greatest concern to the Department of Defense pose significant groundwater contamination problems. Examples include 1,4-dioxane, perchlorate, nitrate, and sulfate. Extensive dissolved-phase groundwater contaminant plumes typically form at sites contaminated by these compounds because of their relatively high aqueous solubilities (in comparison to regulatory standards), limited retardation, and generally low (or very site dependent) transformation potential. In many cases, the plumes are hundreds of meters to several kilometers long. These large plumes are very expensive to contain and remediate, and present difficult challenges to long-term management of contaminated sites. Pump and treat is currently the primary method used to contain and treat groundwater contaminant plumes at these sites.

The results of this project support the observations reported in prior studies that most sites with large groundwater plumes comprising these contaminants will require many decades before cleanup will be achieved under current methods and standards. The continued use of pump and treat to manage plumes at these sites for the many additional decades anticipated will result in an enormous aggregate operations and maintenance cost. Hence, there is a critical need to evaluate alternative methods, such as monitored natural attenuation, permeable reactive barriers, and deep reactive treatment zones that can be used to cost-effectively manage these plumes while continuing to meet all remedial objectives. Methods for assessment and implementation have been developed for individual remedial alternatives. However, no robust, comprehensive framework currently exists to support objectives-based site assessments for transitioning from pump and treat to these alternative methods. Development of such a framework would facilitate site assessments and improve long-term management.

Cost-effective High-Resolution Site Characterization

It is now well established that spatial variability (or heterogeneity) of physical and biogeochemical properties of the subsurface greatly impacts the effectiveness of site characterization, risk assessment, and remediation. For example, the spatial distribution of permeability mediates the flow field, which influences contaminant transport and delivery of remedial vectors. It also influences the distribution of contamination, which in turn impacts the effectiveness of remedial operations. Additionally, physical and biogeochemical heterogeneity can impart spatial variability to the magnitudes and rates of mass-transfer and transformation processes. Furthermore, it is now recognized that operation of remediation systems will at some point significantly modify the distribution and accessibility of contamination, such that operational effectiveness will typically diminish significantly with time. Currently, the vast

majority of characterization efforts conducted at hazardous-waste sites do not provide sufficient resolution of subsurface heterogeneity nor of temporal variability of subsurface properties and conditions.

Higher-resolution characterization of contaminant distributions, hydrogeological properties, and biogeochemical conditions can significantly enhance risk assessment and the selection, design, and operation of remediation systems. However, current methods used for high-resolution site characterization, such as fine-scale sediment coring, tracer tests, and tomography, are expensive and often disruptive to remediation-system operations. There is a critical need to develop methods that can provide higher-resolution characterization that: (a) are cost effective, (b) are specifically designed to minimize disruption of operating remedial systems, and (c) can readily provide temporal updates of site conditions, thus supporting adaptive responses of the remedial systems to changing site conditions.

Treatment of Sources in Low-Permeability Systems

Source zones located in relatively deep, low-permeability formations provide special challenges for remediation. Given these site conditions, source containment using hydraulic-based methods or permeable reactive barriers may be impractical, and aggressive mass-removal approaches based on reagent injection (e.g., ISCO, enhanced-solubility reagents) are likely to be ineffective using standard implementation methods. In-situ thermal or electrokinetic methods may be feasible, but are likely to be relatively expensive. Additional research is needed to develop and test alternatives for treating poorly accessible contaminant mass in source zones. Technologies under consideration include (a) the use of shear-thinning fluids (STF) to provide improved control of solution injection into heterogeneous subsurface environments, (b) hydraulic and pneumatic fracturing to improve extraction of contaminants from lower-permeability formations, and (c) coupling advanced oxidation reagents with facilitated-transport and timed-release reagents to enhance ISCO applications. The efficacy and cost-effectiveness of such approaches to reduce CMD to the plume is a key performance factor.

Another possible approach for treating sources in lower-permeability systems is to create a persistent treatment zone for purposes of containment. This concept was tested at a site within the TIAA complex. The objective of this approach is to reduce the contaminant mass discharge from the source zone via source containment. In this case, containment is effected by creation of a persistent treatment zone through injection of permanganate solution. Given the site conditions (low permeability, low hydraulic gradient), it was hypothesized that the reagent solution would remain primarily within the source area for several years. Thus, a single round of injection was designed, minimizing costs. Results of the field study indicated the approach was successful in reducing the discharge of contaminant to the plume. This may be a viable, lower-cost approach for source containment in systems such as the one investigated.

6.2 Practical Tools for Site Characterization and Remediation Performance Assessment

6.2.1 Time-Continuous Contaminant Mass Discharge

A key issue for implementing source-zone remediation methods at a given site is their relative costs and benefits in comparison with existing (typically pump and treat) and other potential remediation efforts. Assessing the quantitative performance of a source-zone remediation effort is central to evaluating associated costs and benefits. The performances of a variety of source-zone remediation efforts have been evaluated in a number of studies. To date, remediation performance assessment has typically been based on analysis of changes in

groundwater contaminant concentrations within the treatment zone, wherein samples are collected from one or more monitoring wells. As is widely recognized, the effectiveness of this point-sampling-based method is often limited for large, complex sites characterized by high degrees of heterogeneity. Interest has increased recently in the use of contaminant mass flux or discharge as a more integrative measure of the performance of source-zone remediation efforts. The use of contaminant mass discharge also has several advantages compared to the other alternative metric, reduction in contaminant mass, including greater accessibility, less uncertainty, and greater relevance for risk-based assessment. The use of contaminant mass discharge has been demonstrated successfully in a number of projects (see recent reviews: DiFilippo and Brusseau, 2008; ITRC, 2010).

Characterization of contaminant mass discharge for purposes of evaluating the performance of source-zone remediation efforts is typically conducted at the source-zone scale. However, it can also be useful to evaluate the impact on plume-scale mass discharge. This is relatively straightforward for sites consisting of a single source zone and a relatively small associated plume. However, it becomes a more complex endeavor for sites with multiple source zones and large plumes. In this project we developed and demonstrated an enhanced approach for characterizing contaminant mass discharge that extends the standard source-zone scale measurements to incorporate additional characterization at the plume scale. We demonstrated that collection of integrated plume-scale contaminant mass discharge data before, during, and after a source-zone remediation effort provided a high-resolution, real-time analysis of discharge perturbations, including rebound effects. This approach provides a robust means by which to link source-zone remediation to impacts on the contaminant plume and associated site-wide risk, and is anticipated to have broad utility for assessing remediation effectiveness.

As noted, the use of contaminant-mass-discharge measurements to characterize site conditions and evaluate remediation performance is becoming a critical component of site assessment. However, almost all applications to date have been based on obtaining one or two discrete measurements of contaminant mass discharge (e.g., collected before and after a remedial action), using multi-point transects or short-term pumping tests that are often applied within the contaminant plume. While this approach provides useful information, additional information and insight can be gained by measuring time-continuous profiles of contaminant mass discharge. In this project, we demonstrated that time-continuous measurements of contaminant mass discharge can provide useful information to characterize mass-transfer processes, assess mass-removal magnitudes and conditions, and estimate contaminant distributions and quantities, as well as measure mass discharge. It is anticipated that collection and analysis of time-continuous contaminant-mass-discharge data at other DOD sites would provide substantial benefits, including improving the assessment and cost-effective operation of remediation systems.

6.2.2 The Contaminant Mass Discharge Test

Time-continuous profiles of contaminant mass discharge can be obtained by conducting extended contaminant mass discharge tests or by capturing operational fluid-extraction data. The latter method is discussed in section 6.2.3 below. The CMD test, which involves using one or more wells to extract groundwater (or vapor) for extended times to measure CMD, is based on the contaminant elution test. The contaminant elution test was developed to characterize mass-removal behavior, and was focused on applications for groundwater plumes (Bahr, 1989). Brusseau and colleagues extended the test to source zones, and demonstrated its utility for measuring contaminant mass discharge (Brusseau et al., 1999, 2007, 2011a, 2011b, 2013). A

significant advantage of the CMD test is its high degree of temporal resolution, much greater than that associated with typical monitoring-well sampling. This high temporal resolution allows the CMD test to provide rapid analysis of potential changes in system conditions due to site perturbations, and supports dynamic updating of the conceptual site model. The results of this project demonstrated the benefits associated with conducting CMD tests, and provided methods for data analysis and interpretation.

A primary disadvantage of the standard CMD test is limited spatial resolution in the vertical dimension, given that typical extraction wells are built with large screened intervals. A modified CMD test, the vrCMD test, is proposed to specifically resolve this issue. For this method, the extraction well is designed or retrofitted to allow groundwater extraction via multiple pumps placed along the vertical axis of the well and separated by packers. This approach allows collection of vertically resolved flow and contaminant-concentration data, and thus vertically resolved CMD over time.

6.2.3 Use of Pump-and-Treat Operations Data for Assessing Remediation Efforts

One primary practical outcome of our project is the demonstration of the enormous wealth of information that can be recovered from analysis of historic data sets obtained from an operating pump-and-treat system. Flow-rate and contaminant-concentration data are routinely collected under regulatory requirement for all pump-and-treat operations. However, these data are rarely used other than to monitor the mass of contaminant removed. Our project, using data sets collected for the TIAA Superfund site, showed that analysis of operational flow-rate and contaminant-concentration data can provide the following information:

(1) estimates of initial contaminant mass,
(2) time-continuous measurements of contaminant mass discharge,
(3) time-continuous measurements of magnitudes and rates of mass removal,
(4) characterization of the relationship between reductions in contaminant mass discharge and reductions in contaminant mass,
(5) delineation of source-zone architecture,
(6) delineation of contaminant-mass-removal conditions,
(7) assessment of contaminant persistence,
(8) identification of specific mass-transfer processes and other factors influencing mass removal,
(9) assessment of the impact of source-zone remedial actions on overall risk reduction.

The information obtained from mining of the data can be used to update the site conceptual model, to revise the design and operation of the remediation systems, and to support decision-making concerning remedy modification, long-term site management, and closure. The method and approach is presented in a manuscript in press (15), and application of the method to site data is illustrated in a manuscript in review (17).

The basic approach of the characterization method involves the following components:

1. Tabulation and quality-assurance evaluation of raw flow-rate and concentration data.
2. Calculation of integrated contaminant mass discharge as a function of operational time.
3. Integration of the temporal mass-discharge data to determine time-continuous measurements of magnitudes and rates of mass removal.

4. Application of a mathematical mass-depletion function to the temporal mass-discharge data to estimate the initial contaminant mass that was present in the treatment zone at the start of remediation. This information is invaluable for the design of remediation systems, for assessing remediation progress, and for evaluating closure. However, it is well known that determining this variable using standard methods is problematic for most sites.
5. Use of calculated initial mass and time-continuous mass removal data to characterize the relationship between reductions in contaminant mass discharge (CMDR) and reductions in contaminant mass (MR) as a function of operational time. The CMDR-MR relationship is a defining characteristic of system behavior, and is mediated by system properties and conditions such as permeability distribution, contaminant distribution, and mass-transfer processes. This index has the potential to be a powerful tool for analyzing the performance of remediation systems, and additional research is needed to fully evaluate its utility.
6. Analysis of the processed data to evaluate contaminant-mass-removal conditions, source-zone architecture, contaminant persistence, specific mass-transfer processes and other factors influencing mass removal, and the impact of source-zone remedial actions on overall risk reduction.

In summary, the project showed that our approach for comprehensive analysis of operational pump-and-treat data is a powerful, cost-effective method for providing higher-resolution, value-added characterization of contaminated sites. Advantages of the method include: (a) use of data that typically exists for operating sites, thus minimizing data-collection costs, (b) no disruption of the operating remediation system, (c) ability to update the analysis at any time, providing a means to periodically revise the site conceptual model, and the operation of the remediation system. It is anticipated that implementation of this tool at other DOD sites will enhance site assessment and operation of remediation systems.

Two methods were used in the project to estimate the mass of contaminant initially present in the source area, and they produced reasonably similar results. The second method is based on fitting a mass-depletion function to temporal CMD data, and has broad potential applicability given the general widespread availability of monitoring-well data for many sites. However, it is anticipated that CMD data (rather than solely concentration data) measured directly for the source area via an extended contaminant mass discharge test as done herein will provide a more robust data set for estimation of source mass. The second method is a useful alternative to standard coring, particularly for cases wherein coring is technically or economically impractical. The method is also useful for cases wherein temporal CMD data can be captured from analysis of operational data for fluid-extraction systems such as pump and treat or soil vapor extraction. Such analysis of historic-operations data provides a simple means by which to estimate initial contaminant mass for the treatment domain.

6.2.4 The CMDR-MR Relationship

Temporal profiles of contaminant mass discharge, combined with knowledge of initial contaminant mass, can be used to evaluate the relationship between reductions in contaminant mass discharge (CMDR) and reductions in contaminant mass (MR). These relationships have been characterized in several laboratory and mathematical-modeling studies (Rao et al., 2002; Jayanti and Pope, 2004; Phelan et al., 2004; Jawitz et al., 2005; Fure et al., 2006; Brusseau et al., 2008; DiFilippo and Brusseau, 2008; Kaye et al., 2008; Maji and Sudicky, 2008; Carroll and Brusseau, 2009; Christ et al., 2009, 2010; Tick and Rincon, 2009; DiFilippo et al., 2010; Marble

et al., 2010). However, very few measurements of CMDR-MR relationships have been reported to date for field systems (Brusseau et al., 2007; DiFilippo and Brusseau, 2008). This is because very few measurements of time-continuous profiles of contaminant mass discharge have been reported to date for field systems, as well as the typical uncertainty regarding initial contaminant mass for most sites. Initial time-continuous-based characterizations of CMDR-MR relationships for field sites were reported by Brusseau et al. (2007) and DiFilippo and Brusseau (2008). Brusseau et al. (2007) determined the integrated CMDR-MR relationship associated with combined pump and treat of the sources and groundwater contaminant plume for the South section of the TIAA complex. DiFilippo and Brusseau (2008) determined the CMDR-MR relationships for emplaced-source experiments conducted at the Borden site in Canada, using raw concentration and flow-rate data reported by Broholm et al. (1999) and Rivett and Feenstra (2005).

Three simplified, prototypical relationships between reductions in contaminant mass discharge and reductions in contaminant mass useful for comparative discussion are illustrated in Figure 6.2.4-1. Such relationships can be readily developed by employing a simple limiting-case analysis of the temporal mass-removal and contaminant-elution functions for contaminated systems (as shown in Figures 6.2.4-2 and 6.2.4-3, respectively), from which the mass-discharge-reduction/mass-removal relationship can be obtained directly. The curve in the lower right of Figure 6.2.4-1 represents the relationship for a system governed by relatively ideal mass-transfer behavior, wherein mass removal is relatively efficient, as illustrated by the corresponding contaminant elution curve presented in Figure 6.2.4-3. Because mass removal is relatively efficient, the aqueous-phase contaminant concentrations are maintained at maximal or near-maximal levels, and thus there is minimal reduction in mass discharge until almost all of the mass has been removed. The curve in the upper left of Figure 6.2.4-1 represents the relationship for a system governed by non-ideal mass-transfer behavior (e.g., poorly accessible mass due to rate-limited dissolution, by-pass flow phenomena, or other factors), wherein mass removal is relatively inefficient (Figure 6.2.4-3), and there is a significant reduction in mass discharge with minimal mass removed. The third curve represents the special case wherein there is a one-to-one relationship between mass discharge reduction and mass reduction (e.g., first-order mass removal).

Given that performance objectives may typically require orders-of-magnitude reductions in CMD or mass, it is instructive to re-plot Figure 6.2.4-1 in log form. The result is presented in Figure 6.2.4-4. An alternative form of the plot is presented in Figure 6.2.4-5, wherein relative CMD and relative mass are used in place of relative reductions in mass discharge and mass.

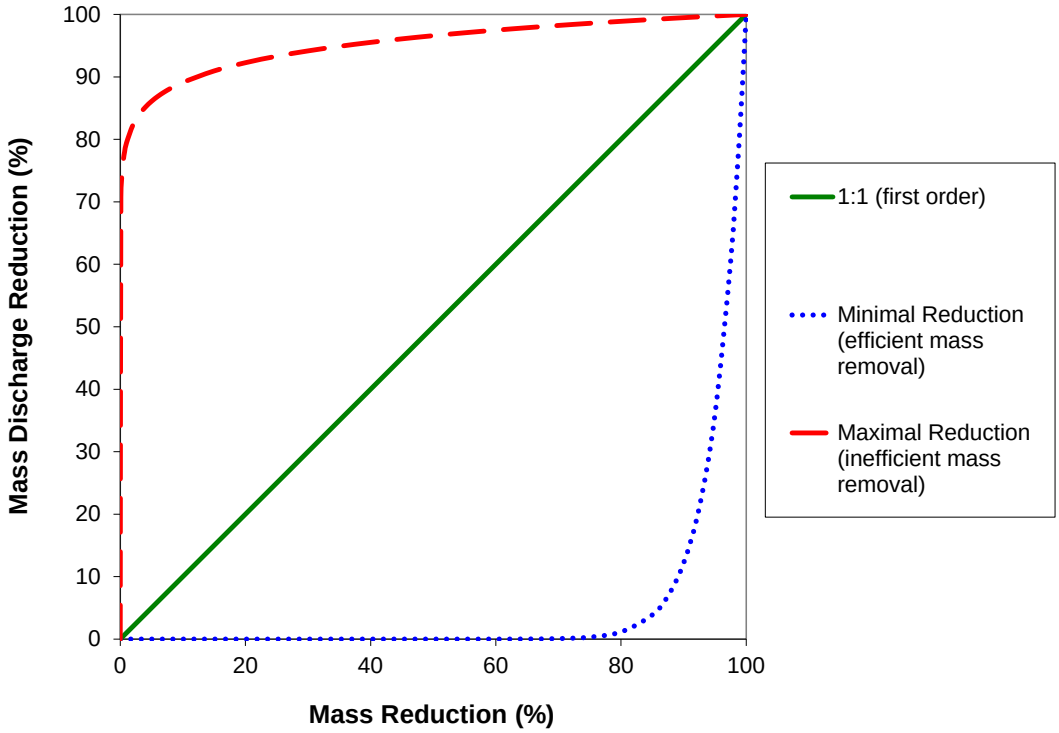

Figure 6.2.4-1. Relationships between reduction in contaminant mass discharge and reduction in contaminant mass for three prototypical cases.

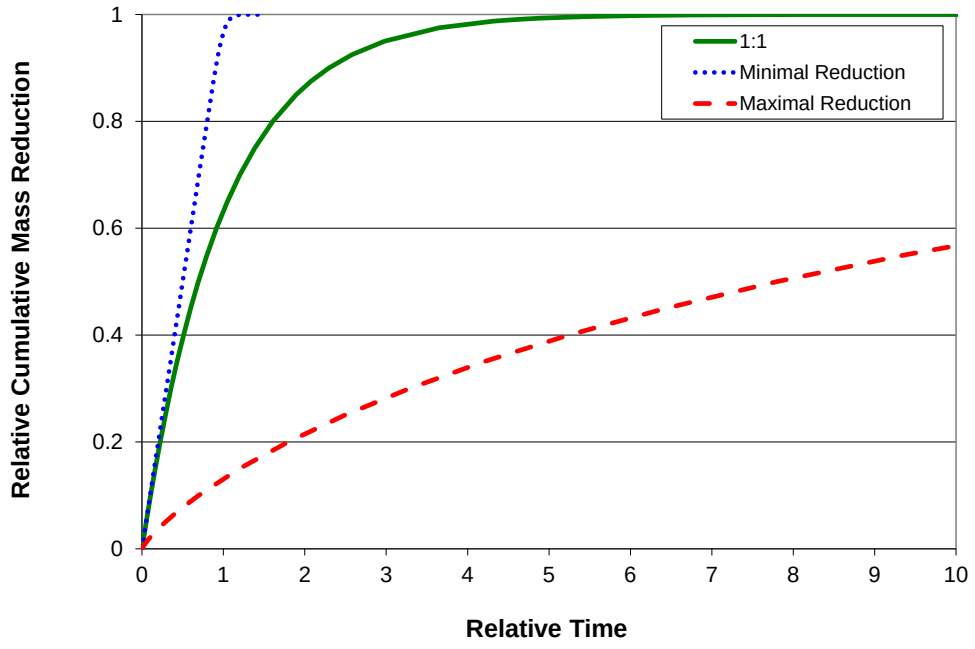

Figure 6.2.4-2. Cumulative mass reduction profiles for three prototypical cases.

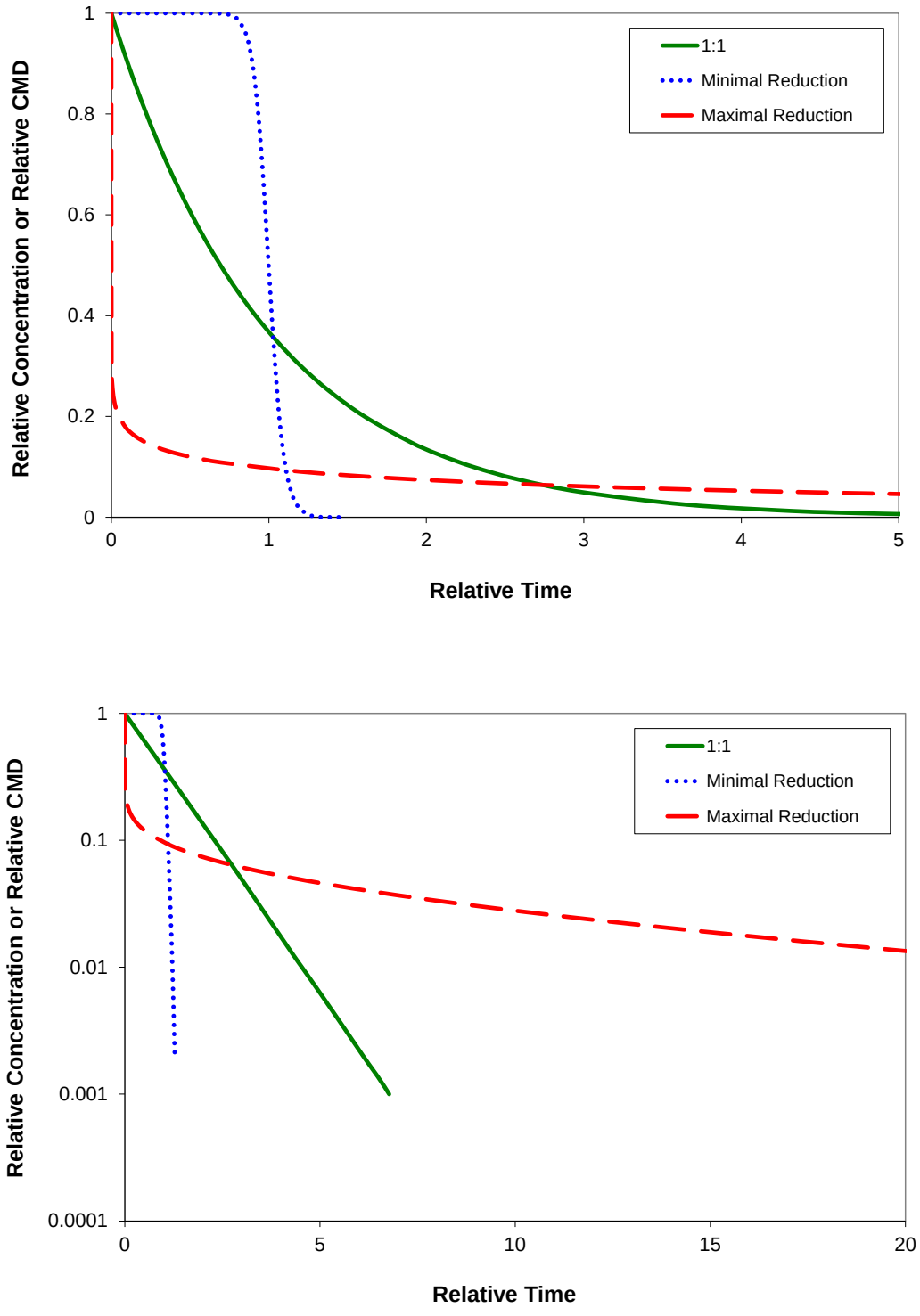

Figure 6.2.4-3. Temporal concentration or CMD profiles for three prototypical cases. Top = arithmetic scale; bottom = log scale.

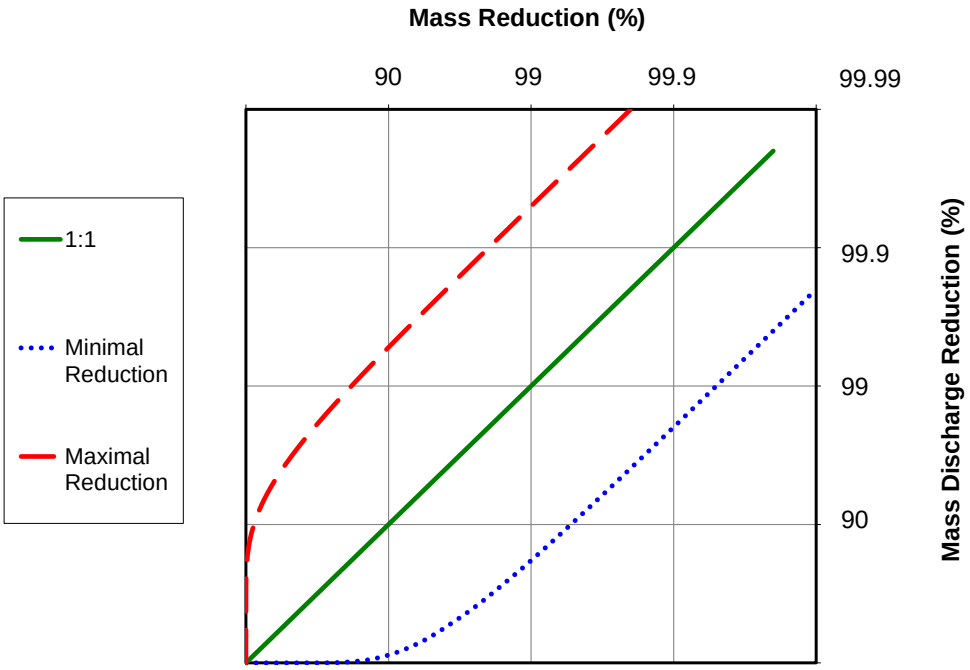

Figure 6.2.4-4. Relationships between reduction in contaminant mass discharge and reduction in contaminant mass for three prototypical cases; log scale.

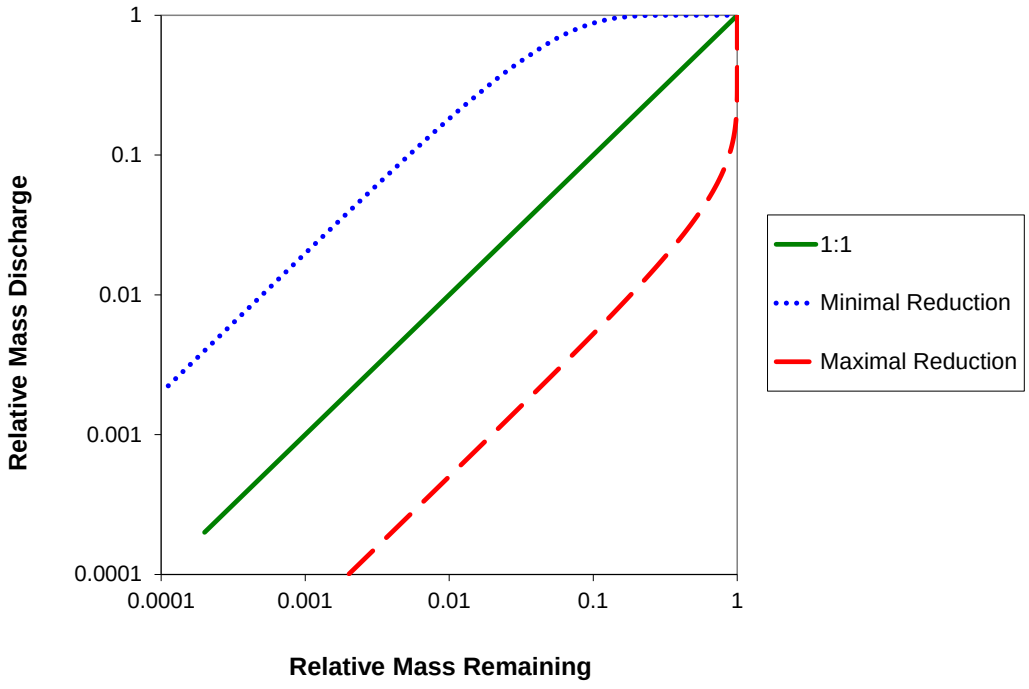

Figure 6.2.4-5. Relationships between relative contaminant mass discharge and relative contaminant mass for three prototypical cases; log scale.

In this project, we developed CMDR-MR relationships for a well-detailed field site, and also for several other prior field projects. These data represent the first comprehensive field-based analysis of this entity. The results indicate that the CMDR-MR relationship is a defining characteristic of system behavior, and is mediated by system properties and conditions such as permeability distribution, contaminant distribution, and mass-transfer processes. It is anticipated that its use for other DOD sites will provide multiple benefits, including enhancing assessment and operation of remediation systems. The results of this work, in conjunction with those discussed in the preceding subsections of section 6.2 meet Objective 4: "Assess the efficacy of methods for estimating mass-flux-reduction/mass-removal behavior".

6.3 Summary Statement

The studies reported herein investigated the impact of source-zone remediation efforts on contaminant mass discharge and associated plume response at an unprecedented resolution and scale. The results obtained thus provide a significant, unique contribution to our understanding of source-zone dynamics and plume persistence for DNAPL sites. It is anticipated that application of the concepts and tools developed from the project to other DOD sites would provide substantial benefits, including improving the assessment and cost-effective operation of remediation systems for, and enhancing long-term management of, sites contaminated by chlorinated solvents.

7.0 Literature Cited

Bahr, J.M. 1989. Analysis of nonequilibrium desorption of volatile organics during field test of aquifer decontamination, J. Contam. Hydrol., 4(3), 205-222.

Basu, N.B., P.S.C. Rao, R.W. Falta, M.D. Annable, J.W. Jawitz, K. Hatfield. Temporal evolution of DNAPL source and contaminant flux distribution: Impacts of source mass depletion, JCH, 2008, 95(3-4), 93-109.

Basu, N.B., Rao, P.S.C., Poyer, I.C., Nandy, S., Mallavarapu, M., Naidu, R., Davis, G.B., Patterson, B.M., Annable, M.D., Hatfield, K. 2009. Integration of traditional and innovative characterization techniques for flux-based assessment of Dense Non-aqueous Phase Liquid (DNAPL) sites. J. Contam. Hydrol. 105, 161-172.

Blue, J.E.; Brusseau, M.L.; Srivastava, R. Simulating Tracer and Resident Contaminant Transport to Investigate the Reduced Efficiency of a Pump-and-Treat Operation. Groundwater Quality: Remediation and Protection (Proceedings of the GQ '98 Conference Held at Tubingen, Germany, September 1998. IAHS Publication no. 250, 1998. 537-543.

Broholm, K., Feenstra, S., Cherry, J.A., 1999. Solvent release into a sandy aquifer. 1. Overview of source distribution and dissolution behavior. Environ. Sci. Technol. 33, 681-690.

Brooks, M.C.; Annable, M.D.; Rao, P.S.C.; Hatfield, K.; Jawitz, J.W.; Wise, W.R.; Wood., A.L.; Enfield, C.G. 2004. Controlled release, blind test of DNAPL remediation by ethanol flushing. J. Contam. Hydrol. 69: 281-297.

Brusseau, M.L. 1993. Complex Mixtures and Groundwater Quality. Environmental Research Brief. EPA/600/S-93/004.

Brusseau, M.L. et al., 2000. Influence of heterogeneity and sampling method on aqueous concentrations associated with NAPL dissolution. Environmental Science & Technology, 34(17): 3657-3664.

Brusseau, M.L., Carroll, K.C., Allen, T., Baker, J., DiGuiseppi, W., Hatton, J., Morrison, C., Russo, A., and Berkompas, J. 2011a. The Impact of In-situ Chemical Oxidation on Contaminant Mass Discharge: Linking Source-zone and Plume-scale Characterizations of Remediation Performance. Environ. Sci. Technol., 45:5352-5358.

Brusseau, M.L., DiFilippo, E.L., Marble, J.C. and Oostrom, M., 2008. Mass-removal and mass-flux-reduction behavior for idealized source zones with hydraulically poorly-accessible immiscible liquid. Chemosphere, 71(8): 1511-1521.

Brusseau, M.L., Hatton, J., and DiGuiseppi, W. 2011b. Assessing the Impact of Source-Zone Remediation Efforts at the Contaminant-Plume Scale: Application to a Chlorinated-Solvent Site. J. Contam. Hydrol., 126:130-139.

Brusseau, M.L.; Matthieu III, D.E.; Carroll, K.C.; Mainhagu, J.; Morrison, C.; McMillan, A.; Russo, A.; Plaschke, M. 2013. Characterizing Long-term Contaminant Mass Discharge and the Relationship Between Reductions in Discharge and Reductions in Mass for DNAPL Source Areas. J. Contam. Hydrol., 149: 1-12.

Brusseau, M.L.; Nelson, N.T.; Oostrom, M.; Zhang, Z. H.; Johnson, G.R.; Wietsma, T.W. Influence of heterogeneity and sampling method on aqueous concentrations associated with NAPL dissolution. Environ. Sci. Technol. 2000, 34, 3657-3664.

Brusseau, M.L.; Nelson, N.T.; Zhang, Z.; Blue, J.E.; Rohrer, J.; Allen, T. Source-Zone Characterization of a Chlorinated-Solvent Contaminated Superfund Site in Tucson, AZ. J. Contam. Hydrol. 2007, 90, 21-40.

Brusseau, M.L., Rohay, V. and Truex, M.J. 2010. Analysis of Soil Vapor Extraction Data to Evaluate Mass-Transfer Constraints and Estimate Source-Zone Mass Flux. Ground Water Monitor. Remed. 30:57-64.

Brusseau, M.L., Rohrer, J.W., Decker, T.M., Nelson, N.T., and Linderfelt, W.R. 1999. Contaminant transport and fate in a source zone of a chlorinated-solvent contaminated superfund site: Overview and initial results of an advanced site characterization project. Chapter 19 in: Innovative Subsurface Remediation: Field Testing of Physical, Chemical, and Characterization Technologies, Brusseau, M.L., Sabatini, D.A., Gierke, J.S., and Annable, M.D., eds., American Chemical Society, Washington DC.

Brusseau, M.L.; Zhang, Z.; Nelson, N.T.; Cain, R.B.; Tick, G.R.; Johnson, G.R.; Oostrom, M. Dissolution of nonuniformly distributed organic liquid: intermediate-scale experiments and mathematical modeling. Environ. Sci. Technol. 2002, 36, 1033-1041.

Butcher, J.B. and Gauthier, T.D. 1994. Estimation of residual dense NAPL mass by inverse modeling. Ground Water. 32:71-78.

Carroll, K.C. and Brusseau, M.L., 2009. Dissolution, cyclodextrin-enhanced solubilization, and mass removal of an ideal multicomponent organic liquid. J. Contam. Hydrol. 106: 62-72.

Chapman, S.W. and Parker, B.L. 2005. Plume Persistence Due to Aquitard Back Diffusion Following Dense Nonaqueous Phase Liquid Source Removal or Isolation. Water Resour. Res., 41:1-16.

Childs, J., Acosta, E., Annable, M.D., Brooks, M.C., Enfield, C.G., Harwell, J.H., Hasegawa, M., Knox, R.C., Rao, P.S.C., Sabatini, D.A., Shiau, B., Szekers, E., Wood, A.L., 2006. Field demonstration of surfactant-enhanced solubilization of DNAPL at Dover Air Force Base, Delaware. J. Contam. Hydrol. 82: 1-22.

Chipera, S.J., Bish, D.L.. 2001. Baseline Studies of the Clay Minerals Society Source Clays: Powder X-Ray Diffraction Analysis. Clays and Clay Minerals. 49, 398-409.

Christ, J.A., Ramsburg, C.A., Pennell, K.D., Abriola, L.M., 2006. Estimating mass discharge fromdense nonaqueous phase liquids source zones using upscaled mass transfer coefficients: an evaluation using multiphase numerical simulations.Water Resour. Res. 42,W11420.

Christ, J.A.; Lemke, L.D.; Abriola, L.M. 2009. The influence of dimensionality on simulations of mass recovery from nonuniform dense non-aqueous phase liquid (DNAPL) source zones. Adv. Water. Res. 32, 401–412.

Christ, J.A., Ramsburg, C.A., Pennell, K.D., Abriola, L.M. 2010. Predicting DNAPL mass discharge from pool-dominated source zones. J. Contam. Hydrol. 114: 18-34.

Conrad, S.H., Glass, R.J. and Peplinski, W.J., 2002. Bench-scale visualization of DNAPL remediation processes in analog heterogeneous aquifers: surfactant floods and in situ oxidation using permanganate. Journal of Contaminant Hydrology, 58(1-2): 13-49.

CRA (CONESTOGA-ROVERS & ASSOCIATES). 2004. Shallow Groundwater Zone (SGZ) Subsurface Investigation, Extraction Well Installation and Aquifer Testing. July, Ref. No. 13711(19).

CRA (Conestoga-Rovers & Associates). 2012. Tenth Performance Evaluation Report, SGZ and SVE Remedy ; March 2012-August 2012 ; Airport Property, Tucson International Airport Area Superfund Site, Tucson, Arizona ; Includes Groundwater Containment Evaluation, September 2011 Through August 2012, and Off-Airport Property Performance Standards Attainment Evaluation (Section 3.8). November 2012. Ref. No. 013711 (66).

CRA (CONESTOGA-ROVERS & ASSOCIATES). 2010. Performance Evaluation Report, Airport Property, Tucson International Airport Area Superfund Site. May, Ref. No. 13711(54).

Detwiler, R.L., Rajaram, H., Glass, R.J., 2001. Nonaqueous-phase-liquid dissolution in variable-aperture fracture: development of a depth-averaged computational model with comparison to a physical experiment. Water Resour. Res. 37 (12), 3115–3130.

DiFilippo, E.L. and Brusseau, M.L., 2008. Relationship between mass-flux reduction and source-zone mass removal: Analysis of field data. Journal of Contaminant Hydrology, 98(1-2): 22-35.

DiFilippo, E.L., Carroll, K.C., and Brusseau, M.L. 2010. Impact of Organic-Liquid Distribution and Flow-Field Heterogeneity on Reductions in Mass Flux. J. Contam. Hydrol. 115: 14-25.

DiFilippo, E.L.; Brusseau, M.L. 2011. A simple Light Reflection Visualization (LRV) method for measuring in-situ organic-liquid saturation in two-dimensional flow cells. Journal of Hazardous Materials.

Dobson, R.; Schroth, M.H.; Oostrom, M.; Zeyer, J. Determination of NAPL-water interfacial areas in well-characterized porous media. Environ. Sci. Technol. 2006, 40, 815-822.

Environmental Protection Agency. 2012. Guidance for Evaluating Technical Impracticability of Ground-Water Restoration. http://www.epa.gov/superfund/health/conmedia/gwdocs/techimp.htm

Falta, R.W., Rao, P.S. and Basu, N., 2005. Assessing the impacts of partial mass depletion on DNAPL source zones I. Analytical modeling of source strength functions and plume response. J. Contam. Hydrol., 78(4), 259-308.

Feenstra, S., D. M. MacKay, and J.A. Cherry. 1991. A Method for Assessing Residual NAPL Based on Organic Chemical Concentrations in Soil Samples, Groundwater Monitoring Review, Vol. 11, No. 2.

Frind, E.O., Molson, J.W., Schirmer, M., and N. Guiguer. 1999. Dissolution and mass-transfer of multiple organics under field conditions: The Borden emplaced source. Water Resour. Res. 35(3), 683-694.

Fure, A.D.; Jawitz, J.W.; Annable M.D. 2006. DNAPL source zone depletion: Linking architecture and response. J. Contam. Hydrol. 85, 118-140.

Garg, S., Rixey, W.G., 1999. The dissolution of benzene, toluene, m-xylene and naphthalene from a residually trapped non-aqueous phase liquid under mass-transfer limited conditions. J. Contam. Hydrol. 36 (3–4), 313–331.

Heiderscheidt, J.L., Siegrist, R.L. and Illangasekare, H., 2008. Intermediate-scale 2D experimental investigation of in situ chemical oxidation using potassium permanganate for remediation of complex DNAPL source zones. Journal of Contaminant Hydrology, 102(1-2): 3-16.

Imhoff, P.T.; Jaffe, P.R.; Pinder, G.F. An experimental-study of complete dissolution of a nonaqueous phase liquid in saturated porous-media. Water Resour. Res. 1994, 30, 307-320.

Interstate Technology and Regulatory Council (ITRC). 2002. Regulatory Overview: DNAPL Source Reduction: Facing the Challenge. www.itrcweb.org.

Interstate Technology and Regulatory Council (ITRC). 2010. Use and Measurement of Mass Flux and Mass Discharge. www.itrcweb.org.

Jawitz, J.W.; A.D. Fure; G.G. Demy; S. Berglund; Rao, P.S.C. 2005. Groundwater contaminant flux reduction resulting from nonaqueous phase liquid mass reduction. Water Resour. Res., 41, 10408-10423.

Jayanti, S.; Pope, G.A. Modeling the benefits of partial mass reduction in DNAPL source zones. In: Remediation of Chlorinated and Recalcitrant Compounds. Battelle Press, Columbus, OH. 2004, Paper 2C-04.

Johnson, R.L., Pankow, J.F., 1992. Dissolution of dense chlorinated solvents in groundwater. 2. Source functions for pools of solvents. Environ. Sci. Technol. 26, 896–901.

Johnson, G.R., Gupta, K., Putz, D.K., Hu, Q., and Brusseau, M.L. 2003b. The effect of local-scale physical heterogeneity and non-linear, rate-limited sorption/desorption on contaminant transport in porous media. J. Contamin. Hydrol., 64, 35-58.

Johnson, G.R., Norris, D.K., and Brusseau, M.L. 2009. Mass removal and low-concentration tailing of trichloroethene in freshly-amended, synthetically-aged, and field-contaminated aquifer material. Chemosphere ,75:542–548.

Johnson, G.R., Zhang, Z., and Brusseau, M.L. 2003. Characterizing and Quantifying the Impact of Immiscible-Liquid Dissolution and Non-linear, Rate-limited Sorption/Desorption on Low-concentration Elution Tailing. Water Resour. Res., 39:6-1 to 6-8.

Kaye, A.J.; Cho, J.; Basu, N.B.; Chen, X.; Annable, M.D.; Jawitz, J.W. 2008. Laboratory investigation of flux reduction from dense non-aqueous phase liquid (DNAPL) partial source zone remediation by enhanced dissolution. J. Contam. Hydrol. 102:17-28.

Keely, J.F. (1989). "Performance evaluations of pump-and-treat remediations." U.S. Environ. Protec. Agency, Ground Water Issue Report, Ada, OK.

Krembs, F.J. R.L. Siegrist, M.L. Crimi, R.F. Furrer, and B.G. Petri. 2010. ISCO for Groundwater Remediation: Analysis of Field Applications and Performance. Ground Water Monitor. Remed. 30, 42-53.

Lemke, L.D.; Abriola, L.M. Modeling dense nonaqueous phase liquid mass removal in nonuniform formations: Linking source zone architecture and system response. Geosphere. 2006, 2, 74-82.

Lemke, L.D.; Abriola, L.M.; Lang, J.R. Influence of hydraulic property correlation on predicted dense nonaqueous phase liquid source zone architecture, mass recovery and contaminant flux. Water. Resour. Res. 2004. 40, W12417, doi:10.1029/2004WR003061.

Li, X.D. and Schwartz, F.W., 2004a. DNAPL mass transfer and permeability reduction during in situ chemical oxidation with permanganate. Geophysical Research Letters, 31(6).

Li, X.D. and Schwartz, F.W., 2004b. DNAPL remediation with in situ chemical oxidation using potassium permanganate Part I. Mineralogy of Mn oxide and its dissolution in organic acids. Journal of Contaminant Hydrology, 68(1-2): 39-53.

Li, X.D. and Schwartz, F.W., 2004c. DNAPL remediation with in situ chemical oxidation using potassium permanganate. II. Increasing removal efficiency by dissolving Mn oxide precipitates. Journal of Contaminant Hydrology, 68(3-4): 269-287.

Liu, C., Ball, W.P., 2002. Back diffusion of chlorinated solvent contaminants from a natural aquitard to a remediated aquifer under well-controlled field conditions: predictions and measurements. Ground Water 40 (2), 175–184.

Mackay, D. M. and Cherry, J. A. 1989. Groundwater contaminantion: Pump-and-treat remediation, Environ. Sci. Technol. 23, 630–636.

Maji, R. and Sudicky, E.A. 2008. Influence of mass transfer characteristics for DNAPL source depletion and contaminant flux in a highly characterized glaciofluvial aquifer. J. Contam. Hydrol. 102, 105–119.

Marble, J.C., DiFilippo, E.L., Zhang, Z., Tick, G.R., Brusseau, M.L., 2008. Application of a lumped-process mathematical model to dissolution of nonuniformly distributed immiscible liquid in heterogeneous porous media. J. Contam. Hydrol. 100, 1–10.

Marble, J.C., Carroll, K.C., Janousek, H., and Brusseau, M.L. 2010. In Situ Oxidation and Associated Mass-Flux-Reduction/Mass-Removal Behavior for Systems with Organic Liquid Located in Lower Permeability Sediments. J. Contam. Hydrol., 117: 82-93.

Maloszewski, P., and Zuber, A., 1993. Tracer experiments in fractured rocks: matrix diffusion and the validity of models. Water Resour. Res., 29:2723-2735.

Matthieu, D.E., M.L. Brusseau, G.R. Johnson, J.L. Artiola, M.L. Bowden, J.E. Curry. 2013. Intercalation of trichloroethene by sediment-associated clay minerals. Chemo. (in press).

Mayer, A.S. and Miller, C.T. 1996. The influence of mass transfer characteristics and porous media heterogeneity on nonaqueous phase dissolution. Water Resour. Res. 32, 1551-1567.

Nambi, I.M.; Powers, S.E. NAPL dissolution in heterogeneous systems: an experimental investigation in a simple heterogeneous system. J. Contam. Hydrol. 2000, 44, 161-184.

National Research Council (NRC). 2005. Contaminants in the Subsurface: Source-zone Assessment and Remediation. Natl. Acad. Press, Washington, D.C.Chemosphere. 90:459-463.

Nelson, N.T. and Brusseau, M.L. 1996. Field Study of the Partitioning Tracer Method for Detection of Dense Nonaqueous Phase Liquid in a Trichloroethene-Contaminated Aquifer. Env. Sci. Tech. 30:9. 2859-2863.

Nelson, N.T. and Brusseau, M.L. 1997. Advanced characterization of a superfund site: tracer tests and contaminant monitoring. PP. 255-257 in: Proc. of the American Chemical

Society National Meetings, Environmental Chemistry Div., San Francisco, CA, April 13-17, 1997. Vol. 37(1), American Chem. Soc., Washington, D.C.

Nelson, N.T.; Hu, Q.; Brusseau, M.L. 2003. Characterizing the Contribution of Diffusive Mass Transfer to Solute Transport in Sedimentary Aquifer Systems at Laboratory and Field Scales. J. Hydrol.. 276:275-286.

NRC (National Research Council). 1994. Alternatives for Ground Water Cleanup. National Research Council (NRC), Washington, DC, 315 pp.

NRC (National Research Council). 2004. Contaminants in the Subsurface: Source-zone Assessment and Remediation. National Research Council (NRC), Washington, DC, 372 pp.

NRC (National Research Council). 2013. Alternatives for Managing the Nation's Complex Contaminated Groundwater Sites. Wash., DC.

Parker, B.L.; Chapman, S.W.; Guilbeault, M.A. 2008. Plume Persistence Caused by Back Diffusion from Thin Clay Layers in a Sand Aquifer Following TCE Source-Zone Hydraulic Isolation. 2008. J. Contam. Hydrol. 102, 86-104.

Parker, J.C., Park, E., 2004. Modeling field-scale dense nonaqueous phase liquid dissolution kinetics in heterogeneous aquifers. Water Resour. Res. 40, W05109.

Phelan, T.J.; Lemke, L.D.; Bradford, S.A.; O'Carroll, D.M.; Abriola, L.M. Influence of textural and wettability variations on predictions of DNAPL persistence and plume development in saturated porous media. Adv. Water Resour. 2004, 27, 411-427.

Powers, S.E., Abriola, L.M. and Weber, W.J., 1994. An Experimental Investigation of Nonaqueous Phase Liquid Dissolution in Saturated Subsurface Systems - Transient Mass-Transfer Rates. Water Resources Research, 30(2): 321-332.

Powers, S.E.; Nambi, I.M.; Curry, G.W. Non-aqueous phase liquid distribution in heterogeneous systems: Mechanisms and a local equilibrium modeling approach. Water Resour. Res. 1998, 34, 3293-3302.

Rao, P.S.C.; Jawitz, J.W.; Enfield, C.G.; Falta, R.W.; Annable, M.D.; Wood, A.L. 2002. Technology integration for contaminated site remediation: clean-up goals and performance criteria. In: Groundwater Quality- Natural and Enhanced Restoration of Groundwater Pollution, IAHS Publ. 275: 571-578.

Rasa, E.; Chapman, S.W.; Bekins, B.A.; Fogg, G.E.; Scow, K.M.; Mackay, D.M. 2011. Role of Back Diffusion and Biodegradation Reactions in Sustaining an MTBE/TBA Plume in Alluvial Media. Jour. Contam. Hydrol. 126, 235-247.

Reitsma, S. and Marshall, M., 2000. Experimental study of oxidation of pooled NAPL. In: G.B. Wickramanayake, A.R. Gavaskar and A.S.C. Chen (Editors), Chemical Oxidation and Reactive Barriers: Remediation of Chlorinated and Recalcitrant Compounds. Battelle Press, Columbus, Ohio, pp. 25-32.

Rivett, M.O.; Chapman, S.W.; Allen-King, R.; Feenstra, S.; and Cherry, J.A. 2006. Pump-and-Treat Remediation of Chlorinated Solvent Contamination at a Controlled Field-Experiment Site. Environ. Sci. Technol., 40, 6770-6781

Rivett, M.O. and Feenstra, S. 2005. Dissolution of an emplaced source of DNAPL in a natural aquifer setting. Environ. Sci. Technol. 39: 447-455.

Saba, T. and Illangasekare, T.H., 2000. Effect of Groundwater Flow Dimensionality on Mass Transfer from Entrapped Nonaqueous Phase Liquid Contaminants. Water Resources Research, 36(4): 971-979.

Saenton, S. and Illangsasekare, T. 2007. Upscaling of mass transfer rate coefficient for the numerical simulation of dense nonaqueous phase liquid dissolution in heterogeneous aquifers. Water Resour. Res., Vol. 43, W02428, doi:10.1029/2005WR004274.

Sale, T.C.; McWhorter, D.B. Steady state mass transfer from single-component dense nonaqueous phase liquids in uniform flow fields. Water Resour. Res. 2001, 37, 393-404

SERDP, 2006. Final Report: SERDP/ESTCP Expert Panel Workshop on Reducing the Uncertainty of DNAPL Source Zone Remediation, Strategic Environmental Research and Development Program (SERDP).

Simon, M.A., and M.L. Brusseau. 2007. Analysis of a gas-phase partitioning tracer test conducted in an unsaturated fractured-clay formation, J. Contamin. Hydrol., 90, 146-158.

Soerens, T.S., D.A. Sabatini, and J.H. Harwell (1998), Effects of flow bypassing and nonuniform NAPL distribution on the mass transfer characteristics of NAPL dissolution, Water Resour. Res., 34(7), 1657-1673.

Soga, K.; Page, J.W.E.; Illangasekare, T.H. 2004. A review of NAPL source zone remediation efficiency and the mass flux approach. J. Hazard. Mater., 110, 13-27.

Strategic Environmental Research and Development Program (SERDP). 2006. Final report: SERDP/ESTCP expert panel on reducing the uncertainty of DNAPL source-zone remediation. http://docs.serdp-estcp.org/viewfile.cfm?Doc=DNAPLWorkshopReport.pdf.

Struse, A.M., Siegrist, R.L., Dawson, H.E. and Urynowicz, M.A., 2002. Diffusive transport of permanganate during in situ oxidation. Journal of Environmental Engineering-Asce, 128(4): 327-334.

Suchomel, E.J.; Pennell, K.D. Reductions in contaminant mass discharge following partial mass removal from dnapl source zones. Environ. Sci. Technol. 2007, 40, 6110-6116.

Tick, G.R.; Lourenso, F.; Wood, A.L.; Brusseau, M.L. 2003. Pilot-Scale Demonstration of Cyclodextrin as a Solubility-Enhancement Agent for Remediation of a Tetrachloroethene-Contaminated Aquifer. Environ. Sci. Technol. 37, 5829-5834.

Tick, G.R. and Rincon, E.A. 2009. Effect of enhanced-solubilization agents on dissolution and mass flux from uniformly distributed immiscible liquid trichloroethene (TCE) in homogeneous porous media. Water Air Soil Poll. 204:315–332.

Thomson, N.R., Fraser, M.J., Lamarche, C., Barker, J.F. and Forsey, S.P., 2008. Rebound of a coal tar creosote plume following partial source zone treatment with permanganate. Journal of Contaminant Hydrology, 102(1-2): 154-171.

U.S. Environmental Protection Agency (EPA). 2003. The DNAPL remediation challenge: is there a case for source depletion? Expert Panel on DNAPL Remediation, Kavanaugh, M.C., and P.S.C. Rao, Co-chairs, EPA/600/R-03/143.

Zhang, Z. and Brusseau, M.L. 1998. Characterizing three-dimensional hydraulic conductivity distributions using qualitative and quantitative geologic borehole data: application to a field site. Ground Water, 36, 671-678.

Zhang, Z. and Brusseau, M.L. 1999. Nonideal Transport of Reactive Solutes in Heterogeneous Porous Media: 5. Simulating Regional-Scale Behavior of a Trichloroethene Plume During Pump-and-Treat Remediation. Water Resour. Res., 35: 2921-2935.

Zhang, C., Yoon, H., Werth, C.J., Valocchi, A.J., Basu, N.B., Jawitz, J.W. Evaluation of simplified mass transfer models to simulate the impacts of source zone architecture on nonaqueous phase liquid dissolution in heterogeneous porous media. J. Contam. Hydrol. 2008, doi:10.1016/j/jconhyd.2008.05.007.

Zhu, J. and Sykes, J.F., 2004. Simple screening models of NAPL dissolution in the subsurface. J. Contam. Hydrol., 72 (1-4). 245-258.

8.0 Appendices

8.1 Supporting Data

Refined data collected during the research project are provided in the *Results and Discussion* section above in the form of tables and graphs.

8.2 List of Scientific/Technical Publications

8.2.1 Journal Articles

1. Johnson G.R., D.K. Norris, and M.L. Brusseau. 2009. Mass Removal and Low-Concentration Tailing of Trichloroethene in Freshly-amended, Synthetically-aged, and Field-contaminated Aquifer Material. Chemosphere 75:542-548.

2. Marble, J.C., K.C. Carroll, H. Janousek, and M.L. Brusseau. 2010. In Situ Oxidation and Associated Mass-flux-reduction/mass-removal Behavior for Systems with Organic Liquid Located in Lower-permeability Sediments. J. Contam. Hydrol. 117:82-93.

3. DiFilippo, E.L., K.C. Carroll, and M.L. Brusseau. 2010. Impact of Organic-liquid Distribution and Flow-field Heterogeneity on Reductions in Mass Flux. J. Contam. Hydrol. 115:14-25.

4. DiFilippo E.L. and M.L. Brusseau. 2011. Assessment of a Simple Function to Evaluate the Relationship Between Mass Flux Reduction and Mass Removal for Organic-liquid Contaminated Source Zones, J. Contam. Hydrol. 123:104-113.

5. Brusseau, M. L., K. C. Carroll, T. Allen, J. Baker, W. DiGuiseppi, J. Hatton, C. Morrison, A. Russo, and J. Berkompas. 2011. Impact of In Situ Chemical Oxidation on Contaminant Mass Discharge: Linking Source-Zone and Plume-Scale Characterizations of Remediation Performance. Environ. Sci. Technol. 45:5352-5358.

6. Brusseau, M.L., J. Hatton, and W. DiGuiseppi. 2011. Assessing the Impact of Source-zone Remediation Efforts at the Contaminant-plume Scale Through Analysis of Contaminant Mass Discharge, J. Contam. Hydrol. 126:130-139.

7. DiFilippo, E.L. and M.L. Brusseau. 2011. Application of Light Reflection Visualization for Measuring Organic-Liquid Saturation for Two-Phase Systems in Two-Dimensional Flow Cells. Environ. Eng. Sci. 28:803-809.

8. McCray, J.E., G.R. Tick, J.W. Jawitz, J.S. Gierke, M.L. Brusseau, R.W. Falta, R.C. Knox, D.A. Sabatini, M.D. Annable, J. Harwell, and A.L. Wood. 2011. Remediation of NAPL Source-Zones: Lessons Learned from Field Studies at Hill and Dover AFB. Ground Water 49:727-744.

9. Matthieu, D.E., M.L. Brusseau, G.R. Johnson, J.L. Artiola, M.L. Bowden, and J.E. Curry. 2013. Intercalation of Trichloroethene by Sediment-associated Clay Minerals. Chemosphere 90:459-463.

10. Brusseau, M.L. D.E. Matthieu, III, K.C. Carroll, J. Mainhagu, C. Morrison, A. McMillan, A. Russo, and M. Plaschke. 2013. Characterizing Long-term Contaminant Mass Discharge and the Relationship Between Reductions in Discharge and Reductions in Mass for DNAPL Source Areas. J. Contam. Hydrol. 49:1-12.

11. Matthieu, III, D.E., M. Plaschke, K.C. Carroll, F. Brinker, and M.L. Brusseau. 2013. Persistence of a Groundwater Contaminant Plume after Hydraulic Source Containment at a Chlorinated-Solvent Contaminated Site (in review).

12. Aykol, N.H., A. Russo, and M.L. Brusseau. 2013. Impact of Organic-Liquid Distribution on Mass Removal and Mass-Discharge Reduction for Enhanced-Solubilization Flushing. Water, Air, Soil Poll. (in press).

13. Johnson, G.R. and M.L. Brusseau. 2013. The Impact of Changes in the Ionic Composition of Groundwater on Solute Transport in High-Fines Aquifer Sediment (in preparation).

14. Brusseau, M.L., Z. Zhang, and A. Russo. 2013. Modeling Nonideal Dissolution of Organic Liquids in Heterogeneous Porous Media (in preparation).

15. Brusseau, M.L. Use of Historical Pump-and-Treat Data to Enhance Site Characterization and Remediation Performance Assessment. Water, Air, Soil Poll. (in press).

16. Marble, J., M. Plaschke, K.C. Carroll, L. Fuhrig, F. Brinker, and M.L. Brusseau. 2013. Application of In-situ Chemical Oxidation for Source Containment in a Low-Permeability System (in review).

17. Brusseau, M.L. and Z. Guo. Assessing Contaminant-Removal Conditions and Plume Persistence through Analysis of Long-term Pump-and-Treat Data (in review).

18. Brusseau, M.L. and Z. Guo. An Overview of Plume Persistence (in preparation).

8.2.2 Presentations

1. Brusseau M.L., DiFilippo, E.L. Time-Continuous Analysis of Mass Flux Reduction as a Function of Source Zone Mass Removal at Two Field Sites. Presented at the Partners in Environmental Technology Technical Symposium & Workshop, Washington D.C., December 2-4, 2008.

2. DiFilippo, E.L., Carroll, K.C., Brusseau, M. L. Impact of Source-Zone Architecture and Flow Field Heterogeneity on Reductions in Mass Flux. Presented at the Partners in Environmental Technology Technical Symposium & Workshop, Washington D.C., Dec 2-4, 2008.

3. Brusseau, M. L., DiFilippo, E.L., Russo, A. Characterizing Mass Flux and Mass Removal for Heterogeneous Systems: From the Pore Scale to the Field Scale. Presented at the American Geophysical Union Fall Meeting, San Francisco, CA, December 15-19, 2008.

4. DiFilippo, E.L., Carroll, K.C., Brusseau, M. L. Impact of Source-Zone Architecture and Flow Field Heterogeneity on Reductions in Mass Flux. Presented at the American Geophysical Union Fall Meeting, San Francisco, CA, December 15-19, 2008.

5. Johnson, G.R., Norris, D.K., Brusseau, M. L. Sorption/Desorption and Transport of Trichloroethene in Freshly-amended, Synthetically-aged, and Field-contaminated Aquifer Material. Presented at the American Geophysical Union Fall Meeting, San Francisco, CA, December 15-19, 2008.

6. DiFilippo, E.L., Brusseau M.L. Time-continuous Analysis of Mass Flux Reduction as a Function of Source Zone Mass Removal at Two Field Sites. Presented at the National Ground Water Association Ground Water Summit, Tucson, AZ, April 19-23, 2009.

7. Marble, J.C., Carroll K.C., Janousek H., Brusseau M.L. In Situ Oxidation and Associated Mass-Flux Reduction/Mass-Removal Behavior for Idealized Source Zones with Poorly-Accessible Organic Immiscible Liquid. Presented at the Geological Society of America National Meeting, Portland, OR, October 18-21, 2009.

8. Johnson, G.R., Brusseau M.L. The Impact of Contaminant Contact Time and Porous-Media Weathering on Transport of Trichloroethene in Aquifer Material. Presented at the Geological Society of America National Meeting, Portland, OR, October 18–21, 2009.

9. Marble, J.C., Carroll K.C., Janousek H., Brusseau M.L. In Situ Oxidation and Associated Mass-Flux Reduction/Mass-Removal Behavior for Idealized Source Zones with Poorly-Accessible Organic Immiscible Liquid. Presented at the SERDP/ESTCP Partners in Environ. Technology Technical Symposium, Washington D.C., December 1-3, 2009.

10. Brusseau, M.L. DNAPL Source Zones. Presented at the National Association of Remedial Project Managers (US EPA) National Meeting, Arlington, VA, May 24-28, 2010.May 24-28, 2010 • Potomac Yard • Arlington, Virginia

11. Brusseau, M.L. Innovative Remediation of Chlorinated Hydrocarbons for Heterogeneous Subsurface Environments. Presented at the NIEHS Superfund Basic Research Program National Meeting, Portland, OR, November 11-12, 2010.

12. Brusseau, M.L., Carroll, K.C., DiGuiseppi, W. Assessing the Impact of In-situ Chemical Oxidation on Source-zone Mass Discharge for a Chlorinated-solvent Contaminated Field Site. Presented at the SERDP and ESTCP's annual Partners in Environmental Technology Technical Symposium & Workshop, Washington D.C., November 30-December 2, 2010.

13. Brusseau, M.L., Carroll, K.C., Allen, T., Baker, J., DiGuiseppi, W., Hatton, J., Morrisson, C., Russo, A., Berkompas, J. Impact of In Situ Chemical Oxidation on Contaminant Mass

Discharge: Linking Source-Zone and Plume-Scale Characterizations of Remediation Performance. Presented at the Partners in Environ. Technology Technical Symposium and Workshop, Washington D.C., November 29-December 1, 2011.

14. Matthieu, D., Brusseau, M.L., Bowden, M.E., Johnson, G.R., Artiola, J.F., Curry, J. Intercalation of TCE by Sediment-Associated Clay Minerals and Implications for Low-Concentration Elution Tailing and Back Diffusion. Presented at the American Geophysical Union Fall Meeting, San Francisco, CA, December 5-9, 2011.

15. Brusseau, M.L., Carroll, K.C., Allen, T., Baker, J., DiGuiseppi, W., Hatton, J., Morrison, C., Russo, A., Berkompas, J. The Impact of In-Situ Chemical Oxidation on Contaminant Mass Discharge: Linking Source-Zone and Plume-Scale Characterizations of Remediation Performance. Presented at the American Geophysical Union Fall Meeting, San Francisco, CA, December 5-9, 2011.

16. Aykol, N.H., Russo, A., Brusseau, M.L. Impact of Enhanced-Flushing Reagents and Organic-Liquid Distribution on Mass Removal and Mass-Flux Reduction. Presented at the American Geophysical Union Fall Meeting, San Francisco, CA, December 5-9, 2011.

17. McCray, J.E., Tick, G.R., Carroll, K.C., Boving, T.B., Johnson, G.R., Brusseau, M.L. Future Direction for the Remediation of Sites Contaminated by Nonaqueous Phase Liquids. Presented at the American Geophysical Union Fall Meeting, San Francisco, CA, December 5-9, 2011.

18. Brusseau, M.L. Remediation of Chlorinated-solvent Contaminated Groundwater. Presented to the Motorola 52nd St. Superfund Site Community Information Group, Phoenix, AZ, April 25, 2012.

19. McCray, J.E., Tick, G., Jawitz, J.J., Annable, M., Brusseau, M.L., Falta, R., Gierke, J., Knox, R., Sabatini, D., Wood, A.L. Remediation of NAPL Source Zones: Lessons Learned from Field Studies at Hill and Dover AFB. Presented at the National Ground Water Association Ground Water Summit, Garden Grove, CA, May 6-10, 2012.

20. Hatton, J., Mohr, T.K.G., Brusseau, M.L., Warner, G.H. Persistence Mechanisms Maintaining a 6-Mile-Long Plume in a Deep, Low-Organic, Heterogeneous Aquifer. Presented at the Eighth International Conference on Remediation of Chlorinated and Recalcitrant Compounds, Monterey, CA, May 21-24, 2012.

21. Brusseau, M.L., Matthieu, III, D.E., Carroll, K.C., Mainhagu, J., Morrison, C., McMillan, A., Russo, A., Plaschke, M. Contaminant Mass Discharge and Mass Removal Behavior for a DNAPL Field Site. Presented at the Annual Meeting of the American Geophysical Union, San Francisco, CA, December 3-7, 2012.

8.3 Other Supporting Material

None.